ENVIRONMENTAL FATE AND BIOLOGICAL EFFECTS OF RADIUM-226 IN FRESHWATER ENVIRONMENTS: EVIDENCE FROM FINGERNAIL CLAMS (SPHAERIIDAE)

Catherine Proulx

Thesis submitted to the University of Ottawa
in partial fulfillment of the requirements for the
Doctorate in Philosophy
in
Earth Sciences
with a
Specialization in Chemical and Environmental Toxicology

Faculty of Science
Department of Earth and Environmental Sciences
University of Ottawa

© Catherine Proulx, Ottawa, Canada, 2026

ABSTRACT

Radium-226 (^{226}Ra) is a naturally occurring radionuclide that is typically present at low concentrations in freshwater environments but can be elevated by industrial activities that disturb or concentrate naturally occurring radioactive materials, including mining, oil and gas extraction, coal production, and wastewater treatment. Despite concerns regarding its mobility, bioaccumulation potential, and radiotoxicity, the ecological effects of ^{226}Ra remain poorly understood. This knowledge gap has contributed to the absence of a Canadian freshwater quality guideline for the protection of aquatic life. This thesis investigated the occurrence, environmental fate, bioaccumulation and toxicity of ^{226}Ra to a sensitive freshwater species of fingernail clams (*Sphaerium striatinum*), with a particular focus on the influence of calcium on its behaviour and toxicity. As alkaline earth metals with similar physicochemical properties, calcium and radium are expected to exhibit comparable environmental and biological behaviours, making calcium a potentially important factor influencing ^{226}Ra fate, bioavailability, bioaccumulation, and toxicity.

Analysis of Canadian mining effluent data demonstrated that ^{226}Ra is released from multiple mining sectors and that uranium mines are not uniquely responsible for elevated discharges. Final treated effluent concentrations ranged from 0.2 to 7800 mBq L^{-1}, with average concentrations in several sectors exceeding the regional background upper tolerance limit of 21.7 mBq L^{-1}. To address ecotoxicological data gaps, laboratory methods were developed for the freshwater fingernail clam *Sphaerium striatinum*, a sensitive bivalve species. Experimental results demonstrated that ^{226}Ra bioaccumulates in both soft tissues and shells, with preferential partitioning to shells. Chronic exposure reduced growth (EC_{10} = 4.1 Bq L^{-1}) and reproduction (EC_{10} = 0.37 Bq L^{-1}) at environmentally relevant concentrations, while survival was comparatively less sensitive. Sorption experiments further showed that the environmental fate of ^{226}Ra is strongly controlled by mineralogy and water chemistry, with adsorption to reactive clay minerals rapidly

reducing dissolved concentrations. Increasing calcium concentrations reduced sorption and increased the persistence of dissolved ^{226}Ra, whereas organic matter had comparatively little influence.

Combined bioaccumulation and toxicity studies demonstrated that calcium exerts competing effects on ^{226}Ra behaviour. Although calcium can reduce biological uptake through competitive interactions at biological membranes, it also increases ^{226}Ra dissolved exposure by limiting sorption to mineral phases. Consequently, calcium did not consistently mitigate toxicity and, for some endpoints, resulted in increased organism sensitivity. Dose modelling further indicated that waterborne exposure was the dominant pathway under the conditions tested. Overall, this research demonstrates that the environmental risk of ^{226}Ra is governed by coupled geochemical and biological processes and that water chemistry can substantially influence both exposure and toxicity. These findings provide critical information for environmental risk assessments and support the future development of science-based freshwater quality guidelines and management strategies for ^{226}Ra releases.

RÉSUMÉ

Le radium 226 (^{226}Ra) est un radionucléide naturel généralement présent à faibles concentrations dans les milieux d'eau douce, mais dont les concentrations peuvent être accrues par diverses activités industrielles perturbant ou concentrant les matières radioactives naturelles, notamment l'exploitation minière, l'exploitation pétrolière et gazière, la production de charbon et le traitement des eaux usées. Malgré des préoccupations liées à sa mobilité, à son potentiel de bioaccumulation et à sa radiotoxicité, les effets écologiques du ^{226}Ra demeurent peu documentés. Cette lacune a contribué à l'absence de recommandations canadiennes pour la qualité des eaux visant la protection de la vie aquatique. Cette thèse examine la présence, le devenir environnemental, la bioaccumulation et la toxicité du ^{226}Ra chez une espèce sensible de petite palourde d'eau douce (*Sphaerium striatinum*), en mettant particulièrement l'accent sur l'influence du calcium sur son comportement et sa toxicité. En tant que métaux alcalino-terreux présentant des propriétés physicochimiques similaires, le calcium et le radium sont susceptibles d'avoir des comportements environnementaux et biologiques comparables; le calcium pourrait donc influencer le devenir, la biodisponibilité, la bioaccumulation et la toxicité du ^{226}Ra.

L'analyse des données d'effluents miniers canadiens a démontré que le ^{226}Ra est rejeté par plusieurs secteurs miniers et que les mines d'uranium ne sont pas les seules responsables des rejets élevés observés. Les concentrations mesurées dans les effluents traités variaient de 0,2 à 7 800 mBq L^{-1}, et plusieurs secteurs présentaient des concentrations moyennes supérieures aux concentrations naturelles de fond. Afin de combler les lacunes écotoxicologiques, des méthodes expérimentales ont été développées pour la petite palourde d'eau douce Sphaerium striatinum, une espèce de bivalve sensible. Les résultats ont démontré que le ^{226}Ra se bioaccumule à la fois dans les tissus mous et les coquilles, avec une accumulation préférentielle dans ces dernières. Une exposition chronique a entraîné une diminution de la croissance (CE_{10} = 4,1 Bq L^{-1}) et de la

reproduction (CE_{10} = 0,37 Bq L^{-1}) à des concentrations environnementalement pertinentes, tandis que la survie s'est révélée moins sensible. Des expériences de sorption ont également montré que le devenir environnemental du ^{226}Ra est fortement contrôlé par la minéralogie et la chimie de l'eau. L'adsorption sur des minéraux argileux réactifs réduit rapidement les concentrations dissoutes, tandis qu'une augmentation de la concentration en calcium diminue cette sorption et favorise le maintien du ^{226}Ra sous forme dissoute. À l'inverse, la matière organique exerce une influence relativement faible.

Les expériences intégrées de bioaccumulation et de toxicité ont démontré que le calcium exerce des effets antagonistes sur le comportement du ^{226}Ra. Bien qu'il puisse réduire l'absorption biologique par compétition aux membranes cellulaires, il accroît également l'exposition au ^{226}Ra dissous en limitant sa sorption sur les phases minérales. Par conséquent, le calcium n'a pas systématiquement atténué la toxicité et a même entraîné une sensibilité accrue pour certains paramètres biologiques. La modélisation dosimétrique a par ailleurs indiqué que l'exposition par voie aqueuse constituait la principale voie d'exposition dans les conditions étudiées. Dans l'ensemble, cette recherche démontre que le risque environnemental associé au ^{226}Ra est régi par des processus géochimiques et biologiques étroitement couplés et que la chimie de l'eau peut influencer de façon importante l'exposition et la toxicité. Ces résultats fournissent des connaissances essentielles aux évaluations des risques environnementaux et soutiennent l'élaboration future de recommandations fondées sur des données scientifiques pour la protection des écosystèmes d'eau douce et la gestion des rejets de ^{226}Ra.

DEDICATION

For Austin and Collins

ACKNOWLEDGEMENTS

I would like to thank my thesis supervisor, Dr. Richard R. Goulet, for the opportunity to work on this project, as well as his continued support and guidance. I also appreciate the flexibility he afforded me as I balanced family life, work, and research. I am grateful to my co-supervisor Dr. Danielle Fortin, for her continued support and helpful feedback. I am also grateful to my committee members Dr. Tom Al and Dr. John Chételat for their time, advice, and knowledge. A special thank you to Dr. Tom Al for his guidance in geochemistry and speciation modelling.

This research was conducted in collaboration with CanmetMINING (Natural Resources Canada). The laboratory experiments (adsorption, toxicity) were conducted at CanmetMINING, with the guidance of Dr. Carrie Rickwood. I also acknowledge laboratory support from Gauri Prabhakar, Emily Suominen, and Ashley Nicholls. I would like to thank Nicolas Guérin, Debbie Behm, and Joseph Ro of Canadian Nuclear Laboratories for the analysis of ^{226}Ra samples.

Funding for this research was provided in part by the Natural Resources Canada Critical Minerals Program funds attributed to CanmetMINING and the Natural Sciences and Engineering Research Council of Canada (NSERC, grant number ALLRP 566677-21), with contributions from BHP Billiton Canada Inc., CAMECO Corp., Canadian Nuclear Laboratories, Canadian Nuclear Safety Commission, Denison Mines Corp., NexGen Energy Ltd., Orano Canada Inc., and the Saskatchewan Ministry of the Environment. I would like to acknowledge Dr. Claude Fortin for his leadership in coordinating the research program (RADIum effects on AquaTIc OrgaNisms (RADIATION)), and for facilitating regular radium working group meetings and conferences, which fostered a highly collaborative and supportive research environment. I would like to acknowledge the broader research team involved in this project, including Dr. Anne Cremazy (INRS), Dr. David Janz and Dr. Karl Liber (University of Saskatchewan), and Dr. Marilyn Stuart (Canadian Nuclear Laboratory), for their contributions and collaboration.

I would like to thank Dr. Bruce Kilgour, for his continued mentorship throughout my professional career. His flexibility allowed me to pursue this work alongside my professional responsibilities. I would also like to thank Charles Hatry for his encouragement and support throughout this process, particularly for stepping in when needed and never making me feel guilty for dedicating time to my studies.

Most of all, thank you to my family. My incredible parents, Lorraine and Denis, and in-laws, Wally and Sandy. I am grateful for their unwavering support, encouragement, and help throughout this journey. Whether it was helping with the kids and dogs, running errands, or lending a hand around the house, their support gave me the opportunity to dedicate time to both work and school. I am particularly grateful to my parents, who taught me the importance of perseverance and hard work. To my mother, Lorraine, for always encouraging me to believe that I could achieve anything I put my mind to, that no goal is out of reach with determination and dedication.

Finally, to my husband, Dave, and children, Austin and Collins, whose patience and encouragement carried me through the many challenges of balancing family life and research; from attending my first class virtually with my one-month-old in my lap to reaching this milestone. This accomplishment is as much yours as it is mine. Dave, thank you for being the supportive partner I needed throughout this journey, for holding down the fort when I had to run experiments on weekends or disappear for long hours to write. Austin and Collins, thank you for sharing so much of your mom with this process over the past four years, for sitting beside me while I worked, drawing pictures next to me while I sat at my computer, or curling up in my lap for cuddles while I wrote. While I often wished for fewer competing demands during this journey, I know these moments are some of the ones I will remember most. I look forward to closing this chapter and spending more weekends, evenings, and uninterrupted time focused on you both. And lastly to Cooper and Finn, for keeping me company through the many late nights of writing, always at my

feet under my desk, while also reminding me to step away from my computer for walks, fresh air, and moments of balance along the way.

TABLE OF CONTENTS

ABSTRACT ..... **II**

RÉSUMÉ ..... **IV**

DEDICATION ..... **VI**

ACKNOWLEDGEMENTS ..... **VII**

1 CHAPTER 1: GENERAL INTRODUCTION **1**
1.1 NATURALLY OCCURRING RADIOACTIVE MATERIALS 1
1.2 RADIUM-226 IN THE AQUATIC ENVIRONMENT 2
1.2.1 Occurrences and Sources 2
1.2.2 Environmental Properties and Behaviour 5
1.2.3 Radiological Effects of ^{226}Ra to Aquatic Biota 7
1.2.4 Bioaccumulation and Dose of ^{226}Ra in Aquatic Biota 8
1.3 REGULATORY CONTEXT AND WATER QUALITY GUIDELINES 10
1.3.1 Environmental Risk Assessments 10
1.3.2 Effluent Regulations 11
1.3.3 Water Quality Guideline 12
1.4 KNOWLEDGE GAPS 13
1.5 ANALYTICAL CONSIDERATIONS 15
1.6 FINGERNAIL CLAMS (SPHAERIIDAE) 17
1.7 STUDY OBJECTIVES 19

2 CHAPTER 2: BASELINE REVIEW OF RADIUM-226 RELEASES FROM CANADIAN MINING OPERATIONS **23**
ABSTRACT 24
2.1 INTRODUCTION 25
2.2 MATERIALS AND METHODS 27
2.2.1 Effluent Data Assembly 27
2.2.2 Data Analyses 29
2.2.3 Background Concentrations 29
2.3 RESULTS & DISCUSSION 30
2.4 CONCLUSION 38

3 CHAPTER 3: BIOACCUMULATION AND CHRONIC TOXICITY OF RADIUM-226 TO THE FRESHWATER BIVALVE *SPHAERIUM STRIATINUM* (SPHAERIIDAE) **40**
ABSTRACT 41
3.1 INTRODUCTION 42
3.2 METHODS 46
3.2.1 Field Collections of Test Organisms 46
3.2.2 Fingernail Clam Acclimation 47
3.2.3 Chronic Toxicity Tests 48
3.2.4 Exposure Water Chemistry 49
3.2.5 Speciation Calculation 51
3.2.6 Bioaccumulation 52
3.2.7 Chronic Endpoints 53

3.2.8 Statistical Analyses 55
3.3 RESULTS & DISCUSSION 56
3.3.1 Supporting Water Quality 56
3.3.2 Radium-226 Speciation 57
3.3.3 Estimated Exposure Concentrations....58
3.3.4 Toxicity Tests 65
3.3.5 Evaluation of Species Sensitivity 71
3.3.6 Uncertainties and Future Research 74
3.4 CONCLUSION 79

4 CHAPTER 4: MINERAL-DEPENDENT AND CALCIUM-INHIBITED ADSORPTION OF RADIUM-226 ONTO QUARTZ AND KAOLINITE IN A NATURAL SAND SUBSTRATE ..81
ABSTRACT 82
4.1 INTRODUCTION 83
4.2 MATERIALS AND METHODS 87
4.2.1 Experimental Solutions....87
4.2.2 Inorganic Substrates 88
4.2.3 Geochemical Modelling 89
4.2.4 Adsorption Experiments 93
4.2.5 Batch Sorption Experiment....95
4.2.6 Adsorption Parameters and Kinetic Model....95
4.2.7 Statistical Analyses 96
4.3 RESULTS 98
4.3.1 Stock Solution Chemistry 98
4.3.2 Radium-226 Speciation 99
4.3.3 Sand Characterization....100
4.3.4 Geochemical Models....101
4.3.5 Tiered Adsorption Experiments 102
4.4 DISCUSSION 111
4.4.1 Limited Interaction between ^{226}Ra and Organic Matter 112
4.4.2 Mineralogical Control on $^{226}Ra^{2+}$ Sorption in Sandy Substrates 113
4.4.3 Influence of Calcium on $^{226}Ra^{2+}$ Sorption Kinetics and Partitioning 114
4.4.4 Implications for ^{226}Ra Mobility and Availability to Aquatic Organisms in Sandy Environments 116
4.5 CONCLUSION 117

5 CHAPTER 5: THE EFFECT OF CALCIUM ON RADIUM-226 BIOACCUMULATION, DOSE RATES, AND TOXICITY TO FINGERNAIL CLAMS (SPHAERIIDAE) 118
ABSTRACT 119
5.1 INTRODUCTION 120
5.2 METHODS 123
5.2.1 Experimental Design 123
5.2.2 Water Quality and Chemistry....124
5.2.3 Bioaccumulation Assessment....125
5.2.4 Dose Rate Estimation....127
5.2.5 Statistical Analysis....129
5.3 RESULTS 131
5.3.1 Chronic Experiments....131
5.3.2 Bioaccumulation of ^{226}Ra....134
5.3.3 Dose Rates in *Sphaerium striatinum* 136

5.3.4 Calcium Effects on Chronic Toxicity 137
5.4 DISCUSSION 146
5.5 CONCLUSION 153

6 CHAPTER 6: GENERAL CONCLUSION 155
6.1 STUDY OUTCOMES 155
6.1.1 Chapter 2 155
6.1.2 Chapter 3 156
6.1.3 Chapter 4 159
6.1.4 Chapter 5 161
6.2 STUDY IMPLICATIONS 165
6.3 UNCERTAINTIES AND LIMITATIONS 166
6.4 FUTURE DIRECTIONS 169
6.5 CLOSING STATEMENT 171

REFERENCES 172

SUPPLEMENTARY MATERIALS 192
CHAPTER 1: SUPPORTING INFORMATION 192
CHAPTER 3: SUPPORTING INFORMATION 194
CHAPTER 4: SUPPORTING INFORMATION 205
CHAPTER 5: SUPPORTING INFORMATION 212

List of Figures

Figure 1.1 Part of the uranium 238 decay chain with the atomic number, decay mode (alpha α or beta β) and half-life of each radioisotope 3
Figure 2.1 Histograms of ^{226}Ra concentrations (mBq L^{-1} log transformed) in final treated effluent collected from mining and milling facilities in Canada in accordance with the Metal and Diamond Mining Effluent Regulations (MDMER), by mining subsector, 2014 to 2022 35
Figure 2.2 Boxplot of ^{226}Ra concentrations (mBq L^{-1} log transformed) in final treated effluent collected from mining and milling facilities in Canada in accordance with the Metal and Diamond Mining Effluent Regulations (MDMER), by mining subsector, 2014 to 2022. The box represents the interquartile range (25%-75%), with the thick bar within representing the median value. The lower whisker represents the minimum value, excluding outliers, up to the lower quartile (Q1), while the upper whisker represents the maximum value, excluding outliers, down to the upper quartile (Q3). The dotted line represents the upper tolerance limit, representing background concentrations, calculated using data (n = 401) collected from reference sites by uranium mines in Northern Saskatchewan from 2000 to 2012. 37
Figure 3.1 Relationship between time-weighted average (TWA) radium-226 (^{226}Ra) activity concentrations in water and tissue activity concentrations in *Sphaerium striatinum* shell and soft tissues following 28-day exposure. Points represent estimates obtained from composite samples (n = 6 composites per treatment, each consisting of 4-9 individuals per composite). Lines indicate linear regressions for each tissue type, with shaded bands representing 95% confidence intervals.....63
Figure 3.2 Variations in growth, measured as the change in total shell length in *Sphaerium striatinum* individuals after exposure to radium-226 (^{226}Ra) over 28 days. Boxes represent the interquartile range (25th–75th percentiles), with the horizontal line indicating the median. Whiskers extend to 1.5 × the interquartile range, and points represent individual observations. Asterisks indicate treatments significantly different from the control based on Dunnett-adjusted comparisons. Sample sizes ranged from n = 49–51 per treatment.....68
Figure 3.3 Variations in relative brood size, number of larvae as a function of total shell length (TSL), in *Sphaerium striatinum* after exposure to radium-226 (^{226}Ra) over 28 days. Boxes represent the interquartile range (25th–75th percentiles), with the horizontal line indicating the median. Whiskers extend to 1.5 × the interquartile range, and points represent individual observations. Asterisks indicate treatments significantly different from the control based on Dunnett-adjusted comparisons. Sample sizes ranged from n = 11–13 per treatment.....69
Figure 4.1 Influence of calcium (Ca) concentration on radium-226 (^{226}Ra) speciation at activity concentrations of 1, 5 and 50 Bq L^{-1}, modelled using PHREEQC. 100
Figure 4.2 Wide field emission scanning electron microscopy of rinsed sand substrate sample showing clay minerals lodged in quartz surface microstructures.....101
Figure 4.3 Activity concentrations of dissolved radium-226 (^{226}Ra) for solution only (Series A), solution + sand (Series B), and solution + sand + organic matter (Series C) systems under various calcium (Ca) concentrations (0.9 – 70 mg L^{-1}) and nominal ^{226}Ra activities (1, 5, and 50 Bq L^{-1}), over 48 hours.....104
Figure 4.4 Time-weighted average estimates of dissolved radium-226 (^{226}Ra) for solution only (Series A), solution + sand (Series B), and solution + sand + organic matter (Series C) systems under various calcium (Ca) concentrations (0.9 – 70 mg L^{-1}) and nominal ^{226}Ra activities (1, 5, and 50 Bq L^{-1}), over 48 hours.....107
Figure 4.5 Sorption of radium-226 ($^{226}Ra^{2+}$) to kaolinite and quartz mineral phases following 48 h of equilibrium under batch condition (solid-solution ratio: 47 g in 94 mL; temperature 21 °C; pH ~ 7). The black circles represent average measured concentrations (n = 3), with error bars representing standard errors (± SE).....111

Figure 5.1 Relationship between time-weighted average (TWA) radium-226 (^{226}Ra) concentrations in water and ^{226}Ra activity concentrations in soft tissue and shell of *Sphaerium striatinum* after 28-day exposure at varying Ca concentrations.....135
Figure 5.2 Total dose rates to *Sphaerium striatinum* as a function of time-weighted average (TWA) radium-226 (^{226}Ra) concentrations under different calcium conditions. Panels A–D correspond to calcium concentrations of 0.9, 7, 35, and 70 mg L^{-1}, respectively. Estimate 1 assumes full water occupancy (water-only exposure); Estimate 2 incorporates both water and sediment exposure using ERICA-derived sediment concentrations (K_d-based); and Estimate 3 incorporates water and sediment exposure using sediment concentrations derived from mass balance. Horizontal dashed and dotted lines indicate screening benchmarks of 10 and 400 µGy h^{-1}, respectively. 137
Figure 5.3 Survival (%) of *Sphaerium striatinum* after 28 days of exposure to nominal radium-226 (^{226}Ra) concentrations across varying calcium concentrations. Boxplots represent the median, interquartile range (box), and range (whiskers), with points showing individual replicates.139
Figure 5.4 Burrowing (%) of *Sphaerium striatinum* after 28 days of exposure to nominal radium-226 (^{226}Ra) concentrations across varying calcium concentrations. Boxplots represent the median, interquartile range (box), and range (whiskers), with points showing individual replicates.141
Figure 5.5 Growth in total shell length (mm) of *Sphaerium striatinum* after 28 days of exposure to nominal radium-226 (^{226}Ra) concentrations across varying calcium concentrations. Boxplots represent the median, interquartile range (box), and range (whiskers), with points showing individual replicates.....143
Figure 5.6 Relative brood size of *Sphaerium striatinum* after 28 days of exposure to nominal radium-226 (^{226}Ra) concentrations across varying calcium concentrations. Boxplots represent the median, interquartile range (box), and range (whiskers), with points showing individual replicates.145

List of Tables

Table 2.1 Number of samples which reported ^{226}Ra concentrations, along with the frequency flags indicating values below detection limits and the range of those detection limits, in samples collected from final treated effluents from mining and milling facilities in Canada in accordance with the Metal and Diamond Mining Effluent Regulations (MDMER), 2014 to 2022 (n = 43,389).....32
Table 2.2 Summary statistics of ^{226}Ra concentrations (mBq L^{-1}) in final treated effluent collected from mining and milling facilities in Canada in accordance with the Metal and Diamond Mining Effluent Regulations (MDMER), by mining sector, 2014 to 2022 33
Table 3.1 Summary statistics for measured activity concentrations of radium-226 (^{226}Ra) in dosed reconstituted soft water used in the *Sphaerium striatinum* 28-day chronic toxicity test for each nominal treatment.....59
Table 3.2 Estimated time-weighted average (TWA) concentrations of radium-226 (^{226}Ra) using paired fresh (T_0) and old (T_{48}) samples collected during the *Sphaerium striatinum* 28-day chronic toxicity test for each nominal treatment.....61
Table 3.3 Radium-226 (^{226}Ra) activity concentrations (mean ± standard deviations) in shell and soft tissues and corresponding bioaccumulation factors for *Sphaerium striatinum* following aqueous exposure over 28 days to ^{226}Ra. 65
Table 3.4 Mean observations (± standard deviations) for the chronic toxicity endpoints from the 28-day chronic toxicity test of radium-226 (^{226}Ra) to *Sphaerium striatinum* 67
Table 3.5 Effect concentrations (Bq L^{-1}) from the 28-day chronic toxicity test of radium-226 (^{226}Ra) to *Sphaerium striatinum*, estimated by hypotheses testing (ANOVA, post-hoc Dunnett's test) and dose-response modelling 70
Table 3.6 Parameter estimates for dose–response models fit to growth and reproduction data from the 28-day chronic toxicity test of radium-226 (^{226}Ra) to *Sphaerium striatinum* 71
Table 4.1 Thermodynamic data used in speciation modelling.....90
Table 4.2 Measured activity of radium-226 (^{226}Ra) in stock solutions with varying calcium (Ca) concentrations.....99
Table 4.3 Estimated sorption parameters for radium-226 (^{226}Ra) in adsorption experiments, including initial (C_0) and equilibrium (C_e) aqueous activities, fraction sorbed (fsorbed), equilibrium solid-phase activity (C_s), distribution coefficients (K_d), and first-order rate constants (k, reported in h^{-1} with associated standard errors (SE)) for Series B (solution + sand) and Series C (solution + sand + organic matter) across calcium (Ca) treatments (0.9-70 mg L^{-1}) and nominal ^{226}Ra activities (1, 5, 50 Bq L^{-1}). 109
Table 4.4 Estimated sorption parameters for radium-226 (^{226}Ra) in batch sorption tests, including initial (C_0) and equilibrium (C_e) aqueous activities, fraction sorbed (fsorbed), equilibrium solid-phase activity (C_s), and distribution coefficients (K_d) at nominal ^{226}Ra activities (1, 5, 50 Bq L^{-1}).....111
Table 5.1 Measured activity concentrations of radium-226 (^{226}Ra) in dosed waters used in the *Sphaerium striatinum* 28-day chronic toxicity tests at varying Ca concentrations, including fresh (T_0) and tested (48 hours old, T48) samples used to estimate fractional loss of ^{226}Ra between water renewals and the average exposure activity over 48 hours using a time-weighted average (TWA).....133
Table 5.2 Bioaccumulation factors (BAF, L kg^{-1}) for *Sphaerium striatinum* following 28-d aqueous exposure to increasing time-weighted average (TWA) radium-226 (^{226}Ra) concentrations (Bq L^{-1}) at varying calcium (Ca) concentrations. 136
Table 5.3 Estimated no-observed-effect concentrations (NOEC) and lowest-observed-effect concentrations (LOEC) for chronic toxicity endpoints of *Sphaerium striatinum* across varying calcium treatments, derived from Dunnett's post-hoc comparisons to control using time-weighted average (TWA) radium-226 (^{226}Ra) concentrations (Bq L^{-1}).....146

SUPPLEMENTARY INFORMATION

Table S1-1 Literature review of endpoint used to determine the acute and sublethal effects to fingernail clam species (Sphaeriidae)
Table S3-1. Chemical recipe of the reconstituted soft water used in the *Sphaerium striatinum* 28-day chronic toxicity test of ^{226}Ra
Table S3-2. Concentrations of select water chemistry parameters in samples collected from the bivalve collection areas, Ottawa River, 2022.
Table S3-3. Thermodynamic data used in speciation modelling in PHREEQC version 3.7.3
Table S3-4. Mean ± standard deviation of *in situ* water quality parameters measured during the *Sphaerium striatinum* 28-day chronic toxicity test for each ^{226}Ra nominal treatment
Table S3-5. Kruskal-Wallis rank sum test comparing *in situ* water parameters measured during the *Sphaerium striatinum* 28-day chronic toxicity across all ^{226}Ra nominal treatments
Table S3-6. Welch two sample t-test comparing *in situ* water quality parameters measured before and after water renewals during the *Sphaerium striatinum* 28-day chronic toxicity across all ^{226}Ra nominal treatments
Table S3-7. Kruskal-Wallis rank sum test comparing water chemistry parameters measured during the *Sphaerium striatinum* 28-day chronic toxicity across all ^{226}Ra nominal treatments
Table S3-8. Mean ± standard deviation of water chemistry parameters measured during the *Sphaerium striatinum* 28-day chronic toxicity test for each ^{226}Ra nominal treatment
Table S3-9. Predicted aqueous speciation of ^{226}Ra in stock solutions using PHREEQC, showing molal concentrations and percent composition of individual species
Table S3-10. Welch two sample t-test comparing total and dissolved fractions of ^{226}Ra measured during the *Sphaerium striatinum* 28-day chronic toxicity across all nominal treatments
Table S3-11. Kruskal-Wallis rank sum test comparing water chemistry parameters measured during the *Sphaerium striatinum* 28-day chronic toxicity across all ^{226}Ra nominal treatments
Table S3-12. Comparison of effect concentrations (Bq L-1) derived from dose-response models using nominal, time-weighted average, and end-of-interval (T_{48}) concentrations from the 28-day chronic toxicity test of ^{226}Ra to *Sphaerium striatinum*
Figure S3-1. Growth in total shell length (mm) of *Sphaerium striatinum* across ^{226}Ra exposure treatments (time-weighted average concentrations, Bq L^{-1}), shown separately for each replicate. Boxes represent the interquartile range (25th–75th percentiles), the horizontal line indicates the median, and whiskers extend to 1.5 × the interquartile range; points represent single observations
Figure S3-2. Relative brood size (# larvae / total shell length) of *Sphaerium striatinum* across ^{226}Ra exposure treatments (time-weighted average concentrations, Bq L^{-1}), shown separately for each replicate. Boxes represent the interquartile range (25th–75th percentiles), the horizontal line indicates the median, and whiskers extend to 1.5 × the interquartile range; points represent single observations
Table S4-2. Surface protonation, deprotonation, and surface complexation constants compiled for Surface Complexation Modelling development in PHREEQC version 3.7.3
Table S4-3. Concentrations of major ions in stock solutions for adsorption experiments (N =1)
Table S4-4. Results from the geochemical analysis of mineral sand substrate (N =1)
Table S4-5. Quartz mineral surface properties for quartz and kaolinite used in the Surface Complexation Modelling in PHREEQC version 3.7.3
Table S4-6. In situ water quality parameters throughout the adsorption experiments
Figure S4-1. Design of the tiered-adsorption experiment used to quantify the potential influence of solution composition (Series A), sand substrate (Series B) and organic matter (Series C) on changes in dissolved 226Ra in solution over 48 hours. The Control consisted of Reconstituted Soft Water (RSW). Treatments consisted of varying ^{226}Ra (1, 5, 50 Bq L^{-1}) and Ca (0.9, 7, 35, 70 mg L^{-1}) concentrations.

List of Acronyms and Abbreviations

^{226}Ra	Radium-226
ANOVA	Analysis of Variance
BAF	Bioaccumulation factor
Bq	Becquerel
Ca	Calcium
CCME	Canadian Council of Ministers of the Environment
CEPA	Canadian Environmental Protection Act
CI	Confidence Interval
CMMP	Canadian Minerals and Metals Plan
CNSC	Canadian Nuclear Safety Commission
CR	Concentration Ratio
CWQGs-PAL	Canadian Water Quality Guidelines for the Protection of Aquatic Life
DCint	Internal dose coefficient in whole organism body
DCext	External dose coefficient in water or sediment
Dext	External radiation dose rate
Dint	Internal radiation dose rate
DIC	Dissolved Inorganic Carbon
DOC	Dissolved Organic Carbon
EC_x	Effect Concentration causing x% effect
EEM	Environmental Effects Monitoring
EPA	Environmental Protection Agency
ERA	Environmental Risk Assessment
IAEA	International Atomic Energy Agency
HC_5	Hazard Concentration
Kd	Distribution (Partitioning) Coefficient
LET	Linear Energy Transfer
LOEC	Lowest-observed-effect concentration
mBq	Millibecquerel
MDMER	Metal and Diamond Mining Effluent Regulations
NOEC	No-observed-effect concentration
NORM	Naturally Occurring Radioactive Material
NSCA	Nuclear Safety and Control Act
OFw	Fraction of time spent in water
OFsed	Fraction of time spent in the sediments
OSMP	Oil Sands Monitoring Program
PWQO	Provincial Water Quality Objective
Ra	Radium
RBE	Relative Biological Effectiveness
RN	Radionuclide
RN_{sed}	Total activity concentrations of a radionuclide in sediment
RN_{water}	Total activity concentrations of a radionuclide in water
RN_{wo}	Total activity concentrations of a radionuclide in whole organism body
ROS	Reactive oxygen species
RSW	Reconstituted soft water
SEQG	Saskatchewan Environmental Quality Guideline
SD	Standard deviations
SSD	Species Sensitivity Distribution
TIC	Total Inorganic Carbon
TOC	Total Organic Carbon
TSL	Total shell length
TWA	Time-weighted average

US EPA	United States Environmental Protection Agency
WHAM	Windemere Humic Acid Model
µGy	Microgray

1 CHAPTER 1: GENERAL INTRODUCTION

1.1 Naturally Occurring Radioactive Materials

Radiation exposures and effects are a source of concern, in part due to a lack of public understanding. Radiation is ubiquitous, as it is present in naturally occurring radioactive material (NORM). NORM are present in many soils and rock formations, as well as the waters that come into contact with them. NORM contain low or moderate concentrations of naturally occurring primordial radionuclides, including uranium isotopes (e.g., ^{238}U, ^{235}U), thorium (^{232}Th), potassium (^{40}K), and their radioactive decay products, such as radium (e.g., ^{226}Ra, ^{228}Ra), radon (^{222}Rn), polonium (e.g., ^{218}Po, ^{210}Po) and lead isotopes (e.g., ^{214}Pb, ^{210}Pb) (Kamunda et al., 2016). Geological formations known to contain elevated levels of NORM include black shales, granite rocks, sandstone formations, phosphate rocks and phosphate-rich formations such as oil fields and gas reservoirs (Bezuidenhout, 2019; Fisher, 1995; Jędrzejek et al., 2022). Industrial activities that disturb these NORM-bearing formations can mobilize or concentrate radionuclides in air, soil, and water, thereby enhancing background levels (Aberikae et al., 2023; Ahmad et al., 2021; IAEA, 2014; Schmandt et al., 2019). These industrial activities include uranium mining and milling, metal and diamond mining, coal ash production, the oil and gas industry, water extraction and wastewater treatment processes, and the production of phosphates and other industrial minerals. Mining and milling activities are expected to increase in Canada per the Canadian Minerals and Metals Plan (CMMP), in order to meet the growing demand for critical minerals (Natural Resources Canada, 2021). The CMMP has identified 31 such minerals which are essential to the sustainable economic success of Canada as a leading mining nation, including uranium, aluminum, cobalt, gold, nickel, iron ore, copper, and coal (Natural Resources Canada, 2021).

Canada is an active participant in the nuclear fuel cycle, and projected increases in demand for nuclear energy are expected to drive expanded uranium mining and milling in regions with rich deposits. Historically, uranium mining and milling also occurred from 1955 to 1996 in Ontario, particularly in the Elliot Lake region (Berthelot et al., 2019; Clulow et al., 1998; Martin et al., 2003), but operations ceased following the discovery of higher-grade ore bodies in northern Saskatchewan. Currently, all active Canadian uranium mines and mills are located in the Athabasca Basin of northern Saskatchewan. The production of uranium concentrates requires the management of large volumes of process water, which can result in the release of radionuclides to the aquatic environment through treated effluent. In addition, seepage from tailings and waste rock may occur during both active operations and post-decommissioning if containment systems are insufficient. A radionuclide that is of particular concern as a contaminant entering the aquatic environment is ^{226}Ra due to its long half-life of 1600 years, persistence and mobility in aquatic systems, high degree of radiotoxicity and bioaccumulation potential (Mothersill et al., 2013; Pröhl, 2014; Thiry & Van Hees, 2008).

1.2 Radium-226 in the Aquatic Environment

1.2.1 Occurrences and Sources

Radium-226 (^{226}Ra) is one of four naturally occurring radioactive isotopes that are environmentally significant due to their relatively long half-lives (^{223}Ra, ^{224}Ra, ^{226}Ra and ^{228}Ra). These isotopes are produced through the decay of the primordial radionuclides of uranium (U) and thorium (Th) (Thiry & Van Hees, 2008). Radium-226 is part of the ^{238}U decay series (Figure 1.1), produced from the decay of ^{230}Th and subsequently decays via alpha emission into radon gas (^{222}Rn). Sources and pathways of ^{226}Ra in freshwater systems include groundwater inflow (Brenner et al., 2007), sediment resuspension and remobilization of sediment-bound radionuclides (Martin

et al., 2003), and atmospheric deposition via precipitation and particle fallout (IAEA, 2014). Activity concentrations of ^{226}Ra in groundwater will vary with source characteristics of the region and the ionic strength of the groundwater itself (IAEA, 2014). In Canadian surface waters, however, background activity concentrations of ^{226}Ra are relatively narrow. In rivers and streams ^{226}Ra activity concentrations have been reported to range between 0.0041 to 0.0137 Bq L^{-1} (Fesenko et al., 2014). In lakes, reported ^{226}Ra activity concentrations range from 0.005 to 0.009 Bq L^{-1} (Fesenko et al., 2014).

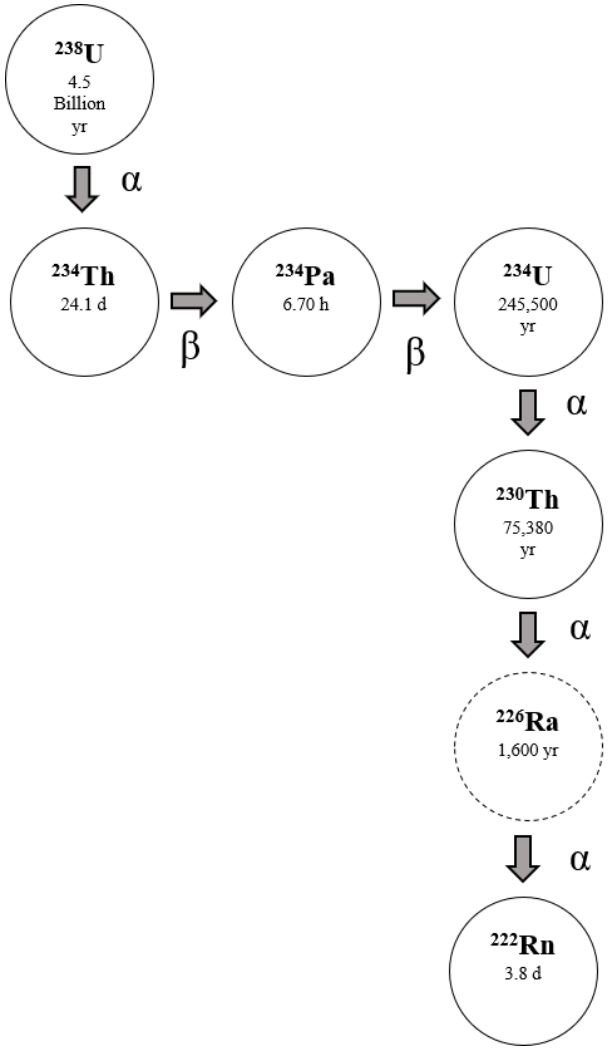


Figure 1.1 Part of the uranium 238 decay chain with the atomic number, decay mode (alpha α or beta β) and half-life of each radioisotope

Figure Notes. Adapted from (IAEA, 2014)

Anthropogenic sources of radium are primarily associated with the mining and milling of uranium (Chellam & Clifford, 2002; Mothersill et al., 2013; Sajih et al., 2014). Uranium mining and milling generate large volumes of tailings and mineralized waste rock that contain elevated concentrations of radionuclides, including ^{226}Ra (Wiramanaden et al., 2015). Uranium mill tailings, in particular, represent a primary reservoir of ^{226}Ra, where activity concentrations can range from 8 to 320 Bq g^{-1}, compared to background soil concentrations of 0.01 to 0.07 Bq g^{-1} (Abdelouas, 2006; Donahue et al., 2000; Fesenko et al., 2014). Both tailings and waste rock are typically stored near mine sites, where they can act as long-term sources of radionuclides to the surrounding environment if not adequately isolated. Rainwater percolation through these materials can mobilize ^{226}Ra, while runoff from waste management areas may transport radionuclides to surface waters. In lakes located downstream of uranium mines in northern Saskatchewan, ^{226}Ra concentrations have been reported to range up to 1.45 Bq L^{-1} (CNSC, 2014), which represents an increase from background conditions.

Water from these areas is typically collected, managed, and treated prior to discharge. Chemical amendments, such as lime or limestone, are added to promote the precipitation of dissolved radionuclides (Averill et al., 1984). However, ^{226}Ra activity concentrations can remain elevated in treated effluent. Elevated ^{226}Ra concentrations are frequently observed in mine and mill waters, particularly under acid-generating conditions where sulfide oxidation produces sulfuric acid and enhances radionuclide mobility (Schmidt and Goulet, 2014). Under these conditions, ^{226}Ra concentrations in groundwater influenced by tailings can reach several thousand Bq L^{-1}. In contrast, under circumneutral to alkaline conditions, attenuation of ^{226}Ra may occur through co-precipitation with carbonate minerals (e.g., calcite) and sorption to organic matter, although these processes are generally secondary to incorporation into sulfate minerals such as barite (Schmidt and Goulet, 2014). During milling, ^{226}Ra is commonly co-precipitated with barite and incorporated

into mineral phases such as cryptomelane, celestite, and, to a lesser extent, gypsum (Averill et al., 1984; Abdelouas, 2006; Lestini et al., 2013; Robin et al., 2017; Rollog et al., 2020). However, sequential extraction studies have demonstrated that ^{226}Ra can also be associated with Fe- and Mn-(hydr)oxides, particularly under neutralization conditions (Liu and Hendry, 2011).

Although these associations initially limit ^{226}Ra mobility, they may not ensure long-term stability. Under reducing conditions, such as those that develop in flooded tailings, microbial Fe(III) reduction can dissolve Fe-(hydr)oxides, releasing sorbed ^{226}Ra into solution (Landa et al., 1991; Stackelberg et al., 2018; Martin et al., 2003). Similarly, sulfate-reducing conditions may destabilize poorly ordered Ba–Ra sulfate phases ($(Ra,Ba)SO_4$), further contributing to mobilization. Mineralogical variability also influences ^{226}Ra retention, with higher porewater concentrations observed in tailings dominated by quartz and sulfide minerals compared to those containing more reactive phases such as chlorite and goethite (Scanlan, 2023). Additional release mechanisms may include oxidative weathering of primary ore minerals and the transport of ^{226}Ra associated with colloidal Fe-(hydr)oxides (Kartick, 2015). Following mine closure, engineered covers are used to limit infiltration and reduce radionuclide release; however, seepage may still occur if containment systems are insufficient or degrade over time (Berthelot et al., 2019; Swanson et al., 1983; Waite et al., 1989).

1.2.2 Environmental Properties and Behaviour

The environmental fate of ^{226}Ra is largely controlled by the physicochemical characteristics of the surrounding water. In freshwaters with pH values ranging from 3 to 10, dissolved ^{226}Ra occurs primarily as the free divalent cation ($^{226}Ra^{2+}$) (Langmuir and Riese 1985). In this form, ^{226}Ra may remain in solution, adsorb to suspended particulate matter, or be taken up by aquatic organisms. Particulate-bound ^{226}Ra can subsequently settle and accumulate onto surface sediments, contributing to long-term environmental reservoirs (Thiry and Van Hees 2008). Due to

its relatively long half-life, ^{226}Ra is considered persistent in aquatic systems (e.g., Hesslein and Slavicek, 1984). A common and simple method for describing the partitioning of a radionuclide between sediment and water is through the use of a distribution (partitioning) coefficient (K_d), defined as the ratio of the total activity concentration of a radionuclide in sediments (RN_{sed}, $Bq \cdot kg^{-1}$ dry mass) to that of water (RN_{water}, $Bq \cdot L^{-1}$) (Goulet at al. 2022).

$$K_d = \frac{RN_{sed}}{RN_{water}} \quad \text{(Eq. 1)}$$

Higher K_d values indicate greater partitioning to the sediment phase (i.e., strong adsorption), whereas lower K_d values indicate weaker adsorption and greater mobility in the aqueous phase.

The extent to which ^{226}Ra partitions between dissolved and particulate phases is strongly influenced by water chemistry, including pH, anions such as carbonate and sulfate, competing cations, and the presence of reactive mineral surfaces (Lofts et al. 2015; Sajih et al. 2014). Studies have shown that water pH influences the sorption of ^{226}Ra, with adsorption (higher K_d) generally increasing as pH increases (Nirdosh et al. 1990; Thiry and Van Hees 2008). Sorption will be influenced by the presence of other alkaline earth cations such as calcium and barium, as they will compete for binding sites due to their similar size and characteristics (Brown et al. 2019). Radium-226 adsorption over a range of physical and chemical parameters is relatively well studied for common rock-forming minerals including quartz (Beneš et al., 1984), muscovite and albite (Beneš & Strejc, 1986) and clay minerals such as kaolinite, montmorillonite, bentonite and smectite (Beneš et al., 1985; Reinoso-Maset & Ly, 2016; Robin et al., 2017; Tachi et al., 2001).

In sediments, redox conditions typically decrease with depth as microbial respiration sequentially consumes oxygen, nitrate, Fe- and Mn-(hydr)oxides, and sulfate during organic matter degradation (Berner, 1980). These redox-driven processes exert an important control on ^{226}Ra mobility and partitioning. Under oxic conditions, Fe- and Mn-(hydr)oxides provide reactive surfaces for ^{226}Ra sorption or co-precipitation, thereby reducing dissolved concentrations and

limiting mobility (Ames et al., 1983; Chellam & Clifford, 2002; Lofts et al., 2015; Nirdosh et al., 1990; Thiry & Van Hees, 2008). As sediments become reducing, microbial Fe(III) and Mn(IV) reduction promotes dissolution of these mineral phases, releasing previously sorbed ^{226}Ra back into porewater and overlying waters (Gonneea et al., 2008; Sajih et al., 2014). Sulfate-reducing conditions may further modify ^{226}Ra behaviour by altering sulfate availability and sulfate mineral equilibria. Co-precipitation with barite ($BaSO_4$) or celestite ($SrSO_4$) can remove ^{226}Ra from solution where sulfate is available; however, under strongly reducing conditions, sulfate depletion may inhibit sulfate mineral formation and increase ^{226}Ra mobility (Rosenberg et al., 2013). Collectively, these geochemical processes influence the partitioning of ^{226}Ra between dissolved and particulate phases, thereby affecting its persistence, mobility, and bioaccumulation potential in aquatic systems.

1.2.3 Radiological Effects of ^{226}Ra to Aquatic Biota

The radiological properties of ^{226}Ra can make it harmful to aquatic biota (Mothersill et al. 2013; Wiramanaden et al., 2015). Ionizing radiation exposure to organisms occurs through two primary pathways: external and internal. External exposure results from organisms living in or in close proximity to a contaminated medium, such as water or sediment, whereas internal exposure results from the uptake and incorporation of radionuclides into biological tissues (IAEA 2014). The magnitude of both external and internal radiation exposure depends on radionuclide activity concentrations and the type and energy of emitted radiation (IAEA, 2014; Ulanovsky, 2016). External exposure is further influenced by environmental contamination levels, habitat characteristics, and organism life-history traits that determine contact with contaminated media (Ulanovsky, 2016). In contrast, internal exposure depends on radionuclide uptake and retention within the organism and is influenced by factors such as organism size, trophic position, and the distribution of radionuclides among tissues and organs (IAEA, 2014).

Different types of ionizing radiation (i.e., alpha, beta, gamma) produce varying biological effects per unit dose, largely due to differences in linear energy transfer (LET) (Fuller et al. 2015). To account for this variability, radiation weighing factors, often expressed as relative biological effectiveness (RBE), are used in dose assessment (Chambers et al. 2006; Kocher and Trabalka 2000). RBE generally increases with LET, with alpha particles exhibiting high LET and therefore causing severe biological damage per unit dose than lower LET radiation such as beta and gamma emissions (Fuller et al. 2015). For alpha emitters, RBE values typically range from 1 to 50 (Mothersill et al. 2013).

Radium-226 is an alpha-emitting radionuclide, and as such, it poses a greater risk to aquatic organisms when internalized. Once incorporated, ^{226}Ra can localize in calcified tissues and cause localized ionization due to the high LET of alpha particles (Whicker and Schultz, 1982). This ionization can result in cellular and DNA damage, including chromosomal aberrations, mutagenesis, and carcinogenesis (Desouky et al., 2015). In contrast, the contribution of ^{226}Ra to external dose is generally limited, as alpha particles are readily attenuated in water and biological tissues, as demonstrated in modelling studies of environments downstream of uranium mines and mills (Goulet et al., 2022). As a result, internal exposure is typically the dominant pathway for radiological effects of ^{226}Ra in aquatic organisms.

1.2.4 Bioaccumulation and Dose of ^{226}Ra in Aquatic Biota

Freshwater biota, including algae, aquatic macrophytes, benthic invertebrates, and fish, have a high demonstrated capacity to accumulate ^{226}Ra across a range of environments (IAEA 2014). These organisms can take up ^{226}Ra directly from the water column (e.g., via gill uptake in fish), from sediments, or through ingestion of contaminated food and particles (IAEA, 2014). In general, ^{226}Ra concentrations in biota increase with increasing aqueous concentrations, with elevated levels typically observed in organisms from regions with high natural background levels

or from areas influenced by anthropogenic activities (IAEA, 2014). Given this potential for accumulation, assessment of radiological risk requires consideration of both internal and external exposure pathways. Goulet *et al.* (2022) recommend an approach for estimating total radiation dose rates to aquatic biota downstream of uranium mines and mills by integrating contributions from both internalized radionuclides and external environmental sources, as summarized below.

First, activity concentrations of radionuclides in biota must be estimated before dose-rate calculations can be performed (Goulet et al. 2022). When direct measurements are unavailable, activity concentrations in biota can be estimated by multiplying the radionuclide activity concentration in the ambient environment ($Bq \cdot L^{-1}$ for water, $Bq \cdot kg^{-1}$ for sediment) by a concentration ratio (CR) (Brown et al. 2008; Goulet et al. 2022). For aquatic organisms, the CR for a radionuclide (RN) is defined as

$$CR = \frac{RN_{wo}}{RN_{water}} \quad \text{(Eq. 2)}$$

where RN_{wo} is the radionuclide activity concentration in the whole organism ($Bg \cdot kg^{-1}$ fresh mass). When only sediment activity concentrations are available, partitioning relationships (e.g., K_d, Eq. 1) can be used to estimate aqueous concentrations. Generic CR values are available in databases such as the Wildlife Transfer Parameter Database (Howard et al. 2013; International Commission on Radiological Protection (ICRP), 2009). Once activity concentrations in environmental media and biota have been derived, internal and external absorbed dose rates for a radionuclide (RN) can be estimated using

$$\sum_{RN} D_{int,RN} = \sum_{RN} \left(DC_{int,RN} x RN_{wo} \right) \quad \text{(Eq. 3)}$$

$$\sum_{RN} D_{ext,RN} = \sum_{RN} DC_{ext,RN} x [OF_{water}\ x\ RN_{water} + OF_{sed}\ x\ RN_{sed}] \quad \text{(Eq. 4)}$$

Where, Dint and Dext are the internal and external dose rates ($\mu Gy \cdot h^{-1}$), respectively, DCint, RN is the internal dose coefficient ($\mu Gy \cdot h^{-1}/Bq \cdot kg^{-1}$), and DCext, RN is the external dose coefficient ($\mu Gy \cdot h^{-1}/Bq \cdot kg^{-1}$ or $Bq \cdot L^{-1}$). The occupancy factors OFwater and OFsed represent the fraction of

time an organism spends in the water column and sediment, respectively (Goulet et al. 2022). A key source of uncertainty in estimating activity concentrations and dose rates is the use of generic CR values, which can vary substantially with water chemistry, sediment composition, and biological factors (Goulet et al. 2022).

1.3 Regulatory Context and Water Quality Guidelines

1.3.1 Environmental Risk Assessments

The Canadian Nuclear Safety Commission (CNSC) regulates the development and production of nuclear energy to protect human health and the environment from the effects of ionizing radiation under the *Nuclear Safety and Control Act* (NSCA). Canada's environmental protection framework aligns with recommendations from the International Atomic Energy Agency (IAEA) and is implemented through legislation, licensing, compliance verification, research and Environmental Risk Assessments (ERA) (CNSC 2014). ERAs are used to evaluate the potential risks of contaminants in the environment in relation to mining operations (Canadian Standards Association (CSA), 2022). For uranium mines and mills, effluent and receiving environment monitoring programs, along with site-specific ERAs (CSA, 2022), are required to demonstrate that regulatory requirements are met and that releases do not pose an unacceptable risk to the environment (CNSC, 2014). Under Section 64 of the *Canadian Environmental Protection Act* (CEPA, 1999), uranium and uranium compounds in mine effluents are classified as toxic. In ERAs, baseline concentrations are typically derived from reference site(s) that are representative of background conditions. These baselines are often defined as the mean concentration at reference site(s) plus two standard deviations, approximating the 95th percentile under the assumption of a normal distribution (Kilgour et al., 1998).

The CNSC works with other federal agencies, including Environment and Climate Change Canada (ECCC), to manage risks associated with radionuclide release from uranium mining and

milling activities. A key component of ERA for radionuclides is the comparison of estimated dose rates in organisms to established screening thresholds. The ERICA Tool (Brown et al., 2008) recommends a screening dose rate of 10 μGy h^{-1}, below which ecological effects are unlikely, and a higher benchmark of 400 μGy h^{-1}, considered protective of aquatic populations (United Nations Scientific Committee on the Effects of Atomic Radiation (UNSCEAR), 2008). Additional guidance has been proposed by the Government of Canada, including dose thresholds specific to fish, benthic invertebrates, and plants in the Priority Substances List Assessment Report: Releases of Radionuclides from Nuclear Facilities (Impact on Non-Human Biota) (Environment Canada, 2003). While these approaches support the protection of aquatic life, they are based on dose and do not identify specific radionuclides that may be driving risk. As a result, there remains a need to develop substance-specific water quality guidelines for radionuclides such as ^{226}Ra.

1.3.2 Effluent Regulations

The Canadian *Metal and Diamond Mining Effluent Regulations* (MDMER), under the *Fisheries Act*, impose limits for prescribed deleterious substances in liquid effluent and prohibit the discharge of effluent that is acutely lethal to fish. Facilities subject to the MDMER are required to collect effluent samples from each final discharge point (FDP) and analyze them for deleterious substances on an ongoing basis. Concentrations must not exceed the authorized limits specified in the regulations. For ^{226}Ra, the maximum authorized concentrations are 0.37 Bq L^{-1}as a monthly mean, 0.74 Bq L^{-1} for a composite sample, and 1.11 Bq L^{-1} for a grab sample. Analytical requirements are defined in Schedule 3 of the MDMER, which specifies a method detection limit (MDL) of 0.01 Bq $L^{-1}$for ^{226}Ra. Reduced monitoring frequency is permitted for facilities other than uranium mines and mills, with sampling reduced to as little as once per calendar year if concentrations remain below 0.037 Bq L^{-1} over ten consecutive tests.

There is currently no ecotoxicological basis for the ^{226}Ra effluent limits established under the Metal and Diamond Mining Effluent Regulations (MDMER). The release limit of 0.37 Bq L^{-1} originates from a drinking water study conducted in the United States (Hess et al., 1985), in which ^{226}Ra concentrations in public water supplies were evaluated against a regulatory threshold of 0.19 Bq L^{-1}. Of the 990 samples analyzed, approximately 200 exceeded this threshold, yielding a mean concentration of 0.37 Bq L^{-1} (Agency for Toxic Substances and Disease Registry (ATSDR), 1990). These values are broadly consistent with effluent limits established by the United States Environmental Protection Agency (USEPA) under Title 40 of the *Code of Federal Regulations* (USEPA, 2016). Under this framework, average daily concentrations over 30 consecutive days must not exceed 0.37 Bq L^{-1} for total ^{226}Ra (and 0.11 Bq L^{-1} for dissolved ^{226}Ra), with corresponding maximum daily limits of 1.1 Bq L^{-1} and 0.37 Bq L^{-1}, respectively. Notably, these limits are derived from the performance of best available technology (BAT), rather than from ecological effects thresholds. Consequently, effluent limits based on drinking water guidelines or technology-based standards may not be sufficiently protective of aquatic ecosystems. This gap underscores the need for ecotoxicologically derived water quality guidelines for ^{226}Ra, which could provide an environmentally relevant basis for discharge limits and inform the development of treatment technologies capable of achieving those limits.

1.3.3 Water Quality Guideline

The Canadian Water Quality Guidelines for the Protection of Aquatic Life (CWQGs-PAL) are defined as "*nationally approved limits of substances and other attributes in the water column where no adverse toxic effects are expected to aquatic plants and animals*" (Canadian Council of Ministers of the Environment (CCME), 2007). Guidelines are derived for both short-term and long-term exposure periods. Long-term CWQGs-PAL are intended to protect all forms of aquatic life under indefinite exposure, whereas short-term guidelines are designed to protect a portion of

species from severe effects during brief exposures (CCME, 2007). Exposure and toxicity-modifying factors (ETMFs), such as pH, temperature, and hardness (e.g., Ca^{2+}, Mg^{2+}), are incorporated into guideline derivation where sufficient data are available (CCME, 2007).

The Species Sensitivity Distribution (SSD) is a statistical approach commonly used to derive water quality guidelines (CCME, 2007; Fox et al., 2021; Posthuma et al., 2019). SSDs describe the distribution of species sensitivities to a substance and are typically used to estimate the 5th percentile, or hazard concentration (HC5), at which 5% of species are expected to exhibit an adverse effect (Fox et al., 2021; Posthuma et al., 2019). Reliable SSD development requires sufficient ecotoxicity data, generally between 10 and 23 data points, with statistical robustness increasing as the dataset expands (Solomon et al., 1996; Wheeler et al., 2002; Zhao and Chen, 2016). For long-term guidelines, CCME (2007) recommends data from a minimum of three fish species (including one salmonid and one non-salmonid), three invertebrates (including at least one planktonic crustacean), and one to three plant species, depending on the substance's phytotoxicity.

There is currently no national CWQG-PAL for ^{226}Ra in Canada. While provincial guidelines exist, they are not derived from ecotoxicological datasets. For example, Saskatchewan has established an Environmental Quality Guideline (SEQG) of 0.11 Bq L^{-1} for total ^{226}Ra, based on United States Environmental Protection Agency (USEPA) effluent limits (Government of Saskatchewan, 2017; USEPA, 2016). Similarly, Ontario has defined a Provincial Water Quality Objective (PWQO) of 1.0 Bq L^{-1}; however, this value is based on historical drinking water objectives rather than ecological data (Ministry of Environment and Energy (MOEE), 1994).

1.4 Knowledge Gaps

Despite increasing attention to ^{226}Ra in freshwater systems, several key knowledge gaps limit the assessment of risk to aquatic environments. First, while ^{226}Ra is monitored in some

regulated effluents, there is limited synthesis of occurrence data across industrial sectors, and the relative contribution of different mining activities to environmental releases remains poorly characterized. This has contributed to the public perception that uranium mining is the dominant source of ^{226}Ra, despite limited comparative analysis across sectors.

Second, there is a lack of chronic toxicity data for freshwater organisms. Although field studies have demonstrated that ^{226}Ra can accumulate across freshwater food webs, from algae to fish (e.g., Clulow et al., 1998; Clulow and Pyle, 1997; Hesslein and Slavicek, 1984; Justyn and Havlik, 1990; Pyle and Clulow, 1998), there are relatively few studies evaluating the biological effects of ^{226}Ra on freshwater organisms. Available toxicity data are limited to a small number of species, including fish such as mullet (*Mugil cephalus*) (Antovic and Antovic, 2011) and fathead minnow (*Pimephales promelas*) (Mothersill et al., 2013, 2014; Shi et al., 2017), as well as invertebrates such as the ragworm (*Hediste diversicolor*) (Grung et al., 2009), the bivalve (*Velesunio angasi*) (Jeffree and Simpson, 1986), and the snail (*Lymnaea stagnalis*) (Van der Borght, 1963). Existing studies are limited in number and often do not account for dynamic exposure conditions, such as changes in aqueous concentrations due to sorption and partitioning processes. As a result, the sensitivity of aquatic organisms to ^{226}Ra, as well as the relative importance of different exposure pathways, remains uncertain. Moreover, many of these studies focus primarily on bioaccumulation rather than chronic toxicity, limiting their utility to dose modelling, which can only be used in predictive risk assessment but cannot be applied for guideline derivation. Where effects have been observed, they are often limited to a narrow set of endpoints; for example, reduced growth was reported in fathead minnows fed diets containing 10 and 100 mBq g^{-1} of ^{226}Ra (Mothersill et al., 2013). Collectively, the scarcity of chronic toxicity data across diverse taxa represents a key limitation in assessing the ecological risk of ^{226}Ra in freshwater systems.

Third, the environmental fate and partitioning of ^{226}Ra in freshwater systems are not well understood, particularly in relation to mineralogy and water chemistry. While it is recognized that ^{226}Ra can sorb to particulate phases, the relative roles of different mineral substrates and the influence of competing ions, such as calcium (Ca^{2+}), on sorption behaviour and aqueous persistence are not well constrained. This limits the ability to predict ^{226}Ra mobility and bioavailability under environmentally relevant conditions. Finally, the combined effects of water chemistry on ^{226}Ra bioaccumulation, dose, and toxicity are poorly characterized. Calcium is known to influence metal bioavailability through competitive interactions, yet its dual role in both reducing uptake and modifying partitioning, and therefore exposure, has not been systematically evaluated for radionuclides. Consequently, it remains unclear whether calcium acts as a protective factor or alters dose–response relationships in more complex ways. Together, these gaps limit the development of robust water quality guidelines for ^{226}Ra and hinder accurate assessment of ecological risk in freshwater systems.

1.5 Analytical Considerations

Accurate measurement of radium isotopes in environmental samples presents several analytical challenges due to their low concentrations, complex decay chains, and the need to distinguish among isotopes (e.g., ^{226}Ra versus ^{228}Ra). Radium is typically reported as an activity concentration (Bq L^{-1}), representing the number of radioactive decays per second per unit volume (1 Bq = 1 decay s^{-1}). For ^{226}Ra, 1 Bq L^{-1} is equivalent to approximately 27 pCi L^{-1} or 27 pg L^{-1}. While radioactivity has historically been expressed in curies (Ci), the becquerel is now the preferred SI unit. However, concentrations reported in mass units (e.g., pg L^{-1}) may become increasingly common as advances in mass spectrometry enable the sensitive and direct quantification of ^{226}Ra.

Because environmental concentrations are often at or near analytical detection limits, careful sample handling and method selection are required to obtain reliable measurements. Sample preservation is critical, as radium can adsorb to container walls or precipitate with mineral phases. To minimize these losses, samples are typically acidified (e.g., with nitric acid, HNO_3) immediately after collection to maintain radium in solution and prevent adsorption or co-precipitation. As highlighted by Guérin *et al.* (2023), variability in reported radium concentrations across studies is often attributable to differences in sample preservation, analytical methods, and detection limits, underscoring the need for standardized approaches and careful interpretation of low-level measurements.

Several analytical techniques are available for quantifying ^{226}Ra, each with advantages and limitations. Alpha spectrometry is commonly used due to its high sensitivity (detection limits on the order of ~0.3 mBq) and specificity for alpha-emitting radionuclides, although it requires chemical separation and is time-intensive. Inductively coupled plasma mass spectrometry (ICP-MS), including isotope dilution or pre-concentration approaches, enables rapid multi-element analysis with detection limits of approximately 3 mBq, but may be influenced by matrix effects and requires careful calibration. Gamma spectrometry provides a non-destructive alternative by measuring gamma emissions associated with the ^{226}Ra decay series but generally has higher detection limits (~5 mBq) and often requires larger sample volumes or extended counting times due to lower sensitivity (ASTM International, 2020; Guérin et al., 2023). These analytical constraints have important implications for experimental design and environmental monitoring. The low concentrations typically encountered in freshwater systems, combined with method-specific limitations, contribute to the scarcity of high-quality ^{226}Ra datasets.

1.6 Fingernail Clams (Sphaeriidae)

Benthic macroinvertebrates are considered indicators of fish habitat condition and overall water quality and, as such, are a key biological component monitored under regulatory programs such as the MDMER (Environment Canada 2012, Proulx et al. 2025b). Among benthic macroinvertebrates, freshwater bivalves are considered particularly valuable bioindicators due to their sensitivity to environmental stressors. Freshwater bivalves are also experiencing widespread global declines (Lopes-Lima et al., 2014; Vaughn & Hakenkamp, 2001), highlighting the importance of understanding stressors that may affect their survival, reproduction, and long-term persistence. Fingernail clams (Bivalvia: Sphaeriidae, Gray 1857) have been identified as being suitable sentinel species for assessing the survival, growth, condition, and reproduction rates of freshwater bivalves in receiving environments under Environmental Effects Monitoring (EEM) programs (Environment Canada 2012, Proulx et al. 2025b).

Several biological and ecological characteristics make fingernail clams particularly well suited as sentinel species. They can be found in great abundances, are easy to handle and sample year-round, and have a relatively simple life cycle with a lifespan typically not exceeding four years (Environment Canada 2012; Mackie 2007). Fingernail clam biology is well known, and considerable research has been conducted regarding the effects of exposure to various anthropogenic and natural environmental stressors (e.g., Mackie 1989; Kilgour and Mackie 1990; Mackie 2007). They are relatively non-mobile, such that exposure to contaminants is assured and representative of the exposure area. Like other bivalves, fingernail clams readily bioaccumulate contaminants through multiple exposure pathways and exhibit measurable sublethal responses to contaminant exposure (Schoonover et al. 2016). Their growth is relatively easy to quantify (Kilgour and Mackie 1990) and has been shown to be more sensitive than survival endpoints in standard test species such as *Daphnia*, Fathead Minnow (*Pimephales promelas*) and Rainbow

Trout (*Oncorhynchus mykiss*) (Mackie 1989). Fingernail clams have been reported to decline or disappear downstream of uranium mine and mill effluent discharges (Kilgour et al., 2018), suggesting their potential utility as bioindicators of ecological impacts.

Fingernail clams have a widespread distribution throughout Canada. Their lifespan is typically up to 4 years, with sexual maturity generally reached within the first year of life. Compared to larger freshwater bivalves such as unionids, fingernail clams remain relatively small and exhibit slower growth rates. Optimal growth generally occurs at temperatures between 10 and 25°C, and the life histories of many species have been well documented (e.g., Mackie 2007). Fingernail clams are hermaphroditic and ovoviviparous, with fertilized eggs developing within brood sacs inside their inner gills (Mackie 1979, Bespalaya et al. 2015). During later developmental stages, larvae incubate extramarsupially between gill filaments. Their life cycle includes four ontogenetic stages: embryos, fetal larvae, prodissoconch larvae, and extramarsupial larvae. Adults may produce between 3 and 24 large eggs (Salazar and Salazar 2000), and multiple ontogenetic stages may occur simultaneously within a single individual (Mackie 1979).

Fingernail clams occupy both lentic and lotic habitats and are found across a wide range of substrate types (Gale 1973). Species of *Pisidium* typically inhabit the upper few millimetres of sediment (< 5 mm), orienting their dorsal side downwards while feeding on material within the interstitial waters (Meier-Brook 1969; Lopez and Holopainen 1987). Water enters the mantle cavity through the foot slit, and cilia on the anterior dorsal and posterior margins of the foot produces water currents flowing through the ctenidia and faeces, before being expelled through the anal siphon (Mackie 2007). Species of *Sphaerium* also inhabit surface sediment and may feed either through gill-ciliary filter feeding or through ciliary action associated with the foot (Mackie 2007). Fingernail clams also function as deposit and detrital feeders, consuming particulate organic matter, algae, bacteria, dissolved organic material, and decomposing plant material (Mackie 2007).

These feeding strategies and close association with sediments increase the potential for exposure to dissolved and particle-associated contaminants.

Various species of fingernail clams have been used to assess both acute and sublethal effects of contaminants on endpoints including mortality, growth, reproduction, behaviour, and bioaccumulation, as summarized in Table S1-1 (see supplementary materials). Studies have employed a range of exposure systems, including static, renewal, and flow-through designs, with exposure durations ranging from 4 h to 63 d (see supplementary materials, Table S1-1). Mortality is commonly assessed using the gaping response, which results from relaxation of the anterior and posterior adductor muscles (Anderson 1977). Growth can be evaluated through changes in shell length over time, as shell dimensions can be measured accurately and repeatedly without sacrificing the organism (Anderson et al. 1978; Hickey and Martin 1999; Mackie 2007). In contrast, wet weight is considered a less reliable growth metric because shell mass and retained water within tissues and the mantle cavity contribute substantially to total weight (Mackie 2007). Reproductive responses may be assessed by quantifying larvae within brood sacs (Mackie 2007) or through the enumeration of released progeny (Fong et al. 1998; Fong and Molnar 2008). Behavioural endpoints, including immobility and valve closure, are also commonly evaluated as generalized stress responses (Heinonen et al. 1997; Kramer et al. 1989).

1.7 Study Objectives

The overall objective of this thesis was to improve understanding of the occurrence, environmental behaviour, bioaccumulation, and toxicity of ^{226}Ra in freshwater systems, with a particular focus on the sensitivity of *Sphaerium striatinum* to ^{226}Ra dosed solutions and the role of water chemistry in modifying its toxicity. The thesis is broken down into four chapters which have been prepared as manuscripts for publication in peer-reviewed scientific journals.

These objectives were designed to address complementary aspects of ^{226}Ra occurrence, fate, and effects in freshwater environments. The research progresses from broad-scale characterization of ^{226}Ra releases from Canadian mining operations (Objective 1) to evaluation of biological uptake and chronic toxicity in a representative freshwater benthic organism (Objective 2). Building on these findings, Objective 3 investigates the geochemical processes governing ^{226}Ra partitioning and mobility, with particular emphasis on the influence of mineralogy and calcium. Finally, Objective 4 integrates these biological and geochemical components by evaluating how calcium mediates ^{226}Ra bioaccumulation, radiation dose, and toxicity. Together, these objectives provide a mechanistic framework linking environmental occurrence, fate, bioavailability, and biological effects of ^{226}Ra in freshwater systems.

To address the identified knowledge gaps, the following specific objectives were pursued:

Objective 1: Baseline review of ^{226}Ra releases from Canadian mining operations.

Evaluate the occurrence and distribution of ^{226}Ra in mining effluents across multiple sectors in Canada, using data reported under federal regulations, to contextualize releases relative to natural background levels and challenge assumptions regarding dominant sources. The following hypotheses were tested:

- During operations, elevated releases of ^{226}Ra occur across multiple mining sectors, including the uranium mining sector.
- Concentrations of ^{226}Ra in treated operational effluents are elevated above regional background upper limit concentrations reported for Canadian freshwater systems.

Objective 2: Bioaccumulation and chronic toxicity of ^{226}Ra to the freshwater bivalve *Sphaerium striatinum* (Sphaeriidae).

Generate a coherent set of ^{226}Ra bioaccumulation and chronic toxicity data in a freshwater benthic invertebrate, the fingernail clam (*Sphaerium striatinum*), under controlled laboratory conditions, including evaluation of multiple biological endpoints and exposure pathways. The following hypotheses were tested:

- Radium-226 bioaccumulates in *Sphaerium striatinum* during chronic aqueous exposure.
- Due to its chemical similarity to calcium, ^{226}Ra preferentially accumulate in shell material relative to soft tissues.
- Chronic exposure to ^{226}Ra causes measurable biological responses in *S. striatinum* including effects on survival, growth, reproduction, and behaviour.

Objective 3: Mineral-dependent and calcium-inhibited adsorption of ^{226}Ra onto quartz and kaolinite in a natural sand substrate.

Investigate the influence of mineralogy, calcium concentration, and organic matter on the partitioning and fate of ^{226}Ra, with the aim of identifying key controls on sorption, mobility, and aqueous persistence, with implications for chronic studies and natural systems. The following hypotheses were tested:

- Radium-226 sorption differs among mineral substrates, with greater sorption to kaolinite than to quartz.
- Increasing calcium concentrations inhibit ^{226}Ra sorption to mineral surfaces and compete with ^{226}Ra for biological uptake sites.

- Organic matter influences ^{226}Ra partitioning between dissolved and particulate phases.

Objective 4: The effect of calcium on ^{226}Ra bioaccumulation, dose rates, and toxicity to fingernail clams (Sphaeriidae).

To evaluate the combined effects of calcium on ^{226}Ra bioaccumulation, dose, and toxicity, including assessment of how calcium modifies dose–response relationships through competing geochemical and biological mechanisms. The following hypotheses were tested:

- Calcium concentration influences ^{226}Ra partitioning among water, sediment, and biological tissues, thereby affecting bioaccumulation and estimated dose rates.

- Increasing calcium concentrations mitigate the sublethal effects of ^{226}Ra on fingernail clams.

- Calcium modifies the relationship between aqueous ^{226}Ra concentrations, absorbed dose, and biological response.

By integrating environmental occurrence, geochemical partitioning, bioaccumulation, dosimetry, and toxicity, this research advances understanding of the processes governing ^{226}Ra exposure and effects in freshwater ecosystems. The findings contribute to the development of science-based approaches for environmental monitoring, ecological risk assessment, and the derivation of ecotoxicologically relevant water quality guidelines for ^{226}Ra.

2 CHAPTER 2: BASELINE REVIEW OF RADIUM-226 RELEASES FROM CANADIAN MINING OPERATIONS

Proulx CL[ab*], B.W. Kilgour[b] and R.R. Goulet[ac]

[a] Department of Earth and Environmental Sciences, University of Ottawa, 150 Louis-Pasteur Private, Ottawa, ON, K1N 6N5, Canada

[b] Kilgour & Associates Ltd., 2285 St. Laurent Blvd, Ottawa, ON, K1G 4Z6, Canada

[c] Canmet-MINING, Natural Resources Canada, 555 Booth St., Ottawa, ON, K1A 0G1, Canada

*Corresponding Author: Catherine L. Proulx

STATEMENT OF CONTRIBUTIONS

Proulx, C.L.: Conceptualization, Methodology, Formal Analysis, Investigation, Writing – Original Draft, Visualization

Kilgour, B.W.: Writing – Review & Editing

Goulet, R.R.: Writing – Review & Editing, Supervision, Funding acquisition

Journal of Environmental Radioactivity published this chapter:

Proulx, C.L., Kilgour, B.W. and R.R. Goulet. 2025. Quantifying historical releases of radium-226 from Canadian mining operations to freshwaters, *Journal of Environmental Radioactivity*, Volume 283, 107629. https://doi.org/10.1016/j.jenvrad.2025.107629.

ABSTRACT

A common misconception is that radium-226 (^{226}Ra) is released into receiving waters exclusively by uranium mines and mills. In fact, ^{226}Ra is routinely analyzed in mining effluent across various sectors. Using data reported under the Canadian *Metal and Diamond Mining Effluent Regulations*, ^{226}Ra releases from mine effluent were evaluated for the period of 2014-2022. Final treated effluent concentrations ranged from 0.2 to 7,800 mBq L^{-1}. Data were grouped by mining sector as being either precious metals, base metals, ferrous metal, non-ferrous metals, uranium ore, or diamonds. Mean ^{226}Ra concentrations were highest for non-ferrous metal mines (51.9 mBq L^{-1}), followed by base metal (31.6 mBq L^{-1}), diamond (23.8 mBq L^{-1}), uranium (22.0 mBq L^{-1}), precious metal (15.0 mBq L^{-1}), and ferrous metal mines (11.0 mBq L^{-1}). Mean concentrations for non-ferrous, base metal, diamond, and uranium mining sectors exceeded the upper tolerance limit (UTL) for natural background concentrations (21.7 mBq L^{-1}), calculated using reference data from Northern Saskatchewan. Median concentrations, however, were below the UTL for all sectors, indicating episodic high ^{226}Ra releases likely influenced by variations in the uranium content of the ore bodies. This study demonstrates that ^{226}Ra activity concentrations in final treated effluent from uranium mining operations are lower than those from other mining sectors, challenging the perception that uranium operations are the primary source of ^{226}Ra releases.

2.1 INTRODUCTION

Public perception is that only uranium mines and mills release radionuclides, a belief that is also reported in the scientific literature (Chellam & Clifford, 2002; Mothersill et al., 2013; Sajih et al., 2014). In fact, naturally occurring radioactive materials (NORM) are present in a variety of geological formations, containing low to moderate concentrations of radionuclides such as uranium (e.g., ^{238}U, ^{235}U), thorium (^{232}Th), potassium (^{40}K), and their decay products, such as radium (e.g., ^{226}Ra, ^{228}Ra), radon (^{222}Rn), lead (^{210}Pb) and polonium (^{210}Po) (Kamunda et al., 2016). Some key formations that are known to contain elevated levels of NORM include black shales, granite, sandstone, pegmatites, coal, phosphate-rich and hydrocarbon-rich formations such as oil fields and gas reservoirs (Bezuidenhout, 2019; Fisher, 1995; Jędrzejek et al., 2022). As such, mining activities which disturb rock containing NORM can potentially contribute to the dispersion of radionuclides into the air, soil, and water. These activities include uranium mining and milling but also the mining and milling of metallic and non-metallic ores, coal production, and oil and gas extraction (Aberikae et al., 2023; Ahmad et al., 2021; IAEA, 2014; Schmandt et al., 2019).

One radionuclide of particular interest is ^{226}Ra because it is water-soluble, has a long half-life of 1600 years, and a high degree of radiotoxicity (Mothersill et al., 2013; Pröhl, 2014; Thiry & Van Hees, 2008; Wiramanaden et al., 2015). Water is a primary pathway by which ^{226}Ra may be dispersed from mining operations into the environment, enhancing concentrations above natural background concentrations (Fesenko et al., 2014). Natural background concentrations represent the range of usual or natural concentrations of a substance in the environment (Bodo, 1993; Kilgour et al., 2002). The use of data from reference locations is common when establishing the normal range of variation for substances in water (Kilgour & Somers, 2017; Kilgour et al., 1998; Proulx et al., 2018). Background concentration ranges of naturally occurring substances in the aquatic environment can be used to identify elevated concentrations in treated effluent and set exposure

ranges in toxicity experiments. Knowledge of background concentrations can also guide in the selection of best available technology economically achievable (BATEA) for mining effluents. Reported activity concentrations of ^{226}Ra in unaffected surface waters is scarse. The International Atomic Energy Agency (2014) reported that globally, ^{226}Ra concentrations in rivers and lakes range between 0.5 and 20 mBq L^{-1} and 0.5 to 15 mBq L^{-1}, respectively. For a watershed in Northern Ontario, Canada, Sauvé *et al.* (2021) derived background ranges of 20 mBq L^{-1} for rivers and 17 mBq L^{-1} for lakes.

Mine or mill site water originates directly from water used in mineral extraction, processing, treatment, and mine dewatering, as well as rainwater percolating through mine waste. This site-collected water can contain various contaminants, including ^{226}Ra, the concentration of which can be variable, depending on the mining processes, ore types, and mine management practices. During operations, contaminated site water is managed and treated before being discharged into the environment, and this water is referred to as final treated effluent. Contaminated site water can be processed through a series of treatment steps designed to remove or reduce ^{226}Ra to acceptable levels. In the uranium mining industry, and other industries where ^{226}Ra is a byproduct of mining and processing activities such as the exploration and processing of niobium (Alves & Coutinho, 2019), ^{226}Ra is often removed from effluent by the addition of barium chloride to precipitate barium-radium sulphate [(Ba, Ra)SO_4] (Averill et al., 1984). Schmidt and Goulet (2014) also reported other common treatment methods including membrane filtration, ion exchange, reverse osmosis, and nanofiltration. These technologies can decrease ^{226}Ra levels in the final treated effluent to BATEA levels.

Management of ^{226}Ra contamination at uranium mining and milling sites relies on accurate predictions or historical data of ^{226}Ra concentrations in effluent. These data are used in environmental risk assessment models to identify and implement mitigation measures aimed at

keeping ^{226}Ra releases as low as reasonably achievable (Goulet et al., 2022a). When effluent ^{226}Ra concentrations are predicted to significantly exceed background levels or applicable water quality guidelines (if available), BATEA may be implemented to improve the effluent quality. Currently, there is no Canadian water quality guideline (CWQG) for ^{226}Ra. Comprehensive knowledge of effluent and natural background concentrations is particularly valuable when designing ^{226}Ra toxicity tests at environmentally relevant concentrations, with the ultimate objective of deriving a CWQG for the protection of aquatic life.

The purpose of this paper is to analyze historical data on treated mining effluent releases of ^{226}Ra across various mining sectors to determine whether the uranium industry is the primary contributor of ^{226}Ra. Additionally, ^{226}Ra concentrations in mining effluents in Canada are characterized and assessed relative to natural background concentrations. This study will be helpful in providing the public, industry, regulators, and the scientific community with insight as to which mining sectors release ^{226}Ra, what ^{226}Ra concentrations are being released, and what natural background ^{226}Ra concentrations are around uranium mines and mills. This information will also be useful for the toxicity testing of ^{226}Ra to aquatic organisms.

2.2 MATERIALS AND METHODS

2.2.1 Effluent Data Assembly

Mining operations and milling facilities in Canada are subject to the *Metal and Diamond Mining Effluent Regulations* (MDMER, SOR/2002-222) under the *Fisheries Act* (R.S.C., 1985, c. F-14). Under the MDMER, mining and milling operations are required to collect treated effluent samples and analyze them for deleterious substances on an ongoing basis. All available MDMER compliance data for this study were obtained and compiled from the Government of Canada Open Data portal (Government of Canada, 2022a). Data were available for nine consecutive years (2014 to 2022). Since Environment and Climate Change Canada (ECCC) launched a new regulatory

reporting software called the Mine Effluent Reporting System (MERS) in 2019, the format of the data available between 2014 and 2018 differed from the data available from 2019 to 2022. The main differences included the following: (1) data available for the years of 2014 to 2018 consisted of individual data files, while data for the years of 2019 to 2022 were already compiled, (2) a column indicating whether data consisted of either single grab or composite samples was provided in the 2019 to 2022 data, (3) flags indicating when data were below detection limits were provided with the 2019 to 2022 data, and (4) a column indicating each facility's product(s) was provided with the 2014 to 2018 data sets. In addition, samples with missing concentrations for one or more deleterious substance(s) in the 2014 to 2018 data sets were classified as either "no deposit" in instances where there was no effluent flow from the final discharge point in a given month, "no measurement required" in instances where it was not required in accordance with the conditions set out in the MDMER, or "reduced frequency" in instances where the facility met the requirements of the MDMER which allowed them to conduct the testing of effluent on a reduced basis instead of weekly.

Compiled data for the years of 2014 to 2022 consisted of 43,389 effluent samples collected from 190 different mining and milling facilities located in all Canadian provinces and territories except for Alberta and Prince Edward Island. No ^{226}Ra monitoring records from MDMER-regulated facilities were available for Alberta or Prince Edward Island during the study period. Missing product(s) information for samples collected between 2019 and 2022 were filled in using data from prior years or via web search. As the MDMER (previously Metal Mining Effluent Regulations) were only amended in 2018 to include diamond mines, effluent samples from these mines were only available for the years of 2018 to 2022.

A total of 190 facilities reported under the MDMER from 2014 to 2022. Amongst those, several facilities produce more than one product, with precious metal mines often also producing

base metals and vice versa. The 190 facilities were grouped by so-called sectors as precious metals (i.e., gold, palladium, platinum, and silver), base metals (i.e., copper, aluminum, lead, nickel, and zinc), non-ferrous metals (i.e., antimony, cadmium, cesium, calcium, cobalt, indium, lithium, magnesium, molybdenum, niobium, rubidium, selenium, strontium, tantalum, tellurium, titanium, and tungsten), ferrous ore (i.e., producing high iron concentrate), uranium ore, and diamonds (modified from ICMM, 2024).

2.2.2 Data Analyses

A variety of basic statistics were computed for ^{226}Ra concentrations in effluent, including the minimum, maximum, median, mean, standard deviation, standard error, and 5th and 95th percentiles for each sector of mines. Differences in concentrations of ^{226}Ra among sectors were assessed using an Analysis of Variance (ANOVA), with sector as the fixed categorical predictor variable and using a significance level (α) of 0.05. A Tukey's multiple comparison post-hoc test was performed to determine between which sectors the differences occurred. For the Tukey's test, a Bonferroni correction was applied to α, given the multiple comparisons (N =15), for a resulting significance level of 0.003. Various types of plots were used to visualize the data. Histograms were used to display the distribution of the ^{226}Ra data, by sector of mines. A boxplot was used to visually summarize discharged ^{226}Ra concentrations in mine effluent by sector of mines. Values flagged as being below detection were considered at the reported value. Data were log transformed ($\log_{10}(x+1)$) for visualization with a boxplot. All statistical analyses were performed using the R software environment and associated base packages (R 4.6.1, R Core Team, 2026).

2.2.3 Background Concentrations

Radium-226 is not commonly monitored in the various freshwater quality programs throughout Canada (e.g., Canada's National Long-term Water Quality Monitoring Data (Government of Canada, 2022b)). However, it has been monitored extensively in northern

Saskatchewan by uranium mining operations. The Canadian Nuclear Safety Commission (CNSC 2014) presented reference environmental data collected from rivers and lakes in Northern Saskatchewan from 2000 to 2012, which ranged from 0.05 to 100 mBq L^{-1}. These data (n = 401) from reference sites were used to estimate normal ranges, calculated as tolerance limits of reported concentrations. Tolerance limits are confidence regions for the lower 5th or upper 95th percentile of the normal range of variation (Smith, 2002) and values falling outside the upper tolerance limit (UTL) would be deemed elevated from natural background concentrations. Here, an UTL for all reference site data was calculated using the following equation:

$$(1)\ Upper\ Tolerance\ Limit\ (UTL) = \bar{x} + k * SD$$

where $\bar{x}$ is the mean of reference data, k is based on the t-score of the 95th quantile of the Student t distribution and dependent of the sample size, and SD is the standard deviation of the reference data.

2.3 RESULTS & DISCUSSION

Of the 190 facilities reported under the MDMER, approximately 54% primarily produce precious metals, 27% primarily produce base metals, 7% produce iron ore, 7% produce non-ferrous metals, 3% produce uranium, and another 3% produce diamonds. Of the 43,389 data entries in the 2014 to 2022 MDMER compliance data, 17,337 samples (40%) had reported ^{226}Ra concentrations (Table 2.1). Of these 17,337 samples, the occurrence of ^{226}Ra concentrations flagged as being below method detection limits (MDL) ranged between 60% and 69% of entries from 2019 to 2022, with over 100 different MDLs ranging between 0.2 and 100 mBq L^{-1} (Table 2.1). The distribution of the ^{226}Ra data in final treated effluent by mining sector data are presented in Table 2.1 and summary statistics are provided in Table 2.2. Reported concentrations of ^{226}Ra were most frequent in effluent from precious metals, ferrous ore, and base metal mines (Table 2.1). Measurable concentrations of ^{226}Ra (i.e., those not flagged as being <MDL) in data from 2019 to

2022 were most frequent in effluent from precious metal mines (n = 1,526), followed by uranium (n = 1,185), base metals (n = 900), diamond (n = 496), ferrous (n = 487) and non-ferrous (n = 437) mines (Figure 2.1).

Summary statistics of reported concentrations of ^{226}Ra in final treated effluent for the various mining sectors are provided in Table 2.2, revealing notable differences in sample size, central tendencies, and data dispersion. Radium-226 concentrations ranged from 0.2 to 7,800 mBq L^{-1} across all mining sectors. Minimum values were comparable across sectors, varying from 0.15 to 1.00 mBq L^{-1}. Median values were also consistent across most sectors, ranging between 5.0 and 10.0 mBq L^{-1}. The SD values indicate substantial variability, particularly for non-ferrous mining (SD = 218.9 mBq L^{-1}) and ferrous mining (SD = 135.2 mBq L^{-1}). By contrast, the uranium (SD = 32.7 mBq L^{-1}) and diamond (SD = 24.9 mBq L^{-1}) mining sectors showed less variation. Standard errors (SE) were low across sectors, reflecting the large sample sizes, with the smallest SE observed for uranium (SE = 0.597 mBq L^{-1}) and the largest for non-ferrous mining (SE = 6.057 mBq L^{-1}). The 5th and 95th percentiles underscore the distribution of values, with non-ferrous mining exhibiting the widest range (2.0 to 230 mBq L^{-1}), while ferrous mining had a narrower range (2.0 to 16 mBq L^{-1}). These statistics provide a comprehensive overview of the data variability and central tendencies across different mining sectors.

Table 2.1 Number of samples which reported ^{226}Ra concentrations, along with the frequency flags indicating values below detection limits and the range of those detection limits, in samples collected from final treated effluents from mining and milling facilities in Canada in accordance with the Metal and Diamond Mining Effluent Regulations (MDMER), 2014 to 2022 (*n* = 43,389)

Compliance Data	Total Number of Samples	Number of Samples which Reported [^{226}Ra]		Frequency of Flags in Samples with ^{226}Ra		Range of Detection Limits[1] (mBq L^{-1})	
		#	% Total	#	% Samples with ^{226}Ra	Min	Max
2014	1,522	867	57				
2015	1,460	860	59				
2016	1,529	844	55		No Data		
2017	1,554	879	57				
2018	1,697	940	55				
2019	9,061	3,356	37	2,002	60	2.0	100
2020	8,407	3,156	38	1,931	61	0.3	100
2021	8,790	3,219	37	2,212	69	0.5	100
2022	9,369	3,216	34	2,109	66	0.2	100

Table Notes: [1]Range of detection limits, as indicated by flags in the data sets

Mean ^{226}Ra concentrations in final treated effluent ranged between 11 mBq L^{-1} and 52 mBq L^{-1} (Table 2.2), with averages being highest for non-ferrous metal mines (51.9 mBq L^{-1}), followed by base metal mines (31.6 mBq L^{-1}), diamond mines (23.8 mBq L^{-1}) and uranium mines (22.0 mBq L^{-1}). Mean concentrations were elevated compared to median values indicating that episodic high ^{226}Ra releases, likely influenced by variations in the uranium content of the ore bodies, are driving the values. Mean concentrations of ^{226}Ra in final treated effluent varied significantly among sectors ($p < 0.001$), with the post-hoc Tukey's test indicating that concentrations differed significantly ($p < 0.003$) in 13 of the 15 pairwise comparisons. These exceptions were for the comparisons of the non-ferrous and uranium sectors ($p = 0.078$) and the non-ferrous and diamond sectors ($p = 0.017$).

Table 2.2 Summary statistics of ^{226}Ra concentrations (mBq L^{-1}) in final treated effluent collected from mining and milling facilities in Canada in accordance with the Metal and Diamond Mining Effluent Regulations (MDMER), by mining sector, 2014 to 2022

Summary Statistics	Precious Metals	Base Metals	Non-Ferrous Metals	Ferrous Metals	Uranium	Diamonds
N of Cases	5,625	3,165	1,304	3,356	3,004	883
Minimum	0.15	0.20	0.50	0.50	0.50	1.00
Maximum	6,940	825	7,410	7,800	520	170
Median	7.0	6.7	5.0	10.0	10.0	10.0
Mean	15.0	31.6	51.9	11.0	22.0	23.8
Mode	5	5	5	10	10	10
Standard Deviation	125.4	62.7	218.9	135.2	32.7	24.9
Standard Error	1.671	1.114	6.057	2.334	0.597	0.837
5th Percentile	2.0	2.5	2.0	2.0	4.9	5.0
95th Percentile	30	170	230	16	92	75

Table Notes: Underlined values exceed the background upper tolerance limit concentration of 21.7 mBq L^{-1}, estimated using data from reference sites in Northern Saskatchewan (CNSC, 2014)

Finally, maximum values showed substantial variability, peaking at 7,800 and 7,410 mBq L^{-1} for the ferrous and non-ferrous metal mining sectors, respectively. Maximum values were lowest for the diamond and uranium sectors, at 170 and 520 mBq L^{-1}, respectively. These results are surprising as anthropogenic sources of ^{226}Ra in Canada are often presumed to be primarily associated with the mining and milling of uranium (Chellam & Clifford, 2002; Mothersill et al., 2013; Sajih et al., 2014). The presence of ^{226}Ra in final treated effluent from other sectors is likely due to its natural occurrence in the geological materials associated with ore deposits. Ore deposits that form in geological settings rich in uranium-bearing rocks, such as granites, black shales, or phosphorites, will likely contain traces of ^{226}Ra (Bezuidenhout, 2019; Fisher, 1995; Jędrzejek et al., 2022). Sulfide minerals commonly associated with gold and copper ore deposits, such as pyrite for example, often contain trace amounts of uranium and ^{226}Ra (Aberikae et al., 2023; Schmandt et al., 2019). This is consistent with the results from this study, which showed concentrations of

^{226}Ra in effluent for precious metals (i.e., gold) with an average of 15.0 mBq $L^{-1}$and in effluent for base metals (i.e., copper) with an average of 31.6 mBq L^{-1}.

During the mining and milling processes, large volumes of rock and soil are excavated, crushed, and ground to extract the metal from the ore. If that metal-bearing ore also contains trace amounts of uranium and its decay daughter ^{226}Ra, water used for ore processing, dust suppression, and transportation can become contaminated, which can lead to mobilization of ^{226}Ra. Mine site water containing radionuclides typically requires specific treatment technologies for removal of these radionuclides prior to being discharged to the aquatic environment (Schmidt and Goulet, 2014; Trenfield et al., 2011). While the uranium industry will typically add barium chloride to precipitate ^{226}Ra, effluent treatment processes for other industries are likely less targeted towards the removal of ^{226}Ra which likely explain the higher ^{226}Ra in other mining sectors observed in this study. Whether effluent containing ^{226}Ra requires treatment depends on how BATEA can remove ^{226}Ra compared to ambient radium concentrations and water quality guidelines.

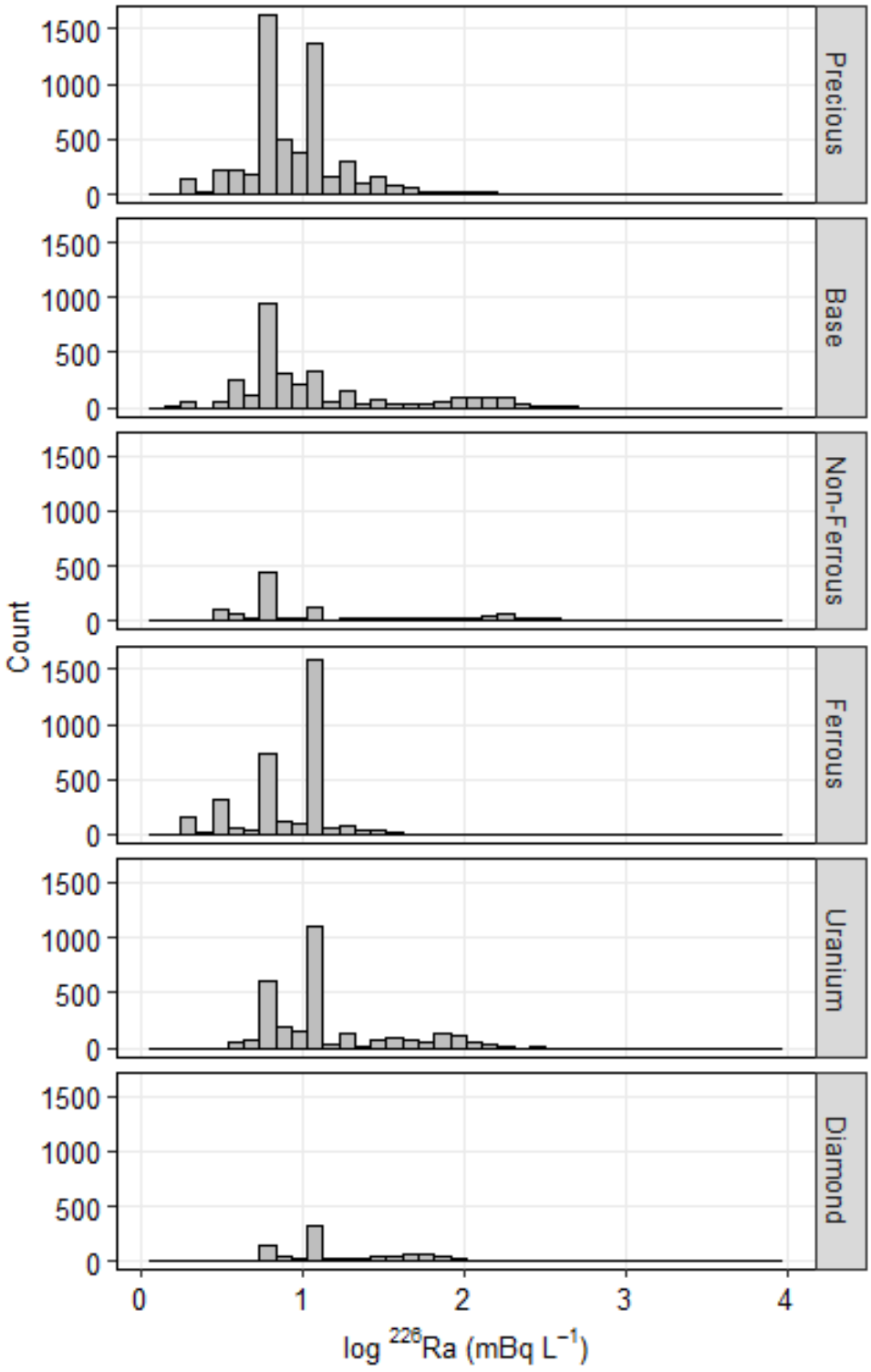


Figure 2.1 Histograms of ^{226}Ra concentrations (mBq L^{-1} log transformed) in final treated effluent collected from mining and milling facilities in Canada in accordance with the Metal and Diamond Mining Effluent Regulations (MDMER), by mining subsector, 2014 to 2022

An upper tolerance limit (UTL) of 21.7 mBq L^{-1} was estimated to represent background concentrations, based on a mean of 5.13 mBq L^{-1}, a sample size of 401, a k of 2.109, and a SD of 7.88 mBq L^{-1} (CNSC, 2014). The UTL of background concentrations of ^{226}Ra used for comparison in this study were computed using data exclusively from Northern Saskatchewan. Notably, the UTL estimate aligns with background concentrations estimates for watersheds in Northern Ontario. Using a similar methodology, Sauvé *et al.* (2021) derived UTLs of 20 mBq L^{-1} for rivers and 17 mBq L^{-1} for lakes. Furthermore, the UTL is consistent with the global range of ^{226}Ra concentrations reported for rivers and lakes, which span from 0.5 and 20 mBq L^{-1} (IAEA 2014). Mean releases of ^{226}Ra exceeded the UTL of 21.7 mBq L^{-1} for non-ferrous mines and base metal mines, while mean releases for diamond and uranium mines fell slightly above the estimated UTL (Table 2.2). The boxplot presented in Figure 2.2 demonstrates variations in releases of ^{226}Ra (i.e., concentrations in final treated effluent) by mining sectors in relation to estimated background UTL (i.e., 21.7 mBq L^{-1}). Interestingly, median effluent concentrations of ^{226}Ra fell below background concentrations in all mining sectors. However, more than 25% of samples reported by the non-ferrous metals and diamond sectors exceeded the background UTL concentrations of 21.7 mBq L^{-1}, as demonstrated by the interquartile ranges (Figure 2.2). Maximum ^{226}Ra concentrations in final treated effluent were above background concentrations in all mining sectors.

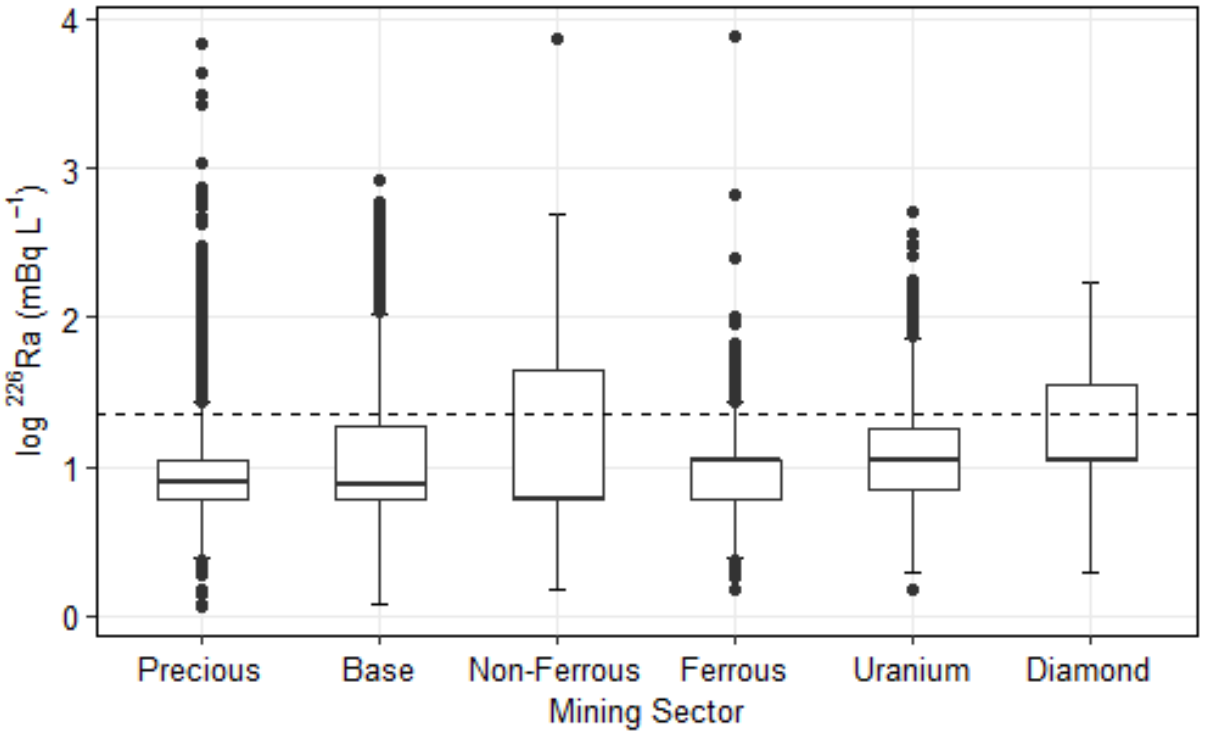


Figure 2.2 Boxplot of ^{226}Ra concentrations (mBq L^{-1} log transformed) in final treated effluent collected from mining and milling facilities in Canada in accordance with the Metal and Diamond Mining Effluent Regulations (MDMER), by mining subsector, 2014 to 2022. The box represents the interquartile range (25%-75%), with the thick bar within representing the median value. The lower whisker represents the minimum value, excluding outliers, up to the lower quartile (Q1), while the upper whisker represents the maximum value, excluding outliers, down to the upper quartile (Q3). The dotted line represents the upper tolerance limit, representing background concentrations, calculated using data (*n* = 401) collected from reference sites by uranium mines in Northern Saskatchewan from 2000 to 2012.

While exceedances of the UTL from the different mining sectors may raise some concerns, it is important to emphasize that the reported data reflect concentrations in final treated mining effluent and do not provide an estimate of loading to the environment. Effluent loadings, together with dilution in receiving waters, ultimately determine environmental concentrations, which are assessed relative to water quality guidelines, when available, to determine potential effects. Therefore, the data presented in this paper only suggest that effluent concentrations vary across different mining sectors. Although chemical concentration plays a significant role in determining the environmental fate and transport of an analyte, other factors must also be considered (Hemond

& Fechner, 2023). High concentrations in effluent may result in low environmental loadings, while low concentrations in effluent may still lead to high environmental loadings. Such scenarios depend on factors such as the volume of effluent discharged, frequency of discharge, and dilution capacity of the receiving water body. For instance, large discharge volumes, continuous effluent discharge, or receiving water bodies with low flow or limited dilution capacity can amplify the environmental impact of low-concentration effluents. Additionally, hydrological factors on a mine site, such as precipitation rates, the size of the mine or mill draining basin, and soil percolation rates, significantly influence flow dynamics and effluent loadings (Thiessen et al., 1999). Predicted or measured ^{226}Ra concentrations in receiving environments under low or high flow conditions reflect these factors, resulting in either high or low ^{226}Ra loadings.

2.4 CONCLUSION

Concentrations of ^{226}Ra in final treated effluent in Canada were compared among six different mining sectors and assessed relative to natural background concentrations. These sectors include those for precious metals, base metals, ferrous metals, non-ferrous metals, uranium ore, and diamonds. Canadian mining operations are evidently contributing ^{226}Ra to receiving environments due to the ubiquitous nature of uranium-bearing ore in Canada, with non-ferrous mines contributing the highest concentrations and ferrous mines contributing the lowest concentrations, on average. This research demonstrates that releases of ^{226}Ra from uranium mining and milling operations are similar, and in some cases lower, than those found in many other types of mining activities. This is likely due to effluent treatment processes in the uranium industry, such as the addition of barium chloride. Despite the likely differences in effluent treatment processes, this challenges the common public and scientific belief that only uranium mines and mills release measurable levels of ^{226}Ra. Although the great majority of samples were below the regional background UTL for ^{226}Ra of 21.7 mBq L^{-1}, each of the mining sectors also produced final treated

effluent concentrations that exceeded background. Although exceedances of natural background do not necessarily translate to effects in receiving environments, they are reasons for potential interest. As mining and milling activities are expected to increase in Canada per The Canadian Minerals and Metals Plan (Natural Resources Canada, 2021) to meet the growing demand for critical minerals, there will potentially be an increase in releases of ^{226}Ra into the aquatic environment, not only from uranium mining and milling but also the mining and milling of other critical minerals such as gold, copper, and ferrous ores. It then follows that a better understanding of ^{226}Ra radiological and chemical toxicity is warranted.

3 CHAPTER 3: BIOACCUMULATION AND CHRONIC TOXICITY OF RADIUM-226 TO THE FRESHWATER BIVALVE *SPHAERIUM STRIATINUM* (SPHAERIIDAE)

Proulx CL[ab], C.J. Rickwood [c], D. Fortin[a] and R.R. Goulet[ac]

[a] Department of Earth and Environmental Sciences, University of Ottawa, 150 Louis-Pasteur Private, Ottawa, ON, K1N 6N5, Canada

[b] Kilgour & Associates Ltd., 2285 St. Laurent Blvd, Ottawa, ON, K1G 4Z6, Canada

[c] Canmet-MINING, Natural Resources Canada, 555 Booth St., Ottawa, ON, K1A 0G1, Canada

*Corresponding Author: Catherine L. Proulx

STATEMENT OF CONTRIBUTIONS

Proulx, C.L.: Conceptualization, Methodology, Formal Analysis, Investigation, Writing – Original Draft, Visualization

Rickwood, C.J.: Conceptualization, Methodology, Resources, Writing - Review & Editing

Fortin, D.: Writing - Review & Editing, Supervision

Goulet, R.R.: Conceptualization, Methodology, Resources, Writing - Review & Editing, Supervision, Funding acquisition

Environmental Toxicology and Chemistry published this chapter:

Proulx, C.L., Rickwood, C.J., Fortin, D.D. and R.R. Goulet. 2026. Bioaccumulation and chronic toxicity of radium-226 to the freshwater bivalve Sphaerium striatinum (Sphaeriidae), *Environmental Toxicology and Chemistry*, https://doi.org/10.1093/etojnl/vgag249.

ABSTRACT

There are limited data on radium-226 (^{226}Ra) activity concentrations that affect freshwater organisms. The chronic toxicity of ^{226}Ra to the native freshwater fingernail clam *Sphaerium striatinum* was tested under controlled laboratory conditions for 28 days. Clams were exposed to reconstituted soft water dosed with seven nominal ^{226}Ra activity concentrations (0.1, 0.5, 1.0, 5, 10, 25 and 50 Bq L^{-1}) and a control (0 Bq L^{-1}). Radium-226 activity concentrations decreased substantially between static renewals, approximately 90% loss attributed to adsorption to the sand substrate. Consequently, time-weighted average (TWA) concentrations were used to estimate exposure. Tissue bioaccumulation (soft and shell) was measured. Results indicated a measurable uptake of ^{226}Ra in clam tissues, increasing with exposure concentration, suggesting potential for trophic transfer and long-term retention. Radium-226 accumulated to a greater extent in shell (278-419 L kg^{-1}) compared to soft tissues (70-180 L kg^{-1}). Toxicity endpoints assessed included survival, burrowing behaviour, growth, and reproduction. Survival and burrowing behaviour were not significantly affected by ^{226}Ra exposure. In contrast, growth and reproduction showed significant concentration-dependent reductions, with TWA effect concentrations (EC_{10}) estimated at 4.1 and 0.37 Bq L^{-1}, respectively. These findings provide new information on the sensitivity of freshwater bivalves to ^{226}Ra exposure and support the conclusion that chronic effects of ^{226}Ra might arise from bioaccumulation and sediment-associated exposure pathways in addition to direct waterborne toxicity. This study contributes to the limited but expanding body of evidence needed to inform water quality guidelines and risk assessments, which are essential for designing mitigation strategies to control radionuclide releases into freshwater ecosystem from mining activities.

3.1 INTRODUCTION

Radium-226 (^{226}Ra) is a naturally occurring decay product of uranium-238 that can become enriched in waste streams during the processing of uranium and other mineral ores and subsequently discharged to the environment in treated effluent (International Atomic Energy Agency (IAEA), 2014; Proulx et al., 2025a). The radiological half-life of ^{226}Ra is 1600 years, making it a persistent radionuclide of particular concern in aquatic environments. As an alpha emitter, its radiation is readily attenuated in water but can result in substantial localized energy deposition when incorporated into biological tissues (Goulet et al., 2022). Furthermore, it is a non-essential element, with no known biological function in organisms (IAEA, 2014). Its unique properties contribute to its bioaccumulation and toxicity in aquatic organisms. As an alkaline earth metal, $^{226}Ra^{2+}$ mimics Ca^{2+} and can enter biological systems through calcium uptake pathways, such as those involved in bone or shell formation (Brenner et al., 2007; Jeffree & Simpson, 1984; Pyle & Clulow, 1998), and is then transported in the bloodstream in its dissolved ionic form ($^{226}Ra^{2+}$). Radium-226 can then become incorporated into hydroxyapatite (calcium phosphate) or other calcium-containing structures, where it may remain for extended periods owing to slow biological turnover. In addition to calcified tissues, ^{226}Ra may also accumulate in soft tissues through association with intracellular calcium pools and calcium-binding structures, including calcium phosphate granules (Ellis & Jeffree, 1982; Jeffree & Simpson, 1984). This mimicry can lead to bioaccumulation by organisms over time.

Field studies have indicated that ^{226}Ra accumulates in freshwater food webs including algae and plants (Havlik, 1970, 1971; Hesslein & Slavicek, 1984; Twining, 1993), benthic invertebrates (Hesslein & Slavicek, 1984), bivalves especially (Bollhöfer et al., 2011; Brenner et al., 2007; Doering & Bollhöfer, 2017; Jeffree, 1985; Ryan et al., 2008), and fish (Clulow & Pyle, 1997; Hesslein & Slavicek, 1984; Pyle & Clulow, 1998). Concentrations of ^{226}Ra in tissues generally

increase proportionally with increasing ^{226}Ra concentrations in water, which can be elevated in regions where anthropogenic activities such as mining mobilize naturally occurring ^{226}Ra (e.g., Ryan et al., 2008). Following free-ion activity model principles (Campbell et al., 2022), ^{226}Ra uptake is expected to vary with the chemical activity of the free $^{226}Ra^{2+}$ ion, which is influenced by pH, carbonate/bicarbonate concentrations, and complexation with dissolved organic carbon. Uptake of $^{226}Ra^{2+}$ may be further modified by water hardness, particularly through competition with Ca^{2+} and Mg^{2+} at uptake sites (Jeffree, 1991; Jeffree & Simpson, 1984, 1986; Sheppard et al., 2006). In addition, strong sorption of ^{226}Ra to Fe-(hydr)oxides and clay minerals may reduce its dissolved, and bioavailable, fraction, thereby limiting uptake (Ames et al., 1983; Sajih et al., 2014). This bioaccumulation can pose health risks to organisms over time.

Radium-226 decays by emission of alpha particles, producing highly ionizing radiation with short penetration distances (typically 50-100 μm in biological tissue), but extremely high linear energy transfer (LET). Consequently, it can cause localized cellular damage when internalized (Fuller et al., 2015; Kim & Brechbiel, 2012; Ulanovsky, 2016). Such exposure may result in cell and DNA damage, chromosomal aberrations, mutagenesis and carcinogenesis (Desouky et al., 2015). DNA damage occurs primarily through emission of alpha radiation that ionizes cellular water and biomolecules, generating highly reactive free radicals (e.g., hydroxyl radicals) and reactive oxygen species (ROS) that chemically damage DNA, as well as through direct ionization of DNA itself, resulting in strand breaks, mutations, and impaired cellular function (Desouky et al., 2015). In addition to direct DNA damage, radiation exposure may induce genomic instability, impair cellular reproductive capacity, and alter gene expression, including in germ cells, potentially leading to reduced fertility, developmental abnormalities, and heritable genetic effects (Desouky et al., 2015). Despite the well-established mechanisms of cellular and genetic damage caused by internalized radionuclides, the reproductive effects of ^{226}Ra exposure in

aquatic organisms remain poorly characterized, particularly under environmentally relevant exposure conditions.

The limited studies on the effects of ^{226}Ra on freshwater aquatic organisms have included fish species such as mullet *Mugil cephalus* (Antovic & Antovic, 2011) and fathead minnow *Pimephales promelas* (Mothersill et al., 2013, 2014; Shi et al., 2017), as well as invertebrates including the ragworm *Hediste diversicolor* (Grung et al., 2009), the bivalve *Velesunio angasi* (Jeffree & Simpson, 1986), and the snail *Lymnaea stagnalis* (Van der Borght, 1963). These studies primarily focused on quantifying ^{226}Ra accumulation in tissues rather than evaluating chronic toxicity, although reduced growth was observed in *Pimephales promelas* fed diets containing 10 and 100 mBq g^{-1} (Mothersill et al., 2013). More recently, research efforts have increasingly aimed to quantify sublethal and chronic toxicity endpoints in aquatic organisms, with the longer-term objective of generating the ecotoxicological data necessary to support the development of a water quality guideline to protect freshwater species. Reductions in the nonlethal endpoint of growth were also reported for *Chironomus dilutus* following waterborne exposure to 25 Bq L^{-1} (Lacroix-Durand et al., 2024). Survival of *Daphnia magna* (Lacroix-Durand et al., 2025) was similarly affected at nominal concentrations of 50 Bq L^{-1}.

Freshwater bivalves (including unionids and sphaeriids) are threatened by anthropogenic activities (Lopes-Lima et al., 2014). Freshwater bivalves are often among the more sensitive freshwater taxa for some contaminants, including certain major ions and metals, particularly during early life stages and at environmentally relevant exposure concentrations (Ciparis et al., 2015; Elder & Collins, 2000). Their filter-feeding behaviour, and interstitial suspension-feeding for some sphaeriids, can increase exposure by bringing dissolved contaminants and particle-associated contaminants into direct contact with gill tissues where exchange with the circulatory

system occurs (Lopez & Holopainen, 1987; Mackie, 2007; Meier-Brook, 1969). Because sphaeriids brood developing young within structures associated with their inner gills, parental exposure through the gills may also plausibly increase exposure of brooded embryos (Mackie, 2007). In addition, fingernail clams (Bivalvia: Sphaeriidae) possess several traits that make them suitable test species for chronic toxicity studies. They are a diverse group of freshwater bivalves with a widespread distribution throughout North America. They are relatively sessile, such that exposure to contaminants is assured (Proulx et al., 2025b). Fingernail clams have a relatively short lifespan (2-4 years), with sexual maturity reached within the first year of life, are hermaphroditic and ovoviviparous (Mackie, 1979; Bespalaya et al., 2015). They live burrowed in surface sediments (top 5 cm) of both lentic and lotic habitats in a variety of substrates (Mackie, 2007). They are filter feeders, digesting mainly detritus, particulate plant remains, live or dead dissolved organic material, algae, and bacteria (Lopez & Holopainen, 1987; Mackie, 2007), providing various routes of exposure to dissolved and particulate-bound contaminants. Bivalves can ingest contaminants adsorbed onto mineral surfaces (e.g., Fe oxides, clays), resulting in accumulation within shell material (Tan et al., 2023).

Fingernail clams have also been successfully used in laboratory and field studies to assess both acute and sublethal effects of contaminant exposure, including effects on survival, growth, and reproduction (e.g., Hickey & Martin, 1999; Ouedraogo et al., 2025; Proulx et al., 2025b). Shell growth in fingernail clams is easy to measure and provides a sensitive and integrative indicator of contaminant exposure (Kilgour & Mackie, 1990; Proulx et al., 2025b). Growth has been shown to be a more sensitive endpoint than mortality in standard aquatic toxicity test species such as *Daphnia magna*, *Pimephales promelas*, and rainbow trout *Oncorhynchus mykiss* (Mackie, 1979). Reproduction of fingernail clams has been shown to vary in response to environmental conditions, including stream acidification (Servos & Mackie, 1986), metal contamination (Kilgour & Mackie,

1990), and exposure to uranium mining and milling effluent (Proulx et al., 2025b). Sphaeriids may be particularly sensitive to radionuclides, as declines in abundance have been observed downstream of uranium mining and milling operations (Kilgour et al., 2018). Radionuclide concentrations in filter-feeding benthic invertebrates have also been shown to exceed those in predatory taxa in uranium tailings-impacted systems (Swanson, 1982). Bioaccumulation and toxicity modelling further suggests that bivalves may accumulate higher concentrations of ^{226}Ra and experience greater radiological dose relative to other aquatic taxa (Doering et al., 2019).

This study aimed to quantify the bioaccumulation of ^{226}Ra in *Sphaerium striatinum* and to assess its chronic toxicity. Understanding the biological responses of these organisms offers valuable insight into the ecological risks posed by ^{226}Ra in freshwater ecosystems. Fingernail clams are just one of several sensitive aquatic species whose chronic toxicity endpoints will contribute to the development of a species sensitivity distribution curve, which enables derivation of water quality guidelines for government jurisdictions. Such guidelines are critical components of environmental risk assessment models, which are essential for designing mitigation strategies to control radionuclide discharges from mining activities into freshwater environments.

3.2 METHODS

3.2.1 Field Collections of Test Organisms

Fingernail clams were collected from the Ottawa River at Britannia Bay in Ottawa, Ontario, Canada (45.36382° N, -75.80448° W). Fingernail clams were collected in October 2022, when ambient air temperatures were approximately 15 °C and water temperature was 12.8 °C. Top sediments were collected from depositional areas approximately 150 m from shore at 0.5 m water depths. A D-net (Wildco) was gently dragged along 100-meter linear transects parallel to the shoreline. To avoid resampling the same areas, the transects progressively extended farther from

the shore. After each transect, D-net contents were emptied and sorted in the field using a 0.0394 mm sieve (W.S. Tyler). Sieved materials were examined by eye for clams which were transferred with live insect forceps (Model 26029-10, Fine Science Tools) in jars containing Ottawa River water. Approximately 3 hr was needed to collect sufficient organisms, which included species of *Pisidium*, *Sphaerium*, and *Musculium*. Collected individuals were transported to the CanmetMINING laboratory (Natural Resources Canada, Ottawa, ON, Canada) within 1 hr of the end of collection for further processing. Fingernail clams were counted and identified to species the same day (Mackie, 2007). *Sphaerium striatinum* was selected as the test organism because it was the most abundant species and larger in size, which increases the likelihood of detecting ^{226}Ra in tissues. Ottawa River water was collected using a wide mouth 1 L Nalgene High-density polyethylene bottle (Millipore Sigma) for chemical analysis and ten 1 L bottles for the acclimation of test organisms to laboratory conditions.

3.2.2 Fingernail Clam Acclimation

The United States Environmental Protection Agency (USEPA) standard reconstituted soft water (RSW; EPA/600/4-90/027F) was used with slight modifications as per Clesceri (1998) for aquatic culturing and toxicity testing (see supplementary materials, Table S3-1). RSW was chosen as the acclimation and 28-day toxicity test required high volumes of water. Chemical analysis of the Ottawa River water (see supplementary materials, Table S3-2) also indicated comparable hardness (38.4 mg L^{-1}) to EPA standard RSW (48.7 mg L^{-1}). Clams were transitioned from Ottawa River water to RSW using the following procedure. Once identified to species, individuals of *S. striatinum* were transferred into 9 L aquaria made of low-density polyethylene (Aquatic Habitats Inc.), each containing 4 L of media which at first consisted of 50:50 Ottawa River water to RSW. Aquaria media were replaced by introducing a tube at the surface and siphoning using gravity. At 24 hr, clams were transitioned to a ratio of 25:75 Ottawa River water to RSW, and a full

replacement with RSW (0:100) was completed at 48 hr, similar to acclimation protocol of Ouedraogo *et al.* (2025). The aquaria also contained 1000 g of fine aquarium sand (CaribSea inc. Super Naturals Premium Aquarium Substrate, color: Marine Sand/Moonlight Sand, hereafter referred to as sand). Organisms were held in groups of ~150 individuals and aeration was provided to ensure that dissolved oxygen levels remained above 60% of saturation. Organisms were fed daily with 150 mL of an algae mixture, consisting of 1 mL Instant Algae Shellfish Diet 1800, and 100 µL instant Algae Nano Diet 3600 in 9 mL RSW, modified from Salerno et al. (2018). A 16:8h light to dark photoperiod was maintained in the laboratory, along with a constant room temperature of 21°C. No deaths were noted during the acclimation process.

3.2.3 Chronic Toxicity Tests

Chronic toxicity test vessels consisted of 800 mL polypropylene plastic beakers (Brandtech Vitlab), each containing 150 g of sand and 300 mL of test solution. Sand substrates (described above) were rinsed three times with ultrapure water (18 MΩ cm) prior to the test. Beakers were wrapped in black plastic to minimize light penetration, approximating natural benthic environments. Beakers were also loosely covered with Parafilm to reduce evaporation. The experiment consisted of eight ^{226}Ra treatments (control (0), 0.1, 0.5, 1.0, 5.0, 10, 25 and 50 Bq L^{-1}), with 3 replicates per treatment ($n = 24$). Exposure concentrations were selected to reflect natural background levels near uranium mines and mill sites (approximately 0.02 Bq L^{-1}) and elevated concentrations reported in precious metal, base metals, non-ferrous metals, ferrous metals, uranium and diamond mining effluents, which can reach up to 8 Bq L^{-1} in ferrous metal mine effluents for instance (Proulx et al., 2025a). Higher concentrations (≥10 Bq L^{-1}) were incorporated to ensure observable biological effects. Test solutions were prepared by pipetting the appropriate aliquot from a 5 mL stock solution of radium chloride (activity: 8 kBq; Stuart Hunt and Associates Ltd., Edmonton, AB, Canada) into one 2 L volumetric glass flask prefilled to approximately three-

quarters with ultra-pure water (18 MΩ cm). Each flask was then brought to volume (2 L), capped, and mixed by inversion. The solutions were transferred to 10 L carboys and volume completed to ten liters by adding 8 liters of ultra-pure water (18 MΩ cm). For each treatment, two 10 L carboys were prepared to provide sufficient volume for the 28-day experiment.

Day 0 of the experiment was defined as the time at which 17 test organisms were randomly distributed into each treatment beaker. The sample size per beaker was chosen to maximize statistical power given the number of individuals captured in the field and as it was similar to other studies (e.g., Hickey & Martin, 1999; Naimo et al., 2000). Given that this was somewhat higher than natural density, density-related stressors were monitored (e.g., dissolved oxygen, ammonia, food). A similar size distribution of test organisms was ensured among treatments, to narrow confidence intervals around effect endpoints (Ouedraogo et al., 2025). The duration of the test was 28 days and involved static renewal exposure, with solutions being replaced every 48 hr by tilting vessels to allow passive draining, followed by gentle replenishment with fresh room-temperature treatment stock solutions. Clams were fed daily using a repeater pipette (Eppendorf) to dispense 300 µL of the algal mixture described above to each beaker. On renewal days, clams were only fed after water replacements.

3.2.4 Exposure Water Chemistry

Water samples were collected from the 10 L stock solutions (i.e., fresh solutions) on Days 0, 14, and 28 to verify ^{226}Ra activity concentrations at test initiation and to confirm that no loss of ^{226}Ra occurred from the stock solutions over the duration of the experiment. Water samples were also collected from one replicate test beaker per treatment immediately prior to each 48-hr water renewal (i.e., old solutions) to quantify ^{226}Ra remaining in solution at the end of each exposure interval. Three sets of duplicate samples were analyzed to assess analytical precision, and relative percent difference (RPD) was calculated.

Paired fresh (stock solution, $C_{fresh,i}$) and old (48 hr test solution, $C_{old,i}$) samples were available for one to three renewal intervals per treatment. These paired measurements were used to estimate interval-specific exposure activity concentrations for each 48-hr renewal interval (n = 14). Time-weighted average (TWA) concentrations were calculated using the trapezoidal integration method (e.g., Belgers et al., 2011; Organisation for Economic Co-operation and Development, 2002), which assumes a linear change in concentration between successive sampling times:

$$TWA = \frac{\sum_{i=0}^{n-1}\left(\frac{C_i+C_{i+1}}{2}\right)(t_{i+1}-t_i)}{t_n-t_0} \quad \text{(Eq. 1)}$$

where C_i and C_{i+1} are the measured dissolved ^{226}Ra concentrations at sampling times t_i and t_{i+1}, respectively, and t_n-t_0 represents the total exposure duration. In the present study, concentrations were measured only at the start (t_0) and end (t_{48}) of each 48-hr renewal interval; therefore, the trapezoidal method simplifies to the arithmetic mean of the paired measurements:

$$TWA_i = \frac{C_{fresh,i}+C_{old,i}}{2} \quad \text{(Eq. 2)}$$

because each interval has equal duration (48 hr). Interval-specific TWAs were then averaged to estimate overall exposure over the 28-d experiment. Sample volumes collected for each treatment varied to obtain a maximum total activity of between 20 to 30 mBq per sample. Water samples were collected into pre-labelled and pre-weighed polypropylene centrifuge (15 mL or 50 mL, Fisherbrand) or micro-centrifuge (1.5 mL or 2 mL, Fisherbrand) tubes as appropriate. Water samples collected for analysis of dissolved ^{226}Ra were filtered using a 0.45 µm mesh (Acrodisc HT Tuffryn Membrane, PALL New York) and 50 mL syringe (Fisher Scientific). All water samples for analysis of both total and dissolved ^{226}Ra were preserved using 1% trace metal grade HNO_3 (Fisher Chemical, 67 to 70% (HNO3, w/w)). Sample masses were recorded using a Shimadzu AUW120 electronic balance (± 0.006 g) to allow ^{226}Ra activity concentrations to be

expressed on a mass-normalized basis (Bq g^{-1}). Samples were sealed with Parafilm and stored at 4°C until shipment to Canadian Nuclear Laboratories (CNL, Chalk River, ON, Canada) for analysis of ^{226}Ra by alpha spectrometry (detection limit = 0.0005 Bq L^{-1}) using the method outlined in Guérin et al. (2023). Samples underwent radiochemical separation using the $PbSO_4$/EDTA/$BaSO_4$ micro-precipitation procedure and were prepared as thin Ba(Ra)SO_4 sources for alpha-spectrometric counting. Activity concentrations were reported in millibecquerel per gram of sample (mBq g^{-1}) and are presented herein in becquerels per litre (Bq L^{-1}). One becquerel (Bq) represents one radioactive decay per s.

In situ water quality parameters (i.e., water temperature (°C), dissolved oxygen (DO, %), pH, and specific conductivity (µS cm^{-1})) were monitored daily throughout the experiment using Hach meters (Hach HQ40d pH/D.O., and HQ14d conductivity). Total ammonia (ppm) was also measured weekly before water renewals using API Ammonia Test Strips for Freshwater and Saltwater Aquariums. Water samples (15 mL) were collected once per week from a single replicate/treatment for analysis of total and dissolved calcium, chloride, potassium, magnesium, and sodium by the CanmetMINING Analytical Laboratory (Ottawa, ON, Canada) by inductively coupled plasma optical emission spectrometry (ICP-OES, Agilent 5110). Sulfate was measured by ion chromatography (ThermoScientific, Dionex VwD). Total and dissolved organic carbon (TOC, DOC) and total and dissolved inorganic carbon (TIC, DIC) were determined using a total organic carbon analyzer (TOC-L, Shimadzu). Quality assurance/quality control by the CanmetMINING Analytical Laboratory included the collection of duplicates, spikes, and blanks.

3.2.5 Speciation Calculation

Speciation of ^{226}Ra was estimated using the PHREEQC Interactive software (version 3.7.3) with the WATEQ4F thermodynamic database (Ball & Nordstrom, 1991). PHREEQC is a widely used geochemical modelling program for calculating aqueous speciation, reaction-path, and

transport (Parkhurst & Appelo, 1999). Aqueous speciation was calculated for each nominal solution using available thermodynamic reactions for dissolved ^{226}Ra species (see supplementary materials, Table S3-3). Speciation of ^{226}Ra was also estimated using the Windemere Humic Acid Model (WHAM, Version 7.0, Tipping (1994)). Because stability constants for ^{226}Ra complexes with fulvic and humic substances are not available in the WHAM database, stability constants for barium were used as a proxy (log K_Ba–HA = 1.30; log K_Ba–FA = 0.97). This substitution is commonly applied because Ba^{2+} and $^{226}Ra^{2+}$ exhibit similar chemical behaviour as alkaline earth metals, occurring predominantly as divalent cations in aqueous systems, having comparable ionic radii (Ba^{2+} 142 pm; Ra^{2+} 148 pm), and similar electronegativities (Brown et al., 2022), further supporting the use of barium as an analogue in geochemical modelling.

3.2.6 Bioaccumulation

Upon completion of the chronic toxicity test, clams were rinsed with RSW and transferred to clear sterile polystyrene 12-well plates (Fisher Scientific) containing clean RSW for depuration without food overnight. Individuals were then dissected to separate the soft tissues from the shells. From each replicate for each treatment, individuals of a similar size were composited (n = 4 to 9 individuals) to obtain enough tissue mass for analysis. Composite samples were placed into pre-labelled and pre-weighed 15 mL polypropylene centrifuge tubes (Fisherbrand™), and wet weights were recorded using a Shimadzu AUW120 electronic balance (± 0.006 g). Samples were then freeze dried (-50°C, Labconco FreeZone 2.5 L Model# 117) to a constant dry weight which took 2 to 3 days. Pooled soft tissue dry weights ranged from 0.5 to 47.6 mg per composite sample, while pooled shell tissue dry weights ranged from 89.1 to 273.1 mg per composite sample. Soft tissues and shell tissues were covered with 100 µL and 500 µL of trace-metal grade HNO_3 (Fisher Chemical, 67 to 70% (HNO_3, w/w)), respectively, and heated (90°C) in a HotBloc system (Environmental Express) for 60 min. Samples were cooled before adding 75 µL and 375 µL of

H_2O_2 (Fisher Chemical, 30% (H_2O_2)) to the soft tissues and shell tissues, respectively. Samples were once again heated at 90°C for 30 min. Extracts were diluted with ultra-pure water (18 MΩ cm) to achieve 5% HNO_3. Samples were sealed using Parafilm and stored under refrigeration until analysis. Samples selected for analysis of ^{226}Ra were those with anticipated detectable concentrations (i.e., samples from the 1, 5, 25 and 50 Bq L^{-1} treatments, plus a control). Selected samples were shipped to the Canadian Nuclear Laboratories (Chalk River, ON, Canada) for analysis of ^{226}Ra, where activity concentrations were reported in millibecquerel per gram of sample (mBq g^{-1} of liquid sample). Activity concentrations were expressed as Bq g^{-1} dry weight and Bq g^{-1} dry weight per individual, accounting for sample dry weight and the number of individuals in each composite. A bioaccumulation factor (BAF) was calculated based on the ^{226}Ra activity concentration in the tissues (Ra_{ti}) and corresponding water (Ra_{wo}) using Equation 3.

$$BAF = \frac{Ra_{ti}\ (Bq\ kg^{-1})}{Ra_{wo}\ (Bq\ L^{-1})} \quad \text{(Eq. 3)}$$

BAF were computed for each sample and estimated for each individual clam. TWA ^{226}Ra activity concentrations were used as Ra_{wo} to provide representative estimates of waterborne exposure over the duration of the experiment. A certified reference material (CLV-1, 0.7 Bq g^{-1}, CANMET, Ottawa, ON, Canada) consisting of spruce twigs from the Cluff Lake uranium mining area in northern Saskatchewan was digested and analyzed following the same approach as the fingernail clam tissues. The recovery in the certified reference material sample was 80% (n = 1).

3.2.7 Chronic Endpoints

Survival was assessed daily, and clams were considered potentially dead when their shells were gaping and removed from the test beakers for closer inspection. Death was confirmed by either the absence of tissue inside the shell, or by gently prodding the clam's foot and observing no movement or valve closure. On Day 28, clams were removed from the test beakers and placed into well plates with RSW for confirmation of survival. The survival endpoint consisted of the

percentage of live test organisms in each treatment replicate. Burrowing behaviour was assessed before each water renewal, with clams on the surface or more than 75% visible not considered burrowed. Each test beaker contained 150 g of sand, which produced an approximate sediment depth of >2 cm based on visual observation during test setup. Sediment depth was not measured directly; however, the sand layer was sufficient to allow organisms to fully burrow. The percentage of burrowed clams was calculated using Equation 4:

$$Burrowed\ (\%) = \frac{(\#\ Living\ clams) - (\#\ Visible\ clams)}{(\#\ Living\ clams)} x\ 100 \quad \text{(Eq. 4)}$$

During each water renewal, beakers were tilted slightly while pouring out the old treatment media, bringing the test organisms back to the surface and resetting individuals on the sand for reassessment of burrowing behaviour. Burrowing behaviour was assessed as the mean percent of organisms that were burrowed over the 28-day test, reflecting the potential cumulative behavioural stress to exposure. Burrowing behaviour was also assessed as the percent of organisms that were burrowed on Day 28, which represents the final state of behavioural function following chronic exposure and may inform on early indication of potential impairment.

Individual growth was assessed using total shell length (TSL, mm), which was the longest distance between the anterior and posterior margins as measured perpendicularly to the umbo. Test organisms were viewed with an Olympus SZ61 dissecting microscope equipped with an Olympus DP73 camera, and pictures were captured on Day 0 and Day 28 for length assessments. Images were imported into ImagePro (Media Cibernetics), calibrated, and TSL was measured. Clams used in the study had an initial TSL ranging from 2.7 to 10.3 mm (mean ± SD = 6.0 ± 1.5 mm). Finally, reproduction was assessed on a subset of clams (n = 4/replicate for a total of n = 12/treatment) after the completion of the test. The largest individuals were selected for the dissections to ensure the *S. striatinum* were mature. Brood sacs were located, and the number of developing larvae were counted. The reproduction endpoint consisted of brood size at TSL (i.e., relative brood size).

3.2.8 Statistical Analyses

Statistical analyses were performed using the R software environment and associated base packages (R 4.6.1, R Core Team, 2026). A nonparametric Kruskal-Wallis test was used to evaluate differences among treatments in general water chemistry, *in situ* water quality parameters, and organism size (TSL) distribution on Day 0. Differences between old and fresh solutions (i.e., before and after water renewals) and between dissolved and total ^{226}Ra activity concentrations (by treatment and sample type) were evaluated using Welch's two-sample *t*-tests, which do not assume equal variances between groups.

Tissue ^{226}Ra activity concentrations were analyzed using linear models to evaluate relationships with exposure (TWA). Differences in exposure–response relationships between shell and soft tissue were assessed by including an interaction term between TWA and tissue type. Burrowing behaviour over the duration of the experiment was analyzed using a linear mixed-effects model with Treatment, Test Day, and their interaction as fixed effects, and replicate nested within treatment as a random effect.

Analysis of variance (ANOVA) was used to test for differences in growth, survival, burrowing, and reproduction among treatments, with ^{226}Ra treatment group as the fixed categorical predictor variable. For growth and reproduction, measurements on individual clams were treated as independent observations. Hypothesis tests (i.e., post-hoc one-tailed Dunnett's multiple comparison test) were used to determine which treatments were statistically different relative to the control and to determine the no-observed-effect concentration (NOEC) and lowest-observed-effect concentration (LOEC) for each endpoint. In addition, four-parameter log-logistic (LL.4) dose-response models were fit using the DRC package in R. The models included parameters for slope, lower and upper asymptotes, and the median effective concentration (ED_{50}). No parameters were fixed during the model fitting. The drm() function was used to estimate effect concentrations

(e.g., EC_{10}, EC_{20}, EC_{50}) and associated confidence intervals. For all statistical analyses, the level of statistical significance (α) was set at 0.05. Data in tables were presented as mean ± standard deviations (SD), unless otherwise stated.

3.3 RESULTS & DISCUSSION

3.3.1 Supporting Water Quality

Water quality parameters, including pH, chloride, sulfate, carbonates, bicarbonates, and dissolved organic matter, can influence ^{226}Ra speciation (Ames et al., 1983; Beneš et al., 1982; Brown et al., 2022; Langmuir & Riese, 1985). In addition, calcium and magnesium concentrations may influence ^{226}Ra uptake by bivalves through competitive interactions with Ca^{2+} transport pathways (Jeffree, 1985; Jeffree & Simpson, 1986). It is therefore essential to verify that water chemistry remains consistent across treatments. Water quality parameters did not differ significantly among treatments (see supplementary materials, Table S3-4 and S3-5). The mean ± SD *in situ* water quality variables measured across all treatments were as follows: temperature 20 ± 0.5 °C (Kruskal-Wallis, $\chi^2 = 3.4$, $p = 0.849$), pH 7.44 ± 0.2 (Kruskal-Wallis, $\chi^2 = 10.7$, $p = 0.153$), dissolved oxygen 92 ± 8% (Kruskal-Wallis, $\chi^2 = 3.4$, $p = 0.872$), and specific conductivity 188 ± 21 µS cm^{-1} (Kruskal-Wallis, $\chi^2 = 3.2$, $p = 0.862$). Although *in situ* water quality parameters varied between renewals (Welch's t-tests; all $p < 0.01$, see supplementary materials, Table S3-6), all values remained within acceptable ranges for aquatic toxicity testing (e.g., temperature within ±1 °C, pH variation <1 unit, and dissolved oxygen maintained between 60–100% saturation; USEPA, 2016), and were therefore not considered to impose additional stress on test organisms. Ammonia ranged between 0.25 and 0.5 mg L^{-1} across treatments throughout the experiment, remaining below the Canadian Council of Ministers of the Environment (CCME) water quality guideline of 1.54 mg L^{-1} for the protection of aquatic life, based on the pH and temperature conditions of our study.

Water chemistry parameters did not differ significantly among treatments, based on Kruskal-Wallis tests conducted separately for dissolved and total fractions (dissolved: $\chi^2 = 1.7$ to 11.5, $p = 0.119$ to 0.973; total: $\chi^2 = 0.5$ to 13.4, $p = 0.064$ to 0.999, see supplementary materials, Table S3-7). The mean ± SD of measured dissolved water chemistry variables across all treatments were as follows: Ca 7.1 ± 1.0 mg L^{-1}, Cl 2.9 ± 0.9 mg L^{-1}, K 0.9 ± 0.4 mg L^{-1}, Mg 7.2 ± 0.9 mg L^{-1}, Na 25.5 ± 3 mg L^{-1}, SO_4 41.0 ± 7 mg L^{-1}, inorganic carbon 1.9 ± 0.9 mg L^{-1}, and organic carbon 3.4 ± 1.3 mg L^{-1} (see supplementary materials, Table S3-8).

3.3.2 Radium-226 Speciation

Aqueous speciation modelling indicated that ^{226}Ra was dominated by the free divalent cation ($^{226}Ra^{2+}$), which accounted for 83.5% of total dissolved ^{226}Ra under the experimental water chemistry conditions, followed by $RaSO_4$(aq) at 9.0% and $RaHCO_3^+$ at 7.6%, with no $RaOH^+$, $RaCO_3$(aq), or $RaCl^+$ (see supplementary materials, Table S3-9). These relative proportions remained constant across all activity concentrations evaluated (nominal ^{226}Ra: 0.1–50 Bq L^{-1}), reflecting linear scaling of species concentrations with total dissolved ^{226}Ra and confirming that complexation reactions were not ligand-limited within the narrow range of assumed ^{226}Ra toxicity modifying factors such pH, Ca, and inorganic carbon. Few studies have examined interactions between ^{226}Ra and natural organic matter, and available evidence suggests that ^{226}Ra exhibits limited complexation with fulvic and humic substances (Rachkova et al., 2010). Because stability constants for ^{226}Ra with humic substances are not available, barium stability constants were used as a proxy in WHAM 7.0 modelling. Model outputs indicated negligible (< 0.001%) interaction between ^{226}Ra and fulvic or humic acids under the experimental water chemistry conditions. Overall, the predominance of the free ion, together with carbonate and sulfate complexes, and negligible interactions with organic matter is consistent with thermodynamic predictions that

sulfate and carbonate systems largely control ^{226}Ra speciation (Brown et al., 2022; Langmuir & Riese, 1985; Rachkova et al., 2010).

3.3.3 Estimated Exposure Concentrations

Radium-226 activity concentrations were measured, and exposure was estimated in 197 water samples (Table 3.1). Duplicate analyses indicated low to moderate variability in measured ^{226}Ra activity concentrations, with RPD values of 8.6%, 27% and 36%. Comparisons conducted within each treatment and sample type (i.e., fresh vs. old) indicated no significant differences between measured dissolved and total ^{226}Ra activity concentrations (Welch's t-test, $p > 0.05$), with only slight variations between fractions (see supplementary materials, Table S3-10). In fresh solutions (T_0 hr), measured ^{226}Ra activity concentrations were lower than nominal concentrations, particularly in the lower ^{226}Ra treatments (Table 3.1). Measured total and dissolved ^{226}Ra activity concentrations in fresh solutions were generally greater than 70% of nominal values across treatments (mean ± SD = 86 ± 15%), except for the 0.1 Bq L^{-1} treatment (37 ± 11%).

In addition, measured ^{226}Ra activity concentrations in the test media (i.e., old solutions) decreased substantially between water renewals (Table 3.1). The percentages of nominal concentrations for measured total and dissolved ^{226}Ra after 48 hr were on average 9%, with even lower recoveries in the 0.1 Bq L^{-1} treatment (Table 3.1). These findings indicate that renewing test solutions every 48 hr was insufficient to maintain stable ^{226}Ra activity concentrations in test chambers containing a 2:1 water-to-substrate ratio. The rapid loss of ^{226}Ra from solution is attributed to sorption to the sand substrates, particularly to fine kaolinite particles associated with the sand (see Chapter 4). Radium-226 readily adsorbs to clay surfaces (e.g., kaolinite, illite, montmorillonite) and is thereby removed from the aqueous phase (e.g., Ames et al., 1983; Beneš et al., 1985; Reinoso-Maset & Ly, 2016; Robin et al., 2017; Tachi et al., 2001). These interactions

suggest that in natural systems, ^{226}Ra discharged from mine or mill effluents would be expected to associate rapidly with fine-grained materials such as clays. Such sorption processes can limit dissolved ^{226}Ra mobility but also enhance its accumulation in depositional environments where benthic invertebrates reside. For *Sphaerium*, which are filter-feeding bivalves inhabiting the upper sediment layers and filtering interstitial waters, this raises the possibility of secondary exposure through ingestion of ^{226}Ra-bearing particles or sorption of ^{226}Ra onto their feeding and respiratory surfaces. Thus, even when dissolved ^{226}Ra concentrations are low due to strong sorptive losses, sediment-associated ^{226}Ra could represent an important pathway of uptake and potential sublethal toxicity.

Table 3.1 Summary statistics for measured activity concentrations of radium-226 (^{226}Ra) in dosed reconstituted soft water used in the *Sphaerium striatinum* 28-day chronic toxicity test for each nominal treatment.

Nominal Activity Concentration (Bq L^{-1})	Measured Fraction	Measured Activity Concentrations (Bq L^{-1})							
		Fresh Solutions at T_0				Old Solutions at T_{48}			
		N	Mean	SD	Mean % Nominal	N	Mean	SD	Mean % Nominal
Control	Dissolved	1	ND	NA	NA	11	ND	NA	NA
	Total	1	ND	NA	NA	11	ND	NA	NA
0.1	Dissolved	2	0.041	0.017	41.1	10	0.002	0.004	1.6
	Total	2	0.034	0.004	33.9	9	0.005	0.007	4.8
0.5	Dissolved	2	0.417	0.024	83.3	9	0.049	0.017	9.9
	Total	3	0.352	0.029	70.3	9	0.049	0.025	9.8
1	Dissolved	2	0.652	0.136	65.2	10	0.089	0.028	8.9
	Total	3	0.858	0.114	85.8	9	0.075	0.029	7.5
5	Dissolved	2	5.284	1.746	88.1	10	0.464	0.179	9.8
	Total	3	4.096	0.461	96.2	10	0.456	0.173	14.4
10	Dissolved	2	9.534	1.599	105.7	10	0.992	0.465	9.3
	Total	2	9.455	2.212	81.9	12	0.985	0.610	9.1
25	Dissolved	2	22.018	0.388	95.3	11	2.440	0.949	9.9
	Total	2	24.042	1.014	94.6	12	3.588	3.825	9.8
50	Dissolved	2	39.188	6.838	78.4	10	4.729	1.084	9.5
	Total	3	46.361	4.289	92.7	10	4.404	1.606	8.8

Table Notes: Analysis of ^{226}Ra by alpha spectrometry (detection limit = 0.0005 Bq L^{-1}) using the method outlined in Guérin *et al.* (2023). Sample size (*n*), standard deviation (SD), non-detects (ND) and not applicable (NA).

Time-weighted average (TWA) ^{226}Ra activity concentrations calculated using paired fresh and old samples (trapezoidal method) were consistently lower than nominal values, reflecting declines in activity between renewals (Table 3.2). For the total fraction, TWAs for the 28-d exposure were 0.017, 0.203, 0.468, 2.25, 5.30, 12.9, and 25.4 Bq L^{-1} for the 0.1, 0.5, 1, 5, 10, 25, and 50 Bq L^{-1} treatments, respectively. The primary approach for determining effect concentrations for the toxicity endpoints was using the TWA as the exposure concentration. The TWA estimates using total fractions were selected over estimates using dissolved fractions as fingernail clams are filter- and detritus-feeders, and exposure can occur through both dissolved and particulate-associated contaminants (Lopez & Holopainen, 1987; Mackie, 2007). Bivalves may also ingest contaminants associated with suspended particles or mineral phases (e.g., calcium-bearing materials), with subsequent accumulation in soft tissues and shells (Tan et al., 2023). As dissolved and total ^{226}Ra activity concentrations did not differ significantly within individual treatments (Welch's t-test, $p > 0.05$), TWA estimates based on either fraction were effectively equivalent.

Table 3.2 Estimated time-weighted average (TWA) concentrations of radium-226 (^{226}Ra) using paired fresh (T_0) and old (T_{48}) samples collected during the *Sphaerium striatinum* 28-day chronic toxicity test for each nominal treatment.

Nominal Activity Concentration (Bq L^{-1})	Measured Fraction	48 h Intervals (*n*)	TWA (Bq L^{-1}) Estimated from Paired Samples
0.1	Total	2	0.02
	Dissolved	2	0.02
0.5	Total	3	0.20
	Dissolved	2	0.23
1	Total	3	0.47
	Dissolved	2	0.36
5	Total	3	2.25
	Dissolved	2	2.84
10	Total	2	5.30
	Dissolved	2	5.12
25	Total	2	12.9
	Dissolved	1	11.8
50	Total	3	25.4
	Dissolved	2	21.8

Table Notes: Analysis of ^{226}Ra by alpha spectrometry (detection limit = 0.0005 Bq L^{-1}) using the method outlined in Guérin et al. (2023). Sample size (*n*).

As exposure concentrations declined over each renewal interval and to account for the uncertainty in the estimation of biologically relevant exposure, effect concentrations were also derived using nominal and end-of-interval (T_{48}) concentrations, providing a range of exposure estimates that collectively support interpretation of toxicity responses. Assuming exposure based solely on nominal concentrations presumes complete and sustained availability of added ^{226}Ra throughout the exposure period, which may underestimate toxicity if activity concentrations decline over time. Conversely, relying only on dissolved ^{226}Ra measured at 48 hr may overestimate toxicity by neglecting earlier exposure to higher concentrations and particulate-associated fractions. The TWA approach integrates temporal changes in exposure and accounts for both dissolved and particulate fractions and therefore provides a more representative estimate of biologically relevant ^{226}Ra exposure.

Radium-226 activity concentrations in unexposed *S. striatinum* soft tissue and shell were detectable (Table 3.3), even though ^{226}Ra activity concentrations in control (unexposed) waters

were non detectable (< 0.0005 Bq L^{-1}) using alpha spectrometry in all samples (n = 24). Radium-226 accumulated in both soft tissue and shell of *S. striatinum* across all exposure treatments in a concentration-dependent manner, with activity concentrations increasing significantly as a function of ^{226}Ra exposure (TWA, $p < 0.001$, Figure 3.1). The relationship differed between tissue types (interaction term: $p < 0.001$), with shell tissue exhibiting a substantially steeper increase in activity with increasing exposure compared to soft tissue. Comparisons to the control using Dunnett-adjusted contrasts indicated that tissue ^{226}Ra activity concentrations were not significantly different from the control at lower exposure levels (≤ 5 Bq L^{-1}) for either tissue type (all $p > 0.05$, see supplementary materials, Table S3-11). At higher exposure levels, significant increases relative to the control were observed. For shell tissue, concentrations at 25 and 50 Bq L^{-1} were significantly greater than the control ($p < 0.001$), while for soft tissue, a significant increase was observed only at 50 Bq L^{-1} ($p < 0.001$).

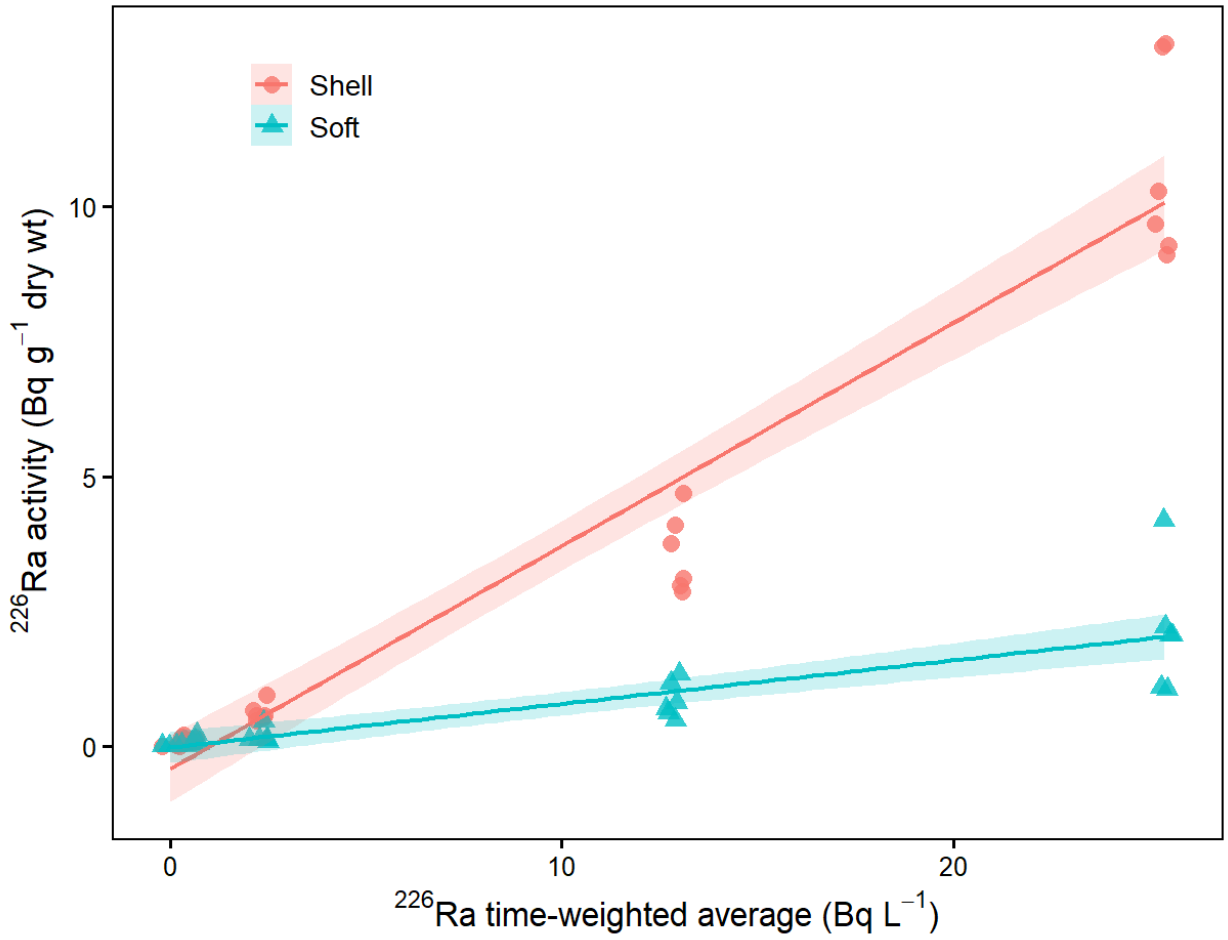


Figure 3.1 Relationship between time-weighted average (TWA) radium-226 (^{226}Ra) activity concentrations in water and tissue activity concentrations in *Sphaerium striatinum* shell and soft tissues following 28-day exposure. Points represent estimates obtained from composite samples (*n* = 6 composites per treatment, each consisting of 4-9 individuals per composite). Lines indicate linear regressions for each tissue type, with shaded bands representing 95% confidence intervals.

Mean soft tissue concentrations in pooled samples ranged from approximately 0.08 to 2.12 Bq g^{-1} dry weight (control = 0.01 Bq g^{-1} dry weight), while shell concentrations were generally higher, ranging between 0.14 to 10.7 Bq g^{-1} dry weight (control = 0.01, Table 3.3). Radium-226 accumulated to a greater extent in shell compared to soft tissues (Figure 3.1). The measured shell ^{226}Ra activity concentrations represent total shell-associated ^{226}Ra and may reflect both passive adsorption to the shell surface and biologically mediated incorporation. The present experimental

design did not allow these processes to be differentiated. The geochemical similarity between Ra^{2+} and Ca^{2+} provides a potential mechanism for biologically mediated incorporation of $^{226}Ra^{2+}$ into the calcium carbonate structure during biomineralization; however, passive adsorption may also have contributed to the comparatively high shell-associated ^{226}Ra activity concentrations.

Shell BAFs ranged from 278 to 419 L kg^{-1} dry weight and were consistently higher than soft tissue BAFs, which ranged from 70 to 180 L kg^{-1} dry weight (Table 3.3). No clear monotonic trend in BAF with increasing exposure concentration was observed; rather, BAFs remained relatively stable across treatments, with a slight increase at the highest exposure in shell tissue. Bioaccumulation factors (BAFs) for *S. striatinum* fall within the range reported for other freshwater invertebrates exposed to aqueous ^{226}Ra and are classified as low according to USEPA benchmarks (<1,000 L kg^{-1}) (USEPA, 1995). Soft tissue BAFs were comparable to those reported for *Daphnia magna* (70 L kg^{-1}, Lacroix-Durand et al. (2025)), while shell BAFs were similar to values reported for *Lymnaea stagnalis* shell and tissues (~376–398 L kg^{-1}; Van der Borght (1963)). Although direct quantitative comparisons among studies should be made cautiously due to differences in species, exposure conditions, and study design, the available literature generally supports accumulation of ^{226}Ra by freshwater molluscs, with both shell adsorption and biological incorporation contributing to shell-associated activity concentrations. For example, recent laboratory studies with freshwater mussels exposed to produced water reported measurable accumulation of ^{226}Ra in both shell and soft tissues and suggested that shell-associated activity during short-term exposures may be dominated by adsorption processes (Pankratz and Warner, 2025), whereas field studies have demonstrated longer-term accumulation of ^{226}Ra in freshwater mussels inhabiting radium-enriched environments (Brenner et al., 2007). Collectively, these studies suggest that freshwater bivalves can accumulate ^{226}Ra to a similar order of magnitude as

observed here, while the overall bioaccumulation potential under aqueous exposure conditions remains relatively low.

Table 3.3 Radium-226 (^{226}Ra) activity concentrations (mean ± standard deviations) in shell and soft tissues and corresponding bioaccumulation factors for *Sphaerium striatinum* following aqueous exposure over 28 days to ^{226}Ra.

Nominal (Bq L^{-1})	TWA (Bq L^{-1})	Composite Samples (*n*)	Activity (Bq g^{-1}, dry weight)	BAF (L kg^{-1}, dry weight)
		Shell Tissue		
Control	ND	3	0.01 ± 0.00	NA
1	0.47	6	0.14 ± 0.05	302 ±103
5	2.25	6	0.63 ± 0.17	278 ± 76
25	12.9	6	3.59 ± 0.72	295 ± 59
50	25.4	6	10.73 ± 1.80	419 ± 70
		Soft Tissue		
Control	ND	3	0.01 ± 0.00	NA
1	0.47	6	0.08 ± 0.08	180 ± 166
5	2.25	6	0.18 ± 0.14	78 ± 62
25	12.9	6	0.85 ± 0.33	70 ± 27
50	25.4	6	2.12 ± 1.13	83 ± 44

Table Notes: Analysis of ^{226}Ra by alpha spectrometry (detection limit = 0.0005 Bq L^{-1}) using the method outlined in Guérin *et al.* (2023). Time-weighted average (TWA), sample size (*n*), bioaccumulation factor (BAF), non-detect (ND), not applicable (NA).

3.3.4 Toxicity Tests

The bioaccumulation data suggest direct uptake and internalisation of ^{226}Ra, which is of radiological concern since it is an alpha emitter with high LET. Mean survival of *S. striatinum* in the control was 98% at the end of the 28-day exposure, meeting the toxicity test acceptability criterion of ≥ 80% control survival (Table 3.4). Survival among treatments ranged from 88 and 100% (mean ± SD: 99 ± 3 %) and did not differ significantly among treatments (ANOVA, $F_{7, 16}$ = 0.633, p = 0.723). Similarly, burrowing behaviour did not differ significantly among treatments when assessed over the 28-day exposure period (ANOVA, $F_{7,16}$ = 1.257, p = 0.33) or at test termination (ANOVA, $F_{7,16}$ = 2.741, p = 0.05). The mean proportion of burrowed individuals over

the 28-day exposure ranged from 76 to 86% (80 ± 11 %), while the proportion burrowed at the end of the test ranged from 47 to 94% (77 ± 12 %). Burrowing behaviour did decline significantly over time (Test Day: $F_{1,142}$ = 14.0, p < 0.001), with a significant Treatment (TWA) × Test Day interaction ($F_{1,142}$ = 4.53, p = 0.035), indicating that temporal trends differed among treatments. The main effect of Treatment was not significant ($F_{1,92}$ = 3.12, p = 0.080), and visual inspection of temporal trends indicated that differences among treatments were not consistently associated with increasing ^{226}Ra exposure concentrations.

The total shell length (TSL) of *S. striatinum* at test initiation (Day 0) ranged from 2.7 to 10.3 mm (mean ± SD: 6.0 ± 1.5 mm, n = 403) across all treatments, with no significant differences among treatment groups (Kruskal-Wallis χ^2 = 3.85, df = 7, p = 0.797). Growth, measured as the change in TSL over the 28-day exposure period, differed significantly among treatments (ANOVA, $F_{7, 395}$ = 13.9, p < 0.001, Figure 3.2). Post-hoc Dunnett's tests indicated that growth at TWA of 12.9 Bq L^{-1} and 25.4 Bq L^{-1} was significantly lower than in the control (p < 0.001), whereas no significant differences were observed at lower concentrations (p = 0.468 to 1.00). Mean growth in the control was 0.37 ± 0.2 mm, compared to 0.16 ± 0.1 mm in treatments exhibiting significant effects, corresponding to a mean reduction of 0.21 mm relative to the control (Table 3.4). Although growth in the 5.3 Bq L^{-1} TWA treatment (0.31 ± 0.2 mm) was slightly reduced, the difference was not statistically significant. Variability among replicates within treatments was generally low to moderate and did not exhibit a consistent pattern across exposure concentrations (see supplementary materials, Figure S3-1).

Dissected individuals ranged from 6.1 to 10.3 mm in TSL (8.0 ± 0.9 mm, n = 96), with no significant difference in size (TSL) of individuals among treatment groups (Kruskal-Wallis χ^2 = 10.2, df = 7, p = 0.176). Brood size ranged from 0 to 8 larvae per individual (mean ± SD: 2.9 ± 1.9

larvae). Brood size varied significantly with both TSL (ANOVA, $F_{1, 80} = 39.05$, $p < 0.001$) and ^{226}Ra treatment (ANOVA, $F_{7,80} = 2.819$, $p = 0.011$), but no significant interaction was observed (ANOVA, $F_{7,80} = 1.54$, $p = 0.166$). Relative brood size (brood size normalized to TSL) also differed significantly among treatments (ANOVA, $F_{7, 88} = 4.92$, $p = 0.0001$, Figure 3.3). Post-hoc Dunnett's tests revealed significant reductions compared to controls at TWA concentrations of 2.3 Bq L^{-1} ($p = 0.006$), 5.2 Bq L^{-1} ($p = 0.001$), 13.8 Bq L^{-1} (p value = 0.006), and 25.4 Bq L^{-1} ($p < 0.001$). Relative brood size was reduced by 0.26, 0.31, 0.25, and 0.32 units, respectively (Table 3.4). Replicate variability within treatments was moderate and inconsistent across exposure levels, with no clear or systematic differences among replicates evident within individual treatments (see supplementary materials, Figure S3-2).

Table 3.4 Mean observations (± standard deviations) for the chronic toxicity endpoints from the 28-day chronic toxicity test of radium-226 (^{226}Ra) to *Sphaerium striatinum*

Time Weighted Average Activity Concentration (Bq L^{-1})	Survival (%)	Burrowing (Mean, %)	Burrowing (Day 28, %)	Growth in TSL (mm)	Brood Size (# larvae)	Relative Brood Size (# larvae/TSL)
Control	98 ± 3	85.9 ± 9.9	90.2 ± 3.4	0.37 ± 0.2	4.3 ± 1.1	0.57 ± 0.13
0.02	100 ± 0	77.9 ± 12.7	60.8 ± 12.2	0.41 ± 0.3	3.8 ± 1.1	0.44 ± 0.10
0.20	98 ± 3	83.5 ± 9.8	80.4 ± 9.0	0.40 ± 0.3	4.2 ± 1.7	0.53 ± 0.18
0.47	98 ± 3	78.4 ± 12.5	82.4 ± 0	0.44 ± 0.3	3.4 ± 2.6	0.42 ± 0.31
2.25	100 ± 0	77.0 ± 10.8	74.5 ± 6.8	0.40 ± 0.2	2.5 ± 2.0	0.31 ± 0.13
5.30	100 ± 0	75.6 ± 7.5	68.6 ± 20.7	0.31 ± 0.2	2.3 ± 1.3	0.26 ± 0.18
12.9	96 ± 7	79.8 ± 12.0	74.5 ± 9.0	0.16 ± 0.1	2.7 ± 1.6	0.32 ± 0.22
25.4	100 ± 0	80.1 ± 9.8	86.3 ± 3.4	0.16 ± 0.1	2.0 ± 1.5	0.25 ± 0.18

Table Notes: Total Shell Length (TSL)

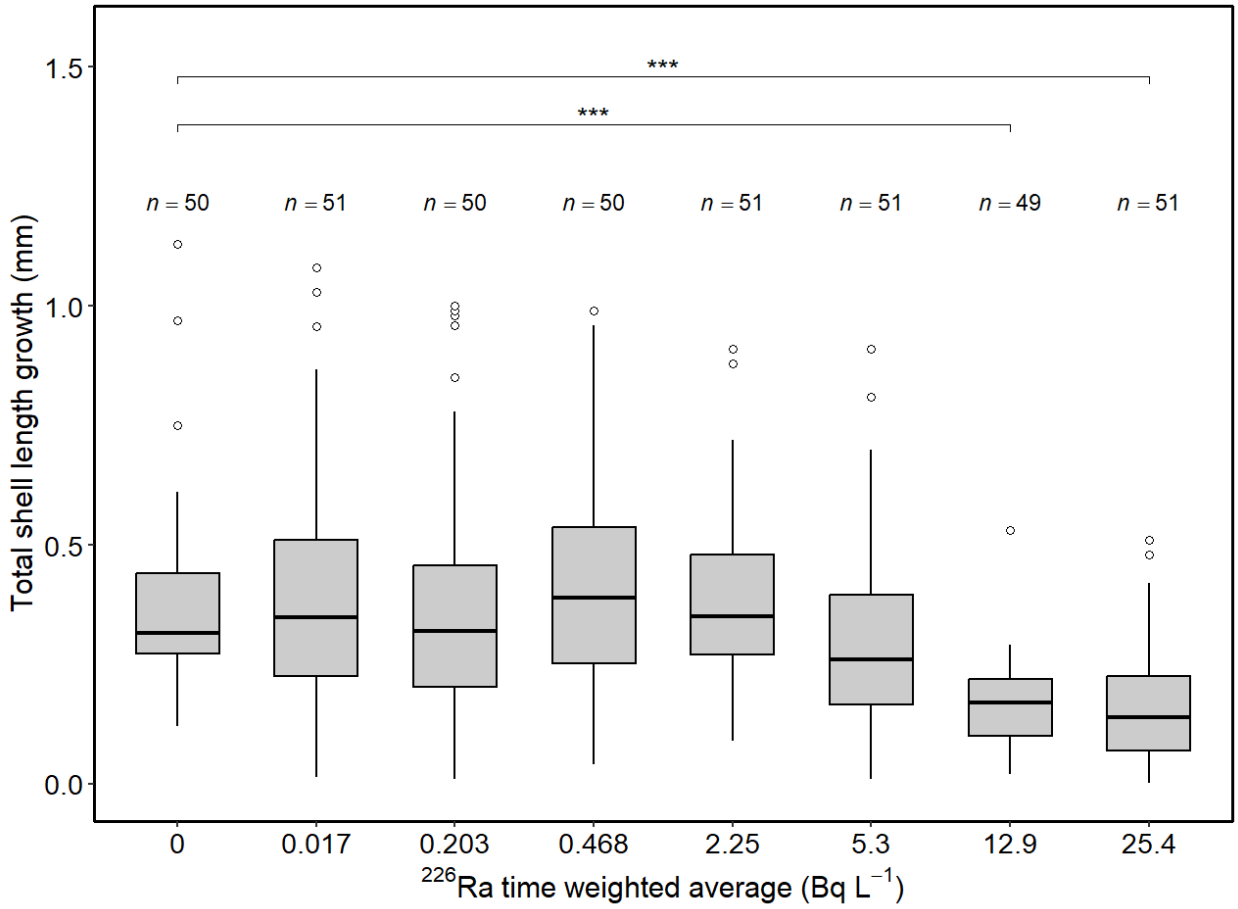


Figure 3.2 Variations in growth, measured as the change in total shell length in *Sphaerium striatinum* individuals after exposure to radium-226 (^{226}Ra) over 28 days. Boxes represent the interquartile range (25th–75th percentiles), with the horizontal line indicating the median. Whiskers extend to 1.5 × the interquartile range, and points represent individual observations. Asterisks indicate treatments significantly different from the control based on Dunnett-adjusted comparisons. Sample sizes ranged from *n* = 49–51 per treatment.

Among all endpoints measured, reproductive output was the most sensitive indicator of ^{226}Ra exposure, followed by growth (Table 3.5). No observable effects occurred on survival or burrowing behaviour of *S. striatinum*, with a no-observed-effect concentration (NOEC) of 25.4 Bq L^{-1} (TWA). For growth, NOEC was estimated to be 5.30 Bq L^{-1}, while the lowest-observed-effect concentration (LOEC) was 12.9 Bq L^{-1}. A 10% reduction in growth (EC_{10}) was estimated at 4.1 Bq L^{-1} (95% CI: -3.7 to 11.9) based TWA concentrations. For reproduction, the NOEC and LOEC

were estimated as 0.468 Bq L^{-1} and 2.25 Bq L^{-1}, respectively. A 10% reduction in reproduction (EC_{10}) was estimated at 0.37 Bq L^{-1} (95% CI: -0.43 to 1.17).

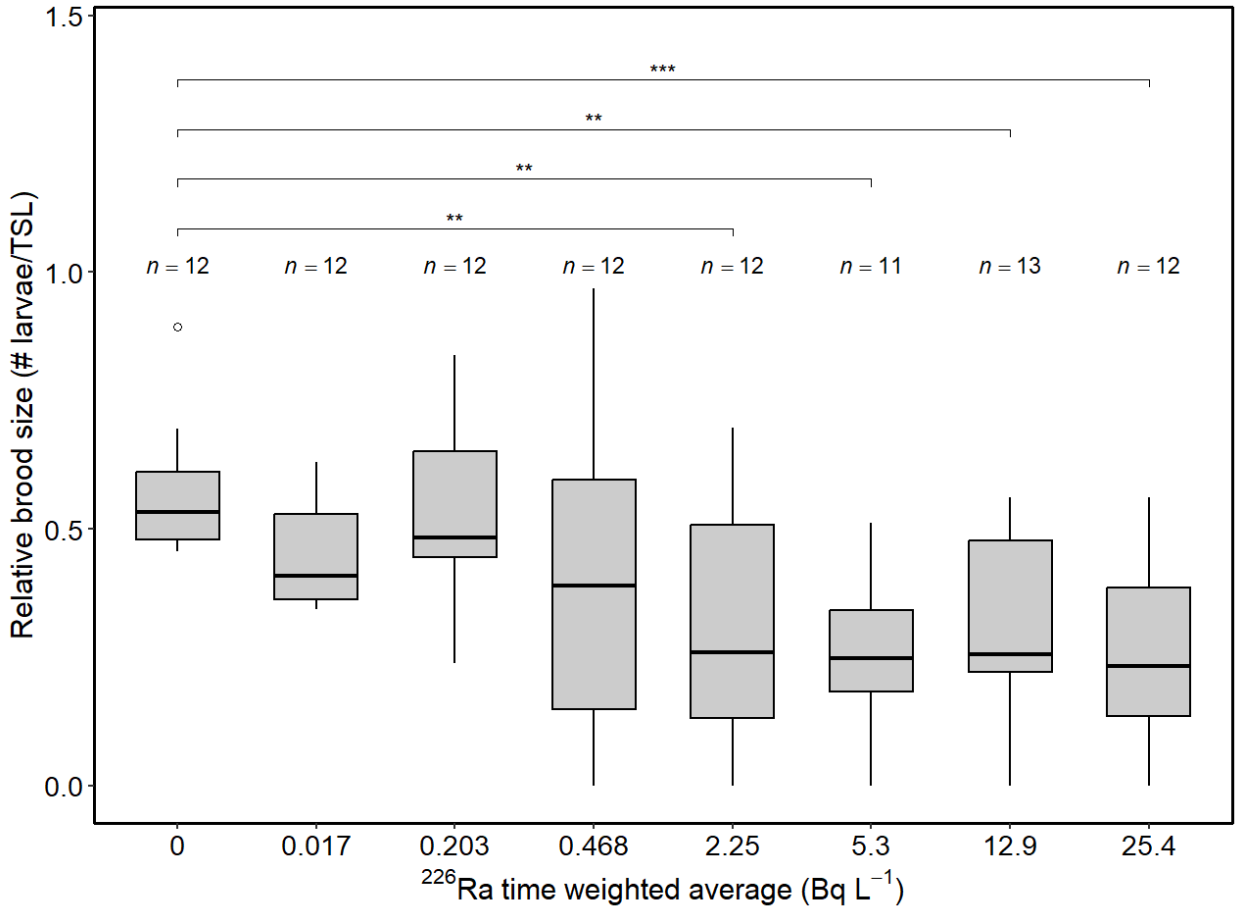


Figure 3.3 Variations in relative brood size, number of larvae as a function of total shell length (TSL), in *Sphaerium striatinum* after exposure to radium-226 (^{226}Ra) over 28 days. Boxes represent the interquartile range (25th–75th percentiles), with the horizontal line indicating the median. Whiskers extend to 1.5 × the interquartile range, and points represent individual observations. Asterisks indicate treatments significantly different from the control based on Dunnett-adjusted comparisons. Sample sizes ranged from *n* = 11–13 per treatment.

Table 3.5 Effect concentrations (Bq L^{-1}) from the 28-day chronic toxicity test of radium-226 (^{226}Ra) to *Sphaerium striatinum*, estimated by hypotheses testing (ANOVA, post-hoc Dunnett's test) and dose-response modelling

Approach	Toxicity Endpoint	Effect Concentration	Time-Weighted Average
Hypothesis Test	Survival	NOEC	25.4
	Burrowing	NOEC	25.4
	Growth	NOEC	5.30
		LOEC	12.9
	Reproduction	NOEC	0.47
		LOEC	2.25
Dose-Response	Growth	EC_{10} (CI)	4.10 (-3.7 to 11.9)
		EC_{20} (CI)	4.64 (0.03 to 9.25)
		EC_{50} (CI)	5.74 (2.14 to 9.34)
	Reproduction	EC_{10} (CI)	0.37 (-0.43 to 1.17)
		EC_{20} (CI)	0.41 (-0.09 to 0.91)
		EC_{50} (CI)	0.49 (0.24 to 0.75)

Table Notes: No Observed Effect Concentration (NOEC), Lowest Effect Concentration (LOEC), Effect Concentration affect *x*% of individuals (EC_x) with confidence intervals (CI)

Log-logistic models provided an adequate fit to both growth and reproduction data, with significant lower and upper asymptotes and ED50 estimates (Table 3.6). However, the slope parameter was not significant for either endpoint, indicating uncertainty in the steepness of the dose–response relationship. As a result, confidence intervals associated with EC estimates for both growth and reproduction were relatively wide, and in some cases included zero (e.g., EC_{10} growth), indicating uncertainty in the precise effect thresholds. Effect concentrations for the three different approaches (i.e., nominal, TWA, measured T48) are reported in the supplementary materials Table S3-12 for comparison and completeness. Across all methods for assessing effect concentrations, while absolute effect concentrations differed as expected, overall patterns in toxicity and treatment ranking were consistent. This indicates that study conclusions are robust to uncertainty in exposure estimation.

Table 3.6 Parameter estimates for dose–response models fit to growth and reproduction data from the 28-day chronic toxicity test of radium-226 (^{226}Ra) to *Sphaerium striatinum*

Toxicity Endpoint	Parameter	Estimate	SE	*p*-value
Growth	Slope	6.53	24.8	0.790
	Lower	0.16	0.02	**< 0.001**
	Upper	0.40	0.01	**< 0.001**
	ED_{50}	5.74	1.83	**0.002**
Relative Brood Size	Slope	7.68	35.1	0.827
	Lower	0.28	0.03	**< 0.001**
	Upper	0.51	0.03	**< 0.001**
	ED_{50}	0.49	0.13	**< 0.001**

Table Notes: Values in bold indicate statistically significant differences at $\alpha = 0.05$. Standard error (SE), median effective dose (ED50)

3.3.5 Evaluation of Species Sensitivity

Comparable responses to those observed for *S. striatinum* growth and reproduction have been reported in other freshwater taxa exposed to ^{226}Ra. For example, *Chironomus dilutus* exhibited reduced growth at 25 Bq L^{-1} (Lacroix-Durand et al., 2024), and survival of *Daphnia magna* was reduced at nominal concentrations of 50 Bq L^{-1} (Lacroix-Durand et al., 2025). In addition, growth of fathead minnow was impacted following dietary exposure to 10 and 100 mBq g^{-1} diet (Mothersill et al., 2013). The sensitivity of *S. striatinum* to somatic endpoints in the low-Bq L^{-1} range is therefore consistent with values reported for other freshwater taxa, whereas its reproductive sensitivity appears greater, highlighting the ecological relevance of these concentrations.

Freshwater bivalves are widely recognized as among the most sensitive aquatic taxa in contaminant toxicity and radiological risk assessment. For instance, Doering et al. (2019) derived a freshwater radiological guideline value of 14 mBq L^{-1} for ^{226}Ra based on mollusc-bivalves, which were identified as the limiting organism for ecosystem protection. Similarly, incorporation of freshwater mussel toxicity data into regulatory datasets has resulted in substantially lower water

quality criteria for contaminants such as ammonia and copper, reflecting their high sensitivity relative to other aquatic organisms (Augspurger et al., 2003; March et al., 2007). Mussel-based guideline estimates for ammonia were 20–75% lower than existing EPA criteria, indicating that existing criteria may not adequately protect sensitive bivalve species (Augspurger et al., 2003). In copper guideline derivation, freshwater mussels represented 10 of the 15 most sensitive taxa, including the most sensitive species, highlighting their critical role in defining protective thresholds (March et al., 2007). Experimental studies have also demonstrated that freshwater mussels exhibit high sensitivity to metals and major ions, particularly when growth or reproductive endpoints are considered (Bringolf et al., 2022). This sensitivity has been linked to impaired ion regulation, reduced growth and filtrate rates, and altered reproductive performance under contaminant stress (Augspurger et al., 2003; Bringolf et al., 2022). Independently of any specific cause, freshwater bivalves are experiencing global declines worldwide (Lopes-Lima et al., 2014).

Physiological and life-history characteristics of bivalves promote efficient uptake and internal exposure to contaminants. As sediment-dwelling organisms, bivalves are exposed to both waterborne and sediment-bound contaminants. As filter- and suspension feeders, they continuously process large volumes of water across their gills, increasing the likelihood of contact with these contaminants of their epithelial surfaces that serve as the primary interface for exchange with the circulatory system (Lopez & Holopainen, 1987; Mackie, 2007). Direct uptake across gill tissues facilitates the absorption of dissolved contaminants, including metal ions and radionuclides, which can then be transported systemically and accumulate in soft tissues and shell (Brenner et al., 2007; Ellis & Jeffree, 1982; Jeffree & Simpson, 1984; Pyle & Clulow, 1998). Because $^{226}Ra^{2+}$ behaves as a Ca^{2+} analogue, it can be taken up via calcium transport pathways and incorporated into calcified structures, contributing to internal accumulation and prolonged biological retention (Brown et al., 2022; Jeffree, 1985; Jeffree & Simpson, 1986; Langmuir & Riese, 1985). In addition,

sphaeriids brood developing young within specialized structures associated with their inner gills, creating a direct pathway for transfer of contaminants taken up across the adult gills to developing embryos (Mackie, 2007; Meier-Brook, 1969). This brooding strategy increases the potential for reproductive effects at exposure concentrations that may not produce overt toxicity in adults. Brood size in sphaeriid clams is dynamic and sensitive to environmental stressors, and substantial brood reductions during gestation have been documented in *S. striatinum* (Beekey & Karlson, 2004). Further, because embryos develop within brood sacs associated with the inner gills, maternal physiological stress can directly affect embryo survival and brood retention (Mackie, 2007). Similar mechanisms have been observed in other brooding freshwater bivalves, where stressors such as hypoxia or elevated temperature can trigger brood evacuation or embryo loss (Aldridge & McIvor, 2003). These physiological and reproductive characteristics provide a mechanistic basis for reduced brood size observed under contaminant exposure.

In natural systems, an upper tolerance limit for background ^{226}Ra activity concentrations was estimated to be approximately 21.7 mBq L^{-1} (Proulx et al., 2025a), while concentrations in effluent-receiving environments in northern Saskatchewan range from 5.0 to 1450 mBq L^{-1} (Fesenko et al., 2014). The present results indicate that both somatic and reproductive impairment in *S. striatinum* could occur at or near environmentally realistic activity concentrations, particularly in depositional zones where ^{226}Ra may become enriched through sediment sorption. Together, continuous filtration, efficient uptake across gill epithelia, accumulation of calcium-analogous contaminants, and adult transfer to brooded offspring contribute to the relatively high sensitivity of these freshwater bivalves and support their importance as indicator taxa in contaminant toxicity and radiological risk assessments. Given the ecological importance of fingernail clams as sediment bioturbators and as prey for higher trophic levels (Mackie, 2007), reductions in growth and reproduction could have cascading effects on benthic ecosystem function

and energy transfer. These findings further support the importance of including freshwater bivalves in species sensitivity distributions used for water quality and radiological guideline derivation, as their sensitivity and ecological role make them critical indicator taxa for ecosystem protection (Proulx et al., 2025b).

3.3.6 Uncertainties and Future Research

Quantifying true ^{226}Ra exposure to fingernail clams in this study was challenging. Radium-226 adsorption over a range of physical and chemical parameters is relatively well studied for common rock-forming minerals and laboratory experiments have demonstrated that ^{226}Ra adsorption to quartz and kaolinite for example is very rapid, with the majority of the $^{226}Ra^{2+}$ being adsorbed within 10 min (Beneš et al., 1984). Although initial measured activity concentrations in prepared stock solutions were generally close to nominal values, activity declined by approximately 90% within 48 hr, likely due to rapid sorptive losses from the water column, consistent with the known affinity of ^{226}Ra for mineral phases (Beneš et al., 1985). As a result, maintaining stable dissolved concentrations through very frequent renewals was not feasible. Renewing 300 mL per triplicate over 28 days would have required more than 3,600 L of stock solution per treatment and increased total activity from 1 to 330 kBq (~300 fold), necessitating 40 vials containing 8kBq of RaCl. The preparation, handling, storage, and disposal of this volume of radioactive solution would have exceeded practical constraints, including cost, nuclear substance storage permit limits, and transport regulations. Renewal frequency was therefore selected to balance exposure stability with radiological safety and regulatory compliance. Future studies could quantify ^{226}Ra activity in water, substrate, and diet and specifically evaluate the relative contributions of these exposure pathways to ^{226}Ra bioaccumulation and toxicity.

Another source of uncertainty is the relative importance of the different exposure pathways and their associated uptake kinetics. Freshwater clams may be exposed to contaminants directly from the water column through filtration, from interstitial (pore) water within the sediment, and through the incidental ingestion of particulate material during filter feeding (Goulet et al. 2007). Toxicity responses may also depend on uptake kinetics (Worms and Wilkinson 2007). Quantifying the relative contribution and kinetics of these pathways would require a complex experimental design and would still involve substantial uncertainties, particularly with respect to sediment-associated exposure. Characterizing sediment-associated exposure would require consideration of several operationally defined fractions. Total ^{226}Ra concentrations in sediment could provide a conservative upper-bound estimate of sediment-associated exposure, although only a fraction of the measured ^{226}Ra may be bioavailable. The potentially bioavailable fraction could be further assessed using leaching or extraction procedures, although this would require careful selection of an appropriate extraction method. Exposure through interstitial (pore) water could also be evaluated by measuring dissolved ^{226}Ra concentrations. Direct measurement of ^{226}Ra in pore water using in situ dialysis was not feasible in the present study because of the limited thickness of the sediment layer. Alternatively, pore water could be separated by centrifugation; however, this approach may also recover colloidal or particulate-associated ^{226}Ra and therefore may not accurately represent the dissolved fraction.

A more robust assessment of these exposure pathways would require controlled laboratory experiments in which clams are exposed separately to (1) ^{226}Ra in water only, (2) sediment-associated ^{226}Ra only, (3) algae previously exposed to ^{226}Ra, and (4) combinations of these exposure scenarios. Such experiments would allow the relative contribution of each exposure pathway to be evaluated. Additional studies examining ^{226}Ra uptake and depuration kinetics for each pathway would help determine whether toxicity responses are influenced by the rate of

internal exposure and the capacity of bivalves to regulate or eliminate accumulated ^{226}Ra. Together, these studies would improve the interpretation of laboratory toxicity tests and help refine environmental risk assessments for radionuclides under varying environmental conditions.

Estimates of ^{226}Ra accumulation in organisms may also be influenced by the duration of the post-exposure depuration period, which is intended to allow clearance of contaminated gut contents prior to analysis. Donaher et al. (2023) reported that marine mussels rapidly eliminated aqueous ^{226}Ra when transferred to ^{226}Ra-free synthetic seawater, with an average elimination rate constant of 1.56 d^{-1}. The biological half-life of aqueous ^{226}Ra ranged from 8.9 h in the gills and labial palps to 15.4 h in muscle tissue. Consequently, the 24-h depuration period used in the present study to allow clams to purge gut contents and minimize the contribution of ingested material to measured tissue ^{226}Ra concentrations may have been insufficient to achieve complete elimination of recently accumulated ^{226}Ra. However, a 24-h depuration period is consistent with previous studies on fingernail clams (e.g., Heinonen et al., 1997), which reported that approximately 94% of ingested material was expelled within the first day of holding in clean water. Furthermore, clams were individually maintained in approximately 2 mL of clean reconstituted soft water (RSW) during the overnight depuration period. While this procedure was intended to minimize the contribution of gut contents to measured ^{226}Ra concentrations, the relatively small water volume may have allowed some reuptake of ^{226}Ra released by the organisms during depuration. As a result, measured tissue concentrations may represent a combination of retained body burdens and limited recycling of ^{226}Ra within the depuration system.

The organism-to-water ratio used in an experimental study can contribute to physiological stress that may confound treatment-related responses. The ratio used in this study (17 clams in 300 mL; ~ 18 mL per clam) is toward the lower end of ratios reported in previous sphaeriid toxicity

studies, where water volumes typically range from approximately 25 to 135 mL per organism (e.g., Heinonen et al., 1997, 2001; Hickey & Martin, 1999; Mackie, 1989; Naimo et al., 2000), with reported values as low as 10 mL (Fong et al., 1998) and 4 mL (Phillips & Hickey, 2010) per organism. The organism to water ratio selected here was intended to maximize the likelihood of determining effect concentrations while ensuring sufficient surviving individuals for measurement of ^{226}Ra activity in tissues. Despite the relatively high organism count, no evidence of density-dependent effects was observed: control survival remained high, no abnormal behaviour or stress-related mortality occurred, and dissolved oxygen and ammonia levels remained within acceptable limits throughout the test. These observations suggest that the test conditions did not impose additional physiological stress that could confound treatment responses. When expressed as a bottom-area density, the experimental setup corresponded to approximately 2,000 individuals per m^2, which falls within the range of natural sphaeriid densities reported in Brittania Bay of the Ottawa River. For example, Kilgour and Mackie (1988) reported mean densities of approximately 4,750 individuals per m^2 for all sphaeriids and 195 individuals per m^2 for *S. striatinum* specifically at 0.5 m depth in Brittania Bay. Given the high survival observed and the sensitivity of ^{226}Ra measurements in clam tissues, future studies could consider using organism densities closer to reported natural densities of *S. striatinum*, while still ensuring sufficient biomass for radiochemical analyses.

Sphaerium striatinum was selected for this study in part because individuals are larger than those of the closely related genus *Pisidium*, which facilitated counting brood larvae and obtaining sufficient tissue mass for reliable measurement of ^{226}Ra activity concentrations. In this study, between four and nine individuals were pooled per sample to quantify ^{226}Ra activity concentrations in soft tissues and shells. However, based on the measured ^{226}Ra activity in pooled clam samples (0.08–10.7 Bq g^{-1} dry weight), individual organism-level quantification appears feasible with a

MDL of 0.0005 Bq L^{-1} for exposures ≥0.02 Bq L^{-1}, suggesting that pooling may not be necessary in future studies conducted at similar or higher exposure concentrations. The larger body size of *Sphaerium* also simplified handling and dissection of soft tissues and shells during sample processing. However, fingernail clams of the genus *Pisidium* are common components of benthic communities; for example, in the Ottawa River nine *Pisidium* species have been reported from Britannia Bay (Kilgour & Mackie, 1988). Although smaller in size, brood size and reproductive output can be assessed in *Pisidium* (Proulx et al., 2025b). Future studies should therefore consider evaluating the effects of ^{226}Ra exposure in *Pisidium* species to determine whether responses are consistent across sphaeriid taxa. This may be particularly important given that *S. striatinum* appears to be the most sensitive freshwater taxa in ^{226}Ra ecotoxicological studies.

Water chemistry, particularly pH and calcium concentration, may also influence both the bioaccumulation and toxicity of ^{226}Ra in freshwater bivalves. Radium-226 behaves as an alkaline earth element and can compete with Ca^{2+} for uptake pathways and incorporation into calcium-bearing structures such as shells (Jeffree, 1988; Jeffree & Simpson, 1984). Consequently, higher calcium concentrations in surrounding waters are expected to reduce the bioaccumulation of ^{226}Ra, while lower calcium conditions may enhance uptake and internal exposure. Because growth and reproduction in sphaeriid bivalves are closely linked to calcium availability and shell formation (Mackie & Flippance, 1983), variation in calcium concentration and pH could also modify the biological response to ^{226}Ra exposure. The bioaccumulation of ^{226}Ra has been reported to be negatively associated with Ca^{2+} concentrations in surrounding waters (Jeffree & Simpson, 1986), suggesting that water hardness may play an important role in modulating internal ^{226}Ra burdens. In addition to influencing total uptake, the rate of metal uptake may also affect toxicity if internal detoxification mechanisms are exceeded. For example, studies of field-collected bivalves have shown that metals such as Cd can occur in both low- and high-molecular-weight protein fractions,

indicating incomplete sequestration by detoxification pathways (Giguère et al., 2003). Future research should therefore examine the influence of pH and calcium across a broader range of water chemistries to better understand how these factors affect ^{226}Ra uptake, growth, and reproductive endpoints in sphaeriid bivalves. In addition, studies examining the kinetics of ^{226}Ra uptake and depuration would help determine whether toxicity responses are influenced by the rate of internal exposure and the capacity of bivalves to regulate or detoxify accumulated radionuclides. Such work would improve interpretation of laboratory toxicity tests and help refine environmental risk assessments for radionuclides under varying natural water conditions.

3.4 CONCLUSION

This study provides the first ^{226}Ra chronic toxicity dataset for fingernail clams, freshwater bivalves widely distributed across Canada. *Sphaerium striatinum* was exposed up to 50 Bq L^{-1} ^{226}Ra for 28 days. Effect concentrations (EC_{10}) were estimated at 4.1 and 0.37 Bq L^{-1} for growth and reproduction, respectively, based on time-weighted average exposure concentrations. Radium-226 accumulated in both soft tissue and shell of *S. striatinum* across all exposure treatments in a concentration-dependent manner. These results indicated that *S. striatinum* exhibits moderate sensitivity to chronic ^{226}Ra exposure, comparable to or slightly more sensitive than standard aquatic test species such as *Chironomus dilutus* and *Daphnia magna* reported in other studies. The relatively low effect concentrations for reproduction suggest that this endpoint is the most sensitive indicator of sublethal stress in these bivalves.

Overall, the findings suggest that direct waterborne exposure to ^{226}Ra at environmentally relevant concentrations poses limited acute risk to freshwater bivalves, and that potential ecological effects are more likely to arise from longer-term bioaccumulation or sediment-mediated exposure pathways. These results provide valuable data for environmental risk assessments of

^{226}Ra in effluent-affected systems, particularly in mining regions where ^{226}Ra can be co-released with other divalent metals. Given the chemical similarity between Ca^{2+} and $^{226}Ra^{2+}$, future studies should examine how varying calcium concentrations influence the chronic toxicity and bioavailability of ^{226}Ra, to better predict effects under different water chemistries typical of Canadian freshwater systems.

4 CHAPTER 4: MINERAL-DEPENDENT AND CALCIUM-INHIBITED ADSORPTION OF RADIUM-226 ONTO QUARTZ AND KAOLINITE IN A NATURAL SAND SUBSTRATE

Proulx C.L.[ab], Cadieux C.[c], Knaack D.R.[c], Fortin D.[a], and R.R. Goulet[ac]

[a] Department of Earth and Environmental Sciences, University of Ottawa, 150 Louis-Pasteur Private, Ottawa, ON, K1N 6N5, Canada

[b] Kilgour & Associates Ltd., 2285 St. Laurent Blvd, Ottawa, ON, K1G 4Z6, Canada

[c] Canmet-MINING, Natural Resources Canada, 555 Booth St., Ottawa, ON, K1A 0G1, Canada

*Corresponding Author: Catherine L. Proulx

STATEMENT OF CONTRIBUTIONS

Proulx, C.L.: Conceptualization, Methodology, Formal Analysis, Investigation, Writing – Original Draft, Visualization

Cadieux, C.: Methodology, Investigation, Writing - Review & Editing

Knaack, D.R.: Methodology, Investigation, Writing - Review & Editing

Fortin, D.: Writing - Review & Editing, Supervision, Funding acquisition

Goulet, R.R.: Conceptualization, Methodology, Resources, Writing - Review & Editing, Supervision, Funding acquisition

Frontiers in Environmental Chemistry published this chapter:

Proulx, C.L., Cadieux, C., Knaack, D.R., Fortin, D.D. and R.R. Goulet. 2026. Mineral-dependent and calcium-inhibited adsorption of radium-226 onto quartz and kaolinite in a natural sand substrate, *Frontiers in Environmental Chemistry*, Volume 7. https://doi.org/10.3389/fenvc.2026.1912040.

ABSTRACT

The availability of radium-226 (^{226}Ra) to aquatic organisms is governed by its aqueous speciation and sorption to mineral substrates. This study evaluated the influence of mineral phases, calcium (Ca) concentration, and organic matter content on the partitioning of ^{226}Ra over 48 hours. Tests were conducted across three nominal ^{226}Ra activity concentrations (1, 5, and 50 Bq L^{-1}) and four Ca levels (0.9, 7, 35, and 70 mg L^{-1}) representative of freshwater systems both affected and unaffected by metal-mining effluent. Under solution-only conditions, dissolved ^{226}Ra remained stable, indicating that Ca concentration alone did not influence ^{226}Ra solubility. The addition of natural sand resulted in rapid removal of dissolved ^{226}Ra from solution, reaching up to 86% after 48 h depending on ^{226}Ra and Ca concentrations. Overall, removal decreased significantly with increasing Ca concentration, suggesting that Ca^{2+} reduced $^{226}Ra^{2+}$ adsorption, consistent with competition between $^{226}Ra^{2+}$ and Ca^{2+} for sorption sites. The presence of organic matter in the form of algal cells produced a small but consistent additional removal of ^{226}Ra (~6%), indicating that interactions between ^{226}Ra and organic matter were limited relative to mineral processes. Mineral-specific experiments demonstrated that ^{226}Ra sorption was strongly mineral-dependent, with extensive sorption onto kaolinite (96 ± 2% within 6h; K_d = 49–62 L kg^{-1}) and minimal sorption onto quartz (10 ± 9% at 48 h, K_d = 0–0.55 L kg^{-1}). These findings demonstrate that ^{226}Ra partitioning in sandy aquatic environments is governed primarily by the presence of reactive clay minerals rather than quartz or organic matter, and by aqueous Ca concentration. Under the controlled laboratory conditions of this study, these findings provide insight into the factors governing ^{226}Ra mobility and bioavailability in sandy sediments where clay content and water chemistry strongly influence the fate of ^{226}Ra.

4.1 INTRODUCTION

Radium-226 (^{226}Ra) is a decay product of the uranium-238 (^{238}U) series and is a radionuclide of environmental concern due to its long half-life (1600 years), high specific activity (3.7×10^{10} Bq g^{-1}), and potential for accumulation in aquatic food chains because of its chemical similarity to Ca^{2+}, an essential element for aquatic organisms (Jeffree, 1988; Jeffree and Simpson, 1986, 1984).

Mining activities can mobilize ^{226}Ra by exposing excavated rock containing ^{238}U or through milling of ore, which produces tailings containing U-series radionuclides. The leaching of ^{226}Ra from mine tailings therefore represents an important pathway for the release of ^{226}Ra to aquatic environments (Chellam and Clifford, 2002; Martin et al., 2003). Radium-226 may also be discharged in treated mining effluents not only from uranium mining and milling operations but from any mining activities involving ore bodies containing ^{238}U (Proulx et al., 2025a). Activity concentrations in mining effluent can reach up to 6940 mBq L^{-1} or 188 pg L^{-1} (Proulx et al., 2025a).

In natural surface waters, ^{226}Ra occurs primarily as a divalent cation ($^{226}Ra^{2+}$) at background activity concentrations ranging between 0.5 and 20 mBq L^{-1} (Fesenko et al., 2014). Its aqueous speciation influences mobility, solubility, and potential availability to aquatic organisms. While $^{226}Ra^{2+}$ may form aqueous complexes with ligands such as nitrate, chloride, and iodate under appropriate chemical conditions (Ames et al., 1983), its behaviour in freshwater is also strongly influenced by co-precipitation with sulfate and carbonate minerals, particularly barite ($BaSO_4(s)$) owing to the close similarity in ionic radius and charge between $^{226}Ra^{2+}$ and Ba^{2+}(Langmuir and Riese, 1985; Zhang et al., 2014).

In addition to aqueous speciation and mineral precipitation, sorption is a dominant process controlling the environmental fate of dissolved ^{226}Ra (Langmuir and Riese, 1985). Sorption refers

to the interaction of an element with the surface of a solid, including suspended particles and bottom sediments (Beneš et al., 1984; Beneš and Strejc, 1986; Landa and Reid, 1983), and encompasses both surface adsorption and absorption into porous solids, while desorption refers to the reverse process (Riese, 1982). Radium-226 adsorption over a range of physical and chemical parameters is relatively well studied for common rock-forming minerals including quartz (Beneš et al., 1984), muscovite and albite (Beneš and Strejc, 1986) and clay minerals such as kaolinite, montmorillonite, bentonite and smectite (Beneš et al., 1985; Reinoso-Maset and Ly, 2016; Robin et al., 2017; Tachi et al., 2001). Laboratory experiments have demonstrated that ^{226}Ra adsorption to quartz and kaolinite is very rapid, with the majority of the Ra^{2+} being adsorbed within 10 minutes (Beneš et al., 1984). Adsorption affinity differs substantially among mineral groups and is strongly influenced by mineral composition and cation-exchange capacity (CEC), with clay minerals generally exhibiting a greater affinity for ^{226}Ra than quartz and other silicates (Ames et al., 1983; Beneš and Strejc, 1986; Robin et al., 2017). Because of its large ionic radius, the interaction of ^{226}Ra with mineral surfaces is expected to be increasingly electrostatic or ionic relative to lighter alkaline earth metals (Langmuir and Riese, 1985). This conceptual understanding provides the mechanistic basis for representing ^{226}Ra partitioning between aqueous and solid phases using cation-exchange and surface complexation models (Riese, 1982).

Beyond quartz and aluminosilicate minerals, Fe-(hydr)oxide phases including both poorly crystalline (amorphous) and crystalline minerals are also important sorbents for dissolved ^{226}Ra (Chellam and Clifford, 2002; Nirdosh et al., 1990; Thiry and Van Hees, 2008). Laboratory experiments have demonstrated that ^{226}Ra adsorption to Fe-(hydr)oxide is rapid, with most Ra^{2+} removed from solution within 10 minutes (Beneš et al., 1984). Iron (hydr)oxides commonly occur in freshwater environments as surface coatings on mineral particles and can play an important role in controlling ^{226}Ra mobility even at low concentrations through electrostatic outer-sphere

complexation with surface hydroxyl groups (Beneš et al., 1984; Chautard et al., 2020). Experimental studies of ^{226}Ra sorption to Fe (hydr)oxides have focused primarily on minerals such as goethite and ferrihydrite (Ames et al., 1983; Sajih et al., 2014), as well as Fe-(hydr)oxide (Beneš et al., 1984). Consistent with these findings, Liu and Hendry (2011) reported that ^{226}Ra associated with precipitates formed during neutralization of uranium mill raffinate was dominated by sorption to amorphous and crystalline Fe-(hydr)oxide phases.

The extent of ^{226}Ra sorption depends not only on mineralogy but also on surrounding water chemistry. Radium-226 adsorption to quartz, kaolinite, Fe- and Mn-(hyr)oxides increases with increasing pH (Nirdosh et al., 1990; Robin et al., 2017; Thiry and Van Hees, 2008) and with decreasing liquid-to-solid ratio (Beneš et al., 1984). The presence of other cations (e.g., Ca^{2+}, Ba^{2+}, Mn^{2+}) can also influence Ra^{2+} adsorption through competitive ion exchange (Brown et al., 2019; Robin et al., 2017). However, the immobilisation of ^{226}Ra through, for example, sorption onto Fe- and Mn-(hydr)oxides and its co-precipitation with $BaSO_4$ is potentially reversible under changing geochemical conditions. Beneš *et al.* (1984) demonstrated that ^{226}Ra adsorbed onto quartz via ion exchange in the electrical double layer can desorb as pH decreases. Similarly, adsorption of ^{226}Ra is reversible from ferrihydrite and goethite (Sajih et al., 2014), and ^{226}Ra can be quantitatively desorbed from kaolinite (Beneš et al., 1985) and quartz (Beneš et al., 1984), although desorption is more limited from minerals such as montmorillonite (Beneš et al., 1985) and certain hydrated metal oxides (Nirdosh et al., 1990).

Although numerous laboratory studies have quantified ^{226}Ra sorption to individual mineral phases, comparatively few have examined the combined influence of mineralogy, Ca concentration, and organic matter under conditions representative of freshwater toxicity testing or sandy aquatic sediments. Consequently, the relative importance of quartz, clay minerals,

competing Ca, and organic matter in controlling dissolved ^{226}Ra remains poorly constrained. A 90% reduction in ^{226}Ra activity concentrations was observed in laboratory exposure experiments with freshwater fingernail clams, *Sphaerium striatinum*, with test solutions renewed every 48 h, indicating that this loss occurred within that interval (see Chapter 3). In these experiments, clams burrowed within a sand substrate and were fed algal cells, suggesting that the observed reduction in dissolved ^{226}Ra may have resulted from sorption of $^{226}Ra^{2+}$ onto either mineral phases present in the sand substrate or onto organic matter. Because the experiments were conducted in reconstituted soft water containing calcium, competitive interactions between Ca^{2+} and $^{226}Ra^{2+}$ may also have influenced adsorption processes. To investigate this hypothesis, the mineralogical composition of the sand substrate was first characterized to identify phases most likely to act as sorbents for ^{226}Ra. This characterization guided the selection of quartz and kaolinite as representative mineral phases for further adsorption experiments.

The objectives of this study were to identify the mechanisms contributing to the loss of dissolved ^{226}Ra observed during the fingernail clam exposure experiments. Specifically, the objectives were to: (1) evaluate the extent to which the sand substrate alone can remove dissolved ^{226}Ra from solution in the absence of fingernail clams; (2) assess the influence of organic matter, represented by algal cells, on the removal of dissolved ^{226}Ra from solution; (3) determine the effect of varying Ca^{2+} concentrations on ^{226}Ra adsorption under conditions where competitive ion-exchange is expected to occur; and (4) compare the relative affinity of ^{226}Ra for key mineral components of the substrate through batch sorption experiments using quartz and kaolinite. Understanding and predicting the mobility of trace radionuclides such as ^{226}Ra is important for assessing the potential environmental impacts of uranium mine tailings and effluent on surrounding aquatic systems, as well as for broader applications such as water resource protection.

4.2 MATERIALS AND METHODS

4.2.1 Experimental Solutions

Base stock solutions were prepared with reconstituted soft water (RSW) following the methodology of Clesceri (1998). The Ca content of the RSW solution (i.e., 7 mg L^{-1}) was modified by removing or adding calcium sulfate dihydrate to obtain three other base stock solutions with low (0.7 mg L^{-1}), moderate (35 mg L^{-1}) and high (70 mg L^{-1}) Ca concentrations (see supplementary materials, Table S4-1). The target calcium concentrations were selected based on levels observed downstream of uranium mines and mills (Goulet et al., 2015). To confirm target Ca concentrations in the base stock solutions, along with concentrations of other major ions, a single water sample was collected from each stock solution. Samples were filtered using a 0.45 µm mesh syringe filters (Acrodisc HT Tuffryn Membrane, PALL New York) and sterile 20 mL luer-lock tip polyethylene-polypropylene syringe (Fisher Scientific), collected into pre-labelled polypropylene centrifuge tubes (15 mL, Fisherbrand™), and preserved by acidifying them to 1% HNO_3 (trace metal grade). Dissolved Ca, Fe, Mg, Mn, K, and Na were analyzed at the CanmetMINING Analytical Laboratory (Ottawa, ON, Canada) using inductively coupled plasma optical emission spectrometry (ICP-OES, Synchronous Vertical Dual View, Agilent Technologies). Concentration of chloride (Cl) and sulfate anions was measured using ion chromatography (ICS, Dionex Inuvion IC System, ThermoFisher). Dissolved organic carbon (DOC) and inorganic carbon (DIC) content were measured using a total organic carbon analyzer (TOC-L, Shimadzu). Quality assurance/quality control by the CanmetMINING Analytical Laboratory included the collection of duplicates, spikes, and blanks. The Ca content of the stock solutions was confirmed to be 0.9 mg L^{-1} (low Ca), 35 mg L^{-1} (moderate Ca) and 70 mg L^{-1} (high Ca).

The stock solutions were dosed with ^{226}Ra to achieve nominal concentrations of 1, 5 and 50 Bq L^{-1}. Calibrated pipettes (Sartorius micropipetter) were used to dose the stock solutions with

the appropriate aliquot from a 5 mL stock solution of radium chloride ($RaCl_2$) with an activity of 8 kBq (Stuart Hunt and Associates Ltd., Edmonton, AB, Canada). Water samples were collected from the stock solutions to confirm nominal concentrations of dissolved ^{226}Ra. Samples were filtered using a 0.45 µm mesh syringe filters (Acrodisc HT Tuffryn Membrane, PALL New York) and sterile 20 mL luer-lock tip polyethylene-polypropylene syringe (Fisher Scientific), collected into pre-labelled polypropylene centrifuge tubes (15 mL, Fisherbrand™), and preserved by acidifying them to 1% HNO_3 (trace metal grade). Sample masses were recorded using an electronic balance (AUW120, Shimadzu Corporation, Kyoto, Japan) with an accuracy of ± 0.006 g to allow ^{226}Ra activity to be expressed on a mass-normalized basis (Bq g^{-1}). Sample vials were sealed with Parafilm and refrigerated until shipment to the Canadian Nuclear Laboratories (CNL, Chalk River, ON, Canada) for analysis of ^{226}Ra by alpha spectrometry (detection limit = 0.0005 Bq L^{-1}) using the method outlined in Guérin *et al.* (2023). Activity concentrations were reported by CNL in millibecquerel per gram of sample (mBq g^{-1}) and reported herein in becquerels per litre of water (Bq L^{-1}). The minimum detectable activity (MDA) ranged from 0.0002 to 0.0005 Bq, which was several orders of magnitude below measured concentrations.

4.2.2 Inorganic Substrates

The inorganic substrate chosen for the adsorption experiments consisted of fine aquarium sand (CaribSea Inc. Super Naturals Premium Aquarium Substrate, color: Marine Sand/Moonlight Sand). This sand substrate was used previously in ^{226}Ra toxicity experiments involving fingernail clams (see Chapter 3). The sand substrate was characterized to determine its mineralogical composition and to identify potential adsorption sites for ^{226}Ra. The approximate mineralogical composition and grain textures of an untreated sand sample were examined using back-scattered electron (BSE) imaging and energy-dispersive X-ray (EDX) spectroscopy on a TESCAN Mira3 field-emission gun scanning electron microscope (FEG-SEM) at the Geological Survey of Canada

(Ottawa, Ontario). The data were collected using a 10 kV (BSE images) or 20 kV (EDX spectra) accelerating voltage. The substrates chosen for the batch sorption experiments consisted of natural kaolinite (Al_2O_3 $2SiO_2$ $2H_2O$, Sigma-Aldrich, Product Number 03584) and trace metal grade white quartz (≥99.995% SiO_2, Sigma-Aldrich, Product Number 204358). The particle size distribution of the substrates was estimated from optical microscope images by calculating the equivalent circular diameter (ECD) of algorithmically segmented particles from three areas of each subsample dispersed on a high-contrast background.

4.2.3 Geochemical Modelling

4.2.3.1 Radium-226 Speciation

Aqueous speciation was modelled for each stock solution using available thermodynamic data for dissolved ^{226}Ra species (Table 4.1). Speciation of ^{226}Ra was performed using the PHREEQC Interactive software (version 3.7.3) with the WATEQ4F thermodynamic database (Ball and Nordstrom, 1991). PHREEQC is a widely used geochemical modelling program for calculating aqueous speciation, reaction-path, and transport (Parkhurst and Appelo, 1999). While PHREEQC was used to evaluate inorganic aqueous speciation, the Windemere Humic Acid Model (WHAM version 7.0, Tipping (1994)) was additionally applied to assess potential complexation of ^{226}Ra with dissolved organic matter (i.e., humic and fulvic acids). Stability constants provided in Table 4.1 were integrated into WHAM's default thermodynamic database. Because stability constants for ^{226}Ra complexes with fulvic and humic substances are not available in the WHAM database, stability constants for barium (Ba^{2+}) were used as a proxy. Stability constants were assumed as log K of 1.3 and 0.97 for humic and fulvic acids, respectively (Tipping, 1994). This substitution is commonly applied because Ba^{2+} and $^{226}Ra^{2+}$ are both alkaline earth metals exhibiting similar chemical behaviour, occurring predominantly as divalent cations in aqueous

systems, having comparable ionic radii (Ba^{2+} 142 pm; Ra^{2+} 148 pm), and similar electronegativities (Brown et al., 2022).

Table 4.1 Thermodynamic data used in speciation modelling

Reaction	Stability Constant (log K)	Reference
$Ra^{2+} + OH^- = RaOH+$	0.57 ± 0.23	(Brown et al., 2022)
$Ra^{2+} + SO_4^{2-} = RaSO_4$	2.61 ± 0.33	(Brown et al., 2022)
$Ra^{2+} + CO_3^{2-} = RaCO_3$	2.53 ± 0.14	(Brown et al., 2022)
$Ra^{2+} + HCO_3 = RaHCO_3^+$	2.89	(Beneš et al., 1982)
$Ra^{2+} + Cl^- = RaCl+$	-0.32 ± 0.23	(Brown et al., 2022)

4.2.3.2 Cation Exchange and Surface Complexation Models

Interactions between ^{226}Ra and the mineral phases were modelled using both: (1) a cation exchange model for kaolinite and (2) a surface complexation model (SCM) for quartz, to account for different mechanisms by which ^{226}Ra may partition to mineral surfaces. Cation exchange modelling was applied to kaolinite using the EXCHANGE formalism in PHREEQC, which represents reversible electrostatic exchange of aqueous cations with negatively charged surface sites. This approach is appropriate for clay minerals such as kaolinite due to their permanent structural charge arising from isomorphic substitution within the crystal lattice, which gives rise to measurable CEC (Kumm and Gier, 2024). Exchange reactions were modelled under equilibrium conditions, allowing $^{226}Ra^{2+}$ and competing cations (i.e., Ca, Mg, Na, and K) to partition between solution and exchange sites. Because an exchange selectivity constant for ^{226}Ra is not widely available in standard thermodynamic databases, including WATEQ4F, the exchange reaction for $^{226}Ra^{2+}$ was assigned the same equilibrium constant as Ba^{2+}.

$$Ba^{2+} + 2X^- = BaX_2,\ \log K = 0.91$$

$$Ra^{2+} + 2X^{-} = RaX_2,\ \log K = 0.91$$

The total number of exchange sites (mol) was calculated from the reported CEC and the experimental solid mass according to Equation 1:

$$n_{exchange} = \frac{CEC * m_{solid}}{100} * \frac{1}{1000} \quad \text{(Eq. 1)}$$

where CEC is expressed in meq 100g^{-1} and m_{solid} is the mass of solid (g). The factor of 100 converts the CEC to the mass of solid used, and division by 1000 converts milliequivalents to moles of charge.

Surface complexation modelling was also performed in PHREEQC using the SURFACE formalism to represent sorption of ^{226}Ra to pH-dependent mineral surface functional groups. Surface complexation models describe sorption as the formation of chemical complexes between aqueous species and reactive surface groups, which are governed by acid–base and metal-binding equilibria (Dzombak and Morel, 1990; Stumm and Morgan, 1996). Surface protonation and deprotonation reactions are represented as:

$$\equiv SOH + H^{+} = \equiv SOH_2^{+}$$

$$\equiv SOH = \equiv SO^{-} + H^{+}$$

where $\equiv S$ denotes a generic surface functional group involved in reactions between aqueous species and mineral surface (e.g., Kitamura et al., 1999; Nair et al., 2014; Rakshit et al., 2015; Szymanek et al., 2021). For quartz, these groups correspond primarily to silanol (≡Si-OH), while for kaolinite they include aluminol (≡Al-OH) and silanol sites (Angove et al., 1997). Surface complexation was simulated using a diffuse double layer (DDL) SCM. The approach was selected to maintain consistency with the literature-derived surface complexation constants, which were developed using the same DDL electrostatic formulation. Surface complexation constants were

defined following literature parameterizations (see supplementary materials, Table S4-2). Because surface complexation constants for ^{226}Ra are not widely available in thermodynamic databases, constants for other alkaline earth metals (e.g., Ca^{2+}, Sr^{2+}, Ba^{2+}) were used as proxies, reflecting their similar geochemical behaviour. This approach is consistent with the use of alkaline earth analogues to represent Ra^{2+} in geochemical modelling due to similarities in ionic radius, charge, and aqueous speciation (Serra-Ventura et al., 2025).

For the quartz substrate, specific surface area (SSA, $m^2\ g^{-1}$) was estimated from measured ECDs, assuming spherical particles following standard geometric relationships between particle size and surface area (Stumm and Morgan, 1996), per Equation 2:

$$SSA = \frac{6}{\rho d} \quad \text{(Eq. 2)}$$

where ρ is particle density ($kg\ m^{-3}$), obtained from the literature (Rühlmann et al., 2006), and d is particle diameter (m) derived from ECDs. This calculation assumes smooth, non-porous spherical particles and therefore represents an estimate of external surface area only. The number of surface sites was then calculated using Equation 3:

$$n_{sites} = \frac{SSA * D * 10^{18}}{N_A} \quad \text{(Eq. 3)}$$

where D are surface site densities, assigned based on literature values for mineral surface functional groups, and N_A is Avogadro's number.

For both exchange and surface complexation simulations, mineral phases were first equilibrated with the experimental solution composition in the absence of ^{226}Ra to establish initial exchange or surface site occupancy. Radium-226 was then introduced at the experimental

concentration of 50 Bq L^{-1}, and equilibrium partitioning between solution and solid phases was calculated. This sequential approach ensured mass-balanced simulation of ^{226}Ra uptake.

4.2.4 Adsorption Experiments

Adsorption test methods, modified from Nautilus Environmental (2021), aimed to quantify effects imparted by Ca concentrations, the sand substrate, and the addition of organic matter on measured dissolved ^{226}Ra activity concentrations over 48 hours. Four experiments were conducted, one for each of the Ca concentrations (0.9, 7, 35, 70 mg L^{-1}), each with the three ^{226}Ra activities (1, 5 and 50 Bq L^{-1}), for a total of 12 treatment groups (i.e., ^{226}Ra x Ca combinations). The design used a tiered approach (see supplementary materials, Figure S4-1) to assess the influence of the various components; solution only (series A), solution + sand (series B), and solution + sand + organic matter (series C). Each series had 3 replicates, for a total of 108 test vessels across the 4 experiments. Experimental conditions, including the 48-hour test duration, sand-to-water ratio, substrate, organic matter amendment, and test vessel configuration, were selected to replicate those used in the previous ^{226}Ra toxicity experiments with fingernail clams (see Chapter 3), thereby allowing the mechanisms responsible for the observed loss of dissolved ^{226}Ra to be investigated under comparable exposure conditions. Sand substrates (described above) were rinsed three times with ultrapure water (18 MΩ cm) prior to the tests. The organic matter consisted of an algae mixture of 1mL Instant Algae Shellfish Diet 1800 and 100 µL instant Algae Nano Diet 3600 in 9 mL RSW, modified from (Salerno et al., 2018). Test vessels consisted of 800 mL plastic Nalgene beakers each containing 300 mL of solution. When added as a component, beakers also contained 150 g of sand and 300 µL of organic matter. Beakers were wrapped in black plastic to minimize light penetration and were loosely covered with Parafilm to reduce evaporation.

In situ water quality parameters (water temperature (°C), dissolved oxygen (DO, %), pH, and specific conductivity (µS cm^{-1})) were monitored daily using Hach meters (Hach HQ40d pH/D.O., and HQ14d conductivity) for a subsample (~20 mL) which was collected from a randomly selected beaker, for each ^{226}Ra x Ca treatment. Water subsamples were also collected from the water column of 1 of the 3 replicates, chosen at random, from each of the 12 treatments at hours 1, 3, 6, 9, 12, 24, and 48. Dissolved ^{226}Ra activity concentrations were measured, following the same procedures as described above (see section 2.1). Measurements of ^{226}Ra in stock solution represented concentrations at time 0h.

Given that dissolved ^{226}Ra concentrations are expected to decline over the 48 h period, exposure concentrations were summarized using a time-weighted average (TWA). The TWA accounts for the variation in instantaneous concentration over time and provides a more representative estimate of exposure than nominal or single-time-point measurements when concentrations change during the test period (Belgers et al., 2011). The TWA was calculated using the trapezoidal integration method, which assumes a linear change in concentration between successive sampling times. For each experimental treatment, the area under the concentration-time curve was calculated and divided by the total elapsed time per Equation 4:

$$TWA = \frac{\sum_{i=0}^{n-1}(C_i + C_{i+1}/2)(t_{i+1} - t_i)}{t_n - t_0} \text{ (Eq. 4)}$$

where C_i and C_{i+1} are the measured dissolved ^{226}Ra concentrations at sampling times t_i and t_{i+1} respectively, and t_n-t_0 represents the total exposure duration of 48 h (Belgers et al., 2011). This approach integrates concentration over time and normalizes by the exposure period, yielding an average concentration that reflects temporal changes in dissolved ^{226}Ra. Time-weighted averages (TWA) were calculated separately for each combination of experimental replicate, treatment concentration, and experimental condition.

4.2.5 Batch Sorption Experiment

Batch sorption experiments were conducted to determine whether quartz and kaolinite provide binding sites for ^{226}Ra. A substrate-to-solution ratio of 47 g per 94 mL in 250 mL plastic Nalgene beakers was selected to match the proportions used in the adsorption experiments and the proportions in the previously conducted toxicity tests using *Sphaerium striatinum* (see Chapter 3). This ratio was intended to reproduce the laboratory exposure conditions rather than to simulate a field-equivalent sediment-to-water ratio in natural environments. Although mixing is commonly used in sorption experiments to ensure transport of ions to adsorption sites is not rate-limiting, the water column was intentionally left unmixed in the present study to replicate the undisturbed conditions used in the adsorption and toxicity experiments. Batch sorption experiments were conducted in triplicate for each of three initial ^{226}Ra activity concentrations (1, 5 and 50 Bq L^{-1} prepared in standard RSW). Subsamples were carefully collected from the water column of each replicate using a sterile 20 mL luer-lock tip polyethylene-polypropylene syringe (Fisher Scientific) to measure dissolved ^{226}Ra (as described above) after 6, 12, 24 and 48 hours.

4.2.6 Adsorption Parameters and Kinetic Model

The fraction of solute adsorbed (fsorbed), or percent of dissolved ^{226}Ra removed from solution, was calculated using Equation 5 (Nair et al., 2014; Raghav and Kumar, 2018):

$$fsorbed = \frac{C_0 - C_t}{C_0} \quad \text{(Eq. 5)}$$

where C_0 is the initial concentration at $t = 0$ and C_t is the measured concentration at time t. The activity concentration associated with the solid phase at equilibrium (C_s), which is equivalent to the equilibrium sorbed concentration (q_e) used in adsorption isotherm analyses, was calculated by mass balance according to Equation 6 (e.g., Abin-Bazaine et al., 2022):

$$C_s = \frac{(C_0 - C_e) * V}{m} \quad \text{(Eq. 6)}$$

where C_e is the equilibrium concentration at t = 48, V is the solution volume (L), and m is the dry mass of sorbent (kg). The partitioning of ^{226}Ra between the aqueous phase and solid surfaces was quantified, under test conditions, by calculating distribution coefficients (K_d). The distribution coefficient for a radionuclide is defined as the ratio of the activity concentration associated with the solid phase at equilibrium (C_s, Bq·kg^{-1} dry mass) to the dissolved equilibrium activity concentration in solution (C_e, Bq·L^{-1}), as shown in Equation 7 (e.g., Goulet et al., 2022).

$$K_d = \frac{C_s}{C_e} \quad \text{(Eq. 7)}$$

Higher K_d values indicate greater partitioning to the solid phase, whereas lower K_d values indicate weaker adsorption and greater mobility in the aqueous phase. Distribution coefficients were calculated using ^{226}Ra concentrations measured at the end of the adsorption experiments (48 h), corresponding to equilibrium, or near-equilibrium, conditions.

Finally, time-dependent changes in dissolved ^{226}Ra concentrations were described using first-order kinetic models in which concentration-time data were fit using an exponential approach to equilibrium model of the form per Equation 8 (e.g., Kajjumba et al., 2019; Liu & Shen, 2008):

$$C(t) = C_e + (C_0 - C_e)e^{-kt} \text{ (Eq. 8)}$$

where k is the first-order rate constant. Rate constants (k) and associated standard errors (SE) were obtained by nonlinear least-squares regression. Large k values indicate faster removal of ^{226}Ra from the water column, and faster equilibrium.

4.2.7 Statistical Analyses

The response variable used to assess the influence of sand and organic matter on ^{226}Ra adsorption was the fraction ^{226}Ra adsorbed, calculated for all sampling time points in both the

adsorption experiments (Series A, B and C) and the batch sorption experiments. To evaluate whether the loss of ^{226}Ra from solution differed between Series A and B (i.e., the influence of sand) or between Series B and C (i.e., the influence of organic matter) in the adsorption experiments, percent removal was compared using paired Wilcoxon signed-rank tests across matched experimental conditions (^{226}Ra concentration, Ca concentration, and time). Agreement between series was further examined using Bland–Altman analysis, which assesses agreement between paired measurements (Bland & Altman, 1986), with bias calculated as the mean paired difference and limits of agreement defined as bias ± 1.96 standard deviations (SD).

The response variables used to assess the influence of Ca concentration on ^{226}Ra adsorption were the sorbed activity (C_s), distribution coefficients (K_d), and first-order rate constant (k). Rate constants (k) were derived from first-order kinetic model fits, whereas sorbed activity (C_s) and distribution coefficients (K_d) were calculated from measured aqueous concentrations at 48 h. Statistical analyses of C_s, K_d, and k were conducted using data from treatments containing a solid phase only (i.e., Series B and C only). Response variables were analysed using linear models including Ca concentration and nominal ^{226}Ra activity as fixed factors. Given the observed non-linear response of these parameters to Ca, Ca was modelled using a second-order polynomial term. Interaction terms between Ca and ^{226}Ra activity were included to assess whether the effect of Ca varied with ^{226}Ra activity. Model significance was evaluated using analysis of variance (ANOVA).

The response variable used to assess the influence of the different mineral substrates (i.e., kaolinite and quartz) on ^{226}Ra adsorption was the percent ^{226}Ra removed from solution, calculated for all sampling time points in the batch sorption experiments. Differences in percent removal between mineral substrates were evaluated using a two-way ANOVA with substrate and time as fixed factors. Estimated marginal means were used to quantify differences between substrates and to evaluate contrasts at each sampling time. Finally, to assess whether sorption had stabilized by

the end of the batch sorption experiments, paired sorbed ^{226}Ra activity measured at 24 and 48 h was compared separately for quartz and kaolinite using Wilcoxon signed-rank tests. All statistical analyses were performed using the R software environment and associated base packages (R 4.6.1, R Core Team, 2026). For all statistical analyses, the level of statistical significance (α) was set at 0.05.

4.3 RESULTS

4.3.1 Stock Solution Chemistry

Measured ^{226}Ra activity concentrations for the stock solutions are outlined in Table 4.2. Measured dissolved ^{226}Ra activities ranged from 0.68–1.16 Bq L^{-1} (mean ± SD = 0.93 ± 0.2), 3.8–5.8 Bq L^{-1} (4.8 ± 0.7), and 40 –50 Bq L^{-1} (46 ± 4.3) for the nominal 1, 5 and 50 Bq L^{-1} treatments, respectively. Measured activities in the moderate Ca treatment were consistently lower than the nominal targets and the corresponding activities in the other Ca treatments. Analytical uncertainties were generally within ± 4–15% depending on activity level. Major ion concentrations for stock solutions are outlined in the supplementary materials Table S4-3. Measured Ca was 0.9 mg L^{-1}, 7.1 mg L^{-1}, 35.6 mg L^{-1}, and 72.3 mg L^{-1}in the low, RSW, moderate and high Ca treatments, respectively. Other water chemistry parameters were consistent among treatments, with mean ± SD of measured dissolved water chemistry variables across all 12 stock solutions (one sample per stock solution) was as follows: Cl 2.0 ± 0 mg L^{-1}, Fe 0.15 ± 0.1 mg L^{-1}, K 1.3 ± 0 mg L^{-1}, Mg 6.4 ± 0.1 mg L^{-1}, Na 18 ± 0 mg L^{-1}, Mn 0.03 ± 0.005 mg L^{-1}, SO_4 34 ± 0 mg L^{-1}, DOC 19 mg L^{-1} (RSW only) and DIC 8.6 ± 1.6 mg L^{-1}.

Table 4.2 Measured activity of radium-226 (^{226}Ra) in stock solutions with varying calcium (Ca) concentrations

Nominal (Bq L^{-1})	Measured Activity (Bq L^{-1}) ± Measurement Uncertainty			
	low Ca (0.9 mg L^{-1})	RSW (7 mg L^{-1})	moderate Ca (35 mg L^{-1})	high Ca (70 mg L^{-1})
1	1.08 ± 0.05	0.79 ± 0.04	0.68 ± 0.04	1.16 ± 0.06
5	5.4 ± 0.2	4.8 ± 0.7	3.8 ± 0.2	5.1 ± 0.2
50	46 ± 2	50 ± 3	40 ± 2	48 ± 2

Table Notes: Minimum detectable activity (MDA) of between 0.0002 and 0.0005 Bq

4.3.2 Radium-226 Speciation

PHREEQC modelling indicated that ^{226}Ra speciation was consistent across the range of tested ^{226}Ra x Ca concentrations (Figure 4.1), with approximately 70% of total dissolved ^{226}Ra occurring as free $^{226}Ra^{2+}$ and the remaining fraction occurring as $RaHCO_3^+$ (~20%), $RaSO_4$ (~6%) and $RaCl^+$ (<1%). Complexes with carbonate ($RaCO_3$) or hydroxide ($RaOH^+$) were not predicted under the experimental conditions. The relative distribution among aqueous species remained unchanged across the range of nominal ^{226}Ra activities (1–50 Bq L^{-1}) and calcium concentrations (0.9–70 mg L^{-1}), indicating that variations in experimental conditions did not alter aqueous ^{226}Ra speciation (Figure 4.1). WHAM modelling indicated negligible (< 0.001%) interaction between ^{226}Ra and fulvic or humic acids under the experimental water chemistry conditions.

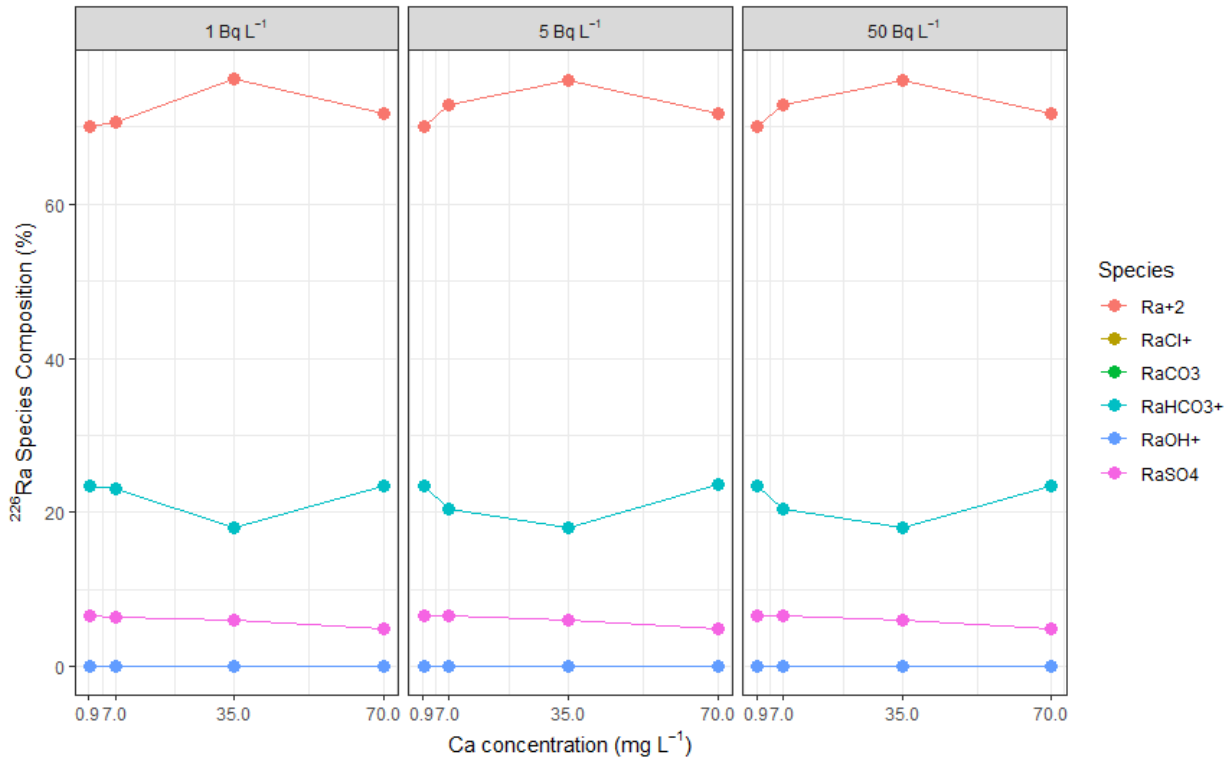


Figure 4.1 Influence of calcium (Ca) concentration on radium-226 (^{226}Ra) speciation at activity concentrations of 1, 5 and 50 Bq L^{-1}, modelled using PHREEQC.

4.3.3 Sand Characterization

The sand substrate was well sorted, with a mean grain size of 219 µm, and the dominant mineral was confirmed to be quartz (SiO2). Textural features (i.e., microfracture and pitting, Figure 4.2) were typically filled with a clay mineral. The EDX analysis of the clay-rich zones confirmed the presence of aluminosilicate with a high aluminum (Al) and low potassium (K) and magnesium (Mg) contents, consistent with kaolinite ($Al_2Si_2O_5(OH)_4$). Other minor impurities were also visible (e.g., ilmenite, zircon, and monazite), but not in excess amounts. There was no visual or geochemical evidence of significant Fe or Mn (hydr)oxides (see supplementary materials, Table S4-4). The geochemical results confirmed the presence of Fe (0.034%) in the sand; however, it appeared to be associated with ilmenite (FeTiO3; Ti 0.037%), large grains of which were identified by EDX, and not Fe coatings. The Mn concentration (<0.010%) was low compared to the Al

concentration (0.124%) and may be associated with other minor unidentified clays in the microfractures.

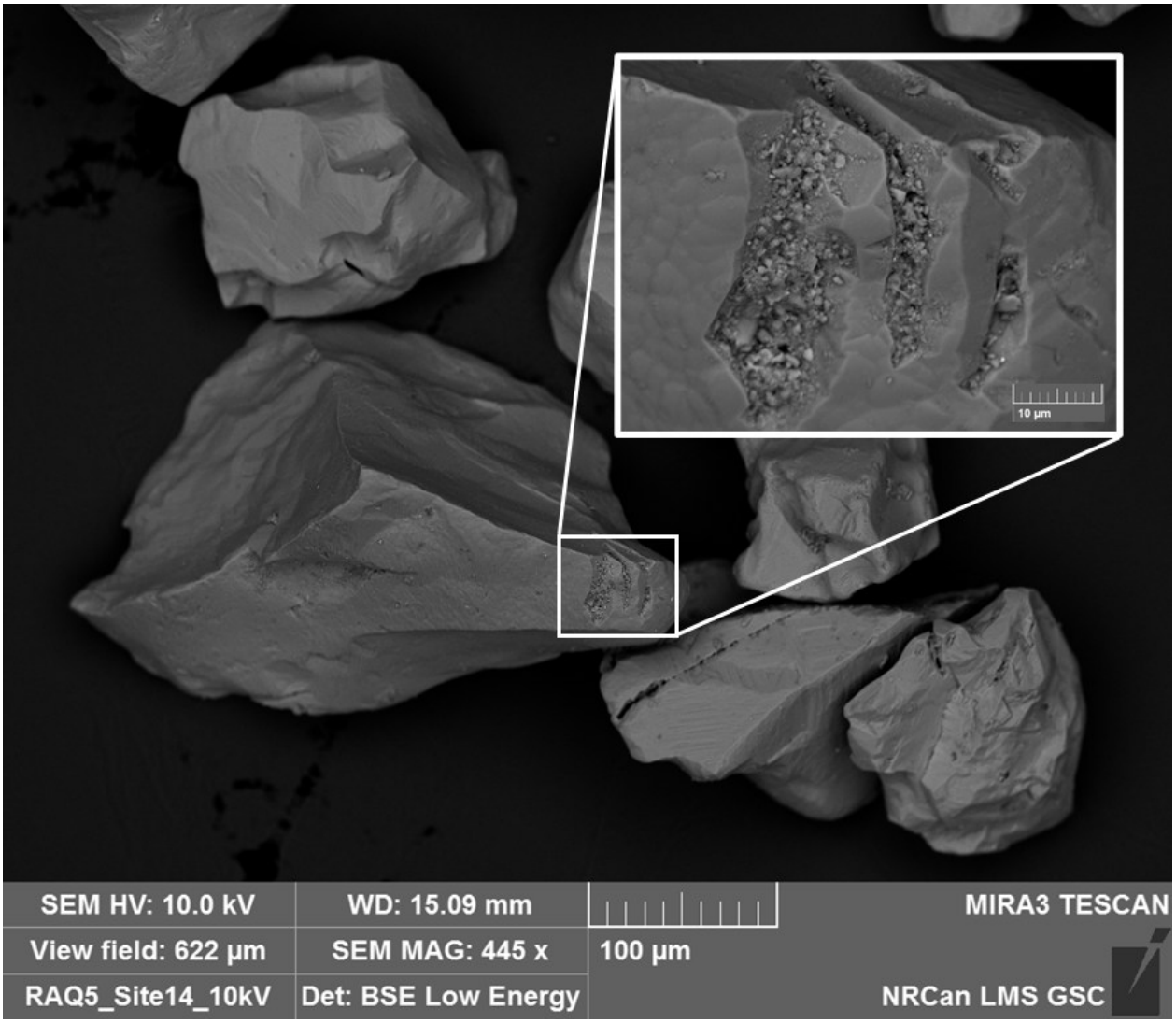


Figure 4.2 Wide field emission scanning electron microscopy of rinsed sand substrate sample showing clay minerals lodged in quartz surface microstructures.

4.3.4 Geochemical Models

The mineral properties used in the exchange and surface complexation models, including measured particle sizes, literature-derived parameters (e.g., CEC, particle density, site density),

and calculated values (e.g., specific surface area and total site concentrations), are provided in Section S1 of the Supplementary Information. Both the kaolinite and quartz substrates exhibited relatively uniform particle sizes, with mean ECDs of 14 ± 7 μm (n = 300) for kaolinite and 188 ± 40 μm (n = 146) for quartz.

Exchange modelling predicted strong partitioning of ^{226}Ra to kaolinite, with approximately 95% of the added ^{226}Ra associated with exchange sites and only 5% remaining in solution under the simulated conditions. Although ^{226}Ra exhibited a strong affinity for kaolinite relative to its initial concentration, exchange-site occupancy remained dominated by Ca^{2+} and Mg^{2+} because of their substantially greater abundance.

The SCM using the DDL approach predicted substantially weaker sorption of ^{226}Ra to quartz. Approximately 27% of the added ^{226}Ra was associated with the quartz surface, while approximately 72% remained in solution. Quartz surface speciation was likewise dominated by Ca-bearing surface complexes and unoccupied surface sites, with ^{226}Ra occupying only a trace fraction of the available surface sites.

4.3.5 Tiered Adsorption Experiments

4.3.5.1 Supporting water quality

During the adsorption experiments, water quality conditions remained stable across treatments (see supplementary materials, Table S4-6). Temperature was between 21–22 °C, dissolved oxygen remained high (91–96% saturation), and pH was circumneutral in all treatments (generally 7.0–7.3), with a slight decrease observed in the low-calcium treatment (6.8–7.2). Specific conductivity reflected the intended calcium gradient, increasing from the low Ca and RSW treatments (~128–182 μS cm^{-1}), to the moderate Ca (~309–337 μS cm^{-1}) and high Ca (~486–523 μS cm^{-1}) treatments, with only minor fluctuations within each treatment.

4.3.5.2 Stability of dissolved ^{226}Ra

Stability of ^{226}Ra in the solution-only treatments (Series A) remained stable over the 48-hour exposure period across all ^{226}Ra and Ca combinations (Figure 4.3). Measured activity concentrations showed no decline, indicating negligible loss of ^{226}Ra from solution in the absence of solid substrates or organic matter. Across the three nominal ^{226}Ra treatments (1, 5, 50 Bq L^{-1}), observed concentrations ranged from 0.75–0.86 Bq L^{-1}, 4.1–4.8 Bq L^{-1}, and 40–50 Bq L^{-1}in RSW (Ca = 7 mg L^{-1}). Similar results were observed for the calcium modified treatments, with variability within each treatment generally ≤ 10%, which was within analytical uncertainty (± 4–15%). The TWA activity concentrations for Series A were estimated to range from 0.8–1.2, 3.7–5.5, and 33–52 Bq L^{-1} for the 1, 5, and 50 Bq L^{-1} nominal treatments, respectively (Figure 4.4). These values reflect the biologically relevant exposure, by integrating temporal changes in ^{226}Ra over the 48 hours.

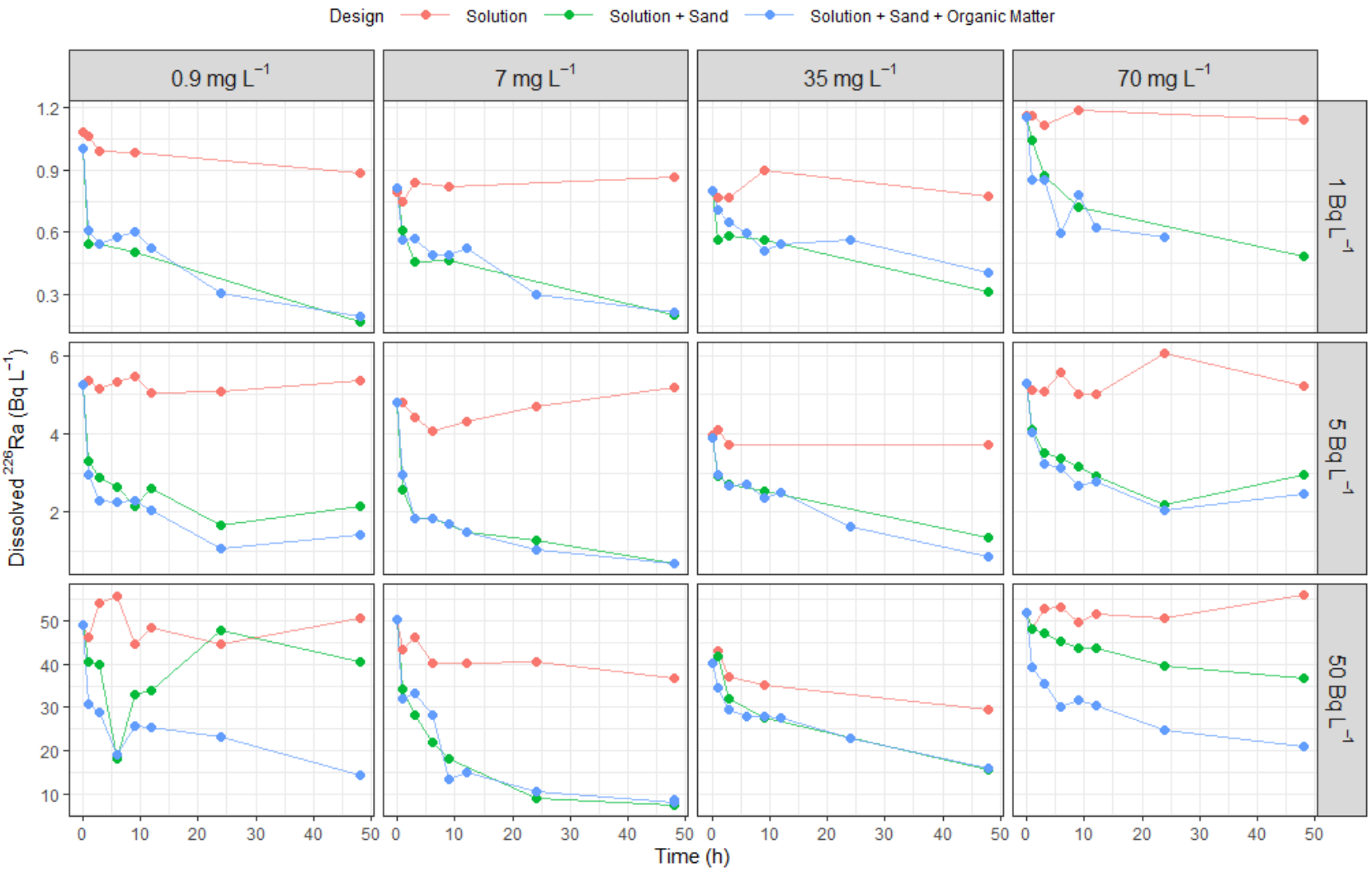


Figure 4.3 Activity concentrations of dissolved radium-226 (^{226}Ra) for solution only (Series A), solution + sand (Series B), and solution + sand + organic matter (Series C) systems under various calcium (Ca) concentrations (0.9 – 70 mg L^{-1}) and nominal ^{226}Ra activities (1, 5, and 50 Bq L^{-1}), over 48 hours.

4.3.5.3 Effect of mineral substrate on ^{226}Ra activity concentrations

In the low Ca (0.9 mg L^{-1}) and RSW (7 mg L^{-1}) treatments the addition of natural sand resulted in rapid removal of dissolved ^{226}Ra from solution, with 46% and 25% of dissolved ^{226}Ra removed within the first hour, increasing to 49% and 43% by 9 h, respectively. Thereafter, removal increased more gradually toward apparent equilibrium. By 48 h, total ^{226}Ra removal reached 83% in the low Ca (0.9 mg L^{-1}) treatment and 75% in the RSW (7 mg L^{-1}) treatment. A comparable pattern was observed under moderate and high Ca concentrations (Figure 4.3). In the moderate Ca treatment (35 mg L^{-1}), 29% of dissolved ^{226}Ra was removed within the first hour, increasing to 61% by 48 h. In the high Ca treatment (70 mg L^{-1}), 9% of dissolved ^{226}Ra was removed within the first hour, increasing to 58% by 48 h. The TWA activity concentrations for Series B were estimated to range from 0.4–0.7, 1.3–2.8, and 13–41 Bq L^{-1} for the 1, 5, and 50 Bq L^{-1} nominal treatments, respectively (Figure 4.4).

The addition of sand (Series B: solution + sand) resulted in a rapid and significant reduction in dissolved ^{226}Ra concentrations relative to solution-only controls (Series A; Wilcoxon signed-rank test, $p < 0.001$; Figure 4.3). Relative to solution-only controls (Series A), the addition of sand (Series B) increased ^{226}Ra removal from solution by a median of 38.4% across matched experimental conditions. This effect was significant overall and within all ^{226}Ra and Ca treatments tested, with median paired differences ranging from 20.7–46.2% ^{226}Ra concentrations and from 25.1–49.1% among Ca concentrations.

4.3.5.4 Effect of organic matter on 226Ra activity concentrations

The addition of organic matter (Series C: solution + sand + organic matter) resulted in a small but consistent additional reduction in dissolved ^{226}Ra concentrations relative to sand-only treatment (Series B; Wilcoxon signed-rank test, $p < 0.001$; Figure 4.3). Across all matched

experimental conditions, median removal increased from 40% in Series B to 46% in Series C at 9 h and from 60% to 70% by 48 h. Similar patterns were observed across calcium treatments. In the low Ca (0.9 mg L^{-1}) treatment, 39% of dissolved ^{226}Ra was removed within the first hour in Series C compared with 46% in Series B, increasing to 80% and 83% by 48 h, respectively. In the RSW (7 mg L^{-1}) treatment, 31% of dissolved ^{226}Ra was removed within the first hour in Series C compared with 25% in Series B, increasing to 74% and 75% by 48 h. In the moderate Ca treatment (35 mg L^{-1}), removal increased from 29% in Series B to 50% in Series C by 48 h. Similarly, in the high Ca treatment (70 mg L^{-1}), removal increased from 58% in Series B to 60% in Series C by 48 h. Overall, the presence of organic matter increased ^{226}Ra removal by a median of approximately 6% across matched experimental conditions. The TWA activity concentrations for Series C were estimated to range from 0.4–0.7, 1.3–2.5, and 14–26 Bq L^{-1} for the 1, 5, and 50 Bq L^{-1} nominal treatments, respectively (Figure 4.4).

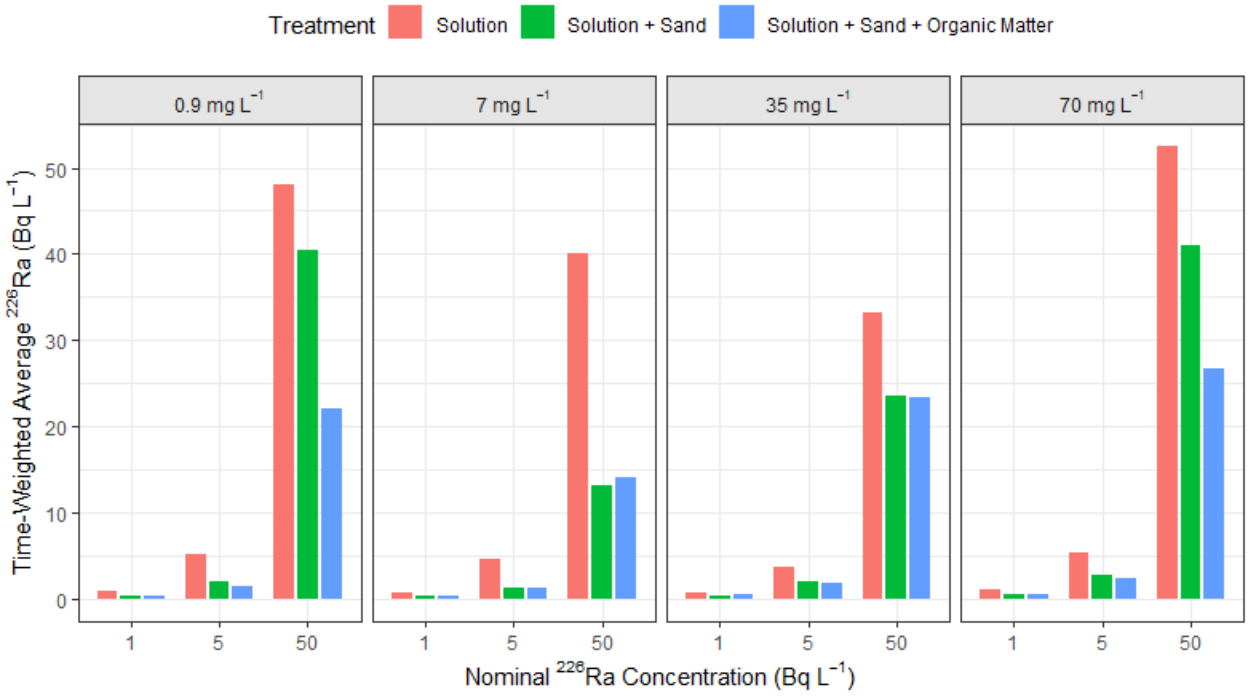


Figure 4.4 Time-weighted average estimates of dissolved radium-226 (^{226}Ra) for solution only (Series A), solution + sand (Series B), and solution + sand + organic matter (Series C) systems under various calcium (Ca) concentrations (0.9 – 70 mg L^{-1}) and nominal ^{226}Ra activities (1, 5, and 50 Bq L^{-1}), over 48 hours.

4.3.5.5 Effect of calcium on ^{226}Ra activity concentrations

The mass of ^{226}Ra sorbed to the solid phase at equilibrium (C_s) was estimated for Series B and Series C by mass balance using aqueous concentrations measured at 48 h (Table 4.3). Estimated C_s values ranged from 0.73 to 85 Bq kg^{-1} for Series B and from 0.55 to 84 Bq kg^{-1} for Series C, depending on ^{226}Ra activity and Ca concentration (Table 4.3). The quadratic model indicated that C_s was strongly dependent on nominal ^{226}Ra ($F_{1,20} = 75.7$, $p < 0.001$), whereas Ca concentration ($p = 0.68$), and the Ca x ^{226}Ra interaction ($p = 0.59$) were not significant. At the lowest nominal ^{226}Ra concentration, sorbed activity generally decreased with increasing Ca concentration; however, at higher nominal ^{226}Ra concentrations the response was non-monotonic.

Although C_s varied among Ca treatments, no consistent directional trend with increasing Ca concentration was evident.

Distribution coefficients (K_d), calculated from aqueous concentrations at 48 h, ranged from 0.3 to 11.8 L kg^{-1} for Series B and 0.6 to 12.0 L kg^{-1} for Series C (Table 4.3). The quadratic model indicated that Ca had a significant non-linear effect on K_d ($F_{2,18} = 4.72$, $p = 0.023$), whereas ^{226}Ra concentration ($p = 0.61$) and the Ca x ^{226}Ra interaction ($p = 0.87$) were not significant. Overall, K_d tended to be lower at higher Ca concentrations, although the relationship was non-linear, with the clearest reduction observed at the lowest nominal ^{226}Ra concentration.

Time-dependent changes in dissolved ^{226}Ra were modelled using first-order kinetics to obtain comparative rate constants (k) for Series B and Series C. Model fits captured the rapid initial removal phase followed by slower asymptotic behaviour (see supplementary materials, Figure S4-2). Estimated rate constants (k) ranged from 0.06 to 0.89 for Series B, and 0.04 to 1.01 for Series C (Table 4.3). The quadratic model indicated that Ca had a significant non-linear effect on k ($F_{2,18} = 5.11$, $p = 0.018$), whereas ^{226}Ra concentration ($p = 0.98$) and the Ca x ^{226}Ra interaction ($p = 0.50$) were not significant. Sorption was generally rapid at low Ca, slowed substantially at 35 mg L^{-1} Ca, and increased again at 70 mg L^{-1} Ca, although remained slower than at the low Ca concentration.

Table 4.3 Estimated sorption parameters for radium-226 (^{226}Ra) in adsorption experiments, including initial (C_0) and equilibrium (C_e) aqueous activities, fraction sorbed (fsorbed), equilibrium solid-phase activity (C_s), distribution coefficients (K_d), and first-order rate constants (k, reported in h^{-1} with associated standard errors (SE)) for Series B (solution + sand) and Series C (solution + sand + organic matter) across calcium (Ca) treatments (0.9-70 mg L^{-1}) and nominal ^{226}Ra activities (1, 5, 50 Bq L^{-1}).

Calcium Treatment	Series	V (L)	m (g)	C_0 (Bq L^{-1})	C_e (Bq L^{-1})	fsorbed (%)	C_s (Bq L^{-1})	K_d (L Kg^{-1})	k (h^{-1})	SE (k) (h_{-1})
Nominal ^{226}Ra = 1 Bq L^{-1}										
0.9 mg L^{-1}	B	0.3	0.15	1.08	0.17	0.84	1.82	10.7	0.13	0.15
	C	0.3	0.15	1.08	0.20	0.82	1.76	8.9	0.06	0.05
7 mg L^{-1}	B	0.3	0.15	0.79	0.20	0.75	1.18	5.9	0.14	0.11
	C	0.3	0.15	0.79	0.21	0.73	1.15	5.4	0.06	0.04
35 mg L^{-1}	B	0.3	0.15	0.68	0.31	0.54	0.73	2.3	0.06	0.08
	C	0.3	0.15	0.68	0.40	0.41	0.55	1.4	0.18	0.08
70 mg L^{-1}	B	0.3	0.15	1.16	0.48	0.58	1.36	2.8	0.13	0.03
	C	0.3	0.15	1.16	0.42	0.64	1.48	3.6	0.46	0.30
Nominal ^{226}Ra = 5 Bq L^{-1}										
0.9 mg L^{-1}	B	0.3	0.15	5.4	2.16	0.60	6.48	3.0	0.83	0.34
	C	0.3	0.15	5.4	1.42	0.74	7.96	5.6	1.01	0.44
7 mg L^{-1}	B	0.3	0.15	4.8	0.70	0.86	8.23	11.8	0.89	0.34
	C	0.3	0.15	4.8	0.69	0.86	8.24	12.0	0.61	0.19
35 mg L^{-1}	B	0.3	0.15	3.9	1.36	0.65	5.05	3.7	0.09	0.07
	C	0.3	0.15	3.9	0.87	0.78	6.02	6.9	0.04	0.03
70 mg L^{-1}	B	0.3	0.15	5.1	2.97	0.42	4.26	1.4	0.33	0.15
	C	0.3	0.15	5.1	2.47	0.52	5.26	2.1	0.39	0.13
Nominal ^{226}Ra = 50 Bq L^{-1}										
0.9 mg L^{-1}	B	0.3	0.15	46	40.55	0.12	10.91	0.3	0.87	1.76
	C	0.3	0.15	46	14.34	0.69	63.33	4.4	0.87	0.47
7 mg L^{-1}	B	0.3	0.15	50	7.28	0.85	85.43	11.7	0.19	0.05
	C	0.3	0.15	50	7.99	0.84	84.03	10.5	0.16	0.05
35 mg L^{-1}	B	0.3	0.15	40	15.52	0.61	48.95	3.2	0.09	0.04
	C	0.3	0.15	40	15.99	0.60	48.02	3.0	0.06	0.03
70 mg L^{-1}	B	0.3	0.15	48	36.79	0.23	22.42	0.6	0.07	0.02
	C	0.3	0.15	48	20.82	0.57	54.37	2.6	0.19	0.08

Table Notes: Volume (V) and mass (g, dry weight)

4.3.5.6 Radium-226 sorption to quartz and kaolinite

The results of the batch sorption experiment demonstrated that $^{226}Ra^{2+}$ sorption differed significantly between quartz and kaolinite substrates (Figure 4.5, Table 4.4). Differences in percent removal between substrates were highly significant across all sampling times (two-way ANOVA, substrate effect: $p < 0.001$), with estimated marginal mean differences ranging from 83.6 to 86.8% between kaolinite and quartz at 6–48 h ($p < 0.001$ for all pairwise contrasts). In treatments containing kaolinite, dissolved $^{226}Ra^{2+}$ concentrations declined rapidly within the first 6 h, with sorption exceeding 90% across all three ^{226}Ra treatments (mean ± SD = 96 ± 2%). Specifically, $^{226}Ra^{2+}$ removal at 6 h was on average 95%, 98%, and 97% for initial nominal concentrations of 1, 5, and 50 Bq L^{-1}, respectively. Following this rapid initial removal, dissolved $^{226}Ra^{2+}$ concentrations remained stable, suggesting that equilibrium or near-equilibrium conditions were reached rapidly for kaolinite treatments. Consistent with this observation, there was no significant difference in sorbed ^{226}Ra activity between paired 24 and 48 h for either kaolinite (Wilcoxon signed-rank, $p = 0.313$) or quartz (Wilcoxon signed-rank, $p = 0.773$).

Mean K_d values for kaolinite were 51, 49 and 62 L kg^{-1} for the nominal 1, 5, and 50 Bq L^{-1} treatments, respectively. In contrast, ^{226}Ra sorption to quartz was minimal ($K_d < 0.6$ L kg^{-1}) and showed limited temporal progression. Within the first 6 h, there was minimal sorption (11 ± 6%). At 12 h, ^{226}Ra removal remained low (0–17%), with little change observed at 24 h (2–21%). By 48 h, ^{226}Ra removal remained low (0–25%), with mean sorption 0%, 22%, and 10% for initial nominal concentrations of 1, 5, and 50 Bq L^{-1}, respectively.

Table 4.4 Estimated sorption parameters for radium-226 (^{226}Ra) in batch sorption tests, including initial (C_0) and equilibrium (C_e) aqueous activities, fraction sorbed (fsorbed), equilibrium solid-phase activity (C_s), and distribution coefficients (K_d) at nominal ^{226}Ra activities (1, 5, 50 Bq L^{-1}).

Nominal ^{226}Ra	Substrate	V (L)	m (g)	C_0 (Bq L^{-1})	C_e (Bq L^{-1})	fsorbed (%)	C_s (Bq L^{-1})	K_d L Kg^{-1}
1 Bq L^{-1}	Kaolinite	0.094	0.047	0.81	0.03	0.96	1.56	50.93
	Quartz				0.83	-0.02	-0.04	-0.03
5 Bq L^{-1}	Kaolinite	0.094	0.047	4.81	0.11	0.98	9.40	49.33
	Quartz				3.77	0.22	2.07	0.55
50 Bq L^{-1}	Kaolinite	0.094	0.047	50.32	1.61	0.97	97.42	62.01
	Quartz				45.14	0.10	10.36	0.23

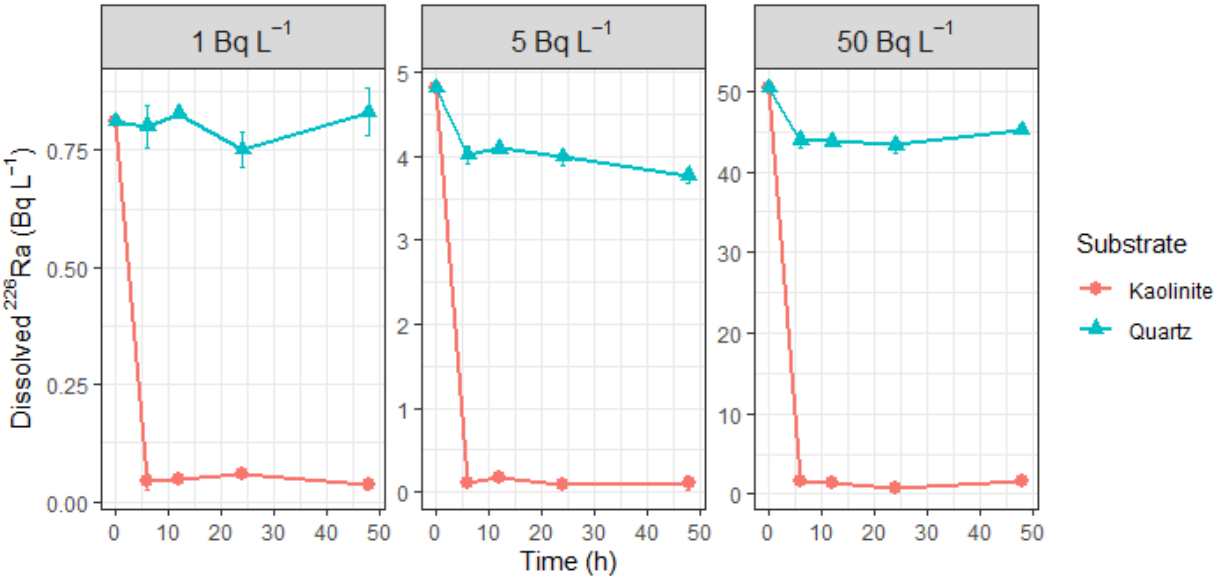


Figure 4.5 Sorption of radium-226 ($^{226}Ra^{2+}$) to kaolinite and quartz mineral phases following 48 h of equilibrium under batch condition (solid-solution ratio: 47 g in 94 mL; temperature 21 °C; pH ~ 7). The black circles represent average measured concentrations (n = 3), with error bars representing standard errors (± SE).

4.4 DISCUSSION

The objective of this study was to determine the main sorbing phases controlling dissolved $^{226}Ra^{2+}$ activity concentrations in sandy aquatic environments and to evaluate the influence of calcium and organic matter on ^{226}Ra partitioning. The results demonstrate that $^{226}Ra^{2+}$ removal

from solution under the experimental conditions of this study was governed primarily by interactions with kaolinite contained within the sand substrate, whereas organic matter and quartz exerted comparatively minor effects.

4.4.1 Limited Interaction between ^{226}Ra and Organic Matter

The addition of particulate organic matter (algal cells) produced a small but consistent additional removal of ^{226}Ra. Despite the fact that the organic matter amendment represented only a minor fraction of the total system volume (300 µL in 300 mL), the observed increase in ^{226}Ra removal (~6%) was statistically significant. However, the magnitude of this effect remained small relative to the much larger influence of kaolinites and calcium concentration on ^{226}Ra partitioning under the oxic, circumneutral conditions examined in this study. This interpretation is consistent with WHAM speciation modelling, which indicated negligible interaction between ^{226}Ra and fulvic or humic acids under the experimental conditions. These findings are also consistent with previous studies demonstrating weak association between $^{226}Ra^{2+}$ and organic phases compared to mineral substrates (Rachkova et al., 2010; Thiry and Van Hees, 2008). Thiry and Van Hees (2008) reported that $^{226}Ra^{2+}$ exhibits low affinity for organic matter due to its large ionic radius, low hydrolysis tendency, and preference for inorganic sorption sites such as clays. Unlike multivalent transition metals, $^{226}Ra^{2+}$ does not form strong surface complexes with functional groups commonly present in organic matter, such as carboxyl or phenolic sites, limiting its incorporation into organic matrices (Brown et al., 2022).

More broadly, field observations further support the limited role of organic matter in directly controlling ^{226}Ra mobility. Organic matter in surface tailings or sediments can enhance biological oxygen demands and promote reducing conditions (Imafidon et al., 2025; Martin et al.,

2003; Xu and Tsang, 2022). Under such conditions, Fe^{3+}-reducing microorganisms can dissolve Fe-(hydr)oxides and release associated ^{226}Ra (Landa et al., 1991; Stackelberg et al., 2018; Martin et al., 2003; Kartick, 2015), while sulfate-reducing bacteria may promote dissolution of Ra-$BaSO_4$ minerals (Fedorak et al., 1986; Landa et al., 1991; McCready et al., 1980). While ^{226}Ra sorbed to clay minerals (e.g., kaolinite) and quartz is not sensitive to redox conditions, reducing environments may indirectly increase ^{226}Ra mobility through the reductive dissolution of Fe-(hydr)oxides, which are known to strongly sorb ^{226}Ra (Chellam and Clifford, 2002; Nirdosh et al., 1990; Thiry and Van Hees, 2008). Similarly, ^{226}Ra incorporation into sulfate minerals (e.g., Ra–$BaSO_4$) may also be mobilized under reducing conditions (Martin et al. 2003). Consequently, under the oxic, circumneutral conditions examined in this study, the direct influence of organic matter on ^{226}Ra partitioning was limited.

4.4.2 Mineralogical Control on $^{226}Ra^{2+}$ Sorption in Sandy Substrates

The addition of sand resulted in rapid and statistically significant removal of dissolved $^{226}Ra^{2+}$ from solution, with 75–85% removal observed after 48 hours under low-calcium conditions. However, subsequent mineral-specific experiments demonstrated that this sorption was attributable almost entirely to kaolinite rather than quartz, the dominant component of the sand used in this experiment. The mineral-specific experiments also indicated that sorption had stabilized by 48 h, indicating that the calculated distribution coefficients (K_d) correspond to near-equilibrium partitioning under the experimental conditions. Sorption of $^{226}Ra^{2+}$ to kaolinite was rapid and extensive (>90% removal), with distribution coefficients ranging from 49 to 62 L kg^{-1}, whereas sorption to quartz was negligible (K_d < 0.6 L kg^{-1}). These experimental observations were consistent with model predictions. Exchange modelling for kaolinite predicted approximately 94% sorption of ^{226}Ra, in good agreement with the observed removal of 95–98%, supporting the

importance of cation exchange processes. In contrast, the SCM for quartz predicted ~38% sorption, which was higher than the observed range (0–25%), but still correctly indicated substantially weaker interaction relative to kaolinite. The overprediction for quartz likely reflects uncertainties associated with the simplified SCM parameterization, including the use of literature-derived surface properties, estimated specific surface area, and surrogate equilibrium constants for ^{226}Ra. Together, these results confirm that the presence of reactive clay minerals such as kaolinites within an otherwise quartz-dominated substrate can dominate ^{226}Ra partitioning.

The strong affinity of kaolinite for ^{226}Ra is consistent with previous laboratory studies reporting enhanced adsorption of $^{226}Ra^{2+}$ to clay minerals relative to quartz and other framework silicates (Beneš et al., 1985; Reinoso-Maset and Ly, 2016; Robin et al., 2017). Clay minerals possess higher surface area, permanent negative structural charge arising from isomorphic substitution, and greater cation exchange capacity than quartz (Davis and Kent, 1990), facilitating sorption of divalent cations such as $^{226}Ra^{2+}$. In contrast, quartz exhibits limited sorption capacity due to its low surface charge density and absence of permanent charge sites, particularly at circumneutral pH (Stumm and Morgan, 1996). The relatively consistent K_d values observed across the tested ^{226}Ra concentration range suggest that sorption sites were not saturated under the experimental conditions, consistent with partitioning controlled by ion-exchange processes at trace concentrations. These findings highlight the importance of mineralogical composition in controlling ^{226}Ra mobility under the experimental conditions examined in this study.

4.4.3 Influence of Calcium on $^{226}Ra^{2+}$ Sorption Kinetics and Partitioning

Calcium concentration exerted a significant influence on both ^{226}Ra partitioning (K_d) and sorption kinetics (k), whereas no significant effect was observed for the mass of ^{226}Ra sorbed to

the solid phase (C_s). Distribution coefficients generally decreased with increasing Ca concentration, particularly at the lowest ^{26}Ra loading, indicating competitive inhibition of ^{226}Ra sorption by Ca^{2+}. The absence of a significant effect on C_s suggests that calcium primarily influenced the partitioning of ^{226}Ra between the aqueous and solid phases rather than the total amount sorbed under the experimental conditions. This behaviour is consistent with the chemical similarity between Ca^{2+} and Ra^{2+}, both of which are alkaline earth metals with similar ionic radii and sorption mechanisms (Langmuir and Riese, 1985; Riese, 1982). Competition for sorption sites on kaolinite and other mineral surfaces reduces the availability of binding sites for Ra^{2+}, resulting in lower sorbed fractions and greater persistence of ^{226}Ra in solution.

The influence of calcium on sorption kinetics was non-linear, with intermediate Ca concentrations producing slower apparent sorption rates compared to both low and high Ca treatments. The partial recovery in sorption rates at 70 mg L^{-1} Ca relative to 35 mg L^{-1} Ca was unexpected and suggests that additional processes may influence ^{226}Ra sorption under increasing calcium concentrations. One possible explanation is that increased ionic strength associated with higher calcium concentrations may compress the electrical double layer, facilitating faster transport of ^{226}Ra to mineral surfaces. However, competition between Ca^{2+} and Ra^{2+} for sorption sites ultimately limits the extent of ^{226}Ra partitioning to mineral surfaces. Because these processes were not directly evaluated in the present study, the mechanism responsible for the observed non-linear kinetic response remains uncertain and warrants further investigation. Nevertheless, the overall influence of calcium observed here is consistent with previous studies demonstrating that major cations such as Ca^{2+} play an important role in controlling ^{226}Ra sorption and mobility in natural waters (Beneš et al., 1985, 1984; Langmuir and Riese, 1985).

4.4.4 Implications for ^{226}Ra Mobility and Availability to Aquatic Organisms in Sandy Environments

The results of this study have implications for predicting ^{226}Ra mobility and availability to aquatic organisms inhabiting sandy substrates. The presence of reactive clay minerals such as kaolinite is likely to substantially reduce dissolved ^{226}Ra concentrations, thereby potentially reducing dissolved exposure and the bioavailable fraction to aquatic organisms. Conversely, environments dominated by quartz-rich sands with low clay content may exhibit limited sorption capacity, potentially resulting in greater ^{226}Ra mobility and dissolved concentrations. These findings are particularly relevant when studying ^{226}Ra toxicity to benthic invertebrates such as fingernail clams (Sphaeriidae), which inhabit sandy and fine-grained substrates and are primarily exposed to ^{226}Ra via overlying water, with additional exposure from interstitial water in sediments and through sediment ingestion. Greater partitioning of ^{226}Ra to sediments would be expected to reduce uptake from the overlying water column. However, uptake through sediment ingestion or contact with sediment-bound particles may also contribute to overall exposure, particularly in ^{226}Ra-impacted environments such as uranium mine tailings and downstream aquatic systems (Goulet et al. 2022).

One limitation of the application of our study to natural sandy sediments is that Fe- and Mn-(hydr)oxide phases were largely absent from our experimental substrate. These minerals are recognized as important sorbents for ^{226}Ra because of their high surface area and strong affinity for divalent cations. Previous studies have identified Fe-(hydr)oxides as important sinks for ^{226}Ra in sediments and uranium mine tailings (Landa and Reid, 1983; Liu and Hendry, 2011). Accordingly, natural sediments containing both clay minerals and Fe- and Mn-(hydr)oxide phases would be expected to exhibit greater ^{226}Ra sorption than the sandy substrate evaluated in the present

study. However, in natural systems, accumulation of organic matter increases biological oxygen demand and creates reducing conditions. Under such conditions, Fe^{3+}-reducing microorganisms can dissolve Fe-(hydr)oxides and release associated ^{226}Ra (Landa et al., 1991; Stackelberg et al., 2018; Martin et al., 2003; Kartick, 2015), while sulfate-reducing bacteria may promote dissolution of Ra-$BaSO_4$ minerals (Fedorak et al., 1986; Landa et al., 1991; McCready et al., 1980). Under such reducing conditions, sorption to Fe-(hydr)oxides and Ra-$BaSO_4$ may become less important, leaving clay minerals as the main retention mechanism of ^{226}Ra in sandy sediments.

4.5 CONCLUSION

Overall, this study demonstrates that ^{226}Ra partitioning under the experimental conditions examined was controlled primarily by mineralogical composition and aqueous geochemistry, particularly the presence of reactive clay minerals and competing major cations such as Ca. Organic matter played a limited direct role in ^{226}Ra sorption under the oxic, circumneutral conditions of this study. Collectively, these findings improve our understanding of the factors controlling ^{226}Ra partitioning in sandy substrates and provide a framework for predicting ^{226}Ra mobility and potential availability to aquatic organisms in natural and contaminated aquatic environments.

5 CHAPTER 5: THE EFFECT OF CALCIUM ON RADIUM-226 BIOACCUMULATION, DOSE RATES, AND TOXICITY TO FINGERNAIL CLAMS (SPHAERIIDAE)

Proulx C.L.[ab], Fortin D.[a], and R.R. Goulet[ac]

[a] Department of Earth and Environmental Sciences, University of Ottawa, 150 Louis-Pasteur Private, Ottawa, ON, K1N 6N5, Canada

[b] Kilgour & Associates Ltd., 2285 St. Laurent Blvd, Ottawa, ON, K1G 4Z6, Canada

[c] Canmet-MINING, Natural Resources Canada, 555 Booth St., Ottawa, ON, K1A 0G1, Canada

*Corresponding Author: Catherine L. Proulx

STATEMENT OF CONTRIBUTIONS

Proulx, C.L.: Conceptualization, Methodology, Formal Analysis, Investigation, Writing – Original Draft, Visualization

Fortin, D.: Writing - Review & Editing, Supervision, Funding acquisition

Goulet, R.R.: Conceptualization, Methodology, Resources, Writing - Review & Editing, Supervision, Funding acquisition

This chapter was prepared for submission in the journal: *Journal of Environmental Radioactivity*

ABSTRACT

Radium-226 (^{226}Ra) is a naturally occurring radionuclide released to aquatic systems from mining and industrial activities. Its bioavailability and toxicity are influenced by water chemistry, particularly calcium, yet the combined effects of calcium on ^{226}Ra partitioning, bioaccumulation, and biological responses remain poorly understood. The objective of this study was to investigate the effect of calcium on ^{226}Ra bioaccumulation and toxicity to fingernail clams (*Sphaerium striatinum*). Controlled laboratory experiments were performed, exposing clams to waters varying in calcium concentrations (0.9, 7, 35, 70 mg L^{-1}) and ^{226}Ra activity concentrations (0.5, 1.0, 5, 10, 25 and 50 Bq L^{-1}), plus a control (0 Bq L^{-1}). Aqueous ^{226}Ra concentrations were characterized using time-weighted averages. Bioaccumulation was measured in soft tissue and shell, and dose rates were estimated using approaches that varied assumptions regarding water and sediment occupancy, as well as sediment partitioning. Survival, burrowing behaviour, growth, and reproduction were evaluated as biological endpoints. Increasing calcium reduced the removal of ^{226}Ra from exposure solution, resulting in higher dissolved concentrations due to decreased sorption. ^{226}Ra accumulated in both soft tissue and shell, with greater partitioning to shell. Bioaccumulation increased with exposure, while calcium modified uptake patterns. Correspondingly, dose rates increased with exposure and were dominated by waterborne pathways, with minimal contribution from sediment under observed conditions. Dose rates were often above screening benchmarks, suggesting potential ^{226}Ra toxicity. Toxicity responses varied among endpoints: survival, growth, and reproduction declined with increasing ^{226}Ra, while behavioural responses were more variable. Calcium modified these responses, with evidence of increased sensitivity at lower ^{226}Ra concentrations under elevated calcium conditions. These patterns reflect competing biological and geochemical mechanisms. Increased calcium likely

reduced ^{226}Ra uptake through competitive interactions at biological membranes while simultaneously increasing dissolved ^{226}Ra concentrations by limiting sorption to mineral phases, thereby sustaining aqueous exposure. The net effect is a shift in exposure–response relationships rather than consistent mitigation of toxicity. These findings demonstrate that water chemistry can significantly influence radionuclide risk and should be explicitly considered in environmental risk assessments of ^{226}Ra.

5.1 INTRODUCTION

Radium-226 (^{226}Ra) is a naturally occurring radionuclide produced through the decay of thorium-230, both part of the uranium-238 (^{238}U) decay series. Activity concentrations of ^{226}Ra in groundwater vary with the geological characteristics of the source region and the ionic strength of the groundwater itself (Fesenko et al., 2014). Naturally elevated concentrations of ^{226}Ra occur in areas with geogenic enrichment in uranium-bearing formations and sedimentary aquifers (Szabo et al., 2012), particularly where geochemical conditions limit the sorptive efficiency of Fe- and Mn-(hydr)oxides (Szabo et al., 2023). Nevertheless, background ^{226}Ra activity concentrations in aquatic environments are typically low, ranging from 4.1-13.7 mBq L^{-1} in streams, and 5.0-9.0 mBq L^{-1} in lakes (Fesenko et al., 2014). Proulx et al. (2025a) reported an upper tolerance limit for background ^{226}Ra of 21.7 mBq L^{-1} in freshwater lakes in Canada.

Anthropogenic sources of ^{226}Ra to aquatic environments are primarily associated with uranium mining and milling activities (Chellam & Clifford, 2002; Mothersill et al., 2013). During uranium ore extraction and processing, ^{226}Ra is largely partitioned into mine tailings using barium chloride (Averill et al., 1984; Liu and Hendry 2011). As tailings age, additional ^{226}Ra accumulates as decay product of ^{238}U and both can become increasingly mobilized and potentially released to surrounding environments through tailings leachate if not adequately mitigated (Martin et al.,

2003). Depending on the uranium content of their ore, other industrial operations such as metal and coal mining and oil and gas extraction, can also elevate ^{226}Ra concentrations through the discharge of wastewater (Ahmad et al., 2021; Brenner et al., 2007; Jamil & Ali, 2001). Consequently, ^{226}Ra enters surface waters through multiple pathways, including direct effluent releases (Proulx et al. 2025a) and groundwater inflow (Brenner et al. 2007).

Once in the aquatic environment, the partitioning and bioavailability of ^{226}Ra is governed by the physicochemical characteristics of water and sediments. In surface water, dissolved ^{226}Ra may adsorb to inorganic particulate surfaces, with Fe- and Mn-oxides generally exhibiting the highest sorption affinity, followed by aluminosilicates and quartz (Chellam and Clifford, 2002; Lofts et al., 2015; Nirdosh et al., 1990; Thiry and Van Hees, 2008). Complexation of ^{226}Ra with dissolved, colloidal or particulate organic matter appears limited (see Chapter 4). The affinity of ^{226}Ra for both the uptake sites of aquatic organisms and inorganic ligands is strongly dependent on water chemistry, particularly pH, anions such as carbonate and sulfate, and the presence of competing cations (Jeffree, 1991; Jeffree & Simpson, 1984; Sheppard et al., 2006; Thiry & Van Hees, 2008). Radium-226 has physicochemical properties similar to those of other alkaline earth metals, such as calcium and barium, leading to competition for sorption sites on mineral surfaces and uptake sites in biological membranes (Brown et al., 2019; Jeffree & Simpson, 1984).

The chemical similarity between ^{226}Ra and calcium is particularly important when considering uptake by aquatic organisms. Calcium is an essential element playing a critical role in physiological processes and biomineralization. Consequently, ^{226}Ra can be incorporated into calcified tissues through the same uptake pathways used for calcium, such as those involved in bone or shell formation (Jeffree, 1988; Jeffree and Simpson, 1986, 1984), contributing to internal accumulation and prolonged biological retention (Brown et al., 2022). Freshwater bivalves are

therefore of particular interest for ecological risk assessment, as they actively accumulate calcium for shell formation (Brenner et al., 2007; Jeffree & Simpson, 1984; Pyle & Clulow, 1998) while maintaining intimate contact with both the water column and sediment, two important environmental reservoirs of ^{226}Ra. Consequently, water chemistry has the potential to strongly influence ^{226}Ra bioavailability, accumulation, and toxicity in these organisms.

The bioaccumulation potential of ^{226}Ra makes internal exposure a radiotoxic concern for aquatic organisms, given its long half-life (1,600 years) and high radiotoxicity. Its radiotoxicity stems from the emission of alpha particles during radioactive decay. Although external exposure to ^{226}Ra is generally negligible because alpha radiation has low penetration (IAEA, 2014), internal exposure through ingestion or absorption can deliver highly localized and biologically significant doses (Fuller et al., 2015). Because alpha particles possess high linear energy transfer (LET), they deposit large amounts of energy over short distances comparable to the diameter of a cell (Fuller et al., 2015). This dense ionization can cause clustered DNA damage, oxidative stress, chromosomal aberrations, mutagenesis, and cell death (Desouky et al., 2015; Fuller et al., 2015). Consequently, relative biological effectiveness (RBE) values have been established to reflect the greater impact of alpha radiation. These values typically range from 10 to 20 and may exceed 50 for certain biological endpoints (Alpen, 1998; Mothersill et al., 2013), making internally incorporated ^{226}Ra a significant radiotoxic concern.

Despite the recognized importance of water chemistry in controlling radionuclide bioavailability, considerable uncertainty remains regarding the influence of calcium concentrations on ^{226}Ra accumulation, toxicity, and associated radiological dose in freshwater benthic organisms. In particular, experimental data examining the interactions between calcium availability, ^{226}Ra bioaccumulation, and biological effects in freshwater bivalves remain limited.

This study aimed to address key knowledge gaps in the ecological risk assessment of ^{226}Ra in freshwater systems. Specifically, this study evaluated the effects of calcium concentration on ^{226}Ra bioaccumulation, estimated absorbed doses, and toxicity in fingernail clams (*Sphaerium striatinum*) exposed under controlled laboratory conditions. Understanding and predicting the risk posed by trace radionuclides such as ^{226}Ra is essential for assessing the potential environmental impacts of uranium mine tailings and effluent on surrounding aquatic systems, as well as in designing mitigation measures such as tailings management facilities and effluent treatment to limit environmental effects of ^{226}Ra.

5.2 METHODS

5.2.1 Experimental Design

Fingernail clams (*Sphaerium striatinum*) were collected from the Ottawa River at Britannia Bay in Ottawa, Ontario, Canada (45.363821°, -75.804477°). Test individuals were acclimated to laboratory conditions in reconstituted soft water (RSW) following the procedures described in Chapter 3. Chronic 28-d toxicity tests were conducted using the same experimental design and protocols described previously, with the exception that Ca concentrations were manipulated among treatments. The Ca content of the RSW solution (i.e., 7 mg L^{-1}) was modified by removing or adding calcium sulfate dihydrate to produce three additional base stock solutions with low (0.9 mg L^{-1}), moderate (35 mg L^{-1}) and high (70 mg L^{-1}) Ca concentrations (see supplementary materials, Table S5-1). The target Ca concentrations were selected to reflect levels reported in freshwater environments downstream of uranium mines and mills (Goulet et al., 2015). Stock solutions were dosed with ^{226}Ra to achieve nominal concentrations chosen to reflect natural background levels near uranium mine and mill sites, elevated concentrations reported in metal mining effluent, and higher concentrations to ensure observable biological effects (see Chapter 3).

Each of the three experiments consisted of seven ^{226}Ra treatments (control, 0.5, 1, 5, 10, 25 and 50 Bq L^{-1}), with 3 replicates per treatment, and 17 individuals per replicate (i.e., 1071 clams within 63 test replicates). Tests were conducted over 28 d in 800 mL plastic beakers containing 300 mL of test solution and 150 g of aquarium sand, following the procedures described in Chapter 3. Day 0 of the experiments was defined as the time at which organisms were randomly distributed among replicates. Clams were fed daily with 300 µL of an algal mixture and test solutions were renewed every 48 h. Biological endpoints of survival, burrowing behaviour, growth in total shell length (TSL), and reproduction as relative brood size (number of larvae per TSL) were assessed as described in Chapter 3.

5.2.2 Water Quality and Chemistry

In situ water quality parameters including temperature, dissolved oxygen, pH, and specific conductivity were monitored weekly using Hach meters, and total ammonia was measured every week. Measurements were always taken prior to water renewals. Water samples were collected from one replicate per treatment weekly to characterize the exposure media. Water samples were filtered (0.45 µm) and preserved with 1% trace metal grade HNO_3. Dissolved Ca, Fe, Mg, Mn, K, and Na were measured by inductively coupled plasma optical emission spectrometry (ICP-OES), chloride and sulfate were measured by ion chromatography, and a total organic carbon analyzer was used to measure both organic (DOC) and inorganic carbon (DIC) at the CanmetMINING Analytical Laboratory (Ottawa, ON, Canada). Dissolved ^{226}Ra was measured by alpha spectrometry at Canadian Nuclear Laboratories (CNL, Chalk River, ON, Canada) following the method of Guérin *et al.* (2023). Water samples were also collected from the stock solutions, so that paired fresh (0 h, from stock solutions) and old (48 h, from replicates) samples could be used to estimate the time-weighted average (TWA) ^{226}Ra activity concentration over the renewal period.

Quality assurance and quality control procedures included the analysis of duplicates, spikes, and blanks.

Speciation of ^{226}Ra was modelled with PHREEQC Interactive software (version 3.7.3) using available thermodynamic reactions for dissolved ^{226}Ra species, as described in Chapter 3 and 4. Speciation calculations did not consider surface complexation to dissolved organic matter.

5.2.3 Bioaccumulation Assessment

Upon completion of the chronic toxicity test, clams were transferred to clear sterile polystyrene 12-well plates (Fisher Scientific) containing clean RSW for depuration without food for 24 h. A 24-h depuration period has commonly been used in freshwater bivalve studies prior to tissue analysis, including studies involving sphaeriid clams, to minimize contributions from undigested gut contents (e.g., Ouedraogo et al. 2025; Redondo-Hasselerharm et al., 2018). Individuals were then dissected to separate the soft tissues from the shells. From each treatment, surviving individuals from all replicates were composited to obtain sufficient tissue mass for reliable determination of ^{226}Ra activity concentrations. Composite samples were placed into pre-labelled and pre-weighed 15 mL polypropylene centrifuge tubes (Fisherbrand™), and wet weights (ww) were recorded using a Shimadzu AUW120 electronic balance (± 0.006 g). Samples were then freeze-dried (-50°C, Labconco FreeZone 2.5 L Model# 117) to a constant dry weight (dw) which took 2 to 3 d. From each treatment in each calcium experiment, individuals from all replicates were composited (n = 2 to 48 individuals, 24.6 ± 12.2). Pooled soft tissue dry weights ranged from 2.6 to 82.4 mg per composite sample (21.7 to 662.8 mg wet weight), while pooled shell tissue dry weights ranged from 24.2 to 1516.2 mg per composite sample (33.6 to 1959.4 mg wet weight).

Soft tissues and shell tissues were covered with 100 µL and 500 µL of trace-metal grade HNO_3 (Fisher Chemical), respectively, and heated (90°C) in a HotBloc system (Environmental Express) for 60 minutes. Samples were cooled before adding 75 µL and 375 µL of H_2O_2 (Fisher Chemical) to the soft tissue and shell samples, respectively. This digestion protocol was modified from Ouedraogo et al. (2025) to account for the larger size of *Sphaerium* compared to *Pisidium*. Samples were once again heated at 90°C for 30 minutes. Extracts were diluted with ultra-pure water (<18.2 ohm·cm) to achieve 5% HNO_3. Samples were sealed Parafilm and stored under refrigeration until analysis. High calcium composite samples were submitted to the Institut national de la recherche scientifique (INRS, Quebec, QC, Canada) for analysis by Inductively Coupled Plasma Mass Spectrometry (ICP-MS). However, given the strong influence of the matrix on the results, the remaining composite samples were shipped to CNL (Chalk River, ON, Canada) for analysis of ^{226}Ra, where activity concentrations were reported in millibecquerel (mBq g^{-1}). Because insufficient sample material remained, the high-calcium samples analyzed at INRS could not be reanalyzed using the CNL method. These data were retained and interpreted with appropriate caution, as they represented the only available measurements for the high-calcium treatment.

Bioaccumulation factors (BAF) were calculated based on the ^{226}Ra activity concentration in the tissues C_{ti} (soft or shell, dw) and corresponding water (Ra_{wo}) using Equation 1.

$$BAF = \frac{C_{ti}\ (Bq\ kg^{-1})}{TWA\ (Bq\ L^{-1})} \qquad \text{(Eq. 1)}$$

A certified reference material (CLV-1, 0.7 Bq g^{-1}, CANMET, Ottawa, ON, Canada), consisting of spruce twigs collected from the Cluff Lake uranium mining area in northern Saskatchewan, was digested and analyzed following the same approach as the fingernail clam tissues. A plant-based certified reference material was used because no certified reference material more representative

of freshwater bivalve tissues, or other comparable biological matrices containing certified ^{226}Ra concentrations, was available. The recovery in the certified reference material sample was 80% (n = 1).

5.2.4 Dose Rate Estimation

Total dose rates to *S. striatinum* were estimated using three approaches that differ in their treatment of organism occupancy and sediment activity concentrations: (1) a water-only scenario (100% occupancy in water; ERICA default sediment = 0), representing purely dissolved water exposure; (2) a mixed exposure scenario using ERICA-derived sediment concentrations (50% water : 50% sediment), representing equilibrium-based partitioning to solids; and (3) a mixed exposure scenario using mass-balance-derived sediment concentrations (50% water : 50% sediment), reflecting experimentally constrained partitioning (Table 5.1).

Absorbed dose rates were estimated using the ERICA Tool (Brown et al., 2008). Given that laboratory analyses provided total activity (mBq) measurements for soft and shell tissues separately, activities were summed to obtain total organism activity per composite, per Equation 2:

$$A_{whole} = A_{soft} + A_{shell} \qquad \text{(Eq. 2)}$$

where activity (A) is expressed in Bq following conversion from mBq. Whole-organism activity concentrations were obtained by normalizing total activity to the combined mass of soft and shell tissues. The whole-organism wet mass ($M_{whole,ww}$) was calculated as the sum of measured wet masses for soft ($M_{soft,ww}$) and shell ($M_{shell,ww}$) tissues. Whole-organism activity concentrations on a wet-weight basis were then calculated per Equation 3:

$$C_{whole,ww} = \frac{A_{whole}}{M_{whole,ww}} \qquad \text{(Eq. 3)}$$

where $C_{whole,ww}$ is expressed in Bq kg^{-1} wet weight. This approach accounts for activity associated with both soft tissue and shell tissue, providing a whole-organism estimate of ^{226}Ra burden suitable for radiological dose assessment. Bioaccumulation measurements were expressed on a dry-weight basis to reduce variability associated with tissue moisture content and improve analytical comparability among samples, whereas wet-weight concentrations were used for dose assessment because ERICA dose coefficients are parameterized relative to whole-organism fresh mass (Brown et al., 2008).

Dose rates (μGy h^{-1}) were calculated using the ERICA tool as the sum of internal exposure from ^{226}Ra accumulated within organisms and external exposure from surrounding environmental media. Internal absorbed dose rates were estimated according to:

$$D_{int} = \sum(DC_{int} * C_{whole,ww}) \qquad \text{(Eq. 4)}$$

where, D_{int} is the internal radiation dose rate (μGy·h^{-1}), DC_{int} is the internal dose coefficient (μGy·h^{-1} per Bq·kg^{-1}), and $C_{whole,ww}$ is the activity concentration in the whole organism on a fresh mass (wet weight) basis (Bq kg^{-1}). Internal dose coefficients were obtained from the ERICA database (Brown et al., 2008). External absorbed dose rates were estimated according to:

$$D_{ext} = \sum(DC_{ext} * [OF_{water}\ x\ A_{water} + OF_{sed}\ x\ A_{sed}]) \qquad \text{(Eq. 5)}$$

where, D_{ext} is the external radiation dose rate (μGy·h^{-1}), DCext is the external dose coefficient (μGy·h^{-1} per Bq·kg^{-1} or Bq·L^{-1}), and A_{water} and A_{sed} are activity concentrations in water and sediment, respectively. Occupancy factors (OF_{water} and OF_{sed}) represent the fraction of time organisms spend in the water column and sediment, respectively, and are required for organisms inhabiting the sediment-water interface (Goulet et al. 2022).

Because ^{226}Ra activity in sand was not directly quantified in this study, multiple approaches were used to evaluate the sensitivity of dose estimates to sediment exposure assumptions. First, a

bounding scenario was implemented assuming no sediment contribution (water:sediment ratio = 1:0). Second, an equal partitioning scenario (0.5:0.5) was applied to represent organisms occupying both water and sediment compartments. Sediment activity concentrations (A_{sed}) were estimated using two independent approaches. In the first approach, sediment activity was inferred within the ERICA tool using default distribution coefficients (K_d = 8470) to estimate partitioning between water and sediment. A distribution coefficient is a common and simple method for describing the partitioning of a radionuclide between sediment and water (e.g., Goulet et al., 2022) and is defined as the ratio of the total activity concentration of a radionuclide in sediments (A_{sed}) and the total activity concentration of a radionuclide in water (A_{water}) per Equation 6.

$$K_d = \frac{A_{sed}}{A_{water}} \qquad \text{(Eq. 6)}$$

In the second approach, sediment activity was independently estimated using a mass balance framework based on measured aqueous activity and observed losses from solution during the experiment, thereby providing an empirical estimate of ^{226}Ra partitioning to solid phases. Over each 48-h water renewal interval, the decrease in dissolved ^{226}Ra activity represents transfer to sediments via sorption, and to organisms via uptake. The activity loss over the duration of the experiment was estimated by

$$A_{loss,28d} = (C_{t0} - C_{t48}) * V * N_{renewals} \qquad \text{(Eq. 7)}$$

where C_{to} and C_{t48} are the measured dissolved concentrations at t = 0 and t = 48, V is the volume of water (0.3 L) and N is the number of water renewals (n = 14).

5.2.5 Statistical Analysis

All statistical analyses were performed using the R software environment and associated base packages (R 4.6.1, R Core Team, 2026) with the level of statistical significance (α) was set at 0.05. Data in text are presented as mean ± standard deviations (SD), unless otherwise stated. A

nonparametric Kruskal-Wallis test was used to test for differences among treatments in general water chemistry. A linear model was used to evaluate the effect of calcium concentration on TWA ^{226}Ra concentrations, while accounting for differences in initial concentrations (T_0). Data from the experiment conducted in RSW, reported in Chapter 3, were incorporated into the present analyses to allow direct comparison with the additional calcium treatments evaluated in this study. The influence of Ca on ^{226}Ra bioaccumulation was evaluated using linear models relating log-transformed tissue activity concentrations to log-transformed TWA exposure concentrations, with Ca concentration included as a categorical predictor and interaction term.

Survival was assessed at the end of the 28-d exposure as the number of surviving and dead individuals in each replicate. Burrowing behaviour was assessed at the end of the exposure, with the number of burrowed and non-burrowed individuals specified as a two-column response, allowing the model to account for variation in the number of individuals per replicate. Differences in initial TSL of *S. striatinum* on Day 0 among treatment groups were also evaluated using a Kruskal–Wallis test. Pairwise Wilcoxon tests with Benjamini-Hochberg (BH) correction were then used to identify significant differences between groups, while correcting for the multiple comparisons. Individual growth was assessed as the increase in TSL between Day 0 and Day 28. Reproduction was assessed on the largest survival clam individuals (n = 10/replicate), with the endpoint consisting of brood size corrected for TSL (i.e., relative brood size). Toxicity endpoints were analyzed using generalized linear models (GLMs) with a binomial error distribution and logit link function (Equation 8).

$$logit(p_i) = \beta_0 + \beta_1 log_{10}(TWA_i + 0.01) + \beta_2 Ca_i + \beta_3[log_{10}(TWA_i + 0.01) * Ca_i]$$

(Eq. 8)

The full model included main effects of radium exposure, represented by the $\log_{10}$ transformed TWA concentrations, and calcium treatment, included as a categorical predictor corresponding to the four discrete experiment treatments, as well as their interaction. Calcium concentration was treated as a categorical predictor to reflect discrete experimental treatments and to avoid imposing a priori assumptions regarding the functional form of its effect on toxicity. The significance of model terms was evaluated using analysis of deviance, with test statistics selected based on the model error structure (F-tests for Gaussian and quasi-likelihood models; likelihood ratio χ^2 tests for binomial models). Hypothesis tests (i.e., post-hoc one-tailed Dunnett's multiple comparison test) were used to determine which treatments were statistically different relative to the control. Effect concentrations (e.g., EC_{10}, EC_{20}) were initially explored using standard dose–response modelling approaches. However, models did not converge or produced unstable parameter estimates across endpoints, likely due to high variability and non-monotonic response patterns. As an alternative, no-observed-effect concentrations (NOEC) and lowest-observed-effect concentrations (LOEC) were determined based on post-hoc comparisons from GLMs.

5.3 RESULTS

5.3.1 Chronic Experiments

5.3.1.1 Supporting Water Chemistry

Temperature, pH, and dissolved oxygen remained stable throughout the experiments across all treatments, with mean values (± SD) of 21.5 ± 0.45 °C, 7.26 ± 0.16, and 90.1 ± 6.0 %, respectively. Temperature and pH differed slightly among calcium treatments (Kruskal-Wallis $\chi 2$ = 27.4 and 19.5, df = 2, $p < 0.01$), although the magnitude of these differences was small (<1 °C and <0.25 pH units). Dissolved oxygen did not differ among treatments (Kruskal-Wallis, $p = 0.08$). Ammonia ranged between 0.00 and 0.25 mg L^{-1} across treatments throughout the experiment,

remaining below the CCME water quality guideline of 1.54 mg L^{-1} for the protection of aquatic life under the pH and temperature conditions observed in our study.

Specific conductivity increased with increasing calcium concentration (Kruskal-Wallis $\chi 2 = 36.5$, df = 2, $p < 0.001$), with 183 ± 29 µS cm^{-1}, 188 ± 21 µS cm^{-1}, 347 ± 10 µS cm^{-1}, and 565 ± 52 µS cm^{-1} in the low, RSW, moderate and high Ca treatments respectively. Measured Ca concentrations were 0.9 ± 0.1 mg L^{-1}, 7.1 ± 1.0 mg L^{-1}, 35.6 ± 0.6 mg L^{-1}, and 72.3 ± 3.8 mg L^{-1} in the low, RSW, moderate and high Ca treatments, respectively. Other water chemistry parameters did not vary significantly among treatments (Kruskal-Wallis χ^2 0.5 to 13.4, $p > 0.05$). The mean ± SD of measured dissolved water chemistry variables across all treatments were as follows: Cl 2.9 ± 0.9 mg L^{-1}, K 1.3 ± 0.03 mg L^{-1}, Mg 6.5 ± 0.2 mg L^{-1}, Na 18.2 ± 0.7 mg L^{-1}, Fe 0.19 ± 0.01 mg L^{-1}, Mn 0.03 ± 0.004 mg L^{-1}, SO4 41.0 ± 7 mg L^{-1}, DOC 19 mg L^{-1} (RSW only) and DIC 8.3 ± 1.9 mg L^{-1}.

5.3.1.2 Radium-226 Exposure

Aqueous speciation modelling indicated that ^{226}Ra was dominated by the free divalent cation ($^{226}Ra^{2+}$), which accounted for >80% of total dissolved ^{226}Ra under the experimental water chemistry conditions, followed by $RaSO_4(aq)$ and $RaHCO_3^+$ (<10%, respectively). These relative proportions remained constant across all activity concentrations evaluated (nominal ^{226}Ra: 0.5–50 Bq L^{-1}) and calcium concentrations (0.9-70 mg L^{-1}), reflecting linear scaling of species concentrations with total dissolved ^{226}Ra and confirming that complexation reactions were not ligand-limited within the narrow range of assumed ^{226}Ra toxicity modifying factors such pH, Ca, and inorganic carbon.

In fresh solutions, measured dissolved ^{226}Ra activity concentrations were generally close to nominal concentrations. Minor deviations were observed in the lowest nominal treatments,

likely reflecting pipetting uncertainty at small volumes. Measured activity concentrations declined substantially over the 48-h renewal period, consistent with previous observations of ^{226}Ra partitioning to mineral substrates (see Chapter 4). Exposure concentrations were therefore characterized by using time-weighted averages (TWA) calculated from paired fresh and test (48-h) samples, as presented in Table 5.1. Nominal treatment concentrations are reported when referring to experimental treatment groups and figures, whereas statistical analyses were conducted using measured TWA exposure concentrations to account for losses of ^226Ra from solution over the renewal period.

Table 5.1 Measured activity concentrations of radium-226 (^{226}Ra) in dosed waters used in the *Sphaerium striatinum* 28-day chronic toxicity tests at varying Ca concentrations, including fresh (T_0) and tested (48 hours old, T48) samples used to estimate fractional loss of ^{226}Ra between water renewals and the average exposure activity over 48 hours using a time-weighted average (TWA)

Measurement	Nominal ^{226}Ra Treatment (Bq L^{-1})						
	0	0.5	1	5	10	25	50
Low Calcium (0.9 mg L^{-1})							
T_0	ND	0.47	1.08	5.40	11.14	23.99	50.22
T_{48}	ND	0.05	0.07	0.59	2.03	2.72	4.71
Fractional loss	NA	0.90	0.93	0.89	0.82	0.89	0.91
TWA	ND	0.26	0.58	3.00	6.58	13.35	27.47
Reconstituted Soft Water (Ca 7 mg L^{-1})							
T_0	ND	0.42	0.65	5.28	9.53	22.02	39.19
T_{48}	ND	0.05	0.09	0.46	0.99	2.44	4.73
Fractional loss	NA	0.88	0.86	0.91	0.90	0.89	0.88
TWA	ND	0.23	0.37	2.84	5.12	11.80	21.80
Moderate Calcium (35 mg L^{-1})							
T_0	ND	0.44	0.68	3.80	7.90	19.20	40.00
T_{48}	ND	0.15	0.29	1.40	3.18	7.88	18.87
Fractional loss	NA	0.66	0.58	0.63	0.60	0.59	0.53
TWA	ND	0.29	0.48	2.60	5.54	13.54	29.44
High Calcium (70 mg L^{-1})							
T_0	ND	0.65	1.16	5.10	10.74	25.32	51.37
T_{48}	ND	0.16	0.25	1.64	1.79	9.35	16.92
Fractional loss	NA	0.75	0.79	0.68	0.83	0.63	0.67
TWA	ND	0.41	0.70	3.37	6.27	17.34	34.15

The fractional loss of ^{226}Ra from solution was 0.89 ± 0.04, 0.89 ± 0.02, 0.60 ± 0.05, and 0.73 ± 0.08 for the low, RSW, moderate and high Ca experiments. A linear model indicated that TWA concentrations scaled nearly proportionally with initial concentrations (slope = 1.01 ± 0.01, $p < 0.001$), confirming that losses from solution were largely proportional to starting ^{226}Ra concentrations. Calcium concentration had a small but statistically significant positive effect on TWA ($\beta = 0.00105 \pm 0.00027$, $p = 0.001$), indicating that increasing Ca reduced the removal of ^{226}Ra from solution. The model explained nearly all variability in TWA concentrations ($R^2 = 0.998$).

5.3.2 Bioaccumulation of ^{226}Ra

Radium-226 accumulated in both soft tissues and shells of *S. striatinum* across all exposure treatments in a concentration-dependent manner, with activity concentrations increasing as a function of dissolved ^{226}Ra in water (Figure 5.1). However, ^{226}Ra accumulated to a greater extent in shells compared to soft tissues. Soft tissue concentrations ranged from 0.03 to 3.31 Bq g^{-1} dry weight (0.72 ± 0.85 Bq g^{-1} dry weight), while shell concentrations were generally higher, ranging between 0.02 to 10.73 Bq g^{-1} dry weight (2.18 ± 2.67 Bq g^{-1} dry weight).

In soft tissue, ^{226}Ra activity concentrations increased significantly with increasing exposure ($\log_{10}$ TWA; $F_{1,17} = 149.9$, $p < 0.001$). A significant interaction between calcium concentration and exposure was observed ($F_{1,17} = 11.77$, $p = 0.003$), indicating that calcium modified the relationship between exposure and accumulation. Specifically, the slope of the exposure–accumulation relationship decreased with increasing calcium concentration. In shell tissue, ^{226}Ra activity concentrations also increased significantly with increasing exposure ($\log_{10}$ TWA; $F_{1,17} = 71.1$, $p < 0.001$). Calcium concentrations did not have a significant main effect on shell accumulation ($p = 0.33$). However, a significant interaction between calcium and exposure was observed ($F_{1,17} = 6.21$,

$p = 0.023$), indicating that the relationship between exposure and shell ^{226}Ra varied among calcium treatments. Specifically, the slope of the exposure–accumulation relationship increased with calcium concentrations.

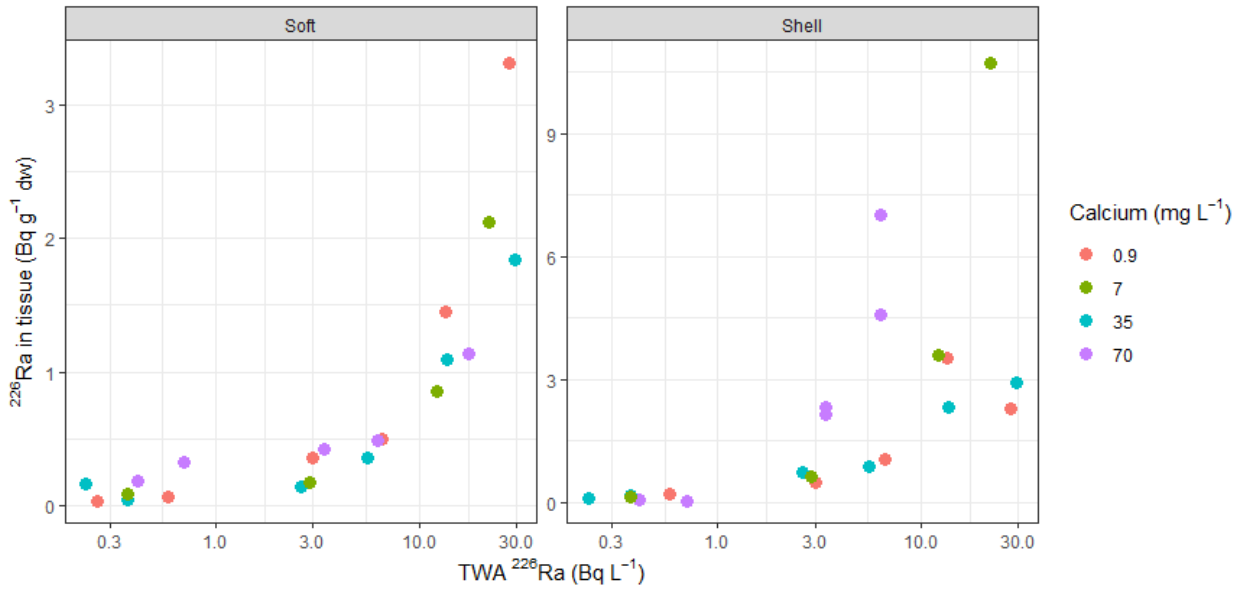


Figure 5.1 Relationship between time-weighted average (TWA) radium-226 (^{226}Ra) concentrations in water and ^{226}Ra activity concentrations in soft tissue and shell of *Sphaerium striatinum* after 28-day exposure at varying Ca concentrations.

Bioaccumulation factors (BAFs) for shells ranged from 25 to 1121 L kg^{-1} dry weight, which was consistently higher than soft tissue BAFs, which ranged from 55 to 722 L kg^{-1} dry weight (Table 5.2). No clear monotonic trend in BAF with increasing exposure concentration was observed; rather, BAFs remained relatively stable across treatments, with a slight increase at the highest exposure in shell tissue.

Table 5.2 Bioaccumulation factors (BAF, L kg^{-1}) for *Sphaerium striatinum* following 28-d aqueous exposure to increasing time-weighted average (TWA) radium-226 (^{226}Ra) concentrations (Bq L^{-1}) at varying calcium (Ca) concentrations.

Nominal ^{226}Ra (Bq L^{-1})	Low (0.9 mg L^{-1})	RSW (7 mg L^{-1})	Moderate (35 mg L^{-1})	High (70 mg L^{-1})
		Soft Tissue		
0.5	117	-	722	457
1	109	228	127	471
5	120	62	55	126
10	76	-	65	77
25	108	70	80	65
50	121	96	63	-
		Shell Tissue		
0.5	-	-	379	163
1	329	383	428	25
5	165	219	276	665
10	158	-	156	926
25	264	293	171	-
50	83	489	99	-

Table Notes: Missing values (-) for samples where ^{226}Ra was not measured.

5.3.3 Dose Rates in *Sphaerium striatinum*

Across all treatments, total dose rates per organism increased with increasing TWA ^{226}Ra concentrations (Figure 5.2). Under full water occupancy assumptions, dose estimates ranged from 5.96 to 727 µGy h^{-1}. Sediment concentrations estimated using ERICA-derived partitioning ranged from 1,950 to 249,000 Bq kg^{-1}, which were approximately 200 times higher than those derived from mass balance (7.24 to 1,255 Bq kg^{-1}). Inclusion of sediment occupancy using ERICA-derived sediment concentrations resulting in only a modest increase in total dose (6.8 to 772 µGy h^{-1}). In contrast, dose estimates based on mass-balance-derived sediment concentrations were identical to water-only values, indicating a minimal contribution of sediment under observed partitioning conditions.

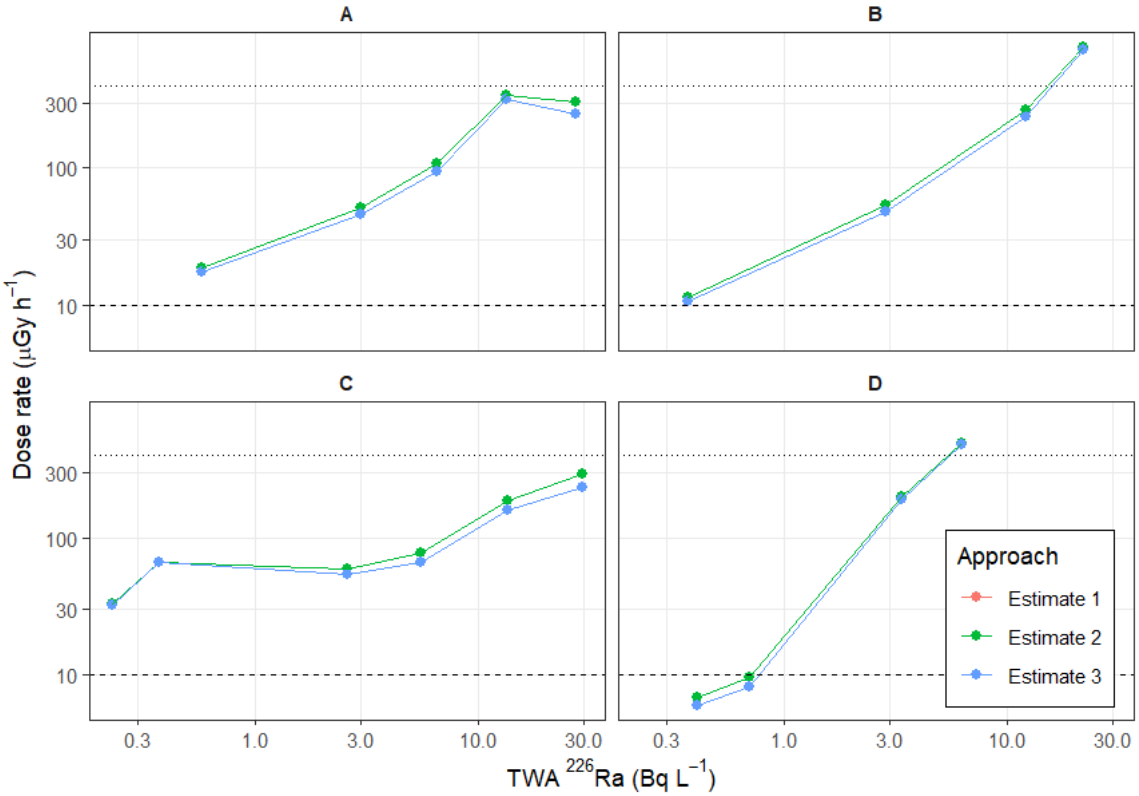


Figure 5.2 Total dose rates to *Sphaerium striatinum* as a function of time-weighted average (TWA) radium-226 (^{226}Ra) concentrations under different calcium conditions. Panels A–D correspond to calcium concentrations of 0.9, 7, 35, and 70 mg L^{-1}, respectively. Estimate 1 assumes full water occupancy (water-only exposure); Estimate 2 incorporates both water and sediment exposure using ERICA-derived sediment concentrations (K_d-based); and Estimate 3 incorporates water and sediment exposure using sediment concentrations derived from mass balance. Horizontal dashed and dotted lines indicate screening benchmarks of 10 and 400 µGy h^{-1}, respectively.

Figure Notes. Results for estimates 1 and 3 were the same and overlap in the figure.

5.3.4 Calcium Effects on Chronic Toxicity

5.3.4.1 Survival

Mean survival of *S. striatinum* at the end of the 28 d exposure was 98%, 98%, 92%, and 76% in the controls for the low, RSW, moderate and high calcium experiments, respectively, meeting the toxicity test acceptability criterion of ≥ 80% control survival in all but the high calcium experiment. Survival was analyzed using a quasibinomial GLM to account for overdispersion.

Survival declined significantly with increasing ^{226}Ra concentration ($F_{1,85} = 21.5$, $p < 0.001$) and differed significantly among calcium treatments ($F_{3,82} = 25.0$, $p < 0.001$). The interaction between ^{226}Ra concentration and Ca treatment was not significant ($F_{3,79} = 1.44$, $p = 0.24$), indicating that the slope of the radium dose–response relationship did not differ significantly among calcium treatments (Figure 5.3).

To further evaluate treatment-level responses, post-hoc Dunnett's tests were performed separately within each calcium treatment, comparing each ^{226}Ra treatment to the respective control (0 Bq L^{-1}). Under low calcium conditions, survival was significantly reduced at multiple nominal ^{226}Ra treatments, including 0.5, 5, 10, 25, and 50 Bq L^{-1} (adjusted $p = 0.006$ to <0.001), whereas survival at 1 Bq L^{-1} did not differ from the control ($p = 0.57$). Under RSW conditions, no significant differences in survival were observed across any ^{226}Ra treatments (all adjusted p ≈ 1.00). Under moderate calcium conditions, survival was significantly reduced at most nominal ^{226}Ra treatments, including 0.5, 1, 5, 10, and 25 Bq L^{-1} (adjusted $p = 0.013$ to <0.001), whereas survival at 50 Bq L^{-1} did not differ significantly from the control ($p = 0.18$). Under high calcium conditions, survival was significantly reduced at all tested ^{226}Ra concentrations (all adjusted $p < 0.001$).

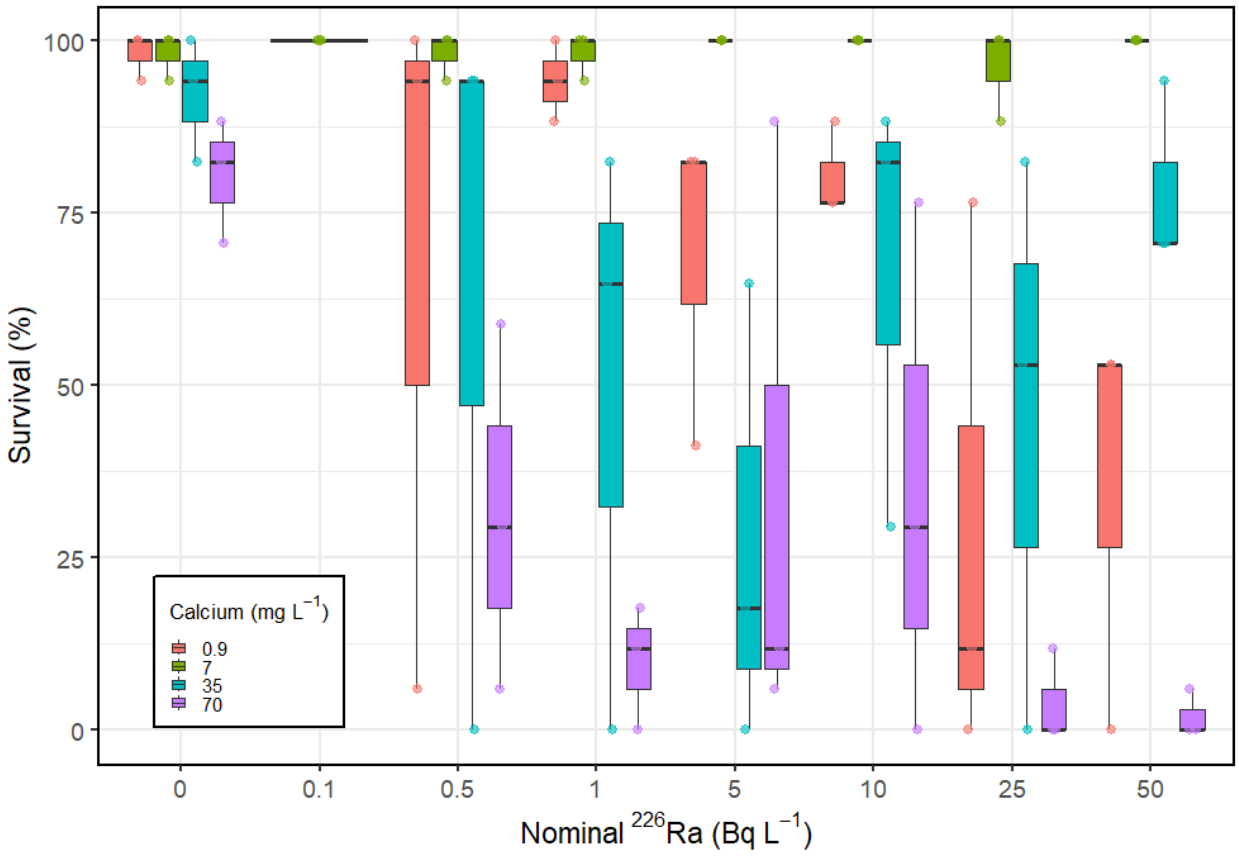


Figure 5.3 Survival (%) of *Sphaerium striatinum* after 28 days of exposure to nominal radium-226 (^{226}Ra) concentrations across varying calcium concentrations. Boxplots represent the median, interquartile range (box), and range (whiskers), with points showing individual replicates.

Figure Notes. Nominal ^{226}Ra treatment concentrations are presented on the x-axis to facilitate comparison among calcium treatments. Statistical analyses were conducted using measured time-weighted average (TWA) ^{226}Ra concentrations to account for activity losses over the exposure period.

5.3.4.2 Behaviour

Burrowing behaviour of *S. striatinum* was significantly affected by ^{226}Ra exposure. A binomial GLM indicated significant effects of ^{226}Ra exposure ($\chi^2 = 8.94$, $p = 0.003$) and Ca concentration ($\chi^2 = 21.2$, $p < 0.001$), but no significant interaction between the two ($\chi^2 = 0.99$, $p = 0.320$), on the proportion of individuals that were burrowed after 28 days of exposure (Figure 5.4). Although burrowing tended to decrease with increasing ^{226}Ra, variability among treatments was

high. Mean burrowing at the end of the test was 72 ± 21 % in the control, 78 ± 32 % at 0.5 Bq L^{-1}, 50 ± 37 % at 1.0 Bq L^{-1}, 69 ± 34 % at 5 Bq L^{-1}, 60 ± 34 % at 10 Bq L^{-1}, 65 ± 36 % at 25 Bq L^{-1}, and 45 ± 47 % at 50 Bq L^{-1}. A similar pattern was observed across Ca treatments, with a general decline in burrowing at higher Ca concentrations but substantial variability among replicates. Mean burrowing was 72 ± 19 % in the low Ca treatments, 77 ± 12 % in the RSW treatments, 59 ± 34 % in the moderate Ca treatments, and 53 ± 42 % in the high Ca treatments. To further evaluate treatment-level responses, post-hoc Dunnett's tests were conducted separately within each Ca treatment, comparing each ^{226}Ra treatment to their corresponding control (0 Bq L^{-1}). However, no significant differences between individual treatments and the control were detected (all adjusted $p > 0.05$).

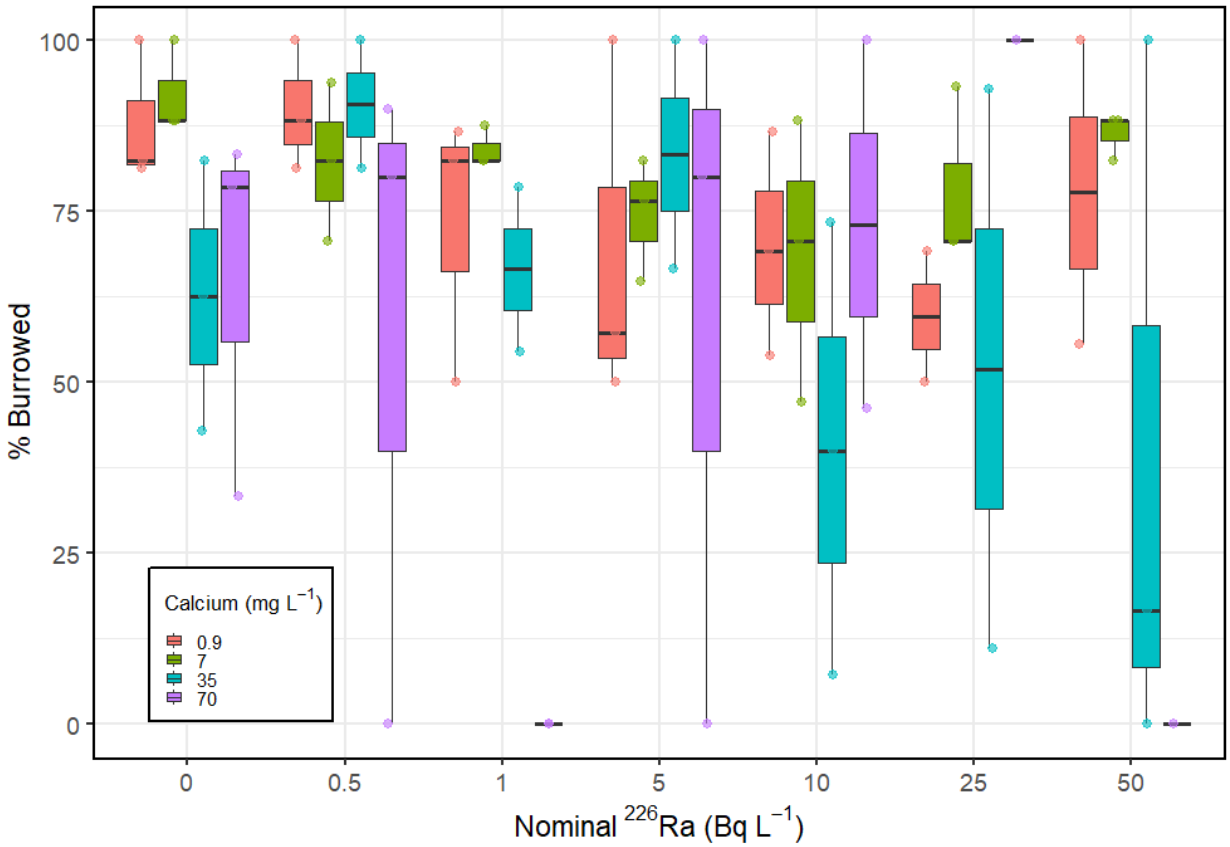


Figure 5.4 Burrowing (%) of *Sphaerium striatinum* after 28 days of exposure to nominal radium-226 (^{226}Ra) concentrations across varying calcium concentrations. Boxplots represent the median, interquartile range (box), and range (whiskers), with points showing individual replicates.

Figure Notes. Nominal ^{226}Ra treatment concentrations are presented on the x-axis to facilitate comparison among calcium treatments. Statistical analyses were conducted using measured time-weighted average (TWA) ^{226}Ra concentrations to account for activity losses over the exposure period.

5.3.4.3 Growth

Results of the Kruskal-Wallis test indicated that initial TSL differed among treatment groups (i.e., all ^{226}Ra x Ca combinations; Kruskal-Wallis $\chi 2 = 76$, df = 28, $p < 0.01$). However, the pairwise comparisons using Wilcoxon ranks, after correcting for multiple comparisons, indicated that no individual differences were statistically significant (all $p > 0.05$). The lack of pairwise differences suggests no systematic baseline bias in initial TSL among treatments, especially given the large number of groups tested, and that the Kruskal-Wallis tests detected small distribution

differences across groups collectively. The GLM used to evaluate the effects of ^{226}Ra exposure and calcium concentration on growth indicated that growth declined significantly with increasing ^{226}Ra exposure ($F_{1,937} = 67.7$, $p < 0.001$, Figure 5.5). While calcium concentration alone did not significantly influence growth ($F_{1,937} = 1.60$, $p = 0.21$), there was a significant interaction between ^{226}Ra exposure and calcium concentration ($F_{1,937} = 8.67$, $p = 0.003$), indicating that the effect of ^{226}Ra on growth varied across calcium treatments.

To further evaluate treatment-level responses, a post-hoc Dunnett's test was performed separately within each calcium treatment, comparing each ^{226}Ra treatment to their respective controls (0 Bq L^{-1}). Under low calcium conditions, no significant differences in growth were observed between any ^{226}Ra treatment and the control (adjusted $p = 0.06$ to 1.00). Under RSW conditions, growth was significantly reduced at the two highest ^{226}Ra treatments (adjusted $p < 0.001$). Under moderate calcium conditions, growth was significantly lower than the control at 1 Bq L^{-1}, 10 Bq L^{-1}, 25 Bq L^{-1}, and 50 Bq L^{-1} nominal treatments ($p < 0.001$ to 0.016). Under high calcium conditions, growth reductions were observed at lower ^{226}Ra concentrations. Growth was significantly lower than the control at 0.5 Bq L^{-1} ($p = 0.008$) and 5 Bq L^{-1} ($p < 0.001$). Growth at nominal 10 Bq L^{-1} was marginally reduced relative to the control ($p = 0.058$), whereas other treatments did not differ significantly. In the high-calcium experiment, interpretation of growth responses at the higher ^{226}Ra treatments is complicated by substantially reduced survival.

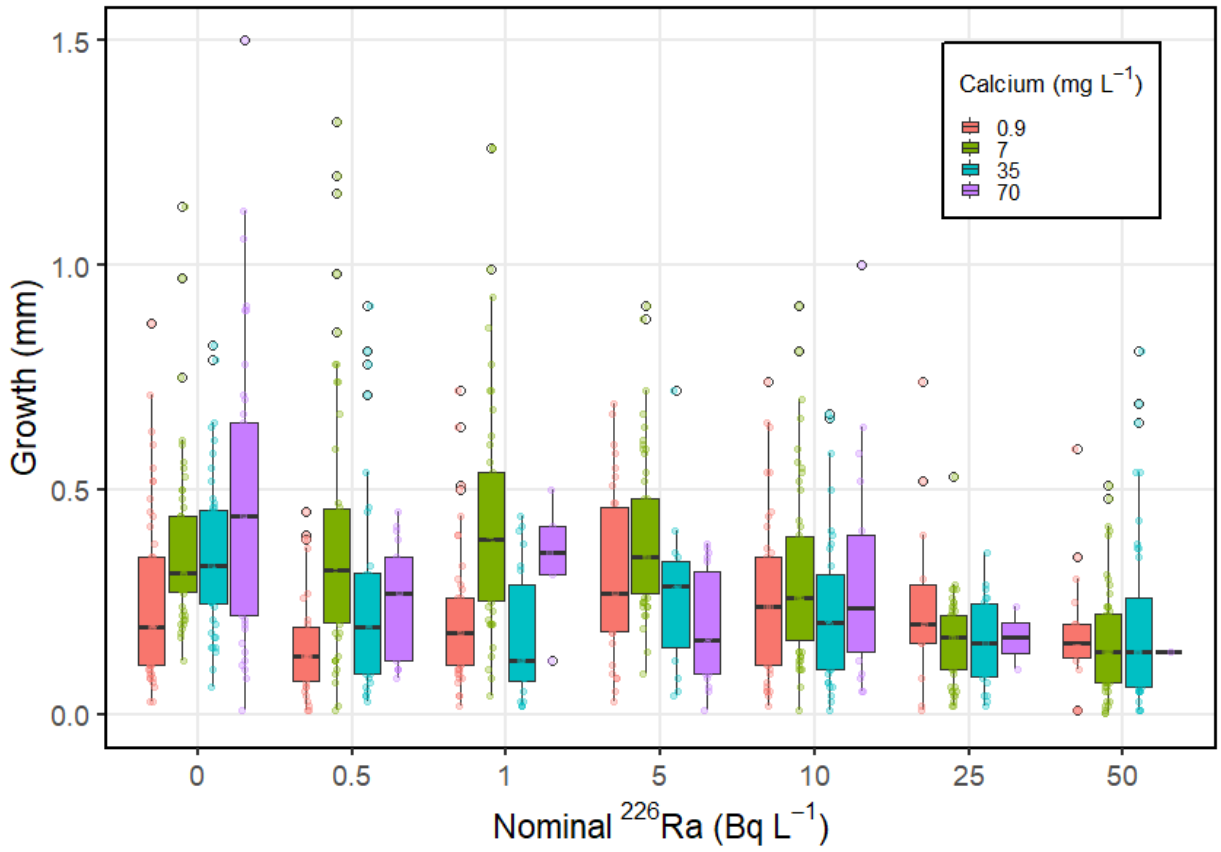


Figure 5.5 Growth in total shell length (mm) of *Sphaerium striatinum* after 28 days of exposure to nominal radium-226 (^{226}Ra) concentrations across varying calcium concentrations. Boxplots represent the median, interquartile range (box), and range (whiskers), with points showing individual replicates.

Figure Notes. Nominal ^{226}Ra treatment concentrations are presented on the x-axis to facilitate comparison among calcium treatments. Statistical analyses were conducted using measured time-weighted average (TWA) ^{226}Ra concentrations to account for activity losses over the exposure period.

5.3.4.4 Reproduction

The GLM used to evaluate the effects of ^{226}Ra exposure and calcium concentration on relative brood size indicated that reproduction declined significantly with increasing ^{226}Ra exposure ($F_{1,414}$ = 81.44, p < 0.001, Figure 5.6). In contrast to previous results, calcium concentration also had a significant positive effect on relative brood size ($F_{1,414}$ = 10.28, p = 0.001), largely driven by a steady increase in relative brood size in the control as a function of calcium

concentration (Figure 5.6). A significant interaction between ^{226}Ra exposure and calcium concentration was observed ($F_{1,414} = 9.83$, $p = 0.002$), indicating that the effect of ^{226}Ra on reproduction varied across calcium treatments. Specifically, the negative effect of ^{226}Ra exposure on relative brood size became more pronounced with increasing calcium concentration.

To further evaluate treatment-level responses, a post-hoc Dunnett's tests were performed separately within each calcium treatment, comparing each ^{226}Ra treatment to their respective controls (0 Bq L^{-1}). Under low calcium conditions, significant reductions were observed at all ^{226}Ra treatments (adjusted $p = 0.05$ to <0.01) except the highest treatment (50 Bq L^{-1}). One exception was the highest treatment of 50 Bq L^{-1} ($p = 0.389$). Under RSW conditions, relative brood size was significantly reduced relative to the control at 5 Bq L^{-1} ($p = 0.012$), 10 Bq L^{-1} ($p = 0.002$), 25 Bq L^{-1} ($p = 0.008$) and 50 Bq L^{-1} ($p = 0.002$). Under moderate calcium conditions, relative brood size was significantly lower than the control at 25 Bq L^{-1}, and 50 Bq L^{-1} ($p = 0.03$ and <0.001, respectively). Under high calcium conditions, reductions in relative brood size were observed at lower radium concentrations. Relative brood size was significantly lower than the control at 0.5 Bq L^{-1} ($p = 0.001$), 1 Bq L^{-1} ($p = 0.03$), 5 Bq L^{-1} ($p < 0.001$) and 10 Bq L^{-1} ($p < 0.001$). Relative brood size could not be evaluated at concentrations > 10 Bq L^{-1} in the high calcium experiment.

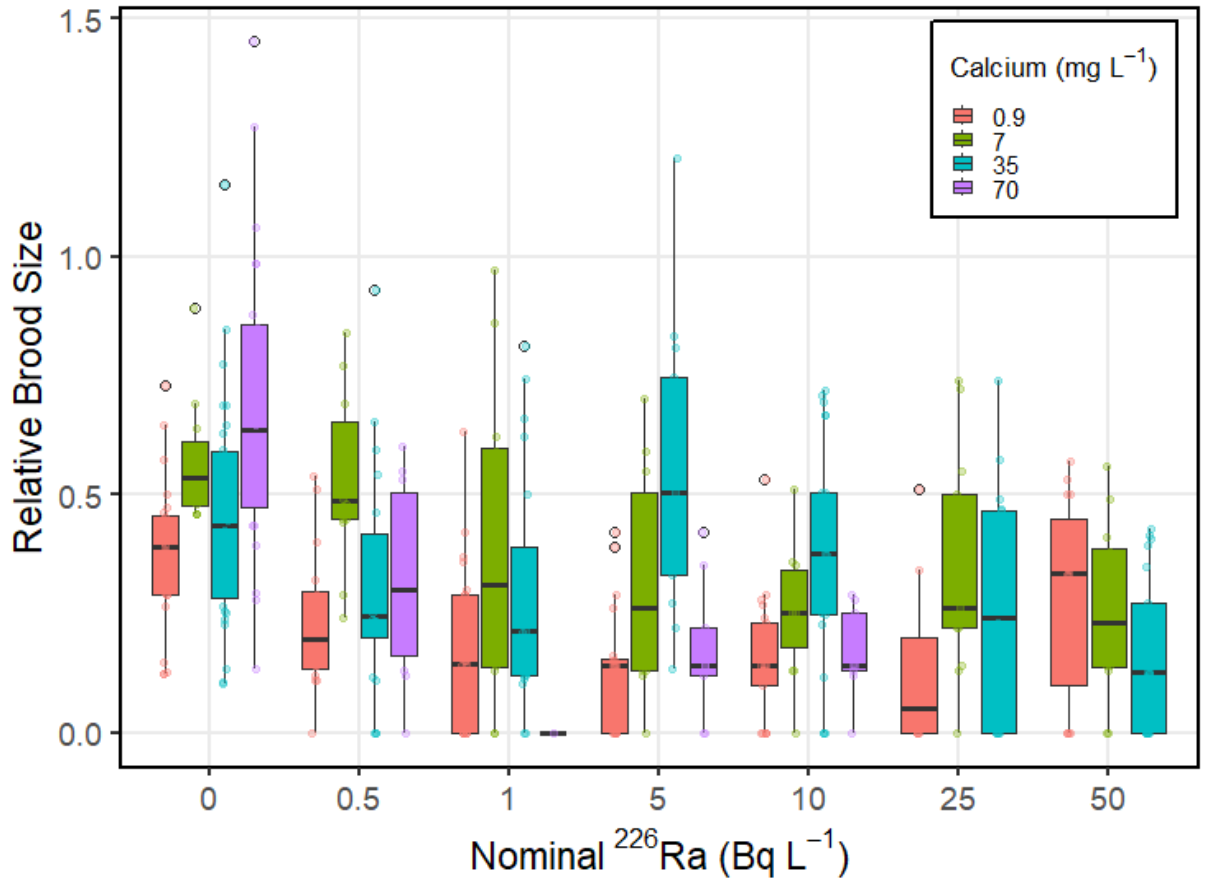


Figure 5.6 Relative brood size of *Sphaerium striatinum* after 28 days of exposure to nominal radium-226 (^{226}Ra) concentrations across varying calcium concentrations. Boxplots represent the median, interquartile range (box), and range (whiskers), with points showing individual replicates.

Figure Notes. Nominal ^{226}Ra treatment concentrations are presented on the x-axis to facilitate comparison among calcium treatments. Statistical analyses were conducted using measured time-weighted average (TWA) ^{226}Ra concentrations to account for activity losses over the exposure period.

5.3.4.5 Endpoint sensitivity

Endpoint sensitivity varied among biological responses, with growth and reproduction generally exhibiting lower effect thresholds than survival and burrowing (Table 5.3). Based on TWA concentrations, reproduction showed the lowest LOEC values across treatments (e.g., 0.26 Bq L^{-1} in the low Ca treatment and 0.41 Bq L^{-1} in the high Ca treatment), followed by growth (e.g., LOECs of 0.48 and 0.41 Bq L^{-1} in moderate and high Ca, respectively). In contrast, survival

and burrowing were less sensitive, with LOECs often occurring at similar or higher concentrations across calcium treatments (e.g., survival LOECs of 0.26–0.41 Bq L^{-1} and consistent burrowing NOECs of 27.5–34.1 Bq L^{-1}). Survival responses also showed limited variation among calcium treatments, with LOECs consistently at or near nominal concentrations of 0.5 Bq L^{-1}. In several cases, NOEC values were equal to or greater than corresponding LOEC values, and responses were not strictly monotonic across the exposure gradient. Effects were sometimes observed at intermediate concentrations but not at higher concentrations, and threshold values varied among calcium treatments and endpoints.

Table 5.3 Estimated no-observed-effect concentrations (NOEC) and lowest-observed-effect concentrations (LOEC) for chronic toxicity endpoints of *Sphaerium striatinum* across varying calcium treatments, derived from Dunnett's post-hoc comparisons to control using time-weighted average (TWA) radium-226 (^{226}Ra) concentrations (Bq L^{-1}).

Calcium Treatment	[Ca] mg L^{-1}	Survival		Burrowing	Growth		Reproduction	
		NOEC	LOEC	NOEC	NOEC	LOEC	NOEC	LOEC
Low	0.9	0.6	0.3	27.5	>27.5	-	-	0.3
RSW	7.0	> 21.8	-	21.8	5.1	11.8	0.4	2.8
Moderate	35	29.4	0.3	29.4	2.6	0.5	5.5	13.5
High	70	-	0.4	34.1	-	0.4	-	0.4

Table Notes. Missing values ("-") were not clearly defined.

5.4 DISCUSSION

Dose modelling exercises frequently identify ^{226}Ra as a key contributor to total dose in aquatic systems downstream of uranium mining operations (Goulet et al. 2022). External exposure pathways are generally minor for ^{226}Ra, with radiotoxic effects to aquatic organisms primarily occurring through internal exposure following uptake and ingestion. Radium-226 can be accumulated from both water and dietary sources; however, in aqueous systems, bioavailability is commonly described using transfer factors and geochemical speciation approaches (Goulet et al., 2022b; Madruga et al., 2001; Wiramanaden et al., 2015). The free ion activity model (FIAM) is

often applied to predict metal bioavailability, with the free ion form considered the most bioavailable species (Brown & Markich, 2000). Consistent with this framework, aqueous speciation modelling in the present study indicated that free $^{226}Ra^{2+}$ was the dominant dissolved species, accounting for >80% of total dissolved ^{226}Ra, with only minor contributions from $RaSO_4(aq)$ and $RaHCO_3^+$ (each <10%). Dissolved organic carbon had minimal influence on ^{226}Ra speciation, consistent with previous findings (see Chapter 4).

A substantial fraction of dissolved ^{226}Ra was removed from solution during exposure, indicating strong partitioning to solid phases (see Chapter 4). Losses from solution were largely proportional to initial concentrations, consistent with rapid sorption processes, and aligning with previous experimental and field observations showing that up to ~90% of ^{226}Ra can be rapidly removed from the water column and associated with surficial sediments (Beneš et al., 1984; Hesslein and Slavicek, 1984). Although aqueous ^{226}Ra dynamics were strongly governed by initial concentrations, they were also modified by calcium-dependent partitioning processes. Calcium exerted a measurable influence on ^{226}Ra partitioning, with increasing Ca concentrations reducing the extent of ^{226}Ra removal from solution. This is consistent with studies showing that Ca^{2+} can inhibit the sorption of other divalent cations through competition for binding sites, reflecting their similar charge and chemical properties (Sugiura et al., 2021; Zachara et al., 1991). Because Ca^{2+} is typically present at much higher concentrations than $^{226}Ra^{2+}$, competitive interactions may reduce partitioning of ^{226}Ra to solid phases and increase its persistence in the dissolved phase. The higher TWA concentrations under elevated calcium conditions are consistent with this interpretation.

Radium-226 accumulated in both soft tissues and shells of *Sphaerium striatinum* in a concentration-dependent manner, with substantially greater accumulation observed in shells.

Although ^{226}Ra is a non-essential element, this uptake is consistent with the geochemical similarity between $^{226}Ra^{2+}$ and Ca^{2+}, which facilitates substitution of $^{226}Ra^{2+}$ for Ca^{2+} into the calcium carbonate structures in shells (Jeffree & Simpson, 1984). In addition to shell incorporation, studies have shown that $^{226}Ra^{2+}$ and Ca^{2+} may co-localize within granular deposits in bivalve soft tissues, reflecting shared biochemical pathways of uptake and intracellular storage (Jeffree, 1988; Jeffree & Simpson, 1984). The calcium content of *S. striatinum* has been shown to increase with Ca concentrations in surrounding water (Mackie & Flippance, 1983), suggesting that environmental Ca availability can directly influence mineralization processes and, consequently, Ra partitioning to tissues. Jeffree and Simpson (1986) observed that ^{226}Ra uptake in mussel tissue was inversely proportional to Ca concentration in water, a relationship that has subsequently been observed in freshwater bivalves across calcium and hardness gradients (Doering & Bollhöfer, 2017). Once incorporated, ^{226}Ra appears to be retained for extended periods, with negligible loss from tissue observed over long depuration periods in multiple bivalve species (Brenner et al., 2007; Jeffree & Simpson, 1986), indicating a long biological half-life and limited elimination. However, retention may vary among tissues, with studies reporting tissue-specific differences in ^{226}Ra turnover and elimination kinetics, suggesting that internal redistribution may influence the long-term fate of ^{226}Ra within organisms (Donaher et al., 2023). Although variability among treatments in this study limited the identification of consistent trends, and several endpoints exhibited non-monotonic responses, patterns in the data broadly support the hypothesized dual role of Ca in ^{226}Ra bioaccumulation. In soft tissues, increased Ca was associated with reduced ^{226}Ra accumulation, consistent with competitive inhibition of ^{226}Ra uptake at biological membranes. In shell tissues, increased Ca was associated with increased ^{226}Ra accumulation, consistent with calcium-mediated

reductions of ^{226}Ra sorption to mineral surfaces (i.e., sand), which increased dissolved ^{226}Ra in the water column (see Chapter 4).

These interacting processes have important implications for dose. As expected, total dose rates increased with increasing aqueous ^{226}Ra concentrations and estimates were not sensitive to assumptions regarding sediment partitioning. Inclusion of sediment using generic ERICA-derived distribution coefficients slightly increased dose estimates, whereas mass-balance-derived sediment concentrations indicated no sediment contribution under the observed conditions. This highlights the importance of water exposure pathways. Regardless of the approach taken, total dose rates to organisms were consistently elevated, with many estimates exceeding commonly applied screening benchmarks. Screening thresholds derived from compilations of radiation effects data are typically on the order of 10 μGy h^{-1}, below which population-level effects are considered unlikely (Brown et al., 2008), and 400 μGy h^{-1} as a protective upper bound for aquatic organisms (Carvalho et al., 2014). In the present study, dose estimates exceeded the lower screening threshold in almost all estimates and, under some scenarios (e.g., 50 Bq L^{-1} in 7 mg L^{-1} Ca; 10 Bq L^{-1} in 70 mg L^{-1} Ca), exceeded the higher benchmark, indicating the potential for radiological effects under elevated ^{226}Ra exposure conditions, although these estimates remain dependent on assumptions regarding occupancy, sediment partitioning, and dose model parameterization.

An important limitation of the dose assessment is that whole-organism activity concentrations included both soft tissue and shell activity. This approach was necessary because the ERICA Tool requires whole-organism activity concentrations and does not distinguish among tissue compartments (Brown et al., 2008). However, because alpha particles have a very short penetration range, shell-associated ^{226}Ra may contribute less to soft-tissue irradiation than activity incorporated directly within biologically active tissues. Consequently, the dose estimates presented

here may represent a conservative estimate of biologically effective internal exposure. Alternatively, dose estimates could be calculated separately for soft tissue and shells.

Given that internal exposure is the primary driver of radiotoxicity for ^{226}Ra due to its high linear energy transfer and RBE (IAEA, 2014), the observed calcium-mediated shifts in uptake and partitioning may influence dose in complex ways. Specifically, while calcium may reduce uptake to biologically active soft tissues through competitive interactions, it also increases the persistence of dissolved ^{226}Ra by inhibiting sorption to particulate phases. As a result, under some conditions, elevated calcium may not reduce, and may even slightly increase, the overall dose. This pattern contrasts with expectations based on the FIAM, which predicts reduced toxicity with increasing calcium, and highlights the importance of considering both exposure concentration and partitioning processes when evaluating radionuclide bioavailability and risk.

The observed bioaccumulation indicates that ^{226}Ra is taken up and retained within tissues, raising radiological concern due to its emission of high LET alpha particles. Based on the chemical similarity of Ra^{2+} to Ca^{2+} and evidence from other alkaline earth and divalent metals, the hypothesis was that higher Ca concentrations would be expected to reduce ^{226}Ra toxicity through competitive inhibition of biological uptake (e.g., Carroll et al., 1979; Welsh et al., 2000). However, the observed patterns in *S. striatinum* survival did not consistently support this hypothesis. Survival was lowest in the high Ca treatment at most ^{226}Ra nominal treatments, and no clear monotonic relationship between Ca concentration and ^{226}Ra toxicity was evident across treatments. This apparent inconsistency may reflect competing effects of Ca on ^{226}Ra exposure and uptake, whereby higher Ca concentrations reduce biological uptake through competitive inhibition, but may also increase dissolved ^{226}Ra concentrations by reducing sorption to mineral phases, as demonstrated by the higher TWA concentrations in the high Ca experiment, resulting in no net change in toxicity.

However, the absence of significant calcium × ^{226}Ra interactions for survival indicates that this interpretation should be considered a working hypothesis rather than a demonstrated mechanism.

Behavioural endpoints are commonly used in ecotoxicological studies as early indicators of sublethal stress, as changes in behaviour can occur rapidly in response to contaminant exposure and may precede effects on survival or reproduction (Melvin & Wilson, 2013). In freshwater bivalves, stress is typically expected to result in altered burrowing activity, most commonly expressed as reduced burrowing or delayed reburial, reflecting avoidance behaviour or impaired physiological function (e.g., Heinonen et al., 2001). In the present study, burrowing behaviour of *S. striatinum* was significantly affected by both ^{226}Ra exposure and Ca concentration, with reduced burrowing observed at higher concentrations. However, substantial variability among treatments limited the identification of distinct threshold responses, suggesting that effects occurred as a gradual decline rather than an abrupt behavioural shift. These findings indicate that burrowing behaviour is a less sensitive endpoint for ^{226}Ra exposure, reflecting subtle physiological stress responses that may not translate directly into clear dose-dependent thresholds.

Growth and reproductive output of *S. striatinum* both declined with increasing ^{226}Ra exposure, with responses varying among calcium treatments, indicating that water chemistry modified the biological response to exposure. Interpretation of both endpoints is constrained by the fact that they were assessed only in surviving individuals and further complicated under high-calcium conditions by control survival (76%), which fell slightly below the recommended test acceptability criterion. Mortality reduced sample size and statistical power, and selective survival of more tolerant individuals may have biased estimates, particularly at higher exposure levels, leading to potential underestimation of population-level effects. The effects of ^{226}Ra on growth and reproduction are likely mediated by its chemical similarity to Ca^{2+}, enabling uptake via calcium

transport pathways and interference with Ca-dependent physiological processes, including ion regulation, reduced growth and filtration rates, and altered reproductive performance under contaminant stress (Augspurger et al., 2003; Bringolf et al., 2022; Wang et al., 2016). While calcium supported higher baseline reproductive output, it did not confer protection under exposure conditions. Instead, the negative effects of ^{226}Ra on both growth and reproduction were maintained, and in some cases became more pronounced at higher calcium concentrations.

Overall, growth and reproduction were the most sensitive endpoints, showing lower effect thresholds than survival and burrowing under both TWA and nominal concentrations. In contrast, survival and burrowing responses were more consistent across calcium treatments, with similar NOECs and LOECs and limited sensitivity. Non-monotonic responses were observed for several endpoints, with NOECs sometimes exceeding LOECs, indicating variable and gradual effects rather than clear concentration–response relationships. These patterns indicate that responses to ^{226}Ra exposure were variable and gradual, with limited evidence of clear dose–response relationships for some endpoints, reflecting competing biological and geochemical mechanisms. Increased calcium can reduce ^{226}Ra uptake through competitive interactions at biological membranes, while simultaneously increasing dissolved ^{226}Ra concentrations by limiting sorption to mineral phases, thereby sustaining aqueous exposure. As a result, the net effect of calcium is not a uniform reduction in toxicity, but a modification of dose–response relationships, including shifts in apparent sensitivity toward lower ^{226}Ra concentrations under elevated calcium conditions. Reproduction appeared particularly sensitive to these changes. Sphaeriids brood developing young within structures associated with their inner gills, and exposure through the gills via filter-feeding behaviour may also plausibly increase exposure of brooded embryos (Mackie, 2007). Overall, these findings suggest that calcium modifies ^{226}Ra toxicity in a non-linear manner and may not

consistently act as a protective factor under the exposure conditions evaluated in this study. This highlights the importance of incorporating both uptake dynamics and geochemical controls on exposure in assessments of radionuclide effects.

5.5 CONCLUSION

This study demonstrates that calcium modifies ^{226}Ra behaviour through coupled geochemical and biological processes, altering bioaccumulation, dose, and toxicity in *Sphaerium striatinum*. Higher calcium increased the persistence of dissolved ^{226}Ra by limiting sorption to inorganic particles, resulting in sustained aqueous exposure. Consequently, calcium did not consistently mitigate effects; instead, it reshaped dose–response relationships, with increased sensitivity observed for some endpoints at elevated calcium. Bioaccumulation patterns indicated preferential partitioning to shell, while dose estimates showed that waterborne exposure dominated under the observed conditions, with limited contribution from sediment. However, because dose calculations included activity associated with both soft tissues and shells, and alpha particles have a limited penetration range, the biological relevance of shell-associated activity to effective internal dose remains uncertain and warrants further investigation.

Growth and reproduction were sensitive endpoints, reflecting both chemical and radiological stress and associated energetic costs. Together, these findings highlight that water chemistry can alter not only the magnitude but also the apparent thresholds of radionuclide toxicity, underscoring the need to incorporate site-specific geochemical conditions into environmental risk assessments of ^{226}Ra. More broadly, the results suggest that radiological protection frameworks based solely on dissolved concentrations or generic transfer parameters may not fully capture the influence of water chemistry on radionuclide exposure and effects.

Future research should focus on uptake rates, tissue-specific dosimetry, radionuclide partitioning among biological compartments, and the kinetic and mechanistic interactions between calcium availability, bioaccumulation, and radiological effects. Because toxicity is ultimately governed by the balance between radionuclide uptake and detoxification, depuration, and repair processes, a better understanding of these rates is needed to improve ecological risk assessments of naturally occurring radionuclides.

6 CHAPTER 6: GENERAL CONCLUSION

Radium-226 (^{226}Ra) is a naturally occurring radionuclide that is ubiquitous in the environment, yet its behaviour, bioavailability, and ecological effects in freshwater systems remain incompletely understood. This knowledge gap is particularly important in Canada, where expanding mining activities and the co-occurrence of ^{226}Ra in a variety of mineral deposits have the potential to increase environmental releases. Despite its inclusion in regulatory frameworks, current management approaches for ^{226}Ra rely largely on assumed technology-based effluent limits, with limited consideration of ecotoxicological data or site-specific environmental conditions. Without adequate water quality guidelines, it is challenging to improve best available treatment technologies that are economically achievable or designing adequate tailings management facilities. The overarching objective of this thesis was to improve understanding of the occurrence, fate, bioaccumulation, and toxicity of ^{226}Ra in freshwater systems, with particular emphasis on the sensitivity of *Sphaerium striatinum* to ^{226}Ra exposure and the role of water chemistry in modifying toxicity.

6.1 Study Outcomes

6.1.1 Chapter 2

The objective of Chapter 2 was to evaluate the occurrence and distribution of ^{226}Ra in mining effluent across multiple sectors in Canada. The approach utilized data reported under federal MDMER regulations. Releases of ^{226}Ra were evaluated relative to an estimated regional background concentration and upper tolerance limit (UTL) for Canadian freshwater systems. Across mining sectors in Canada, ^{226}Ra was present in treated effluents, but concentrations were generally comparable to or below the estimated UTL of background levels (21.7 mBq L^{-1}), with

only occasional exceedances. Although exceedances of natural background do not necessarily translate to effects in receiving environments, they are reasons for potential interest.

Importantly, releases were not limited to uranium mining and milling operations, from which mining effluents are treated with barium chloride to limit releases. Releases were also observed across other mining sectors (e.g., non-ferrous mines), challenging the common assumption that uranium mining is the dominant source of ^{226}Ra to aquatic environments. These findings highlight that ^{226}Ra contamination is a broader issue associated with mining activities involving naturally occurring uranium-bearing ore bodies and reinforce the need for improved understanding of its environmental behaviour and effects, particularly as mining expands to meet demand for critical minerals. While operational effluent releases were observed across multiple mining sectors, releases of ^{226}Ra from tailings and waste rock facilities may become more important following closure, particularly at uranium mines and mills when active effluent treatment ceases and legacy mine waste become a dominant source of ^{226}Ra if mitigation measures to limit seepages are not adequately implemented.

6.1.2 Chapter 3

The objective of Chapter 3 was to generate a coherent set of ^{226}Ra bioaccumulation and chronic toxicity data using the freshwater bivalve *Sphaerium striatinum*. Clams were exposed for a duration of 28-days to reconstituted soft water dosed with seven nominal ^{226}Ra activity concentrations (0.1, 0.5, 1.0, 5, 10, 25 and 50 Bq L^{-1}) and a control (0 Bq L^{-1}). Bioaccumulation was quantified in both soft tissues and shells, while biological endpoints included survival, burrowing behaviour, growth, and reproduction. Time-weighted average (TWA) concentrations were used to estimate ^{226}Ra exposure to clams as ^{226}Ra activity concentrations decreased

substantially between static renewals. That is, approximately 90% loss of ^{226}Ra was observed, which was attributed to adsorption to the sand substrate used in the tests.

Results demonstrated that ^{226}Ra is readily taken up and accumulated in both soft tissues and shells in a concentration-dependent manner. Radium-226 accumulated to a greater extent in shell than in soft tissue, consistent with the geochemical similarity between Ra^{2+} and Ca^{2+}, which facilitates substitution of Ra^{2+} into calcium carbonate during biomineralization (Jeffree & Simpson, 1984). Once incorporated into tissues and shell, ^{226}Ra appears to be eliminated slowly, with previous studies reporting minimal loss during extended depuration periods in bivalves, suggesting limited elimination and potentially long biological half-lives, although retention may vary among species and tissues because of differences in uptake, storage, and turnover processes (Brenner et al., 2007; Donaher et al., 2023; Jeffree & Simpson, 1986). Bioaccumulation factors for *S. striatinum* were generally low (<1,000 L kg^{-1} dw; US EPA, 1995) and fell within the range reported for other freshwater invertebrates exposed to aqueous ^{226}Ra. Soft tissue BAFs were comparable to values reported for *Daphnia magna* (Lacroix-Durand et al., 2025), while shell BAFs were similar to those observed in *Lymnaea stagnalis* (Van der Borght, 1963). Overall, these findings suggest that *S. striatinum* accumulates ^{226}Ra to a similar extent as other freshwater invertebrates, with shell acting as a stronger sink for ^{226}Ra than soft tissue despite relatively low overall bioaccumulation potential under aqueous exposure conditions.

Chronic toxicity testing identified growth and reproduction as sensitive endpoints, with effect concentration (EC_{10}) values of 4.1 and 0.37 Bq L^{-1}, respectively, based on TWA ^{226}Ra exposure concentrations. Survival and burrowing behaviour were not significantly affected by ^{226}Ra exposure. These results indicated that *S. striatinum* exhibits relatively high sensitivity to chronic ^{226}Ra exposure that is equal to or greater than that reported for other freshwater taxa

evaluated to date. Reduced growth in *C. dilutus* was observed at 25 Bq L^{-1} (Lacroix-Durand et al., 2024), while *Raphidocelis subcapitata* exhibited an EC_{20} of 14 Bq L^{-1} for cell density (Desreac, 2025), and early life stage survival of the great pond snail *Lymnaea stagnalis* had a lowest-observed-effect concentration (LOEC) of 26.7 Bq L^{-1} (Guimard et al., 2026). Survival of *D. magna* was reduced at nominal concentrations of 50 Bq L^{-1} (Lacroix-Durand et al., 2025), while growth effects have also been reported in fathead minnows following dietary exposure to ^{226}Ra-contaminated feed (Mothersill et al., 2013).

Collectively, these studies indicate that somatic effects associated with ^{226}Ra exposure generally occur within the low- to mid-Bq L^{-1} range across freshwater taxa. In contrast, reproduction in *S. striatinum* was affected at comparatively lower concentrations, suggesting that reproductive processes may represent a particularly sensitive endpoint for chronic ^{226}Ra exposure. This heightened sensitivity may be related to the reproductive biology of sphaeriid clams, in which developing embryos are brooded within structures associated with the inner gills, potentially increasing exposure of embryos to contaminants taken up across maternal tissues and increasing susceptibility to brood loss under physiological stress (Mackie, 2007; Meier-Brook, 1969).

Typical background ^{226}Ra concentrations in freshwater systems are generally low, ranging from approximately 4.1–13.7 mBq L^{-1} in streams and 5.0–9.0 mBq L^{-1} in lakes (Fesenko et al., 2014). Overall, the findings suggest that direct waterborne exposure to ^{226}Ra at environmentally relevant concentrations (i.e., concentrations typical of most natural freshwater systems) poses limited risk to freshwater bivalves, and that ecological effects are more likely to arise from chronic exposure, bioaccumulation, or sediment-mediated pathways. These results provide valuable data for environmental risk assessments of radium in effluent-affected systems, particularly in mining regions where ^{226}Ra may be co-released with other divalent metals. Given the chemical similarity

between calcium (Ca^{2+}) and radium (Ra^{2+}), future studies should further evaluate how water chemistry, particularly calcium concentrations, influences the chronic toxicity, bioavailability, and partitioning behaviour of ^{226}Ra under environmentally relevant freshwater conditions. Additional research examining interactions with sediments, multiple sentinel species, and co-occurring contaminants would improve understanding of the environmental fate and ecological risks of ^{226}Ra under realistic exposure scenarios. Together, these research needs highlight the importance of integrated approaches that consider geochemical, biological, and ecological processes across multiple levels of organization.

6.1.3 Chapter 4

The objective of Chapter 4 was to evaluate the influence of mineral phases, calcium concentration, and organic matter content on the partitioning of ^{226}Ra over 48 hours. The approach used adsorption experiments with a tiered design to assess the influence of the various components: solution-only, solution + sand, solution + sand + organic matter. Tests were conducted across three nominal ^{226}Ra activity concentrations (1, 5, and 50 Bq L^{-1}) and four calcium levels (0.9, 7, 35, and 70 mg L^{-1}) representative of freshwater systems both affected and unaffected by metal-mining effluent. Batch sorption experiments were also conducted across three nominal ^{226}Ra activity concentrations (1, 5, and 50 Bq L^{-1}) in reconstituted soft water to determine whether quartz and kaolinite provide binding sites for ^{226}Ra.

In the solution-only treatments, dissolved ^{226}Ra concentrations remained stable over the 48-h exposure period across all ^{226}Ra and Ca combinations, indicating limited precipitation or removal from solution under the experimental water chemistry conditions. Aqueous speciation modelling indicated that ^{226}Ra occurred predominantly as the free divalent cation ($^{226}Ra^{2+}$; ~70%), followed by $RaHCO_3^+$ (~20%), with smaller contributions from $RaSO_4(aq)$ (~6%) and $RaCl^+$ (<1%). This

predominance of dissolved Ra^{2+} is consistent with observations from natural freshwater systems, where ^{226}Ra typically occurs primarily as a divalent cation (Fesenko et al., 2014). Radium speciation is an important determinant of its mobility and bioavailability in aquatic systems, as soluble chloride and nitrate complexes may enhance persistence in solution, whereas carbonate- and sulfate-associated species may reduce solubility under some geochemical conditions (Ames et al., 1983; Langmuir & Riese, 1985).

The addition of sand resulted in rapid and substantial removal of dissolved ^{226}Ra from solution, particularly under low-calcium conditions. Subsequent mineral-specific experiments demonstrated that this removal was driven almost entirely by kaolinite rather than quartz, despite quartz being the dominant component of the experimental sand substrate. Sorption of ^{226}Ra to kaolinite was rapid and extensive (>90% removal; K_d = 49–62 L kg^{-1}), whereas sorption to quartz was negligible (K_d < 0.6 L kg^{-1}). These findings are consistent with previous studies reporting greater affinity of ^{226}Ra for clay minerals relative to quartz and other framework silicates (Beneš et al., 1985; Reinoso-Maset & Ly, 2016; Robin et al., 2017), likely due to the higher surface area, permanent negative charge, and greater cation exchange capacity of clay minerals (Davis & Kent, 1990). The linear partitioning observed across the tested concentration range further suggests that sorption sites were not saturated under the experimental conditions and that ^{226}Ra partitioning was governed primarily by ion exchange or surface complexation processes.

The particulate algal organic matter evaluated in this study played only a minor direct role in ^{226}Ra sorption under circumneutral oxic conditions, consistent with WHAM modelling and previous studies demonstrating weak association between Ra^{2+} and organic phases relative to mineral substrates (Rachkova et al., 2010; Thiry & Van Hees, 2008). However, organic matter may indirectly influence ^{226}Ra mobility by promoting reducing conditions that facilitate dissolution

of Fe- and Mn-(oxy)hydroxides and the remobilization of previously sorbed ^{226}Ra (Chellam & Clifford, 2002; Thiry & Van Hees, 2008). These findings demonstrate that ^{226}Ra mobility is governed by dynamic interactions among mineralogy, redox conditions, and water chemistry, complicating predictions of transport and bioavailability in aquatic systems.

The presence of calcium (Ca^{2+}) further modified ^{226}Ra partitioning behaviour by competing for sorption sites on mineral surfaces, thereby reducing ^{226}Ra adsorption and increasing its persistence in the aqueous phase. This behaviour is consistent with the chemical similarity between Ca^{2+} and Ra^{2+} and agrees with previous studies demonstrating that major cations play an important role in controlling ^{226}Ra sorption and mobility in natural waters (Beneš et al., 1984, 1985; Langmuir & Riese, 1985).

Overall, the environmental fate of ^{226}Ra was shown to be strongly influenced by mineralogical composition and aqueous geochemistry. Sorption experiments demonstrated that even small fractions of reactive clay minerals can dominate ^{226}Ra partitioning in sandy substrates, substantially reducing dissolved concentrations and potential bioavailability, whereas quartz exhibits negligible sorption capacity and may promote greater ^{226}Ra mobility in aquatic systems.

6.1.4 Chapter 5

The objective of Chapter 5 was to evaluate the combined effects of calcium on ^{226}Ra bioaccumulation, dose, and toxicity in the freshwater fingernail clam *Sphaerium striatinum*, including assessment of how calcium modifies dose–response relationships through competing geochemical and biological mechanisms. Controlled laboratory experiments were conducted using waters varying in calcium concentration (0.9, 7, 35, and 70 mg L^{-1}) dosed with six nominal ^{226}Ra activity concentrations (0.5, 1.0, 5, 10, 25, and 50 Bq L^{-1}) and a control (0 Bq L^{-1}). Aqueous ^{226}Ra concentrations were characterized using TWA, while bioaccumulation was quantified in both soft

tissue and shell. Dose rates were estimated using multiple approaches incorporating different assumptions regarding water and sediment occupancy and sediment partitioning. Survival, burrowing behaviour, growth, and reproduction were evaluated as biological endpoints.

A key contribution of this research is the demonstration that calcium exerts a complex and non-linear influence on ^{226}Ra bioaccumulation, dose, and toxicity. While calcium is often assumed to reduce metal toxicity through competitive inhibition, this study showed that its effects on ^{226}Ra are more nuanced. Increased calcium concentrations reduced sorption to mineral phases, leading to higher dissolved ^{226}Ra concentrations and sustained aqueous exposure. Although calcium may reduce uptake to biologically active tissues through competition at biological membranes (e.g., Jeffree, 1991; Jeffree & Simpson, 1984, 1986; Sheppard et al., 2006), this effect appeared to be offset by increased exposure, resulting in modified, and in some cases enhanced, biological responses at higher calcium concentrations. These findings challenge simplified assumptions derived from the Free Ion Activity Model (FIAM) that competition between Ca^{2+} and Ra^{2+} alone is sufficient to predict bioaccumulation and toxicity (Brown & Markich, 2000), emphasizes the limitations of the models (Hassler et al., 2004). These results also highlight the importance of coupled geochemical and biological processes influencing dissolved exposure, partitioning, and uptake.

Radium-226 accumulated in both soft tissue and shell in a concentration-dependent manner, with substantially greater accumulation observed in shells. This pattern is consistent with the geochemical similarity between Ra^{2+} and Ca^{2+} and the incorporation of ^{226}Ra into calcium carbonate structures during biomineralization (Jeffree & Simpson, 1984). Previous studies have also demonstrated prolonged retention of incorporated ^{226}Ra in bivalve tissues, suggesting limited elimination and a relatively long biological half-life (Brenner et al., 2007; Jeffree & Simpson,

1986). Although responses varied among treatments, the observed patterns support a dual role of calcium in modifying ^{226}Ra bioaccumulation: increased Ca may reduce uptake to soft tissues through competitive interactions at biological membranes, while simultaneously increasing dissolved ^{226}Ra availability by limiting sorption to mineral phases. Consequently, elevated calcium did not consistently reduce toxicity, highlighting the importance of considering both uptake competition and geochemical controls on aqueous exposure when evaluating radionuclide bioavailability and effects.

Dose estimation further highlighted the importance of exposure pathways in determining ^{226}Ra radiological risk. Although whole-organism dose estimates suggested that waterborne exposure dominated under the conditions evaluated, interpretation should consider that shell-associated ^{226}Ra was included in dose calculations and may contribute less to biologically effective dose than activity accumulated within soft tissues because of the short penetration range of alpha particles. Across all approaches, internal exposure was the dominant contributor to total dose, reflecting the high linear energy transfer and biological effectiveness of alpha radiation emitted by ^{226}Ra (IAEA, 2014). Sediment contributions through external exposure and sediment uptake to dose were minimal under the observed conditions, indicating that waterborne exposure is likely the primary pathway of concern for benthic filter-feeding organisms such as *S. striatinum*. Total dose rates increased with increasing aqueous ^{226}Ra concentrations and frequently exceeded commonly applied radiological screening benchmarks (10 and 400 μGy h^{-1}), indicating the potential for adverse effects under elevated exposure conditions (Brown et al., 2008; Carvalho et al., 2014). These findings are consistent with recent freshwater radiological assessments identifying *S. striatinum* as among the more sensitive freshwater organism groups for ^{226}Ra exposure (Hourtané, 2025), and with modelling studies suggesting that bivalves may accumulate

higher concentrations of ^{226}Ra and experience greater radiological dose relative to other aquatic taxa (Doering et al., 2019). However, the environmental relevance of the observed effects must be considered in the context of typical exposure concentrations. Natural ^{226}Ra concentrations in freshwater systems are generally low, with reported concentrations ranging from approximately 4.1–13.7 mBq L^{-1} in streams and 5.0–9.0 mBq L^{-1} in lakes (Fesenko et al., 2014). These concentrations are substantially lower than the chronic effect concentrations observed in the present study. In contrast, concentrations in mining-influenced receiving environments have been reported to range from approximately 5 to 1,450 mBq L^{-1} (Fesenko et al., 2014), overlapping the lower end of the observed chronic effect range. Consequently, the results suggest that adverse effects to sensitive freshwater bivalves are unlikely under typical background conditions but may become increasingly relevant in contaminated or effluent-influenced environments where ^{226}Ra concentrations are elevated. Collectively, these results demonstrate that assumptions regarding partitioning behaviour, habitat use, and water chemistry can substantially influence dose estimates and radiological risk characterization as recommended by Goulet et al. (2022).

Toxicity responses varied among biological endpoints, with growth and reproduction identified as the most sensitive indicators of chronic ^{226}Ra exposure. These effects likely reflect the efficient uptake and prolonged retention of ^{226}Ra in bivalves, facilitated by continuous filter-feeding activity and the chemical similarity between Ra^{2+} and Ca^{2+}, which enables uptake through calcium transport pathways and incorporation into biological tissues (Jeffree & Simpson, 1984; Langmuir & Riese, 1985). In contrast, survival and burrowing behaviour exhibited more variable and less sensitive responses. Calcium modified toxicity patterns in a non-linear manner, with evidence that competitive inhibition of uptake at biological membranes was offset by increased dissolved ^{226}Ra exposure resulting from reduced sorption to mineral phases. Consequently,

elevated calcium did not consistently reduce toxicity, but instead altered exposure–response relationships and, in some cases, increased apparent sensitivity at lower ^{226}Ra concentrations. Reproductive responses appeared particularly sensitive to these changes, potentially reflecting the brooding strategy of sphaeriid clams, in which developing embryos are retained within structures associated with the inner gills and may therefore be vulnerable to contaminant exposure through maternal uptake pathways (Mackie, 2007).

6.2 Study Implications

Collectively, the findings of this thesis demonstrate that the environmental behaviour and effects of ^{226}Ra are governed by coupled geochemical and biological processes. Mineralogy and calcium concentration interact to control partitioning between dissolved and particulate ^{226}Ra phases, which in turn influences exposure pathways, bioaccumulation, dose, and toxicity. Consequently, the relationship between environmental concentration and biological effects is not fixed but varies according to site-specific geochemical conditions. These findings have important implications for environmental risk assessment, as current frameworks often rely on simplified assumptions that dissolved concentrations alone adequately represent exposure and bioavailability. However, by filtering water samples and focusing primarily on dissolved concentrations, important interactions among sorption, partitioning, and aqueous persistence may not be fully captured.

From a regulatory perspective, the absence of a Canadian Water Quality Guideline for the Protection of Aquatic Life (CWQG-PAL) for ^{226}Ra represents a critical gap. The existing ^{226}Ra effluent limit are derived from a drinking water study conducted in the United States (Hess et al. 1985) and provincial guidelines are currently not derived from ecotoxicological datasets and may not adequately protect sensitive aquatic organisms. As a result, there is currently limited regulatory incentive to improve ^{226}Ra treatment technologies or to incorporate ^{226}Ra-specific considerations

into tailings and effluent management strategies. The toxicity data generated in this thesis, together with improved understanding of ^{226}Ra fate, partitioning, and calcium-modified exposure dynamics, provide an important foundation for the development of scientifically robust, ecotoxicologically derived guidelines. Recent preliminary guideline derivation work by Hourtané (2025) incorporated toxicity data from 15 freshwater species, including five microalgae, one aquatic plant, six invertebrates, and three fish species, across a range of exposure durations, life stages, and biological endpoints. Species sensitivity distribution (SSD) modelling produced a preliminary HC_5 value of 1.94 Bq L^{-1} for ^{226}Ra. This value is broadly comparable to Ontario's Provincial Water Quality Objective (PWQO) of 1.0 Bq L^{-1}, which was historically derived from drinking water objectives rather than ecological effects data (MOEE, 1994), but substantially higher than Saskatchewan's Environmental Quality Guideline (SEQG) of 0.11 Bq L^{-1} (Government of Saskatchewan, 2017), which is based on USEPA effluent criteria (USEPA, 2016) derived from a drinking water study conducted in the United States (Hess et al. 1985). Incorporating exposure- and toxicity-modifying factors, particularly calcium concentration and geochemical partitioning processes, will be essential to ensure that future guidelines remain protective across diverse freshwater systems.

6.3 Uncertainties and Limitations

Several uncertainties and limitations should be acknowledged. First, the estimated regional background concentration and associated UTL developed in Chapter 2 provide useful benchmarks for contextualizing ^{226}Ra concentrations in Canadian mining effluents. However, these values should be interpreted as screening-level tools rather than definitive thresholds for identifying mine-related contamination. Natural ^{226}Ra concentrations can vary substantially among watersheds due to differences in geology, groundwater inputs, and the occurrence of NORM. Consequently, while

the regional background estimates provide context for the current uranium mining regions of Canada, site-specific baseline monitoring remains essential for distinguishing anthropogenic inputs from naturally elevated background concentrations and for accurately assessing potential mine-related impacts.

Furthermore, the release estimates presented in Chapter 2 were derived from effluent monitoring data reported for operating facilities and therefore primarily reflect contemporary operational discharges. These data do not capture potential long-term releases from tailings management facilities, waste rock deposits, or legacy mine sites following closure. Mining activities substantially alter natural geochemical conditions by increasing mineral surface area exposed to weathering, oxygen, and water, potentially accelerating radionuclide mobilization over extended time scales. Consequently, the release estimates presented in Chapter 2 should not be interpreted as representing the full life-cycle environmental contribution of mining activities to ^{226}Ra loading, particularly for mine wastes that may remain reactive for decades or longer following mine closure.

A key limitation of the chronic toxicity studies was the rapid partitioning of dissolved ^{226}Ra from solution to particulate phases, resulting in substantial declines in aqueous concentrations between static renewals. Consequently, TWA concentrations were used to characterize exposure. This approach introduces uncertainty in linking exposure concentrations to biological responses, as true organism exposure likely varied temporally and among exposure pathways. Sediment-associated ^{226}Ra concentrations were not directly measured in this study, and sediment contributions to dose were therefore estimated using partitioning approaches. Although dose modelling identified waterborne exposure as the dominant pathway under the observed conditions,

some uncertainty remains regarding the relative importance of sediment-associated versus dissolved exposure pathways.

In addition, laboratory experiments were conducted under controlled conditions that may not fully capture the complexity of natural systems, including the presence of Fe- and Mn-(hydr)oxides, fluctuating redox conditions, variable dissolved organic carbon, heterogeneous mineralogy, and seasonal changes in water chemistry. Furthermore, the organic matter evaluated in Chapter 4 consisted of autochthonous particulate algal material and therefore may not represent the full range of organic matter encountered in natural freshwater systems. In particular, dissolved organic carbon fractions, including humic and fulvic acids derived from terrestrial sources, were not evaluated. While empirical evidence suggests weak association between ^{226}Ra and organic phases compared to mineral substrates (Rachkova et al., 2010; Thiry and Van Hees, 2008), high concentrations of humic and fulvic acids compared to mineral substrate could lead to increased ^{226}Ra complexation with organic matter. Experimental exposures also evaluated ^{226}Ra in isolation, whereas mining-affected environments often contain complex mixtures of radionuclides, metals, and major ions that may alter bioavailability and toxicity through additive or antagonistic interactions.

Although chronic endpoints were evaluated over a 28-day exposure period, longer-term and multigenerational effects of ^{226}Ra exposure remain uncertain, particularly for reproductive endpoints and internally retained radionuclides with long biological half-lives. Finally, the use of a single species limits the ability to generalize findings across taxa. While *S. striatinum* appears to be among the more sensitive freshwater taxa evaluated for ^{226}Ra exposure, extrapolation of results to broader aquatic communities remains uncertain due to differences in physiology, life history, habitat use, and exposure pathways among taxa.

6.4 Future Directions

Several important areas for future research were identified through this work. First, future research should extend assessment of ^{226}Ra releases beyond operational effluent monitoring to incorporate a life-cycle perspective. Although the present study demonstrated that measurable ^{226}Ra releases occur across multiple mining sectors, the long-term behaviour of radionuclides in mine wastes remains an important knowledge gap. Tailings and waste rock facilities may continue to release ^{226}Ra long after mining operations cease, particularly if mitigation measures implemented progressively fail over time and allow geochemical weathering processes to become active again. Quantifying cumulative or time-integrated releases from operational, closure, and post-closure phases would provide a more comprehensive assessment of radionuclide loading and environmental risk. Such work would also improve understanding of the long-term effectiveness and sustainability of mine waste management strategies and help evaluate environmental risks associated with mine wastes under closure and post-closure conditions, including scenarios where long-term treatment or ongoing management may be required.

Second, reducing uncertainty in exposure characterization should be prioritized through the development of flow-through or semi-static exposure systems capable of maintaining stable dissolved ^{226}Ra concentrations over time, which is currently constrained by the quantity of ^{226}Ra and associated high price of such sources. Future studies should also directly quantify ^{226}Ra concentrations in sediments and porewaters to confirm the low ^{226}Ra contribution from the sediment using mass balance and dose rate modelling.

Further investigation of geochemical controls on ^{226}Ra partitioning and bioavailability is also warranted. In particular, the influence of pH on sorption behaviour, aqueous speciation, bioavailability, bioaccumulation, dose, and toxicity should be evaluated under environmentally

relevant freshwater conditions. The role of Fe- and Mn-(hydr)oxides should also be investigated, as these mineral phases were not present in the current study despite being ubiquitous in natural sediments and potentially important sinks for ^{226}Ra (Beneš et al., 1984, Sajih et al., 2014). Enhanced sorption to these phases may substantially reduce dissolved concentrations and mitigate radiological risk through reduced bioavailability. Future studies should also investigate the influence of dissolved organic matter, particularly humic and fulvic substances, on ^{226}Ra speciation, mobility, bioavailability, and transport. Although particulate organic matter exhibited limited direct sorption of ^{226}Ra under the conditions evaluated in this thesis, dissolved organic matter, if present at high concentrations, may influence radionuclide behaviour through complexation and interactions with mineral surfaces.

Future bioaccumulation studies should further investigate uptake kinetics (Li et al., 2010; Worms & Wilkinson, 2007) and internal partitioning (Campana et al., 2015; Goto & Wallace, 2010) of ^{226}Ra. Analysis of individual organisms rather than pooled composite samples would improve resolution of inter-individual variability, while time-course sampling of tissues and shells would allow characterization of uptake and depuration kinetics (Mahaliyana et al., 2025). Subcellular partitioning studies would also help identify the localization and retention of ^{226}Ra within biological compartments and improve mechanistic understanding of links between accumulation, growth, and reproductive effects (Perceval et al., 2006).

Additional toxicity testing across a broader range of freshwater organisms is needed to improve ecological relevance and support guideline development. Further testing with other sphaeriid species such as *Pisidium* spp. (e.g., Ouedraogo et al., 2025) would help determine whether the high sensitivity observed in *S. striatinum* is representative of the family more broadly, or species-specific. Future studies should also prioritize assessment of chronic reproductive

toxicity across aquatic taxa, as reproduction was identified as the most sensitive endpoint in the present study. Such work would further improve understanding of radionuclide transfer within aquatic food webs, particularly given that ^{226}Ra bioaccumulated in *S. striatinum* and may persist within aquatic environments and benthic food webs over extended periods. Finally, multigenerational studies (e.g., Osborne et al., 2020) are needed to better characterize the long-term ecological consequences of chronic ^{226}Ra exposure. Allowing organisms to reproduce under exposure conditions, while evaluating growth, reproduction, and bioaccumulation in subsequent generations, would provide insight into the potential transgenerational effects, developmental sensitivity, and the persistence of radiological impacts in freshwater populations.

6.5 Closing Statement

In conclusion, this research advances understanding of ^{226}Ra in freshwater systems by linking occurrence, environmental fate, bioaccumulation, dose, and toxicity within a unified geochemical and biological framework. The findings demonstrate that water chemistry and mineralogical composition play critical roles in controlling radionuclide mobility, bioavailability, and ecological effects, and that these interactions must be incorporated into environmental risk assessments that are used in the design of tailings management facilities and in identifying mining effluent treatment requirements. Collectively, this work provides important ecotoxicological data and mechanistic insight to support improved management of ^{226}Ra-contaminated systems and the future development of scientifically robust water quality guidelines for the protection of aquatic life in Canada.

REFERENCES

Abdelouas, A. (2006). Uranium mill tailings: Geochemistry, mineralogy, and environmental impact. *Elements, 2*(6), 335–341. https://doi.org/10.2113/gselements.2.6.335

Aberikae, E. A., Nyantakyi, E. K., Kpeglo, D. O., Abubakar, M., Gbeddy, G., Ackerson, N. O. B., Yeboah, S. I. I. K., Domfeh, M. K., Atta-Darkwa, T., Amankwah, E., & Owusu, M. (2023). Baseline assessment of naturally occurring radionuclides in borehole water of Asikam gold mining community in Ghana. *Scientific African, 20*, e01730. https://doi.org/10.1016/j.sciaf.2023.e01730

Abin-Bazaine, A., Campos Trujillo, A., & Olmos-Marquez, M. (2022). Adsorption isotherms: Enlightenment of the phenomenon of adsorption. In M. Ince & O. Kaplan Ince (Eds.), *Wastewater treatment*. IntechOpen. https://doi.org/10.5772/intechopen.104260

Ahmad, F., Morris, K., Law, G. T. W., Taylor, K. G., & Shaw, S. (2021). Fate of radium on the discharge of oil and gas produced water to the marine environment. *Chemosphere, 273*, 129550. https://doi.org/10.1016/j.chemosphere.2021.129550

Aldridge, D. C., & McIvor, A. L. (2003). Gill evacuation and release of glochidia by *Unio pictorum* and *Unio tumidus* (Bivalvia: Unionidae) under thermal and hypoxic stress. *Journal of Molluscan Studies, 69*(1), 55–59. https://doi.org/10.1093/mollus/69.1.55

Alpen, E. L. (1998). High linear energy transfer radiation effects. In *Radiation biophysics* (pp. 365–392). Elsevier. https://doi.org/10.1016/B978-012053085-4/50016-8

Alves, A. R., & Coutinho, A. D. R. (2019). Life cycle assessment of niobium: A mining and production case study in Brazil. *Minerals Engineering, 132*, 275–283. https://doi.org/10.1016/j.mineng.2018.11.041

Ames, L. L., McGarrah, J. E., & Walker, B. A. (1983). Sorption of trace constituents from aqueous solutions onto secondary minerals: II. Radium. *Clays and Clay Minerals, 31*(5), 335–342. https://doi.org/10.1346/CCMN.1983.0310502

Anderson, K. B. (1977). *Musculium transversum in the Illinois River and an acute potassium bioassay method for the species*. Master's thesis, Western Illinois University.

Anderson, K. B., Sparks, R. E., & Paparo, A. A. (1978). *Rapid assessment of water quality using the fingernail clam, Musculium transversum*. Water Resources Center Research Report No. 133, Project B-097-ILL, University of Illinois.

Angove, M. J., Johnson, B. B., & Wells, J. D. (1997). Adsorption of cadmium (II) on kaolinite. *Colloids and Surfaces A: Physicochemical and Engineering Aspects, 126*, 137–147. https://doi.org/10.1016/S0927-7757(96)03990-8

Antovic, I., & Antovic, N. M. (2011). Concentration factors for radium-226 in the mullet (*Mugil cephalus*) from the South Adriatic Sea. *Journal of Radioanalytical and Nuclear Chemistry, 290*(1), 31–37. https://doi.org/10.1007/s10967-011-1087-x

Agency for Toxic Substances and Disease Registry (ATSDR). (1990). *Toxicological profile for radium*. U.S. Environmental Protection Agency.

Arthur, J. W., West, C. W., Allen, K. N., & Hedtke, S. F. (1987). Seasonal toxicity of ammonia to five fish and nine invertebrate species. *Bulletin of Environmental Contamination and Toxicology, 38*(2), 324–331. ASTM International. (2020). *Standard test method for radium-226 in water by gamma-ray spectrometry* (ASTM D7283-17). ASTM International.

Augspurger, T., Keller, A. E., Black, M. C., Cope, W. G., & Dwyer, F. J. (2003). Water quality guidance for protection of freshwater mussels (Unionidae) from ammonia exposure. *Environmental Toxicology and Chemistry, 22*(11), 2569–2575. https://doi.org/10.1897/02-339

Averill, D. W., Moffett, D., Webber, R. T., Whittle, L., & Wood, J. A. (1984). *Removal of radium-226 from uranium mining effluents* (p. 41).

Ball, J. W., & Nordstrom, D. K. (1991). *User's manual for WATEQ4F, with revised thermodynamic database and test cases for calculating speciation of major, trace, and redox elements in natural waters* (Report 91–183). U.S. Geological Survey.

Beekey, M. A., & Karlson, R. H. (2004). Apparent sibling rivalry in the freshwater fingernail clam *Sphaerium striatinum*. *Behavioral Ecology and Sociobiology, 57*(1), 17–22. https://doi.org/10.1007/s00265-004-0835-0

Belgers, J. D. M., Aalderink, G. H., Arts, G. H. P., & Brock, T. C. M. (2011). Can time-weighted average concentrations be used to assess the risks of metsulfuron-methyl to *Myriophyllum spicatum* under different time-variable exposure regimes? *Chemosphere, 85*, 1017–1025. https://doi.org/10.1016/j.chemosphere.2011.07.025

Beneš, P., Borovec, Z., & Strejc, P. (1985). Interaction of radium with freshwater sediments and their mineral components: II. Kaolinite and montmorillonite. *Journal of Radioanalytical and Nuclear Chemistry, 89*(2), 339–351. https://doi.org/10.1007/BF02040598

Beneš, P., Obdrzalek, M., & Cejchanova, M. (1982). The physicochemical forms of traces of radium in aqueous solutions containing chlorides, sulfates and carbonates. *Radiochemical and Radioanalytical Letters, 50*(4), 227–241.

Beneš, P., & Strejc, P. (1986). Interaction of radium with freshwater sediments and their mineral components: IV. Wastewater and riverbed sediments. *Journal of Radioanalytical and Nuclear Chemistry, 99*(2), 407–422. https://doi.org/10.1007/BF02037602

Beneš, P., Strejc, P., & Lukavec, Z. (1984). Interaction of radium with freshwater sediments and their mineral components: I. Ferric hydroxide and quartz. *Journal of Radioanalytical and Nuclear Chemistry, 82*(2), 275–285. https://doi.org/10.1007/BF02037050

Berner, R. A. (1980). *Early diagenesis: A theoretical approach*. Princeton University Press.

Berthelot, D., Place-Hoskie, D., Willems, D., & Black, K. (2019). Elliot Lake, Ontario uranium mines: A legacy perpetual care case study. In *Proceedings of the 13th International Conference on Mine Closure*. https://doi.org/10.36487/acg_rep/1915_92_berthelot

Bespalaya, Y., Bolotov, I., Aksenova, O., Kondakov, A., Paltser, I., & Gofarov, M. (2015). Reproduction of *Pisidium casertanum* (Poli, 1791) in an Arctic lake. *Royal Society Open Science, 2*(1), 140212. https://doi.org/10.1098/rsos.140212

Bezuidenhout, J. (2019). The relationship among naturally occurring radionuclides, geology, and geography: Tsodilo Hills, Botswana. *Journal of Radiation Research and Applied Sciences, 12*(1), 93–100. https://doi.org/10.1080/16878507.2019.1593717

Bland, J. M., & Altman, D. G. (1986). Statistical methods for assessing agreement between two methods of clinical measurement. *The Lancet, 327*(8476), 307–310. https://doi.org/10.1016/S0140-6736(86)90837-8

Bodo, B. A. (1993). *Assessment in concordance between terrestrial ecodistricts and surface water chemistry in central and southeastern Ontario: Research report*. Byron A. Bodo & Associates.

Bollhöfer, A., Brazier, J., Humphrey, C., Ryan, B., & Esparon, A. (2011). A study of radium bioaccumulation in freshwater mussels, *Velesunio angasi*, in the Magela Creek catchment, Northern Territory, Australia. *Journal of Environmental Radioactivity, 102*(10), 964–974. https://doi.org/10.1016/j.jenvrad.2010.04.001

Boryslawskyj, M., Garrood, A. C., Pearson, J. T., & Woodhead, D. (1987). Rates of accumulation of dieldrin by a freshwater filter feeder: *Sphaerium corneum*. *Environmental Pollution, 43*(1), 3–13. https://doi.org/10.1016/0269-7491(87)90163-1

Boryslawskyj, M., Garrood, T., Stanger, M., Pearson, T., & Woodhead, D. (1988). Role of lipid/water partitioning and membrane composition in the uptake of organochlorine pesticides into a freshwater mussel. *Marine Environmental Research, 24*(1–4), 57–61. https://doi.org/10.1016/0141-1136(88)90254-1

Brenner, M., Smoak, J. M., Leeper, D. A., Streubert, M., & Baker, S. M. (2007). Radium-226 accumulation in Florida freshwater mussels. *Limnology and Oceanography, 52*(4), 1614–1623. https://doi.org/10.4319/lo.2007.52.4.1614

Bringolf, R. B., Raines, B. K., Ratajczak, R. E., & Haskins, D. L. (2022). Major ion toxicity to glochidia of common and imperiled freshwater mussel species. *Diversity, 14*(2), 95. https://doi.org/10.3390/d14020095

Brown, J. E., Alfonso, B., Avila, R., Beresford, N. A., Copplestone, D., Pröhl, G., & Ulanovsky, A. (2008). The ERICA tool. *Journal of Environmental Radioactivity, 99*(9), 1371–1383. https://doi.org/10.1016/j.jenvrad.2008.01.008

Brown, P. L., Ekberg, C., & Matyskin, A. V. (2019). On the solubility of radium and other alkaline earth sulfate and carbonate phases at elevated temperature. *Geochimica et Cosmochimica Acta, 255*, 88–104. https://doi.org/10.1016/j.gca.2019.04.009

Brown, P. L., Matyskin, A. V., & Ekberg, C. (2022). The aqueous chemistry of radium. *Radiochimica Acta, 110*(6–9), 505–513. https://doi.org/10.1515/ract-2021-1141

Brown, P., & Markich, S. (2000). Evaluation of the free ion activity model of metal–organism interaction: Extension of the conceptual model. *Aquatic Toxicology, 51*(2), 177–194. https://doi.org/10.1016/S0166-445X(00)00115-6

Campana, O., Taylor, A. M., Blasco, J., Maher, W. A., & Simpson, S. L. (2015). Importance of Subcellular Metal Partitioning and Kinetics to Predicting Sublethal Effects of Copper in Two Deposit-Feeding Organisms. *Environmental Science & Technology*, 49(3), 1806–1814. https://doi.org/10.1021/es505005y

Campbell, P. G. C., Hodson, P. V., Welbourn, P. M., & Wright, D. A. (2022). *Ecotoxicology* (1st ed.). Cambridge University Press. https://doi.org/10.1017/9781108819732

Carroll, J. J., Ellis, S. J., & Oliver, W. S. (1979). Influences of hardness constituents on the acute toxicity of cadmium to brook trout (*Salvelinus fontinalis*). *Bulletin of Environmental Contamination and Toxicology, 22*(1), 575–581. https://doi.org/10.1007/BF02026990

Carvalho, F., Chambers, D., Fesenko, S., Moore, W. S., Porcelli, D., Vandenhove, H., & Yankovich, T. (2014). Environmental pathways and corresponding models. In *The environmental behaviour of radium: Revised edition* (p. 282). International Atomic Energy Agency.

Canadian Council of Ministers of the Environment (CCME). (2007). *A protocol for the derivation of water quality guidelines for the protection of aquatic life (2007)*.

Canadian Nuclear Safety Commission (CNSC). (2014). *Environmental performance of a uranium mine or mill regulated under the Nuclear Safety and Control Act: Based on environmental data associated with operating uranium mines and mills (2000–2012)*.

Canadian Standards Association (CSA). (2022). *Environmental risk assessments at nuclear facilities and uranium mines and mills (CSA N288.6:22)*.

Chandler, J. H., & Marking, L. L. (1975). *Toxicity of the lampricide 3-trifluoromethyl-4-nitrophenol (TFM) to selected aquatic invertebrates and frog larvae* (Investigations in Fish Control No. 62). U.S. Fish and Wildlife Service.

Chautard, C., Beaucaire, C., Gerard, M., Roy, R., Savoye, S., & Descostes, M. (2020). Geochemical characterization of uranium mill tailings (Bois Noirs Limouzat, France) highlighting the U and radium-226 retention. *Journal of Environmental Radioactivity, 218*, 106251. https://doi.org/10.1016/j.jenvrad.2020.106251

Chellam, S., & Clifford, D. A. (2002). Physical–chemical treatment of groundwater contaminated by leachate from surface disposal of uranium tailings. *Journal of Environmental Engineering, 128*(10), 942–952. https://doi.org/10.1061/(ASCE)0733-9372(2002)128:10(942)

Ciparis, S., Phipps, A., Soucek, D. J., Zipper, C. E., & Jones, J. W. (2015). Effects of environmentally relevant mixtures of major ions on a freshwater mussel. *Environmental Pollution, 207*, 280–287. https://doi.org/10.1016/j.envpol.2015.09.023

Clesceri, L. S. (1998). *Standard methods for the examination of water and wastewater* (20th ed.). American Public Health Association, American Water Works Association, & Water Environment Federation.

Clulow, F. V., Davé, N. K., Lim, T. P., & Avadhanula, R. (1998). Radionuclides (lead-210, polonium-210, thorium-230, and thorium-232) and thorium and uranium in water,

sediments, and fish from lakes near the city of Elliot Lake, Ontario, Canada. *Environmental Pollution, 99*(2), 199–213. https://doi.org/10.1016/S0269-7491(97)00187-5

Clulow, F. V., & Pyle, G. G. (1997). Radium-226 equilibrium between water and lake herring (*Coregonus artedii*) tissues attained within fish lifetime: Confirmation of one assumption in the simple linear concentration factor model. *Environmental Pollution, 96*(1), 75–78. https://doi.org/10.1016/S0269-7491(97)00006-7

Davis, J. A., & Kent, D. B. (1990). Surface complexation modeling in aqueous geochemistry. In *Mineral–water interface geochemistry* (pp. 177–260). Mineralogical Society of America.

Desreac, F. (2025). *Radium-226 subcellular fractionation and binding to biomolecules in Chlamydomonas reinhardtii.* Paper presented at the Canadian Ecotoxicity Workshop (CEW), Victoria, BC, Canada.

Desouky, O., Ding, N., & Zhou, G. (2015). Targeted and non-targeted effects of ionizing radiation. *Journal of Radiation Research and Applied Sciences, 8*(2), 247–254. https://doi.org/10.1016/j.jrras.2015.03.003

Doering, C., & Bollhöfer, A. (2017). Water hardness determines radium-226 uptake in the tropical freshwater mussel. *Journal of Environmental Radioactivity, 172*, 96–105. https://doi.org/10.1016/j.jenvrad.2017.03.019

Doering, C., Carpenter, J., Orr, B., & Urban, D. (2019). Whole-organism concentration ratios in freshwater wildlife from an Australian tropical uranium-mining environment and the derivation of a water radiological quality guideline value. *Journal of Environmental Radioactivity, 198*, 27–35. https://doi.org/10.1016/j.jenvrad.2018.12.01

Donaher, S. E., Dunn, R. P., Gonzales, A. K., Wattier, B. D., Powell, B. A., & Martinez, N. E. (2023). Tissue-specific toxicokinetics of aqueous radium-226 in an estuarine mussel, *Geukensia demissa*. *Environmental Science & Technology, 57*(8), 3187–3197. https://doi.org/10.1021/acs.est.2c09421

Donahue, R., Hendry, M. J., & Landine, P. (2000). Distribution of arsenic and nickel in uranium mill tailings, Rabbit Lake, Saskatchewan, Canada. *Applied Geochemistry, 15*(8), 1097–1119. https://doi.org/10.1016/S0883-2927(99)00114-6

Dzombak, D. A., & Morel, F. M. M. (1990). *Surface complexation modeling: Hydrous ferric oxide*. Wiley.

Elder, J. F., & Collins, J. J. (2000). Freshwater molluscs as indicators of bioavailability and toxicity of metals in surface-water systems. In *Reviews of environmental contamination and toxicology* (Vol. 122). Springer.

Ellis, W. R., & Jeffree, R. A. (1982). Determination of the distribution of alpha emitters in the tissues of the freshwater mussel *Velesunio angasi* using the alpha track etch method. In *Solid state nuclear track detectors* (pp. 683–689). *Elsevier*. https://doi.org/10.1016/B978-0-08-026509-4.50142-2

Environment Canada. (2003). *Priority substances list assessment report: Releases of radionuclides from nuclear facilities (impact on non-human biota)*. Canadian Environmental Protection Act.

Environment Canada. (2012). *Metal mining technical guidance for environmental effects monitoring*.

Ernst, W. R., Jonah, P., Doe, K., Julien, G., & Hennigar, P. (1991). Toxicity to aquatic organisms of off-target deposition of endosulfan applied by aircraft. *Environmental Toxicology and Chemistry, 10*(1), 103–114. https://doi.org/10.1002/etc.5620100112

Fedorak, P. M., Westlake, D. W., Anders, C., Kratochvil, B., Motkosky, N., Anderson, W. B., & Huck, P. M. (1986). Microbial release of radium-226 from (Ba,Ra)SO_4 sludges from uranium mine wastes. *Applied and Environmental Microbiology, 52*, 262–268. https://doi.org/10.1128/aem.52.2.262-268.1986

Fesenko, S., Carvalho, F., Martin, P., Moore, W. S., & Yankovich, T. (2014). Radium in the environment. In *The environmental behaviour of radium: Revised edition* (p. 282). International Atomic Energy Agency.

Fisher, R. S. (1995). *Naturally occurring radioactive materials (NORM) in produced water and scale from Texas oil, gas, and geothermal wells* (Geological Circular). University of Texas at Austin, Bureau of Economic Geology. https://doi.org/10.23867/GC9503D

Fisheries Act (R.S.C., 1985, c. F-14). (2019). Government of Canada. https://laws-lois.justice.gc.ca/eng/acts/f-14/

Fong, P. P., Huminski, P. T., & D'Urso, L. M. (1998). Induction and potentiation of parturition in fingernail clams (*Sphaerium striatinum*) by selective serotonin re-uptake inhibitors (SSRIs). *Journal of Experimental Zoology, 280*(3), 260–264. https://doi.org/10.1002/(SICI)1097-010X(19980215)280:3%3C260::AID-JEZ7%3E3.0.CO;2-L

Fong, P. P., & Molnar, N. (2008). Norfluoxetine induces spawning and parturition in estuarine and freshwater bivalves. *Bulletin of Environmental Contamination and Toxicology, 81*(6), 535–538. https://doi.org/10.1007/s00128-008-9558-7

Fox, D. R., van Dam, R. A., Fisher, R., Batley, G. E., Tillmanns, A. R., Thorley, J., Schwarz, C. J., Spry, D. J., & McTavish, K. (2021). Recent developments in species sensitivity distribution modeling. *Environmental Toxicology and Chemistry, 40*(2), 293–308. https://doi.org/10.1002/etc.4925

Fu, X., Niu, Z., Peng, C., Han, H., Sun, W., & Yue, T. (2025). Quantitative synergistic adsorption affinity of Ca(II) and sodium oleate to predict the surface reactivity of hematite and quartz. *Separation and Purification Technology, 360*, 131196. https://doi.org/10.1016/j.seppur.2024.131196

Fuller, N., Lerebours, A., Smith, J. T., & Ford, A. T. (2015). The biological effects of ionising radiation on crustaceans: A review. *Aquatic Toxicology, 167*, 55–67. https://doi.org/10.1016/j.aquatox.2015.07.013

Gale, W. F. (1973). Substrate preference of the fingernail clam, *Sphaerium striatinum* (Lamarck) (Sphaeriidae). *The Southwestern Naturalist, 18*(1), 31–37. https://doi.org/10.2307/3669908

Gerhardt, A. (1992). Acute toxicity of Cd in stream invertebrates in relation to pH and test design. *Hydrobiologia, 239*(2), 93–100. https://doi.org/10.1007/BF00012575

Giguère, A., Couillard, Y., Campbell, P. G. C., Perceval, O., Hare, L., Pinel-Alloul, B., & Pellerin, J. (2003). Steady-state distribution of metals among metallothionein and other cytosolic ligands and links to cytotoxicity in bivalves living along a polymetallic gradient. *Aquatic Toxicology, 64*(2), 185–200. https://doi.org/10.1016/S0166-445X(03)00052-3

Gonneea, M. E., Morris, P. J., Dulaiova, H., & Charette, M. A. (2008). New perspectives on radium behavior within a subterranean estuary. *Marine Chemistry, 109*(3–4), 250–267. https://doi.org/10.1016/j.marchem.2007.12.002

Goto, D., & Wallace, W. G. (2010). Metal intracellular partitioning as a detoxification mechanism for mummichogs (*Fundulus heteroclitus*) living in metal-polluted salt marshes. *Marine Environmental Research*, 69(3), 163–171. https://doi.org/10.1016/j.marenvres.2009.09.008

Goulet, R. R., Krack, S., Doyle, P., Hare, L., Vigneault, B., & McGeer, J. C. (2007). Dynamic multipathway modeling of Cd bioaccumulation in *Daphnia magna* using waterborne and dietborne exposures. *Aquatic Toxicology, 81*(2), 117–125. https://doi.org/10.1016/j.aquatox.2006.11.008

Goulet, R. R., Newsome, L., Vandenhove, H., Keum, D.-K., Horyna, J., Kamboj, S., Brown, J., Johansen, M. P., Twining, J., Wood, M. D., Černe, M., Beaugelin-Seiller, K., & Beresford, N. A. (2022). Best practices for predictions of radionuclide activity concentrations and total absorbed dose rates to freshwater organisms exposed to uranium mining/milling. *Journal of Environmental Radioactivity, 244–245*, 106826. https://doi.org/10.1016/j.jenvrad.2022.106826

Goulet, R. R., Thompson, P. A., Serben, K. C., & Eickhoff, C. V. (2015). Impact of environmentally based chemical hardness on uranium speciation and toxicity in six aquatic species. *Environmental Toxicology and Chemistry, 34*(3), 562–574. https://doi.org/10.1002/etc.2834

Government of Canada. (2022a). *Metal and diamond mining effluent regulations compliance data* [Dataset]. https://open.canada.ca/data/en/dataset/6ceba940-efaa-4994-bee7-3ea1930bedad

Government of Canada. (2022b). *National long-term water quality monitoring data* [Dataset]. https://open.canada.ca/data/en/dataset/67b44816-9764-4609-ace1-68dc1764e9ea

Government of Canada. (2024). *Metal and diamond mining effluent regulations (SOR/2002-222)*. https://laws-lois.justice.gc.ca/eng/regulations/sor-2002-222/FullText.html

Government of Saskatchewan. (2017). *Radium-226 in surface water* (Saskatchewan Environmental Quality Guidelines EPB #602).

Grung, M., Ruus, A., Holth, T. F., Sidhu, R. S., Eriksen, D. Ø., & Hylland, K. (2009). Bioaccumulation and lack of oxidative stress response in the ragworm *Hediste diversicolor* following exposure to radium-226 in sediment. *Journal of Environmental Radioactivity, 100*(5), 429–434. https://doi.org/10.1016/j.jenvrad.2009.03.001

Guérin, N., Behm, D., Leppinen, J., & Gagné, A. (2023). Determination of radium-226 in environmental samples by alpha spectrometry: A new separation method based on the rapid co-precipitation of radium-226 with $PbSO_4$. *Journal of Radioanalytical and Nuclear Chemistry, 332*(10), 4311–4323. https://doi.org/10.1007/s10967-023-09130-w

Guimard, L., Racine, K., Fortin, C., & Crémazy, A. (2026). Radium-226 bioaccumulation and toxicity in the great pond snail *Lymnaea stagnalis*. *Aquatic Toxicology*, *296*, 107832. https://doi.org/10.1016/j.aquatox.2026.107832

Hassler, C. S., Slaveykova, V. I., & Wilkinson, K. J. (2004). Some fundamental (and often overlooked) considerations underlying the free ion activity and biotic ligand models. *Environmental Toxicology and Chemistry, 23(2),* 283–291. https://doi.org/10.1897/03-149

Havlik, B. (1970). Radium-*226 content of water and plankton from the Chalk River area* (AECL-3687). Atomic Energy of Canada Ltd., Chalk River Nuclear Laboratories. https://www.osti.gov/biblio/4087899

Havlik, B. (1971). Radium in aquatic food chains: Radium uptake by freshwater algae. *Radiation Research, 46*(3), 490. https://doi.org/10.2307/3573429

Heinonen, J., Kukkonen, J., Penttinen, O.-P., & Holopainen, I. J. (1997). Effects of hypoxia on valve-closure time and bioaccumulation of 2,4,5-trichlorophenol by the freshwater clam *Sphaerium corneum*. *Ecotoxicology and Environmental Safety, 36*(1), 49–56. https://doi.org/10.1006/eesa.1996.1486

Heinonen, J., Kukkonen, J. V. K., & Holopainen, I. J. (2001). Temperature- and parasite-induced changes in toxicity and lethal body burdens of pentachlorophenol in the freshwater clam *Pisidium amnicum*. *Environmental Toxicology and Chemistry, 20*(12), 2778–2784. https://doi.org/10.1002/etc.5620201217

Heinonen, J., Penttinen, O.-P., Holopainen, I. J., & Kukkonen, J. V. K. (2003). Sublethal energetic responses by *Pisidium amnicum* (Bivalvia) exposed to pentachlorophenol at two temperatures. *Environmental Toxicology and Chemistry, 22*(2), 433–438.

Hemond, H. F., & Fechner, E. J. (2023). *Chemical fate and transport in the environment* (4th ed.). Elsevier.

Hess, C. T., Michel, J., Horton, T. R., Prichard, H. M., & Coniglio, W. A. (1985). *Occurrence of radioactivity in public water supplies in the United States* (EDB-85-106121). University of Maine.

Hesslein, R. H., & Slavicek, E. (1984). Geochemical pathways and biological uptake of radium in small Canadian Shield lakes. *Canadian Journal of Fisheries and Aquatic Sciences, 41*(3), 459–468. https://doi.org/10.1139/f84-055

Hickey, C. W., & Martin, M. L. (1999). Chronic toxicity of ammonia to the freshwater bivalve *Sphaerium novaezelandiae*. *Archives of Environmental Contamination and Toxicology, 36*(1), 38–46. https://doi.org/10.1007/s002449900440

Hourtané, O. (2025). *Assessment of the sensitivity of freshwater species to radium-226*. Paper presented at the Canadian Ecotoxicity Workshop (CEW), Victoria, BC, Canada.

Howard, B. J., Beresford, N. A., Copplestone, D., Telleria, D., Pröhl, G., Fesenko, S., Jeffree, R. A., Yankovich, T. L., Brown, J. E., Higley, K., Johansen, M. P., Mulye, H., Vandenhove, H., Gashchak, S., Wood, M. D., Takata, H., Andersson, P., Dale, P., Ryan, J., Bollhöfer, A., Doering, C., Barnett, C. L., & Wells, C. (2013). The IAEA handbook on radionuclide transfer to wildlife. *Journal of Environmental Radioactivity, 121*, 55–74.

Illinois Natural History Survey. (2005). *Effects of water quality on acute and chronic toxicity of sulfate to freshwater bivalves, Ceriodaphnia dubia, and Hyalella azteca* (Third quarterly report). Report submitted to U.S. Environmental Protection Agency, Region 5.

International Atomic Energy Agency. (2014). *The environmental behaviour of radium: Revised edition*. https://www.iaea.org/publications/10478/the-environmental-behaviour-of-radium-revised-edition

International Commission on Radiological Protection (ICRP). (2009). *Environmental protection: Transfer parameters for reference animals and plants* (ICRP Publication 114; Annals of the ICRP).

Imafidon, O., Akpojivi, V. O., Okosun, J. Z., & Ediagbonya, T. F. (2025). Redox chemistry of natural organic matter: A review of mechanisms, environmental applications, and implications for sustainable development. *Journal of Water Process Engineering, 77*, 108566. https://doi.org/10.1016/j.jwpe.2025.108566

Jamil, K., & Ali, S. (2001). Estimation of radon concentrations in coal mines using a hybrid technique calibration curve. *Journal of Environmental Radioactivity, 54*(3), 415–422. https://doi.org/10.1016/S0265-931X(00)00175-2

Jędrzejek, F., Szarłowicz, K., & Stobiński, M. (2022). A geological context in radiation risk assessment to the public. *International Journal of Environmental Research and Public Health, 19*(18), 11750. https://doi.org/10.3390/ijerph191811750

Jeffree, R. A. (1985). The accumulation of radium-226 by populations of the freshwater mussel *Velesunio angasi* from the Alligator Rivers uranium province, Northern Territory, Australia. *SIL Proceedings, 22*(4), 2486–2492. https://doi.org/10.1080/03680770.1983.11897709

Jeffree, R. A. (1988). Patterns of accumulation of alkaline-earth metals in the tissue of the freshwater mussel *Velesunio angasi*. *Archiv für Hydrobiologie, 112*(1), 67–90. https://doi.org/10.1127/archiv-hydrobiol/112/1988/67

Jeffree, R. A. (1991). An experimental study of radium-226 and calcium-45 accumulation from the aquatic medium by freshwater turtles (family Chelidae) under varying calcium and magnesium water concentrations. *Hydrobiologia, 218*(3), 205–231. https://doi.org/10.1007/BF00038836

Jeffree, R. A., & Simpson, R. D. (1984). Radium-226 is accumulated in calcium granules in the tissues of the freshwater mussel *Velesunio angasi*: Support for a metabolic analogue hypothesis. *Comparative Biochemistry and Physiology Part A: Physiology, 79*(1), 61–72. https://doi.org/10.1016/0300-9629(84)90708-4

Jeffree, R. A., & Simpson, R. D. (1986). An experimental study of the uptake and loss of radium-226 by the tissue of the tropical freshwater mussel *Velesunio angasi* (Sowerby) under varying calcium and magnesium water concentrations. *Hydrobiologia, 139*(1), 59–80. https://doi.org/10.1007/BF00770242

Justyn, H., & Havlik, B. (1990). Radium uptake by freshwater fish. In *The environmental behaviour of radium* (No. 310, pp. 529–543). International Atomic Energy Agency. https://inis.iaea.org/records/89ayk-jh222

Kajjumba, G. W., Emik, S., Öngen, A., Özcan, H. K., & Aydın, S. (2019). Modelling of adsorption kinetic processes—Errors, theory and application. In S. Edebali (Ed.), *Advanced sorption process applications*. IntechOpen. https://doi.org/10.5772/intechopen.80495

Kamshilov, M. M., & Flerov, B. A. (1976). Experimental research on phenol intoxication of aquatic organisms and destruction of phenol in model communities. In D. I. Mount, W. R. Swain, & N. K. Ivanikiw (Eds.), *Proceedings of the first and second USA–USSR symposia on the effects of pollutants upon aquatic ecosystems* (pp. 181–192).

Kamunda, C., Mathuthu, M., & Madhuku, M. (2016). An assessment of radiological hazards from gold mine tailings in the province of Gauteng in South Africa. *International Journal of Environmental Research and Public Health, 13*(1), Article 1. https://doi.org/10.3390/ijerph13010138

Kartick, M. (2015). *Geochemical and mineralogical assessment of uranium mine tailings at Denison Mine, Elliot Lake, Ontario, Canada: Implications for mobility of radium-226* [Thesis, University of Toronto].

Kilgour, B. W., & Mackie, G. L. (1988). Factors affecting the distribution of sphaeriid bivalves in Britannia Bay of the Ottawa River. *The Nautilus, 102*(2), 73–77.

Kilgour, B. W., & Mackie, G. L. (1990). Relationships between reproductive output and shell morphometrics of the pill clam, *Pisidium casertanum* (Bivalvia: Sphaeriidae). *Canadian Journal of Zoology, 68*(7), 1568–1571. https://doi.org/10.1139/z90-231

Kilgour, B. W., Dixon, D. G., & Paine, M. D. (2002). *Alternative approaches to deriving provincial water quality objectives*. Report submitted to the Ontario Ministry of the Environment.

Kilgour, B. W., Dowsley, B., McKee, M., & Mihok, S. (2018). Effects of uranium mining and milling on benthic invertebrate communities in the Athabasca Basin of northern Saskatchewan. *Canadian Water Resources Journal / Revue canadienne des ressources hydriques, 43*(3), 305–320. https://doi.org/10.1080/07011784.2018.1445560

Kilgour, B. W., Somers, K. M., & Matthews, D.E. (1998). Using the normal range as a criterion for ecological significance in environmental monitoring and assessment. *Écoscience, 5*(4). https://doi.org/10.1080/11956860.1998.11682485

Kilgour, B. W., & Somers, K. M. (2017). Challenges with the use of normal ranges in environmental monitoring. *Integrated Environmental Assessment and Management, 13*(2), 444–446. https://doi.org/10.1002/ieam.1874

Kim, Y.-S., & Brechbiel, M. W. (2012). An overview of targeted alpha therapy. *Tumor Biology, 33*(3), 573–590. https://doi.org/10.1007/s13277-011-0286-y

Kitamura, A., Fujiwara, K., Yamamoto, T., Nishikawa, S., & Moriyama, H. (1999). Analysis of adsorption behavior of cations onto quartz surface by electrical double-layer model. *Journal of Nuclear Science and Technology, 36*, 1167–1175. https://doi.org/10.1080/18811248.1999.9726312

Kocher, D. C., & Trabalka, J. R. (2000). On the application of radiation weighting factor for alpha particles in protection of non-human biota. *Health Physics, 79*(4), 407–411. https://doi.org/10.1097/00004032-200010000-00009

Kramer, K. J. M., Jenner, H. A., & De Zwart, D. (1989). The valve movement response of mussels: A tool in biological monitoring. *Hydrobiologia, 188–189*, 433–443. https://doi.org/10.1007/BF00027811

Kumm, Z. A., & Gier, S. (2024). Cation exchange capacity: An alternative method to investigate the geological barrier for landfills. *Applied Clay Science, 259*, 107513. https://doi.org/10.1016/j.clay.2024.107513

Lacroix-Durand, C., Janz, D., & Liber, K. (2024). Chronic radium-226 toxicity and oxidative stress in the aquatic invertebrate *Chironomus dilutus*. *Toxicology Research, 14*(1), tfaf001. https://doi.org/10.1093/toxres/tfaf001

Lacroix-Durand, C., Janz, D., & Liber, K. (2025). Chronic radium-226 bioaccumulation and toxicity in the aquatic invertebrate *Daphnia magna*. *Archives of Environmental Contamination and Toxicology, 88*(1), 123–133. https://doi.org/10.1007/s00244-024-01109-2

Landa, E. R., Phillips, E. J. P., & Lovley, D. R. (1991). Release of radium-226 from uranium mill tailings by microbial Fe(III) reduction. *Applied Geochemistry, 6*(6), 647–652. https://doi.org/10.1016/0883-2927(91)90075-Z

Landa, E. R., & Reid, D. F. (1983). Sorption of radium-226 from oil-production brine by sediments and soils. *Environmental Geology, 5*, 1–8. https://doi.org/10.1007/BF02381293

Lange, J.E. (1985). *Toxicity of Aluminum to Selected Freshwater Invertebrates in Water of pH 7.5*. Manuscript, Prepared for D.J.Call and L.T.Brooke, University of Wisconsin, Superior, WI:20 p.

Langmuir, D., & Riese, A. C. (1985). The thermodynamic properties of radium. *Geochimica et Cosmochimica Acta, 49*(7), 1593–1601. https://doi.org/10.1016/0016-7037(85)90264-9

Lestini, L., Beaucaire, C., Vercouter, T., & Descostes, M. (2013). Radium uptake by recrystallized gypsum: An incorporation study. *Procedia Earth and Planetary Science, 7*, 479–482. https://doi.org/10.1016/j.proeps.2013.03.002

Li, X., Li, J., Wang, Y., Fu, L., Zhu, J., & Duan, Q. (2010). Kinetic study of the bioaccumulation of heavy metals (Cu, Pb, and Cd) in Chinese domestic oyster Ostrea plicatula. Journal of Environmental Science and Health, Part A, 45(7), 836–845. https://doi.org/10.1080/10934521003709032

Liu, D. J., & Hendry, M. J. (2011). Controls on radium-226 during raffinate neutralization at the Key Lake uranium mill, Saskatchewan, Canada. *Applied Geochemistry, 26*(12), 2113–2120. https://doi.org/10.1016/j.apgeochem.2011.07.009

Liu, Y., & Shen, L. (2008). From Langmuir kinetics to first- and second-order rate equations for adsorption. *Langmuir, 24*, 11625–11630. https://doi.org/10.1021/la801839b

Lofts, S., Fevrier, L., Horemans, N., Gilbin, R., Bruggeman, C., & Vandenhove, H. (2015). Assessment of co-contaminant effects on uranium and thorium speciation in freshwater using geochemical modelling. *Journal of Environmental Radioactivity, 149*, 99–109. https://doi.org/10.1016/j.jenvrad.2015.07.011

Logan, J. W. M., & Perkins, E. J. (1972). Toxicity of Essolvene. *Marine Pollution Bulletin, 3*(10), 155–157.

Lopes-Lima, M., Teixeira, A., Froufe, E., Lopes, A., Varandas, S., & Sousa, R. (2014). Biology and conservation of freshwater bivalves: Past, present and future perspectives. *Hydrobiologia, 735*(1), 1–13. https://doi.org/10.1007/s10750-014-1902-9

Lopez, G. R., & Holopainen, I. J. (1987). Interstitial suspension feeding by *Pisidium* sp. (Pisidiidae: Bivalvia): A new guild in the lenthic benthos.

Lozano, S. J., Brazner, J. C., Knuth, M. L., Heinis, L. J., Sargent, K. W., Tanner, D. K., Anderson, L. E., O'Halloran, S. L., & Ber, S. L. (1989). *Effects, persistence and distribution of esfenvalerate in littoral enclosures* (Report No. DU E104/PPA 06/7592A). U.S. Environmental Protection Agency and University of Wisconsin–Superior.

Mackie, G. L. (1979). Growth dynamics in natural populations of sphaeriid clams (*Sphaerium*, *Musculium*, *Pisidium*). *Canadian Journal of Zoology, 57*(2), 441–456. https://doi.org/10.1139/z79-052

Mackie, G. L. (1989). Tolerances of five benthic invertebrates to hydrogen ions and metals (Cd, Pb, Al). *Archives of Environmental Contamination and Toxicology, 18*(1–2), 215–223. https://doi.org/10.1007/BF01056206

Mackie, G. L. (2007). *Biology of freshwater corbiculid and sphaeriid clams of North America: XV*. Ohio Biological Survey, Bulletin New Series.

Mackie, G. L., & Flippance, L. A. (1983). Intra- and interspecific variations in calcium content of freshwater mollusca in relation to calcium content of the water. *Journal of Molluscan Studies, 49*(3), 204–212. https://doi.org/10.1093/oxfordjournals.mollus.a065714

Madruga, M. J., Brogueira, A., Alberto, G., & Cardoso, F. (2001). Radium-226 bioavailability to plants at the Urgeiriça uranium mill tailings site. *Journal of Environmental Radioactivity, 54*(1), 175–188. https://doi.org/10.1016/S0265-931X(00)00173-9

Mahaliyana, A. S., Pirker, J., Abhiram, G., Pantos, O., Marsden, I. D., & Gaw, S. (2025). Uptake and depuration kinetics of emerging organic contaminants (EOCs) in the New Zealand green-lipped mussel (Perna canaliculus): Seafood safety implications. Marine Environental Research, 212, 107492. https://doi.org/10.1016/j.marenvres.2025.107492

Maki, A. W., Geissel, L., & Johnson, H. E. (1975). Comparative toxicity of larval lampricide (TFM: 3-trifluoromethyl-4-nitrophenol) to selected benthic macroinvertebrates. *Journal of the Fisheries Research Board of Canada, 32*, 1455–1459. https://doi.org/10.1139/f75-168

Maki, A. W., & Johnson, H. E. (1977). Kinetics of lampricide (TFM, 3-trifluoromethyl-4-nitrophenol) residues in model stream communities. *Journal of the Fisheries Research Board of Canada, 34*, 276–281. https://doi.org/10.1139/f77-042

March, F. A., Dwyer, F. J., Augspurger, T., Ingersoll, C. G., Wang, N., & Mebane, C. A. (2007). An evaluation of freshwater mussel toxicity data in the derivation of water quality guidance and standards for copper. *Environmental Toxicology and Chemistry, 26*(10), 2066–2074. https://doi.org/10.1897/06-560R.1

Marking, L. L. (1974). Toxicity of 2-(digeranylamino)-ethanol, a candidate selective fish toxicant. *Transactions of the American Fisheries Society, 103*(4), 736–742. https://doi.org/10.1577/1548-8659(1974)103%3C736:TODACS%3E2.0.CO;2

Martin, A. J., Crusius, J., McNee, J. J., & Yanful, E. K. (2003). The mobility of radium-226 and trace metals in pre-oxidized subaqueous uranium mill tailings. *Applied Geochemistry, 18*(7), 1095–1110. https://doi.org/10.1016/S0883-2927(02)00243-3

McCready, R. G. L., Bland, C. J., & Gonzales, D. E. (1980). Preliminary studies on the chemical, physical, and biological stability of Ba/$RaSO_4$ precipitates. *Hydrometallurgy, 5*, 109–116. https://doi.org/10.1016/0304-386X(80)90032-8

Meier-Brook, C. (1969). Substrate relations in some *Pisidium* species (Eulamellibranchiata: Sphaeriidae).

Melvin, S. D., & Wilson, S. P. (2013). The utility of behavioral studies for aquatic toxicology testing: A meta-analysis. *Chemosphere, 93*(10), 2217–2223. https://doi.org/10.1016/j.chemosphere.2013.07.036

Ministry of the Environment and Energy (MOEE). (1994). Water management policies, guidelines, provincial water quality objectives of the Ministry of Environment and Energy. Queen's Printer for Ontario.

Mothersill, C., Larivière, D., Smith, R. W., Thompson, M. P., Byun, S. H., Prestwich, W., & Seymour, C. B. (2014). Dosimetric analysis of fathead minnow (*Pimephales promelas*) exposed via ingestion to environmentally relevant activities of radium-226 for two years. *International Journal of Radiation Biology, 90*(2), 169–178. https://doi.org/10.3109/09553002.2014.868614

Mothersill, C., Smith, R., Larivière, D., & Seymour, C. (2013). Chronic exposure by ingestion of environmentally relevant doses of radium-226 leads to transient growth perturbations in fathead minnow (*Pimephales promelas*). *International Journal of Radiation Biology, 89*(11), 950–964. https://doi.org/10.3109/09553002.2013.809817

Naimo, T. J., Cope, W. G., Monroe, E. M., Farris, J. L., & Milam, C. D. (2000). Influence of diet on survival, growth, and physiological condition of fingernail clams (*Musculium transversum*). *Environmental Toxicology and Chemistry, 19*, 23–28.

Nair, S., Karimzadeh, L., & Merkel, B. J. (2014). Surface complexation modeling of uranium(VI) sorption on quartz in the presence and absence of alkaline earth metals. *Environmental Earth Sciences, 71*, 1737–1745. https://doi.org/10.1007/s12665-013-2579-5

Nautilus Environmental. (2021). *The fate of rare earth elements in aquatic toxicity tests: Solubility, speciation and bioaccumulation of lanthanum, neodymium, yttrium and cerium*.

Natural Resources Canada. (2021). *The Canadian minerals and metals plan*. https://www.nrcan.gc.ca/sites/www.nrcan.gc.ca/files/CMMP/CMMP_The_Plan-EN.pdf

Nirdosh, I., Trembley, W. B., & Johnson, C. R. (1990). Adsorption–desorption studies on the radium-226–hydrated metal oxide systems. *Hydrometallurgy, 24*(2), 237–248. https://doi.org/10.1016/0304-386X(90)90089-K

Organisation for Economic Co-operation and Development. (2002). *Guidance document on aquatic toxicity testing of difficult substances and mixtures* (OECD Series on Testing and Assessment). OECD Publishing. https://doi.org/10.1787/9789264078406-en

Osborne, R. K., Gillis, P. L., & Prosser, R. S. (2020). Transgenerational Effects of Copper on a Freshwater Gastropod, Planorbella pilsbryi. Freshwater Mollusk Biology and Conservation, 23(1), 42. https://doi.org/10.31931/fmbc.v22i2.2020.42-54

Ouedraogo, A. M. M. A., Rickwood, C. J., Huntsman, P., Proulx, C. L., Pick, F., & Goulet, R. R. (2025). Chronic toxicity of lithium to the fingernail clam *Pisidium dubium* and the water flea *Daphnia pulex*. *Environmental Toxicology and Chemistry*. https://doi.org/10.1093/etojnl/vgaf204

Pankratz, K., & Warner, N. R. (2025). Evaluating radium exposure in *Elliptio dilatata*: Insights from controlled laboratory studies of oil and gas produced water. *ACS ES&T Water, 5*, 1240–1247. https://doi.org/10.1021/acsestwater.4c01020

Parkhurst, D. L., & Appelo, C. A. J. (1999). *User's guide to PHREEQC (Version 2): A computer program for speciation, batch-reaction, one-dimensional transport, and inverse geochemical calculations* (Water-Resources Investigations Report 99–4259). U.S. Geological Survey.

Perceval, O., Couillard, Y., Pinel-Alloul, B., & Campbell, P. G. C. (2006). Linking changes in subcellular cadmium distribution to growth and mortality rates in transplanted freshwater bivalves (Pyganodon grandis). Aquatic Toxicology, 79(1), 87–98. https://doi.org/10.1016/j.aquatox.2006.05.008

Phillips, N. R., & Hickey, C. W. (2010). Genotype-dependent recovery from acute exposure to heavy metal contamination in the freshwater clam *Sphaerium novaezelandiae*. *Aquatic Toxicology, 99*(4), 507–513. https://doi.org/10.1016/j.aquatox.2010.07.004

Posthuma, L., Van Gils, J., Zijp, M. C., Van de Meent, D., & De Zwart, D. (2019). Species sensitivity distributions for use in environmental protection, assessment, and management of aquatic ecosystems for 12,386 chemicals. *Environmental Toxicology and Chemistry, 38*(4), 905–917. https://doi.org/10.1002/etc.4373

Pröhl, G. (2014). Dose assessment. In *The environmental behaviour of radium: Revised edition* (p. 282). International Atomic Energy Agency.

Proulx, C. L., Kilgour, B. W., Francis, A. P., Bouwhuis, R. F., & Hill, J. R. (2018). Using a conductivity–alkalinity relationship as a tool to identify surface waters in reference condition across Canada. *Water Quality Research Journal, 53*(4), 231–240. https://doi.org/10.2166/wqrj.2018.030

Proulx, C. L., Kilgour, B. W., & Goulet, R. R. (2025a). Quantifying historical releases of radium-226 from Canadian mining operations to freshwaters. *Journal of Environmental Radioactivity, 283*, 107629. https://doi.org/10.1016/j.jenvrad.2025.107629

Proulx, C. L., Kilgour, B. W., Petelina, E., & Benson, S. (2025b). Evaluating wild freshwater bivalves as alternative sentinel species in Canadian Environmental Effects Monitoring (EEM). *Environmental Monitoring and Assessment*, *197*(11), 1192. https://doi.org/10.1007/s10661-025-14661-8

Pyle, G. G., & Clulow, F. V. (1998). Radionuclide equilibria between the aquatic environment and fish tissues. *Journal of Environmental Radioactivity, 40*(1), 59–74. https://doi.org/10.1016/S0265-931X(97)00063-5

R Core Team. (2026). *R: A Language and Environment for Statistical Computing. R Foundation for Statistical Computing*, Vienna, Austria. doi:10.32614/R.manuals

Rachkova, N. G., Shuktomova, I. I., & Taskaev, A. I. (2010). The state of natural radionuclides of uranium, radium, and thorium in soils. *Eurasian Soil Science, 43*(6), 651–658. https://doi.org/10.1134/S1064229310060050

Raghav, S., & Kumar, D. (2018). Adsorption equilibrium, kinetics, and thermodynamic studies of fluoride adsorbed by tetrametallic oxide adsorbent. *Journal of Chemical & Engineering Data, 63*, 1682–1697. https://doi.org/10.1021/acs.jced.8b00024

Rakshit, S., Sarkar, D., & Datta, R. (2015). Surface complexation of antimony on kaolinite. *Chemosphere, 119*, 349–354. https://doi.org/10.1016/j.chemosphere.2014.06.070

Redondo-Hasselerharm, P. E., Falahudin, D., Peeters, E. T. H. M., & Koelmans, A. A. (2018). Microplastic effect thresholds for freshwater benthic macroinvertebrates. *Environmental Science & Technology, 52*, 2278–2286. https://doi.org/10.1021/acs.est.7b05367

Reinoso-Maset, E., & Ly, J. (2016). Study of uranium(VI) and radium(II) sorption at trace level on kaolinite using a multisite ion exchange model. *Journal of Environmental Radioactivity, 157*, 136–148. https://doi.org/10.1016/j.jenvrad.2016.03.014

Riese, A. C. (1982). Adsorption of radium and thorium onto quartz and kaolinite: A comparison of solution–surface equilibria models.

Rice, C. P., & White, D. S. (1987). PCB availability assessment of river dredging using caged clams and fish. *Environmental Toxicology and Chemistry, 6*(4), 259–274. https://doi.org/10.1002/etc.5620060404

Robin, V., Tertre, E., Beaucaire, C., Regnault, O., & Descostes, M. (2017). Experimental data and assessment of predictive modeling for radium ion-exchange on beidellite, a swelling clay mineral with a tetrahedral charge. *Applied Geochemistry, 85*, 1–9. https://doi.org/10.1016/j.apgeochem.2017.07.009

Rollog, M., Cook, N. J., Ehrig, K., & Gilbert, S. E. (2020). Rapid, competitive radium uptake in strontium, barium, and lead sulfates during sulfuric acid leaching. *Applied Geochemistry, 115*, 104549. https://doi.org/10.1016/j.apgeochem.2020.104549

Rosenberg, R. M. (2013). *Radium isotope geochemistry in groundwater systems: The role of environmental factors* (Doctoral dissertation, Duke University). Duke University. https://dukespace.lib.duke.edu/items/eaddaf09-44f9-4934-858c-021c5c9f6acb

Rühlmann, J., Körschens, M., & Graefe, J. (2006). A new approach to calculate the particle density of soils considering properties of the soil organic matter and the mineral matrix. *Geoderma, 130*, 272–283. https://doi.org/10.1016/j.geoderma.2005.01.024

Ryan, B., Bollhöfer, A., & Martin, P. (2008). Radionuclides and metals in freshwater mussels of the upper South Alligator River, Australia. *Journal of Environmental Radioactivity, 99*(3), 509–526. https://doi.org/10.1016/j.jenvrad.2007.08.019

Salerno, J., Gillis, P. L., Bennett, C. J., Sibley, P. K., & Prosser, R. S. (2018). Investigation of clearance rate as an endpoint in toxicity testing with freshwater mussels (Unionidae). *Ecotoxicology and Environmental Safety, 163*, 165–171. https://doi.org/10.1016/j.ecoenv.2018.07.054

Sajih, M., Bryan, N. D., Livens, F. R., Vaughan, D. J., Descostes, M., Phrommavanh, V., Nos, J., & Morris, K. (2014). Adsorption of radium and barium on goethite and ferrihydrite: A kinetic and surface complexation modelling study. *Geochimica et Cosmochimica Acta, 146*, 150–163. https://doi.org/10.1016/j.gca.2014.10.008

Salazar, M. H., & Salazar, S. M. (2001). *Using caged mussels to characterize exposure from point and nonpoint stressors in the Cherry Point Reach: The value of in situ monitoring*.

Sauvé, D., Clulow, V., & Goulet, R. R. (2021). Quantifying historical releases and pre-operation levels of metals and radionuclides. *Journal of Environmental Radioactivity, 237*, 106683. https://doi.org/10.1016/j.jenvrad.2021.106683

Scanlan, A. R. (2023). *Geochemical evolution of the remediated Denison uranium mine tailings* [Thesis, Carleton University].

Scheil, H. G., & Hinz, W. (1974). Influence of divalent mercury ions on the filtration rate of *Pisidium casertanum* Poli (Bivalvia). *Hydrobiologia, 45*(4), 543–545. https://doi.org/10.1007/BF00012035

Schmandt, D. S., Cook, N. J., Ehrig, K., Gilbert, S., Wade, B. P., Rollog, M., Ciobanu, C. L., & Kamenetsky, V. S. (2019). Uptake of trace elements by baryte during copper ore processing: A case study from Olympic Dam, South Australia. *Minerals Engineering, 135*, 83–94. https://doi.org/10.1016/j.mineng.2019.02.034

Schmidt, S., & Goulet, R. R. (2014). Mitigation and remediation issues. In *The environmental behaviour of radium: Revised edition* (p. 282). International Atomic Energy Agency.

Schoonover, C. M., Wieker, J., Pope, R., Brown, C., Cooper, E., DeWitt, J., Gunselman, S., Jensen, C., Stevens, W., Yri, J., Nezat, C., & Joyner-Matos, J. (2016). Development of functional trait biomarkers for trace metal exposure in freshwater clams (*Musculium* spp.). *Comparative Biochemistry and Physiology Part A: Molecular & Integrative Physiology, 200*, 21–34. https://doi.org/10.1016/j.cbpa.2016.04.012

Serra-Ventura, J., Sabaté-Herrero, G., Rigol, A., & Vidal, M. (2025). Chemical analogues and probabilistic functions to derive distribution coefficients of radium in soils. *Journal of Environmental Radioactivity, 289*, 107769. https://doi.org/10.1016/j.jenvrad.2025.107769

Servos, M. R., & Mackie, G. L. (1986). The effect of short-term acidification during spring snowmelt on selected mollusca in south-central Ontario. *Canadian Journal of Zoology, 64*(8), 1690–1695. https://doi.org/10.1139/z86-254

Sheppard, S. C., Sheppard, M. I., Tait, J. C., & Sanipelli, B. L. (2006). Revision and meta-analysis of selected biosphere parameter values for chlorine, iodine, neptunium, radium, radon and uranium. *Journal of Environmental Radioactivity, 89*(2), 115–137. https://doi.org/10.1016/j.jenvrad.2006.03.003

Shi, X., Smith, R., Seymour, C., & Mothersill, C. (2017). Radium-226 bioaccumulation and growth indices in fish. *International Journal of Radiation Biology, 93*(6), 617–626. https://doi.org/10.1080/09553002.2017.1297900

Solomon, K. R., Baker, D. B., Richards, R. P., Dixon, K. R., Klaine, S. J., La Point, T. W., Kendall, R. J., Weisskopf, C. P., Giddings, J. M., Giesy, J. P., Hall, L. W., & Williams, W. M. (1996). Ecological risk assessment of atrazine in North American surface waters. *Environmental Toxicology and Chemistry, 15*(1), 31–76. https://doi.org/10.1002/etc.5620150105

Soucek, D. J., & Dickinson, A. (2012). Acute toxicity of nitrate and nitrite to sensitive freshwater insects, mollusks, and a crustacean. *Archives of Environmental Contamination and Toxicology, 62*(2), 233–242. https://doi.org/10.1007/s00244-011-9705-8

Soucek, D. J., & Kennedy, A. J. (2005). Effects of hardness, chloride, and acclimation on the acute toxicity of sulfate to freshwater invertebrates. *Environmental Toxicology and Chemistry, 24*(5), 1204–1210. https://doi.org/10.1897/04-142.1

Soucek, D. J., Linton, T. K., Tarr, C. D., Dickinson, A., Wickramanayake, N., Delos, C. G., & Cruz, L. A. (2011). Influence of water hardness and sulfate on the acute toxicity of chloride to sensitive freshwater invertebrates. *Environmental Toxicology and Chemistry, 30*(4), 930–938. https://doi.org/10.1002/etc.454

Sparks, R. E., & Sandusky, M. J. (1981). *Identification of factors responsible for decreased production of fish food organisms in the Illinois and Mississippi rivers* (Final Report, Project No. 3-291-R). Illinois Natural History Survey, River Research Laboratory.

Smith, R. W. (2002). The use of random-model tolerance intervals in environmental monitoring and regulation. *Journal of Agricultural, Biological, and Environmental Statistics, 7*(1), 74–94. https://doi.org/10.1198/108571102317475071

Stackelberg, P. E., Szabo, Z., & Jurgens, B. C. (2018). Radium mobility and the age of groundwater in public drinking-water supplies from the Cambrian–Ordovician aquifer system, north-central USA. *Applied Geochemistry, 89*, 34–48. https://doi.org/10.1016/j.apgeochem.2017.11.002

Stumm, W., & Morgan, J. J. (1996). *Aquatic chemistry: Chemical equilibria and rates in natural waters* (3rd ed.). Wiley.

Sugiura, Y., Ishidera, T., & Tachi, Y. (2021). Surface complexation of calcium and competitive sorption of divalent cations on montmorillonite under alkaline conditions. *Applied Clay Science, 200*, 105910. https://doi.org/10.1016/j.clay.2020.105910

Swanson, S. (1982). *Levels and effects of radionuclides in aquatic fauna of the Beaverlodge area (Saskatchewan)*. Saskatchewan Research Council and Environment Canada.

Swanson, S. M. (1983). Levels of radium-226, lead-210, and total uranium in fish near a Saskatchewan uranium mine and mill. *Health Physics, 45*(1), 67–80. https://doi.org/10.1097/00004032-198307000-00007

Szabo, Z., Cravotta, C. A., Stackelberg, P. E., & Belitz, K. (2023). Gross alpha-particle activity and high radium-226 concentrations do not correspond with high polonium-210 in the Atlantic and Gulf Coastal Plain aquifers of the United States. *ACS ES&T Water, 3*(2), 262–274. https://doi.org/10.1021/acsestwater.2c00027

Szabo, Z., dePaul, V. T., Fischer, J. M., Kraemer, T. F., & Jacobsen, E. (2012). Occurrence and geochemistry of radium in water from principal drinking-water aquifer systems of the United States. *Applied Geochemistry, 27*(3), 729–752. https://doi.org/10.1016/j.apgeochem.2011.11.002

Szymanek, K., Charmas, R., & Piasecki, W. (2021). Investigations of mechanism of calcium adsorption on silica and alumina based on Ca-ISE monitoring, potentiometric titration, electrokinetic measurements and surface complexation modeling. *Adsorption, 27*, 105–115. https://doi.org/10.1007/s10450-020-00280-x

Tachi, Y., Shibutani, T., Sato, H., & Yui, M. (2001). Experimental and modeling studies on sorption and diffusion of radium in bentonite. *Journal of Contaminant Hydrology, 47*(2–4), 171–186. https://doi.org/10.1016/S0169-7722(00)00147-9

Tan, K., Cai, X., Tan, K., & Kwan, K. Y. (2023). A review of natural and anthropogenic radionuclide pollution in marine bivalves. *Science of the Total Environment, 896*, 165030. https://doi.org/10.1016/j.scitotenv.2023.165030

Thiessen, K. M., Thorne, M. C., Maul, P. R., Pröhl, G., & Wheater, H. S. (1999). Modelling radionuclide distribution and transport in the environment. *Environmental Pollution, 100*(1–3), 151–177. https://doi.org/10.1016/S0269-7491(99)00090-1

Thiry, Y., & Van Hees, M. (2008). Evolution of pH, organic matter and radium-226/calcium partitioning in U-mining debris following revegetation with pine trees. *Science of the Total Environment, 393*(1), 111–117. https://doi.org/10.1016/j.scitotenv.2007.12.020

Tipping, E. (1994). WHAMC—A chemical equilibrium model and computer code for waters, sediments, and soils incorporating a discrete site/electrostatic model of ion-binding by humic substances. *Computers & Geosciences, 20*, 973–1023. https://doi.org/10.1016/0098-3004(94)90038-8

Trenfield, M. A., McDonald, S., Kovacs, K., Lesher, E. K., Pringle, J. M., Markich, S. J., Ng, J. C., Noller, B., Brown, P. L., & van Dam, R. A. (2011). Dissolved organic carbon reduces uranium bioavailability and toxicity: 1. Characterization of an aquatic fulvic acid and its complexation with uranium(VI). *Environmental Science & Technology, 45*(7), 3075–3081. https://doi.org/10.1021/es103330w

Twining, J. R. (1993). A study of radium uptake by the water-lily *Nymphaea violacea* (Lehm.) from contaminated sediment. *Journal of Environmental Radioactivity, 20*(3), 169–189. https://doi.org/10.1016/0265-931X(93)90008-U

Ulanovsky, A. (2016). Dosimetry for animals and plants: Contending with biota diversity. *Annals of the ICRP, 45*(1_suppl), 225–238. https://doi.org/10.1177/0146645316630710

United States Environmental Protection Agency. (1995). *Great Lakes water quality initiative technical support document for the procedure to determine bioaccumulation factors* (EPA-820-B-95-005). Office of Water.

United States Environmental Protection Agency. (2016). *Code of Federal Regulations, Title 40—Protection of environment*. https://www.govinfo.gov/content/pkg/CFR-2015-title40-vol30/xml/CFR-2015-title40-vol30-part440.xml

United Nations Scientific Committee on the Effects of Atomic Radiation (UNSCEAR). (2008). *Sources and effects of ionizing radiation* (Vol. II: Scientific annexes C, D and E).

Van der Borght, O. (1963). Accumulation of radium-226 by the freshwater gastropod *Lymnaea stagnalis*. *Nature, 197*(4867), 612–613. https://doi.org/10.1038/197612a0

Van Wijngaarden, R. P. A., Arts, G. H. P., Belgers, J. D. M., Boonstra, H., Roessink, I., Schroer, A. F. W., & Brock, T. C. M. (2010). The species sensitivity distribution approach compared with a microcosm study: A case study with the fungicide fluazinam. *Ecotoxicology and Environmental Safety, 73*(2), 109–122. https://doi.org/10.1016/j.ecoenv.2009.09.019

Vaughn, C. C., & Hakenkamp, C. C. (2001). The functional role of burrowing bivalves in freshwater ecosystems. *Freshwater Biology, 46*(11), 1431–1446. https://doi.org/10.1046/j.1365-2427.2001.00771.x

Waite, D. T., Joshi, S. R., & Sommerstad, H. (1989). Movement of dissolved radionuclides from submerged uranium mine tailings into the surface water of Langley Bay, Saskatchewan,

Canada. *Archives of Environmental Contamination and Toxicology, 18*(6), 881–887. https://doi.org/10.1007/BF01160304

Wang, N., Ivey, C. D., Ingersoll, C. G., Brumbaugh, W. G., Alvarez, D., Hammer, E. J., Bauer, C. R., Augspurger, T., Raimondo, S., & Barnhart, M. C. (2016). Acute sensitivity of a broad range of freshwater mussels to chemicals with different modes of toxic action. *Environmental Toxicology and Chemistry, 36*(3), 786–796. https://doi.org/10.1002/etc.3642

Welsh, P. G., Lipton, J., Chapman, G. A., & Podrabsky, T. L. (2000). Relative importance of calcium and magnesium in hardness-based modification of copper toxicity. *Environmental Toxicology and Chemistry, 19*(6), 1624–1631. https://doi.org/10.1002/etc.5620190620

Wiramanaden, C. I. E., Orr, P. L., & Russell, C. K. (2015). Assessment of radium-226 bioavailability and bioaccumulation downstream of decommissioned uranium operations, using the caged oligochaete (*Lumbriculus variegatus*). *Environmental Toxicology and Chemistry, 34*(3), 507–517. https://doi.org/10.1002/etc.2852

Wheeler, J. R., Grist, E. P. M., Leung, K. M. Y., Morritt, D., & Crane, M. (2002). Species sensitivity distributions: Data and model choice. *Marine Pollution Bulletin, 45*(1–12), 192–202. https://doi.org/10.1016/S0025-326X(01)00327-7

Whicker, F. W., & Schultz, V. (1982). *Radioecology: Nuclear energy and the environment*. CRC Press.

Worms, I. A. M., & Wilkinson, K. J. (2007). Ni Uptake by a Green Alga. 2. Validation of Equilibrium Models for Competition Effects. Environmental Science & Technology, 41(12), 4264–4270. https://doi.org/10.1021/es0630341

Wurtz, C. B., & Bridges, C. H. (1961). Preliminary results from macroinvertebrate bioassays. *Proceedings of the Pennsylvania Academy of Science, 35*, 51–56.

Xu, Z., & Tsang, D. C. W. (2022). Redox-induced transformation of potentially toxic elements with organic carbon in soil. *Carbon Research, 1*, 9. https://doi.org/10.1007/s44246-022-00010-8

Zachara, J. M., Cowan, C. E., & Resch, C. T. (1991). Sorption of divalent metals on calcite. *Geochimica et Cosmochimica Acta, 55*(6), 1549–1562. https://doi.org/10.1016/0016-7037(91)90127-Q

Zhang, T., Gregory, K., Hammack, R. W., & Vidic, R. D. (2014). Co-precipitation of radium with barium and strontium sulfate and its impact on the fate of radium during treatment of produced water from unconventional gas extraction. *Environmental Science & Technology, 48*, 4596–4603. https://doi.org/10.1021/es405168b

Zhao, J., & Chen, B. (2016). Species sensitivity distribution for chlorpyrifos to aquatic organisms: Model choice and sample size. *Ecotoxicology and Environmental Safety, 125*, 161–169. https://doi.org/10.1016/j.ecoenv.2015.11.039

SUPPLEMENTARY MATERIALS

Chapter 1: Supporting Information

Table S1-1 Literature review of endpoint used to determine the acute and sublethal effects to fingernail clam species (Sphaeriidae)

Author	Species Scientific Name	Parameter	Lifestage	Exposure Type	Effect	Effect Measurement	Duration (Days)
Anderson 1977	*Musculium transversum*	KCl	Adult	Flow-through	Mortality		1.5 to 4
Anderson et al. 1978	*Musculium transversum*	KCl	Adult; Juvenile	Static	Growth	Length	28
		KCl		Static	Mortality		2 to 42
		NH_4Cl		Static	Growth	Length	42
		NH_4Cl		Static	Mortality		42
Arthur et al. 1987	*Musculium transversum*	NH_4Cl	Adult	Flow-through	Mortality		4
Boryslawskyj et al. 1987	*Sphaerium corneum*	$C_{12}H_8C_{L6}O$		Static	Bio-accumulation	Soft Tissue	3
Boryslawskyj et al. 1988	*Sphaerium corneum*	$C_{12}H_8C_{L6}O$		Static	Bio-accumulation	Soft Tissue	1
Chandler and Marking 1975	*Sphaerium sp.*	$C_7H_4F_3NO_3$		Static; Flow-through	Behaviour	Immobile (Intoxication)	4
Ernst et al. 1991	*Pisidium sp.*	Endosulfan II		Static	Mortality		1
Fong and Molnar 2008	*Sphaerium striatinum*	$C_{10}H_{13}ClN_2O$		Static	Reproduction	Spawning frequency	0.1667
Fong et al. 1998	*Sphaerium striatinum*	Fluoxetine $C_{10}H_{13}ClN_2O$	Adult	Static	Reproduction	Spawning frequency	0.1667
				Static	Reproduction	Progeny counts/numbers	0.1667 to 0.5
		Fluoxetine	Adult	Static	Reproduction	Progeny counts/numbers	0.1667
		Fluvoxamine	Adult	Static	Reproduction	Progeny counts/numbers	0.1667 to 0.2917
		Paroxetine	Adult	Static	Reproduction	Progeny counts/numbers	0.1667
Gerhardt 1992	*Pisidium sp.*	Cadmium Sulfate		Static; Flow-through	Mortality		5
Heinonen et al. 1997	*Sphaerium corneum*	$C_6H_3Cl_3O$		Static	Behaviour	Valve closure	0.25
	Sphaerium corneum	$C_6H_3Cl_3O$		Static	Bio-accumulation	Soft Tissue	0.25 to 4
	Pisidium amnicum	C_6HCl_5O		Renewal	Behaviour	Valve closure	28
Heinonen et al. 2001	*Pisidium amnicum*	C_6HCl_5O		Renewal	Bio-accumulation	Whole Organism	28
Heinonen et al. 2003	*Pisidium amnicum*	C_6HCl_5O		Static	Mortality		1
	Sphaerium novaezelandiae	C_6HCl_5O			Mortality		4
Hickey and Martin 1999		NH_4Cl	Immature	Flow-through	Growth	Length	60
		NH_4Cl	Adult; Immature	Renewal; Flow-through	Mortality		4 to 60
		NH_4Cl	Immature	Flow-through	Reproduction	Progeny counts/numbers	60
		Phenol			Mortality		0.0417
INHS 2005	*Sphaerium simile*	Na_2O_4S		Static	Mortality		4

Author	Species Scientific Name	Parameter	Lifestage	Exposure Type	Effect	Effect Measurement	Duration (Days)
Kamshilov and Flerov 1976	*Sphaerium corneum*	Phenol			Mortality		2
Lange 1985	*Sphaerium sp.*	$AlCl_3$		Aquatic - not reported	Behaviour	Immobile (Intoxication)	4
Logan and Perkins 1972	*Sphaerium corneum*	Essolvene		Static; Renewal	Mortality		1 to 63
Lozano et al. 1989	*Sphaerium sp.*	C8H8O	Adult	Static	Mortality		2
Mackie 1989	*Pisidium compressum*	Aluminum		Static	Mortality		4
	Pisidium casertanum	Aluminum		Static	Mortality		4
	Pisidium compressum	$CdCl_2$		Static	Mortality		4
	Pisidium casertanum	$CdCl_2$		Static	Mortality		4
	Pisidium casertanum	HNO_3Pb		Static	Mortality		4
	Pisidium compressum	HNO_3Pb		Static	Mortality		4
Maki and Johnson 1977	*Pisidium sp.*	$C_7H_4F_3NO_3$		Renewal	Bio-accumulation	Residue	1
Maki et al. 1975	*Sphaerium sp.*	$C_7H_4F_3NO_3$		Flow-through	Behaviour	Immobile (Intoxication)	1 to 4
	Pisidium sp.	$C_7H_4F_3NO_3$		Flow-through	Behaviour	Immobile (Intoxication)	1 to 4
Marking 1974	*Sphaerium sp.*	$C_{22}H_{39}NO$		Static	Mortality		4
Rice and White 1987	*Sphaerium striatinum*	PCB 1254		Static	Bio-accumulation	Whole Organism	45 to 68
Scheil and Hinz 1974	*Pisidium casertanum*	$HgCl_2$		Static	Mortality		21
Soucek and Dickinson 2012	*Sphaerium simile*	$NNaO_2$	Juvenile	Static	Mortality		4
		$NNaO_3$	Juvenile	Static	Mortality		4
Soucek and Kennedy 2005	*Sphaerium simile*	Na_2O_4S	Juvenile	Static	Mortality		4
Soucek et al. 2011	*Musculium transversum*	NaCl	Juvenile	Static	Mortality		4
Sparks and Sandusky 1981	*Musculium transversum*	NH4Cl		Flow-through	Mortality		42
Van Wijngaarden et al. 2010	*Sphaerium sp.*	Fluazinam	Subadult	Static	Behaviour	Stimulus avoidance	4
					Mortality		4
Wurtz and Bridges 1961	*Sphaerium sp.*	NaCl		Static	Mortality		1 to 4

Chapter 3: Supporting Information

Table S3-1. Chemical recipe of the reconstituted soft water used in the *Sphaerium striatinum* 28-day chronic toxicity test of ^{226}Ra

Chemical	Units	Concentration
$CaSO_4 \cdot 2H_2O$	g	1.5
$MgSO_4 \cdot 7H_2O$	g	3.07
$NaHCO_3$	g	2.4
KCl	g	0.1
Vitamin Mix	µL	500
Selenium	µL	500
Ultrapure Water	L	50

Table Notes. The vitamin mix solution is prepared by adding thiamine hydrochloride (750 mg L^{-1}), cyanocobalamin B12 (10 mg L^{-1}) and biotine (7.5 mg L^{-1}) to 1 litre ultra-pure water (<18.2 ohm·cm)

Table S3-2. Concentrations of select water chemistry parameters in samples collected from the bivalve collection areas, Ottawa River, 2022.

Analyte	Units	Unfiltered Samples (Total Concentrations)			Filtered Samples (Dissolved Concentrations)		
		Sample 1	Sample 2	Sample 3	Sample 1	Sample 2	Sample 3
Calcium	mg L^{-1}	11.28	10.95	11	10.88	11.02	11.02
Fluoride	mg L^{-1}	< 0.1	< 0.1	< 0.1	< 0.1	< 0.1	< 0.1
Potassium	mg L^{-1}	<3.38	<3.38	<3.38	<3.38	<3.38	<3.38
Magnesium	mg L^{-1}	2.68	2.65	2.71	2.66	2.67	2.66
Sodium	mg L^{-1}	8.89	8.49	8.59	8.53	8.61	8.8
Nitrogen	mg L^{-1}	0.44	0.43	0.45	0.42	0.47	0.4
Nitrite	mg L^{-1}	< 0.1	< 0.1	< 0.1	< 0.1	< 0.1	< 0.1
Nitrate	mg L^{-1}	0.4	0.4	< 0.2	0.2	0.3	< 0.2
Phosphorus	mg L^{-1}	<0.63	<0.63	<0.63	<0.63	<0.63	<0.63
Total Organic Carbon	mg L^{-1}	19.23	16.27	20.64	15.93	19	18.4
Hardness (as $CaCO_3$)	mg L^{-1}	39.20	38.25	38.63	38.12	38.51	38.47

Table S3-3. Thermodynamic data used in speciation modelling in PHREEQC version 3.7.3.

Reaction	Stability Constant (log_{10} K)	Reference
$Ra^{2+} + OH^- = RaOH+$	0.57 ± 0.23	(Brown et al., 2022)
$Ra^{2+} + SO_4^{2-} = RaSO_4$	2.61 ± 0.33	(Brown et al., 2022)
$Ra^{2+} + CO_3^{2-} = RaCO_3$	2.53 ± 0.14	(Brown et al., 2022)
$Ra^{2+} + HCO_3 = RaHCO_3^+$	2.89	(Beneš et al., 1982)
$Ra^{2+} + Cl^- = RaCl+$	-0.32 ± 0.23	(Brown et al., 2022)

Table S3-4. Mean ± standard deviation of in situ water quality parameters measured during the *Sphaerium striatinum* 28-day chronic toxicity test for each ^{226}Ra nominal treatment.

Treatment	Temperature (°C)	pH	Dissolved Oxygen (%)	Specific Conductivity (µS/cm)
All	20.0 ± 0.5	7.4 ± 0.2	92 ± 8	188 ± 21
Statistics by Treatment				
Control	20.1 ± 0.9	7.4 ± 0.2	92 ± 6	194 ± 35
0.1 Bq L^{-1}	20.2 ± 0.5	7.4 ± 0.2	92 ± 7	184 ± 15
0.5 Bq L^{-1}	19.9 ± 0.5	7.4 ± 0.2	92 ± 8	185 ± 18
1 Bq L^{-1}	20.0 ± 0.4	7.5 ± 0.1	93 ± 7	186 ± 18
5 Bq L^{-1}	20.0 ± 0.4	7.4 ± 0.2	91 ± 8	188 ± 16
10 Bq L^{-1}	19.9 ± 0.4	7.5 ± 0.1	93 ± 8	190 ± 20
25 Bq L^{-1}	20.0 ± 0.5	7.5 ± 0.2	93 ± 8	190 ± 20
50 Bq L^{-1}	20.0 ± 0.4	7.5 ± 0.2	94 ± 8	189 ± 20
Statistics Before and After Water Renewals				
Control				
Before	20.4 ± 0.6	7.3 ± 0.1	88 ± 4	214 ± 34
After	19.7 ± 1.0	7.6 ± 0.1	98 ± 1	167 ± 2
0.1 Bq L^{-1}				
Before	20.2 ± 0.5	7.3 ± 0.1	88 ± 3	194 ± 6
After	20 ± 0.5	7.5 ± 0.0	102 ± 1	164 ± 1
0.5 Bq L^{-1}				
Before	20.1 ± 0.4	7.3 ± 0.1	86 ± 3	198 ± 11
After	19.6 ± 0.6	7.5 ± 0.1	101 ± 3	166 ± 5
1 Bq L^{-1}				
Before	20.1 ± 0.5	7.4 ± 0.2	88 ± 4	199 ± 8
After	19.8 ± 0.3	7.6 ± 0.1	100 ± 2	166 ± 3
5 Bq L^{-1}				
Before	20.2 ± 0.4	7.4 ± 0.2	85 ± 4	197 ± 9
After	19.8 ± 0.2	7.6 ± 0.2	102 ± 1	167 ± 2
10 Bq L^{-1}				
Before	19.9 ± 0.5	7.4 ± 0.2	89 ± 6	201 ± 14
After	19.8 ± 0.2	7.6 ± 0.0	102 ± 2	166 ± 2
25 Bq L^{-1}				
Before	19.9 ± 0.7	7.4 ± 0.2	87 ± 4	202 ± 14
After	20.0 ± 0.1	7.6 ± 0.0	102 ± 1	168 ± 1
50 Bq L^{-1}				
Before	20.0 ± 0.5	7.4 ± 0.1	88 ± 3	202± 11
After	20.1 ± 0.1	7.6 ± 0.0	104 ± 3	166 ± 1

Table S3-5. Kruskal-Wallis rank sum test comparing in situ water parameters measured during the *Sphaerium striatinum* 28-day chronic toxicity across all ^{226}Ra nominal treatments

Parameter	chi-squared	df	p-value
Temperature (°C)	3.4	7	0.849
pH	10.7	7	0.153
Dissolved Oxygen (%)	3.2	7	0.862
Specific Conductivity (µS/cm)	3.1	7	0.872

Table Notes. Bold values indicate statistically significant results at $\alpha = 0.05$

Table S3-6. Welch two sample t-test comparing in situ water quality parameters measured before and after water renewals during the *Sphaerium striatinum* 28-day chronic toxicity across all ^{226}Ra nominal treatments

Parameter	Before (Mean)	After (Mean)	t	df	p-value
Temperature (°C)	19.8	20.1	-3.17	113	**0.002**
pH	7.56	7.37	11.0	131	**<0.001**
Dissolved Oxygen (%)	101	87.3	26.0	142	**<0.001**
Specific Conductivity (µS/cm)	166	201	-20.9	101	**< 0.001**

Table Notes. Bold values indicate statistically significant results at $\alpha = 0.05$

Table S3-7. Kruskal-Wallis rank sum test comparing water chemistry parameters measured during the *Sphaerium striatinum* 28-day chronic toxicity across all ^{226}Ra nominal treatments

Fraction	Parameter	chi-squared	df	p-value
Dissolved	Ca	2.1	7	0.952
	Cl	1.7	7	0.973
	K	11.2	7	0.131
	Mg	6.2	7	0.520
	Na	11.5	7	0.119
	SO4	2.2	7	0.948
	Inorganic Carbon	2.7	7	0.910
	Organic Carbon	3.6	7	0.828
Total	Ca	0.5	7	0.999
	Cl	4.3	7	0.747
	K	13.4	7	0.064
	Mg	6.5	7	0.483
	Na	10.6	7	0.156
	SO4	7.0	7	0.425
	Inorganic Carbon	1.4	7	0.987
	Organic Carbon	3.0	7	0.888

Table Notes. Bold values indicate statistically significant results at $\alpha = 0.05$

Table S3-8. Mean ± standard deviation of water chemistry parameters measured during the *Sphaerium striatinum* 28-day chronic toxicity test for each ^{226}Ra nominal treatment.

Group	Ca (mg L^{-1})	Cl (mg L^{-1})	K (mg L^{-1})	Mg (mg L^{-1})	Na (mg L^{-1})	SO4 (mg L^{-1})	Inorganic Carbon (mg L^{-1})	Organic Carbon (mg L^{-1})
Dissolved	7.1 ± 1.0	2.9 ± 0.9	0.9 ± 0.4	7.2 ± 0.9	25.5 ± 3.0	41.0 ± 6.9	1.9 ± 0.9	3.4 ± 1.3
Total	6.9 ± 0.7	14.4 ± 1.0	0.9 ± 0.4	7.0 ± 0.5	24.8 ± 3.3	48.2 ± 3.5	2.4 ± 1.2	2.4 ± 1.1
Statistics for Dissolved and Total Concentrations								
Control								
Dissolved	7.0 ± 0.7	2.9 ± 0.9	1.4 ± 0.2	7.6 ± 0.3	31.0 ± 3.2	42.6 ± 7.2	3.0 ± 1.7	3.4 ± 1.6
Total	7.0 ± 0.6	14.6 ± 1.0	1.3 ± 0.7	7.7 ± 0.4	31.2 ± 3.6	51.2 ± 4.3	3.1 ± 1.9	2.9 ± 1.3
0.1 Bq L^{-1}								
Dissolved	6.8 ± 0.9	2.7 ± 0.9	0.8 ± 0.4	6.7 ± 0.5	24.4 ± 1.7	37.3 ± 5.8	2.0 ± 1.1	3.5 ± 1.7
Total	6.8 ± 0.8	13.9 ± 0.5	0.6 ± 0.0	6.9 ± 0.4	24.6 ± 1.9	47.5 ± 0.8	2.6 ± 1.5	2.8 ± 1.3
0.5 Bq L^{-1}								
Dissolved	6.7 ± 0.8	2.5 ± 0.6	0.6 ± 0.0	6.8 ± 0.4	23.7 ± 2.8	38.2 ± 3.6	1.8 ± 0.7	3.1 ± 1.4
Total	6.9 ± 0.8	14.3 ± 1.1	0.8 ± 0.4	6.9 ± 0.3	24.2 ± 3.0	46.7 ± 2.2	2.6 ± 1.7	2.1 ± 1.5
1 Bq L^{-1}								
Dissolved	6.8 ± 0.7	2.7 ± 0.7	0.9 ± 0.4	6.9 ± 0.4	23.8 ± 2.0	39.5 ± 4.0	1.9 ± 0.8	3.1 ± 1.4
Total	7.0 ± 0.6	14.3 ± 1.1	1.0 ± 0.4	6.9 ± 0.3	24.0 ± 2.0	48.2 ± 3.8	2.3 ± 1.7	2.3 ± 1.0
5 Bq L^{-1}								
Dissolved	7.1 ± 1.5	3.2 ± 0.8	0.8 ± 0.5	7.1 ± 1.4	24.2 ± 2.6	40.5 ± 8.5	1.7 ± 1.1	3.1 ± 1.5
Total	6.7 ± 1.0	13.8 ± 0.7	0.6 ± 0.0	6.7 ± 0.8	22.8 ± 2.1	44.7 ± 4.3	2.3 ± 1.1	2.0 ± 1.1
10 Bq L^{-1}								
Dissolved	7.2 ± 1.3	2.8 ± 1.4	0.6 ± 0.0	7.3 ± 1.0	24.9 ± 2.0	42.1 ± 8.0	1.9 ± 0.8	3.2 ± 1.3
Total	6.8 ± 0.8	14.6 ± 1.1	0.6 ± 0.0	7.0 ± 0.4	23.5 ± 1.7	48.7 ± 2.9	1.9 ± 0.8	2.3 ± 1.0
25 Bq L^{-1}								
Dissolved	7.4 ± 1.4	3.1 ± 1.1	1.0 ± 0.5	7.5 ± 1.2	25.5 ± 1.7	43.1 ± 8.6	1.9 ± 0.7	3.8 ± 1.2
Total	6.9 ± 0.7	14.2 ± 1.4	0.8 ± 0.4	7.0 ± 0.4	24.1 ± 3.0	48.0 ± 2.1	2.2 ± 0.7	2.7 ± 1.1
50 Bq L^{-1}								
Dissolved	7.4 ± 1.3	3.1 ± 1.4	1.2 ± 0.4	7.6 ± 1.2	27.5 ± 2.7	44.1 ± 10.9	1.6 ± 0.5	4.0 ± 1.2
Total	6.9 ± 0.8	15.1 ± 1.1	1.3 ± 0.1	7.2 ± 0.5	25.8 ± 3.1	51.0 ± 3.9	2.2 ± 1.1	2.4 ± 1.2

Table S3-9. Predicted aqueous speciation of ^{226}Ra in stock solutions using PHREEQC, showing molal concentrations and percent composition of individual species.

Distribution of Species	Molality	% Composition
Ra+2	5.05E-14	83.47%
RaSO4	5.42E-15	8.96%
RaHCO3+	4.57E-15	7.56%
RaCl+	3.73E-18	0.01%
RaCO3	1.60E-18	0.00%
RaOH+	4.03E-20	0.00%

Table Notes. Conversion of nominal ^{226}Ra concentrations from mol L^{-1} to Bq L^{-1} for experimental treatments, using a specific activity of 8.27×10^{12} Bq mol^{-1}.

Table S3-10. Welch two sample t-test comparing total and dissolved fractions of ^{226}Ra measured during the *Sphaerium striatinum* 28-day chronic toxicity across all nominal treatments

Nominal	Source	Dissolved (Mean)	Total (Mean)	df	p-value
0.1 Bq L^{-1}	Fresh	0.04	0.0339	1.1	0.666
	Test	0.00	0.00476	13.1	0.25
0.5 Bq L^{-1}	Fresh	0.42	0.352	2.7	0.0818
	Test	0	0.0491	13.9	0.974
1 Bq L^{-1}	Fresh	0.652	0.858	1.95	0.223
	Test	0.0888	0.0748	16.7	0.3
5 Bq L^{-1}	Fresh	5.28	4.1	1.09	0.509
	Test	0.464	0.456	18	0.922
10 Bq L^{-1}	Fresh	9.53	9.46	1.82	0.971
	Test	0.992	0.985	19.9	0.976
25 Bq L^{-1}	Fresh	22	24	1.29	0.184
	Test	2.44	3.59	12.5	0.334
50 Bq L^{-1}	Fresh	39.2	46.4	1.54	0.349
	Test	4.73	4.4	15.8	0.603

Table Notes. Bold values indicate statistically significant results at $\alpha = 0.05$

Table S3-11. Kruskal-Wallis rank sum test comparing water chemistry parameters measured during the *Sphaerium striatinum* 28-day chronic toxicity across all ^{226}Ra nominal treatments

Tissue Type	Nominal	TWA	chi-squared	df	p-value
Soft	1 Bq L^{1}	0.47	0.1	22	0.993
	5 Bq L^{1}	2.25	0.2	22	0.955
	25 Bq L^{1}	12.9	0.8	22	0.149
	50 Bq L^{1}	25.4	2.1	22	**<0.001**
Shell	1 Bq L^{1}	0.47	0.1	22	0.992
	5 Bq L^{1}	2.25	0.6	22	0.728
	25 Bq L^{1}	12.9	3.6	22	**<0.001**
	50 Bq L^{1}	25.4	10.7	22	**<0.001**

Table Notes. Bold values indicate statistically significant results at $\alpha = 0.05$

Table S3-12. Comparison of effect concentrations (Bq L^{-1}) derived from dose-response models using nominal, time-weighted average, and end-of-interval (T_{48}) concentrations from the 28-day chronic toxicity test of ^{226}Ra to *Sphaerium striatinum*

Approach	Toxicity Endpoint	Nominal Activity Concentration	Time-Weighted Average	Measured Concentration T48
Hypothesis Test	Survival	50.0	25.4	4.40
	Burrowing	50.0	25.4	4.40
	Growth	10.0	5.30	0.985
		25.0	12.9	3.59
	Reproduction	1.00	0.468	0.075
		5.00	2.25	0.456
Dose-Response	Growth	7.51 (-0.94 to 16.0)	4.10 (-3.7 to 11.9)	0.73 (-0.56 to 2.02)
		8.63 (3.50 to 13.8)	4.64 (0.03 to 0.93)	0.84 (0.05 to 1.63)
		10.9 (6.42 to 15.5)	5.74 (2.14 to 9.34)	1.08 (0.46 to 1.71)
	Reproduction	0.85 (-1.07 to 2.76)	0.37 (-0.43 to 1.17)	0.06 (0.01 to 0.12)
		0.91 (-0.24 to 2.06)	0.41 (-0.09 to 0.91)	0.07 (0.03 to 0.10)
		1.04 (0.51 to 1.56)	0.49 (0.24 to 0.75)	0.08 (0.06 to 0.10)

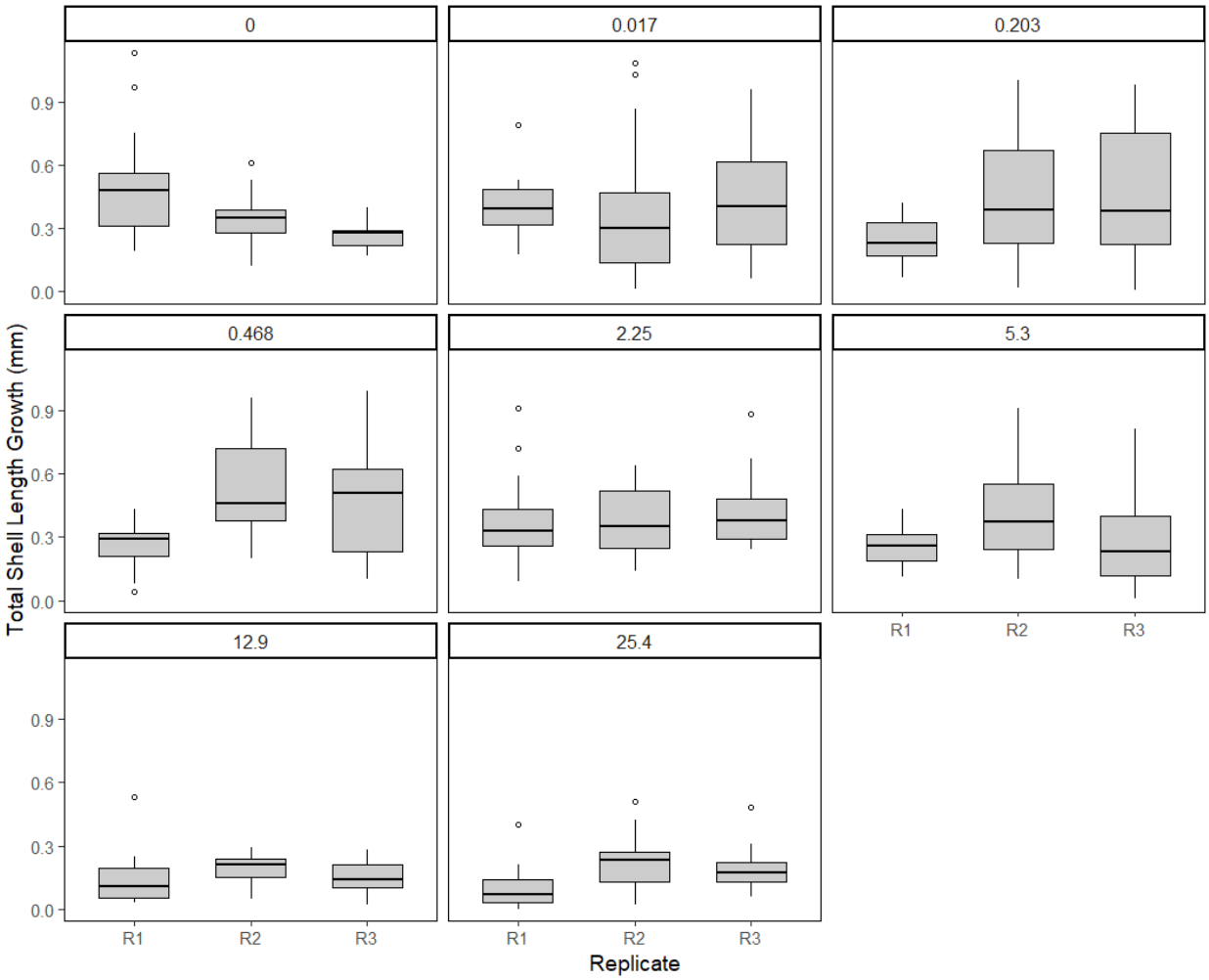


Figure S3-1. Growth in total shell length (mm) of *Sphaerium striatinum* across ^{226}Ra exposure treatments (time-weighted average concentrations, Bq L^{-1}), shown separately for each replicate. Boxes represent the interquartile range (25th–75th percentiles), the horizontal line indicates the median, and whiskers extend to 1.5 × the interquartile range; points represent single observations.

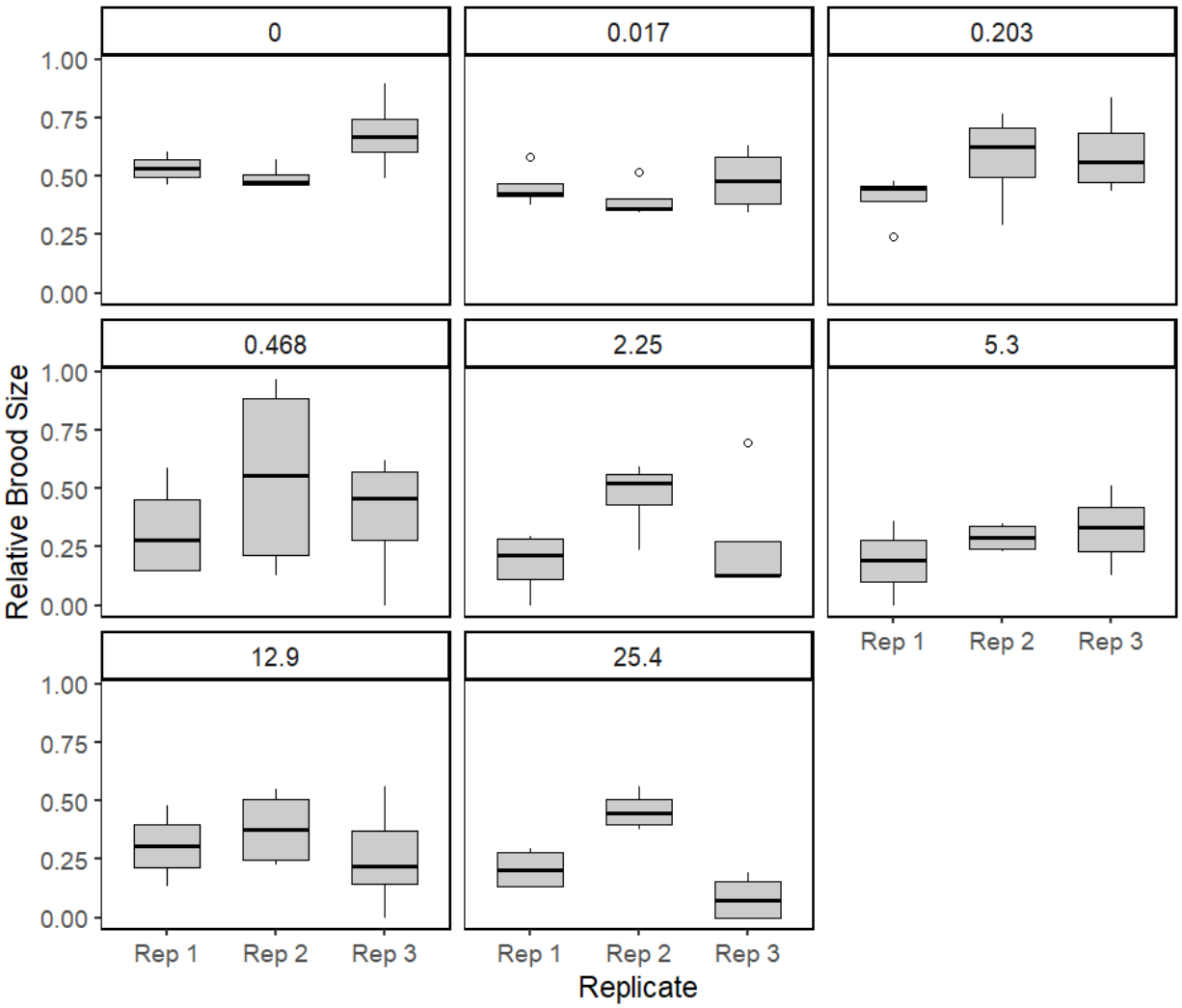


Figure S3-2. Relative brood size (# larvae / total shell length) of *Sphaerium striatinum* across ^{226}Ra exposure treatments (time-weighted average concentrations, Bq L^{-1}), shown separately for each replicate. Boxes represent the interquartile range (25th–75th percentiles), the horizontal line indicates the median, and whiskers extend to 1.5 × the interquartile range; points represent single observations.

Chapter 4: Supporting Information

Table S4-1. Composition of reconstituted soft water (RSW) modified to obtain low, moderate, and high calcium stock solutions

Chemical	Units	RSW (7 mg L^{-1})	Modified RSW		
			low Ca (0.9 mg L^{-1})	moderate Ca (35 mg L^{-1})	high Ca (70 mg L^{-1})
$CaSO_4 \cdot 2H_2O$	g	1.5	0.15	7.5	15
$MgSO_4 \cdot 7H_2O$	g	3.07	3.07	3.07	3.07
$NaHCO_3$	g	2.4	2.4	2.4	2.4
KCl	g	0.1	0.1	0.1	0.1
Vitamin Mix	µL	500	500	500	500
Selenium	µL	500	500	500	500
Ultrapure Water	L	50	50	50	50

Table Notes. The vitamin mix solution is prepared by adding thiamine hydrochloride (750 mg L^{-1}), cyanocobalamin B12 (10 mg L^{-1}) and biotine (7.5 mg L^{-1}) to 1 litre ultra-pure water (<18.2 ohm·cm)

Table S4-2. Surface protonation, deprotonation, and surface complexation constants compiled for Surface Complexation Modelling development in PHREEQC version 3.7.3

Reaction	log K	References
$\equiv SOH + H^+ = \equiv SOH_2^+$	0.40	Nair et al., 2014
$\equiv SOH = \equiv SO^- + H^+$	-6.70	Nair et al., 2014
$\equiv SOH + Ca^{2+} = \equiv SOCa + H^+$	-1.62	Fu et al. 2025
$\equiv SOH + Sr^{2+} = \equiv SOSr + H^+$	-1.23	Kitamura et al. 1999
$\equiv SOH + Ba^{2+} = \equiv SOBa + H^+$	-0.97	Kitamura et al. 1999
$\equiv SOH + Ra^{2+} = \equiv SORa + H^+$	-0.95	*estimated from Quartz Ca, Sr and Ba analogues*

Table S4-3. Concentrations of major ions in stock solutions for adsorption experiments (N =1).

Parameter	Units	Measured Concentration			
		low Ca	RSW	moderate Ca	high Ca
Ca	mg L^{-1}	0.9	7	35	70
Cl	mg L^{-1}	2	2	2	2
Fe	mg L^{-1}	0.1	0.1	0.3	0.1
K	mg L^{-1}	1.3	1.3	1.3	1.3
Mg	mg L^{-1}	6.2	6.4	6.4	6.5
Mn	mg L^{-1}	0.03	0.04	0.03	0.03
Na	mg L^{-1}	18	18	18	18
SO4	mg L^{-1}	34	34	34	34
DOC	mg L^{-1}	-	19	-	-
DIC	mg L^{-1}	10	7.7	6.8	10

Table S4-4. Results from the geochemical analysis of mineral sand substrate (N =1).

Parameter	Units	Sand Sample
Al	%	0.124
Ca	%	<0.030
Fe	%	0.034
K	%	<0.150
Mg	%	<0.060
Mn	%	<0.010
Na	%	<0.021
Si	%	30.17
Ti	%	0.037
Zr	%	0.001

Table S4-5. Quartz mineral surface properties for quartz and kaolinite used in the Surface Complexation Modelling in PHREEQC version 3.7.3

Model	Parameter	Units	Quartz
Surface Complexation Model (SCM) - Double Diffuse Layer (DDL)	Equivalent circular diameter (ECD)[b]	μm	188 ± 40
	Particle density (ρ)[a]	kg/m^3	2530
	Specific Surface Area (SSA)[c]	m^2/g	0.0126
	Site density (D)[a]	sites/nm^2	4.5
	Mass	g	47
	Total Surface Area	m^2	0.5929
	Number of sites	sites	2.67E+18
	Moles of surface sites	mol	4.43E-06

Table Notes. Parameters were obtained from the literature[a], measured[b], or calculated[c]

Table S4-6. In situ water quality parameters throughout the adsorption experiments

Day	Time	Nominal Treatment	Beaker Measurements			
			Temp (°C)	pH	Cond µS/cm	DO %
Low Calcium (0.9 mg L^{-1})						
Day 1	T_0	1 Bq L^{-1}	21.7	7.03	128	95.0
		5 Bq L^{-1}	21.7	7.03	128	95.0
		50 Bq L^{-1}	21.7	7.03	128	95.0
Day 1	T_6	1 Bq L^{-1}	22.0	7.03	128	95.3
		5 Bq L^{-1}	21.7	7.16	128	95.5
		50 Bq L^{-1}	22.1	6.95	127	96.5
Day 2	T_{24}	1 Bq L^{-1}	21.9	6.91	138	95.3
		5 Bq L^{-1}	21.8	6.97	138	95.3
		50 Bq L^{-1}	21.8	6.96	143	95.3
Day 3	T_{48}	1 Bq L^{-1}	21.6	7.01	182	93.4
		5 Bq L^{-1}	21.6	7.03	183	92.1
		50 Bq L^{-1}	21.5	7.01	183	91.0
RSW (7.0 mg L^{-1})						
Day 1	T_0	1 Bq L^{-1}	21.7	7.07	166	95.0
		5 Bq L^{-1}	21.7	7.07	166	95.0
		50 Bq L^{-1}	21.7	7.07	166	95.0
Day 1	T_6	1 Bq L^{-1}	21.7	7.07	166	95.5
		5 Bq L^{-1}	21.8	7.02	166	95.4
		50 Bq L^{-1}	21.7	7.11	166	95.1
Day 2	T_{24}	1 Bq L^{-1}	21.6	7.19	178	94.4
		5 Bq L^{-1}	21.5	7.21	177	95.1
		50 Bq L^{-1}	21.6	7.23	177	95.4
Day 3	T_{48}	1 Bq L^{-1}	21.7	7.03	146	92.4
		5 Bq L^{-1}	21.7	7.11	147	91.5
		50 Bq L^{-1}	21.7	7.24	147	91.6
Moderate Calcium (35 mg L^{-1})						
Day 1	T_0	1 Bq L^{-1}	21.7	7.02	309	95.0
		5 Bq L^{-1}	21.7	7.02	309	95.0
		50 Bq L^{-1}	21.7	7.02	309	95.0
Day 1	T_6	1 Bq L^{-1}	21.7	7.02	309	95.0
		5 Bq L^{-1}	21.6	7.02	311	94.8
		50 Bq L^{-1}	21.6	7.02	315	95.1
Day 2	T_{24}	1 Bq L^{-1}	21.5	7.10	333	93.5
		5 Bq L^{-1}	21.3	7.24	333	94.7
		50 Bq L^{-1}	21.3	7.24	337	94.8
Day 3	T_{48}	1 Bq L^{-1}	21.3	7.22	330	92.5
		5 Bq L^{-1}	21.3	7.25	329	91.4
		50 Bq L^{-1}	21.3	7.26	337	91.4
High Calcium (70 mg L^{-1})						

Day	Time	Nominal Treatment	Beaker Measurements			
			Temp	pH	Cond	DO
			(°C)		µS/cm	%
		1 Bq L^{-1}	21.7	7.13	487	95.0
Day 1	T_0	5 Bq L^{-1}	21.7	7.13	487	95.0
		50 Bq L^{-1}	21.7	7.13	487	95.0
		1 Bq L^{-1}	21.6	7.13	487	95.0
Day 1	T_6	5 Bq L^{-1}	21.6	7.13	486	94.9
		50 Bq L^{-1}	21.7	7.16	487	95.1
		1 Bq L^{-1}	21.1	7.33	521	93.9
Day 2	T_{24}	5 Bq L^{-1}	21.1	7.36	518	94.2
		50 Bq L^{-1}	21.0	7.40	523	94.2
		1 Bq L^{-1}	21.1	7.33	513	92.3
Day 3	T_{48}	5 Bq L^{-1}	21.2	7.34	509	91.4
		50 Bq L^{-1}	21.1	7.31	511	91.2

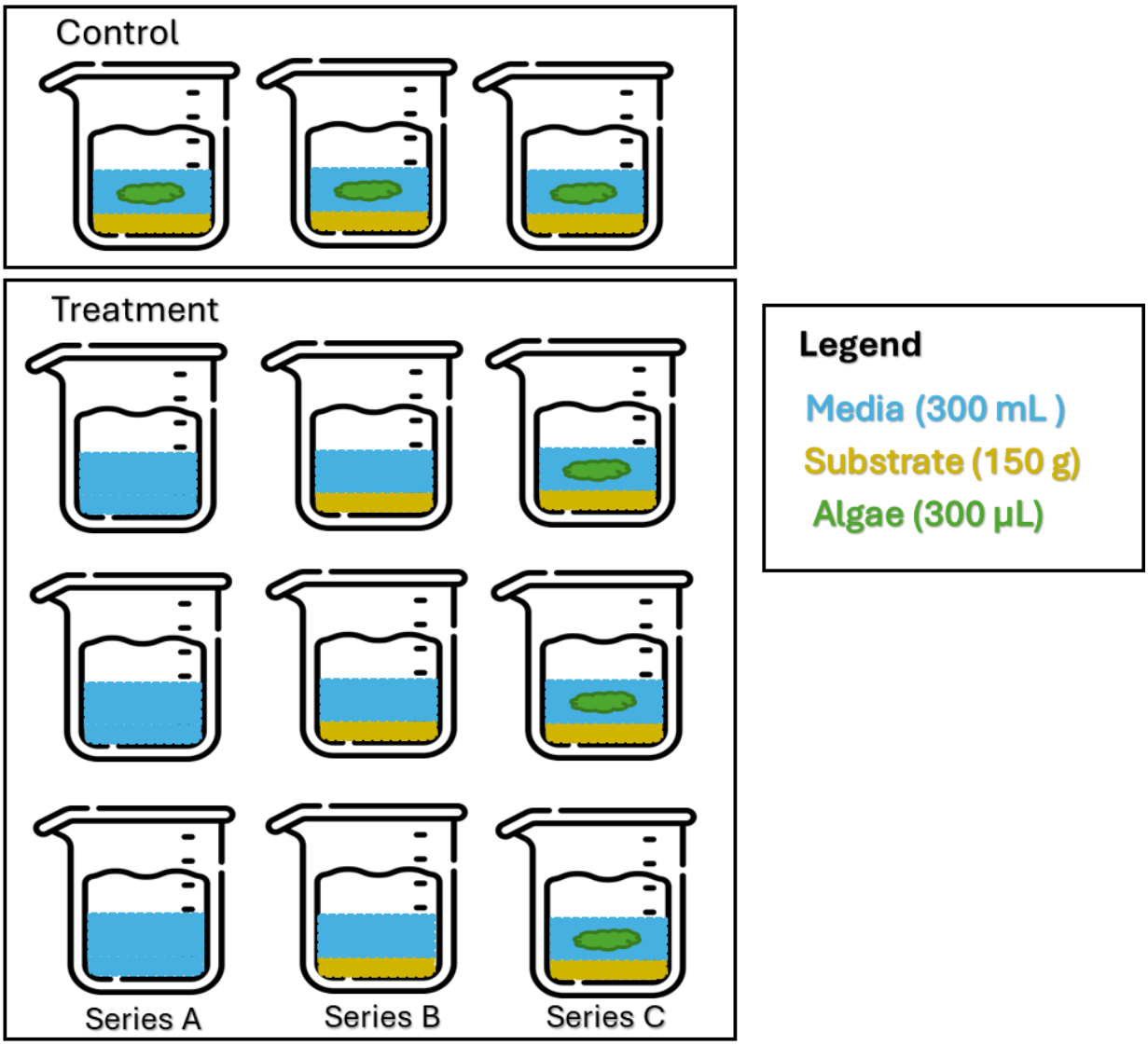


Figure S4-1. Design of the tiered-adsorption experiment used to quantify the potential influence of solution composition (Series A), sand substrate (Series B) and organic matter (Series C) on changes in dissolved ^{226}Ra in solution over 48 hours. The Control consisted of Reconstituted Soft Water (RSW). Treatments consisted of three ^{226}Ra activity concentrations (1, 5, 50 Bq L^{-1}). Experiments were run four times, for each Ca concentration (0.9, 7, 35, 70 mg L^{-1}).

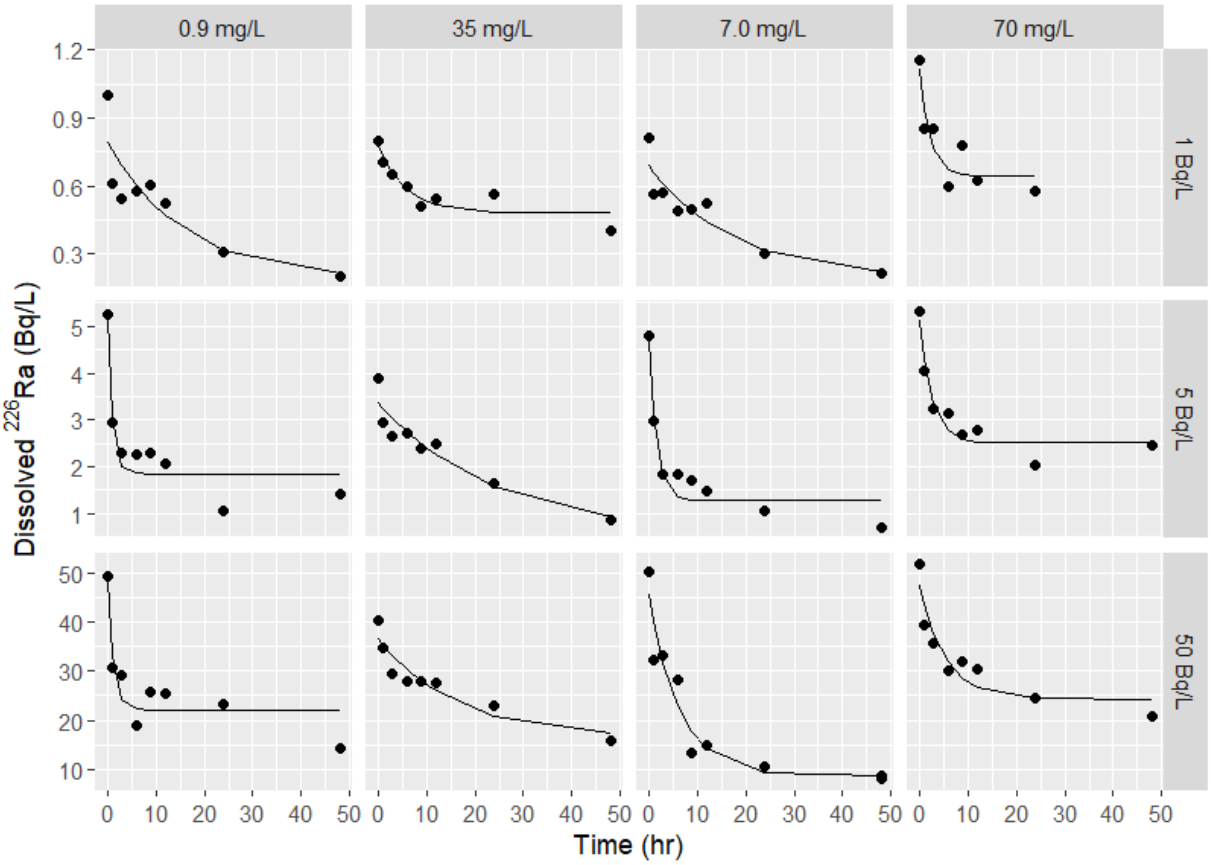


Figure S4-2 Time-series of dissolved ^{226}Ra concentrations for Series C (solution + sand + organic matter) under various Ca concentrations (0.9–70 mg L^{-1}) and nominal ^{226}Ra activities (1, 5, and 50 Bq L^{-1}). The black circles represent measured concentrations, and lines represent fitted first-order kinetic models describing the approach to equilibrium.

Chapter 5: Supporting Information

Table S5-1. Composition of reconstituted soft water (RSW) modified to obtain low, moderate, and high calcium stock solutions

Chemical	Units	RSW (7 mg L^{-1})	Modified RSW		
			low Ca (0.9 mg L^{-1})	moderate Ca (35 mg L^{-1})	high Ca (70 mg L^{-1})
$CaSO_4 \cdot 2H_2O$	g	1.5	0.15	7.5	15
$MgSO_4 \cdot 7H_2O$	g	3.07	3.07	3.07	3.07
$NaHCO_3$	g	2.4	2.4	2.4	2.4
KCl	g	0.1	0.1	0.1	0.1
Vitamin Mix	µL	500	500	500	500
Selenium	µL	500	500	500	500
Ultrapure Water	L	50	50	50	50

Table Notes. The vitamin mix solution is prepared by adding thiamine hydrochloride (750 mg L^{-1}), cyanocobalamin B12 (10 mg L^{-1}) and biotine (7.5 mg L^{-1}) to 1 litre ultra-pure water (<18.2 ohm·cm)

Table S5-2. Summary dose rate estimates (µGy h^{-1}) using ERICA tool for *Sphaerium striatinum* across ^{226}Ra and calcium treatments.

Experimental Design			Activity Concentrations				Total Dose Rate per Organism (uGy h^{-1})		
				Sediment (Bq kg^{-1})					
Test	Calcium (mg L^{-1})	Nominal ^{226}Ra (Bq L^{-1})	Water (Bq L^{-1})	ERICA Estimate	Mass Balance Estimated	Whole Organism (Bq kg^{-1}, ww)	Water 1 : Sediment 0	Water 0.5 : Sediment 0.5 (ERICA Estimate)	Water 0.5 : Sediment 0.5 (Mass Balance)
Low	0.9	1	0.58	4910	26	117.32	**17.5**	**18.6**	**17.5**
		5	3.00	25400	131	286.49	**45.5**	**51.7**	**45.5**
		10	6.58	55700	245	586.0	**93.9**	**107**	**93.9**
		25	13.4	113000	586	2088	**316**	**344**	**316**
		50	27.5	233000	1255	1410.9	**247**	**304**	**247**
RSW	7	1	0.37	3130	16	72.9	10.6	**11.4**	10.6
		5	2.84	24300	134	336.4	**47.7**	**53.6**	**47.7**
		25	11.8	104000	545	1666	**238**	**263**	**238**
		50	21.8	186000	958	5130	**727**	**772**	**727**
Moderate	35	0.5	0.23	1950	7	54.17	**32.2**	**32.7**	**32.2**
		1	0.37	3130	10	88.20	**66**	**66.7**	**66**
		5	2.60	22000	61	384.3	**54.5**	**59.8**	**54.5**
		10	5.54	46900	126	459.4	**65.5**	**76.9**	**65.5**
		25	13.5	115000	303	1083.0	**158**	**185**	**158**
		50	29.4	249000	570	1584.7	**233**	**293**	**233**
High	70	0.5	0.41	3470	14	37.81	**6.0**	6.8	**6.0**
		1	0.70	5930	25	20.59	8.1	9.54	8.1
		5	3.37	28500	85	1198.3	**190**	**197**	**190**
		10	6.27	53100	220	3140	**479**	**492**	**479**

Table Notes. Bold values exceed screening benchmarks of 10 µGy h^{-1}, while grey shading represent exceedance of 400 µGy h^{-1}.